UNIVERSITÀ DEGLI STUDI DI MILANO

FACOLTÀ DI SCIENZE E TECNOLOGIE

Doctorate course in Chemistry - XXXII Cycle

Department of Chemistry

Exploration of the chemical space: diversity-oriented and chemoenzymatic approaches

CHIM/06

Ph.D. Thesis of
Elisa BONANDI
R11778

Tutor: Prof. Daniele Passarella

Coordinator: Prof. Emanuela Licandro

Academic Year: 2018/2019

A Enzo e Daniela

"... Natural selection works like a tinker who does not know exactly what he is going to produce but uses whatever he finds around him to produce some kind of workable object. None of the material at the tinker's disposal has a precise and definite function. Each can be used in different ways. Novelty comes from previously unseen association of old material. To create is to recombine"

François Jacobs

Table of contents

Abstract

This dissertation is an overview of a three-years project, aimed at the exploration of new regions of the chemical space, that could contain new unusual bioactive compounds. The already discovered small molecules cover only a small portion of the chemical universe, that becomes even narrower when bioactive compounds are considered. In this context, two different strategies for the investigation of the chemical space have been considered: the diversity oriented-synthesis (DOS), that constitute the major topic of the work, and a chemoenzymatic approach, developed during a period spent at the University of Warwick (UK), in the laboratory of Professor M. Tosin.

Chapter 1 deals with the general principles of the DOS approach, focusing then the attention on a library of piperidine-based compounds previously synthesised in Professor Passarella's research group, starting from a common precursor, 2-piperidine ethanol (**1**). An overview of the main results previously accessed in this field is reported. At the end of the chapter, the planning of a further expansion of this library is presented. The structure of the newly accessed piperidine-based products is appreciable in Figure 1; their obtainment was the main goal of this thesis.

Chapter 2 is focused on the stereoselective synthesis of eight highly diversified polyheterocyclic compounds, characterized by three different scaffolds.

In particular, the different scaffolds were originated by the same precursor, considering that its different *syn*- or *anti*- stereocenter configuration, influenced the reaction outcome. This project opens the possibility of accessing analogs of some natural products, such as lupin and lycopodium alkaloids.

Chapter 3 concerned the obtainment of a library of potential Hedgehog (Hh) signalling pathway inhibitors, rationally designed exploiting docking simulations and taking inspiration from a class of natural products, the withanolides. The designed scaffold contains two key motif, a bicyclic carbamate and an *α,β*-unsaturated lactone, and presents three stereocenters. So far, two out of the four racemic isomers have been accessed and biological evaluation revealed two interesting intermediates, that have been synthesised also as separate enantiomers. Moreover, preliminary studies toward the obtainment of 2nd generation inhibitors have been performed in our laboratory. Biological evaluation of these compounds is currently in progress and will orient the future development of this work.

Chapter 4 is aimed at the synthesis of (-)-anaferine as an unexpected further ramification of our DOS approach. Key intermediate **10**, already exploited for the

synthesis of the inhibitors of chapter 3, has been employed as starting material, converting its homoallylic alcohol into an *α,β*-unsaturated lactam. To this extent, the same approach used in chapter 1, to transform **9** into a similar lactam (left compound in the pink box of Figure 1) was applied. After that, the synthesis of (-)-anaferine was accomplished in few steps, reducing the lactam to piperidine and oxidizing the 2-hydoxypropane bridge to the corresponding ketone.

Chapter 5 deals with the synthesis of thiocolchicine-based bivalent compounds, possibly acting as microtubules binders. A hybrid compound, bearing the key structural features of pironetin (one of the few known *α*-tubulin binder), previously synthesised on our laboratory from 2-piperidine ethanol, was exploited as key building block. In fact, it was connected through different linkers to *N*-10-deacteyl-thiocolchicine, a model of *β*-tubulin binder. Biological tests revealed that the lipophilic nature of the linkers rendered our conjugates better substrates for P-glycoprotein, leading to a drop in activity on resistant cancer cells. Therefore, new bivalent compounds will be soon produced in our laboratory, changing linkers chemo-physical properties.

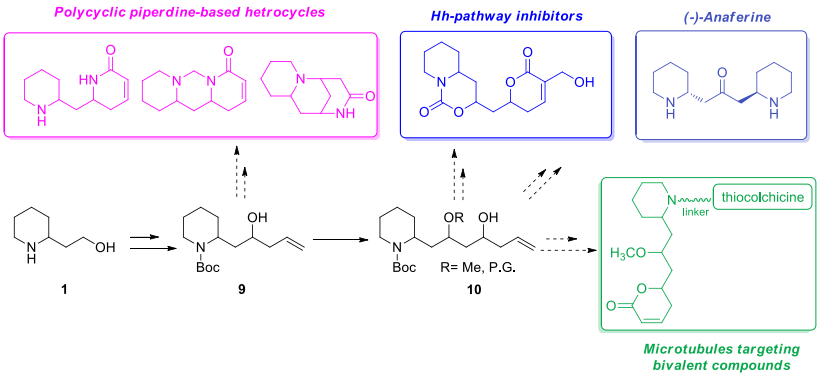

Figure 1. Structures of the new compounds resulting from the expansion of the DOS-approach from 2-piperidine ethanol **1**.

Finally, chapter 6 concerned a project aimed at the generation of unnatural, diversified derivatives of lasalocid A and salinomycin, through feeding experiments of malonate-mimicking chemical probes to the natural *Streptomyces* producers, in an approach resembling mutasynthesis. The efforts were focused on the devopment of different strategies for an easier recovery and analysis of the unnatural products from the complex mixtures of the fermentation broths. To this extent, four chemical probes have been synthesised and proof on concept experiments were performed to verify their applicability in this field.

1. Diversity-oriented synthesis in drug discovery

1.1. Diversity-oriented synthesis: general principles

Small molecules are defined as low molecular weight entities (usually < 900-1000 dalton), that include monosaccharides, small lipids, secondary metabolites, xenobiotics and natural products. Small molecules are known for their possible applications as drug candidates: in fact, the modulation of proteins function exerted by small molecules is one of the fundamental paradigms in medicinal chemistry and chemical genetic.

Nowadays, the screening of libraries of small molecules is one of the most common strategies in drug discovery and development process, to identify possible hit or lead compounds.

In this context, the diversity and the structural complexity of the library members are critical factors, as well as the size of the library itself. This is true in particular when a screening is performed without a precise knowledge of the biological target involved in a certain disease. In these "random" screenings it's impossible to determine *a priori* a set of features that small molecules should possess to display a certain biological activity. In these cases, the availability of a library including a large collection of compounds, diversified as much as possible from a structural point of view, enhances the probability of identifying a promising hit candidate.[1]

Thus, the correlation between the intrinsic diversity of a library and the probability of finding an interesting protein modulator appears to be clear.

Therefore, if target-oriented synthesis (namely the synthesis of a particular product, rationally designed to give a certain biological effect) is the most common strategy when a biological target is known, diversity-oriented synthesis (DOS) finds widespread applications in the preparation of small-molecules libraries, for screening against known and unknown biological targets.[2]

DOS is defined as the "deliberate, simultaneous and efficient synthesis of more than one target compound in a diversity-driven approach",[3] generating a collection of products that, from a structural and functional point of view, covers a portion of the chemical space as wide as possible. The chemical space, accordingly to the concept of cosmological universe, includes all the possible existing small carbon-based molecules.[4] Obviously, the chemical space is huge. It has been estimated that it should

[1] W. R. J. D. Galloway, A. Isidro-Llobet, D. R. Spring, *Nat. Commun.* **2010**, *1*, 1–13.
[2] S. L. Schreiber, *Science* **2000**, *287*, 1964–1969.
[3] D. R. Spring, *Org. Biomol. Chem.* **2003**, *1* , 3867 – 3870.
[4] J. Medina-Franco, K. Martinez-Mayorga, M. Giulianotti, R. Houghten, C. Pinilla, *Curr. Comput. Aided-Drug Des.* **2008**, *4*, 322–333.

contains 10^{60} compounds, characterised by a maximum number of 30 carbon, nitrogen, oxygen and sulphur atoms; of course, the number of possible compounds increases when more complex entities are considered.[5]

The already discovered small molecules cover only a small portion of the chemical universe, that becomes even narrower when bioactive small molecules are considered.

The most part of the chemical universe, that can contain interesting and unusual bioactive compounds, is still inaccessible to chemists. Thus, diversity-oriented synthesis emerged as a promising strategy to reach its unexplored portions.[6]

The goal of a DOS is quite different from targeted-oriented synthesis or combinatorial synthesis, that aim at obtaining a single compound or collections of similar products, respectively.

Ideally, DOS should convert simple starting material into complex and diversified scaffolds, in a limited number of synthetic steps, to maximize the efficiency of the process. The search for "complexity and diversity" is the main difference with combinatorial synthesis, more dedicated to the obtainment of "complex and similar" products, to verify how slight structural differences could impact the biological properties. Therefore, DOS approaches are analysed in a forward synthetic sense, rather than in a retrosynthetic way, typical of target oriented- and combinatorial synthesis. On the basis of the search for diversity, the members of DOS libraries should assume a broader distribution in the chemical space, compared with the case of combinatorial synthesis, in which only a limited portion is explored (Figure 1).

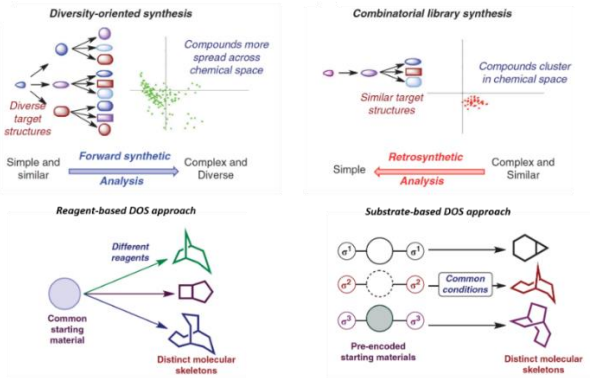

Figure 1. Comparison between DOS and combinatorial synthesis and between reagent-based and substrate-based DOS approaches. Adapted by permission from Springer/Nature, copyright 2010, according to ref 1

[5] R. S. Bohacek, C. McMartin, W. C. Guida, *Med. Res. Rev.* **1996**, *16*, 3-50.

[6] G. L. Thomas, E. E. Wyatt, D. R. Spring, *Curr. Opin. Drug Discov. Devel.* **2006**, *9*, 700–712.

To achieve diversification, two main strategies could be adopted: the reagent-based approach and the substrate-based approach.
In the first case a common, simple precursor is elaborated in different ways, through a branched synthetic route, to obtain differentiated atomic skeletons.
In the substrate-based approach, differentiated starting materials are treated in the same reaction conditions. The selected reagents should present suitable appendages (called σ-elements), characterised by "pre-encoded" skeletal information, convertible into different scaffolds under the same conditions set (Figure 1).
DOS usually exploits reliable, well-known reactions and methodologies, that should work on a wide range of functional groups. Differently from combinatorial synthesis, As aforementioned, DOS strategies are initially planned in a "forward sense", rather than in a retrosynthetic way, starting from the simple precursor and evaluating how to modify it, in order to assess the maximum structural differentiation.
The validity of DOS approach in drug discovery and development has been demonstrated by the individuation of novel bioactive compounds, through the screening of diversified libraries.
Examples of these pharmacologically interesting small molecules include Robotnikin, a hedgehog signalling pathway inhibitor with anticancer properties,[7] and some antibacterial agents, such as gemmacin, gemmacin-B and emmacin, that proved to be active also against multi-drug resistant *Staphylococcus aureus* strains.[8,9]
Moreover, some compounds identified through DOS approach displayed a certain activity against challenging biological targets, for which was difficult or even impossible to find proper leads.[10]
An area in which DOS should find a natural application is fragment-based drug discovery, the branch of drug discovery process in which small fragments that could bind weakly to a biological target are expanded or connected, to ameliorate the interaction with the target, and obtaining potential leads. In this field, better results should be accessed if the library of fragments presents relevant structural diversity, rather than focusing the screening on a specific class of compounds.[1]

[7] B. Z. Stanton, L. F. Peng, N. Maloof, K. Nakai, X. Wang, J. L. Duffner, K. M. Taveras, J. M. Hyman, S. W. Lee, A. N. Koehler, et al., *Nat. Chem. Biol.* **2009**, *5*, 154–156.
[8] G. L. Thomas, R. J. Spandl, F. G. Glansdorp, M. Welch, A. Bender, J. Cockfield, J. A. Lindsay, C. Bryant, D. F. J. Brown, O. Loiseleur, et al., *Angew. Chemie - Int. Ed.* **2008**, *47*, 2808–2812.
[9] A. Robinson, G. L. Thomas, R. J. Spandl, M. Welch, D. R. Spring, *Org. Biomol. Chem.* **2008**, *6*, 2978–2981.
[10] S. Di MiccMiccoo, R. Vitale, M. Pellecchia, M. F. Rega, R. Riva, A. Basso, G. Bifulco, *J. Med. Chem.* **2009**, *52*, 7856 – 7867.

Thus, DOS constitutes a valid approach in chemical biology and drug discovery, being a powerful tool for the identification of potential interesting hit and lead compounds. In the next paragraph, a DOS approach starting from 2-piperidine ethanol will be discussed.

1.2 2-piperidine ethanol: starting point for diversification

2-Piperidine ethanol (**1**) is a piperidine derivative characterised by a stereocenter in α-position to the piperidinic nitrogen and by two functional groups, the amine and the hydroxyl, that constitute two "handles" suitable for further functionalisation of this scaffold (Figure 2).

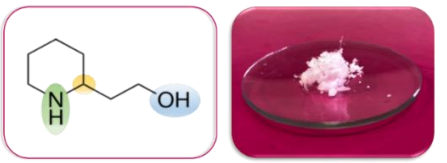

Figure 2. Structure of 2-piperidine ethanol **1**, highlighting the fundamental structural motives. This reagent appears as a fluffy white solid.

This reagent appears as a white solid and it is commercially available as both racemate and pure enantiomers. The racemic form is cheap, and it is synthesised on industrial scale from catalytic hydrogenation of 2-(2-hydroxyethyl)pyridine,[11] while the two enantiomers are definitely more expensive and less available.

Piperidines are common motives in nature and in medicinal chemistry and in the last decades, 2-piperidine ethanol was identified as a promising starting material, for the synthesis of natural products and of pharmacologically interesting compounds.

For example, racemic **1** was exploited as precursor for the synthesis of some patented compounds, such as orexin receptor antagonists,[12] (aryloxyalkyl)piperidines as calcium channel antagonists,[13] sulfonamide derivatives as 5-hydroxytryptamine receptor 7 (5-HT7) antagonists[14] and aminoalcohol-based insect repellent.[15]

[11] M. Freifelder, R. M. Robinson, G. R. Stone, *J. Org. Chem.* **1962**, *27*, 284–286.

[12] P. Gaillard, C. N. Johnson, R. Novelli, R. A. Porter, G. Stemp, K. M. Thewlis, *PCT Int. Appl. Patent* WO 2002089800, 14 November 2002.

[13] T. H. Brown, D. G. Copper, *PCT Int. Appl. Patent* WO 9533723, 14 December 1995.

[14] I. T. Forbes, S. K. Rahman, *PCT Int. Appl. Patent* WO 9749695, 31 December 1997.

[15] a) B. W. Krueger, K. Sasse, F. P. Hoever, G. Nentwig, W. Behrenz, *Eur. Appl. Patent* EP 289842, 9 November 1988. b) He, H.; Zhao, D.; Zhu, Y. Process for Preparation of Insect Repellent Icaridin. Chinese Patent CN 102167681, 31

Enantiopure forms of this versatile scaffold were required to secure the bioactivity of several compounds, including sodium channel inhibitors, TRPV1 receptor activators,[16] non-peptide quinolone GnRH (gonadotropin-releasing hormone) receptor antagonists,[17] gonadotropin-releasing hormone antagonists,[18] selective thrombin inhibitors[19] and cyclin-dependent kinases inhibitors.[20] Interestingly, 2-piperidine ethanol found applications also in industrial chemistry, being used for CO_2 capture[21] and for the synthesis of the catalysts for Ziegler–Natta polymerisation.[22] In general, the racemic compound appears to be the most widely exploited, thanks to its low cost. However, as has been reported in the cited examples, the use of a specific enantiomer is often crucial to obtain compounds characterised by a certain biological activity. Thus, the use of the enantiopure forms of 2-piperidine ethanol is often mandatory. In the next paragraph, the main strategies for their obtainment will be summarised.

[16] S. K. Thompson, T. Priestley, R. A. Smith, A. K. Saha, S. Rudra, A. K. Hajra, D. Chatterjee, C. H. Behrens, Y. He, H. Y.; Li, *PCT Int. Appl. Patent* WO 2012112969, 23 August 2012.

[17] R. J. DeVita, M. T. Goulet, M. J. Wyvratt, M. H. Fisher, J. Lo, Y. T. Yang, K. Cheng, R. G. Smith, *Bioorg. Med. Chem. Lett.* **1999**, *9*, 2621–2624.

[18] J. R. Young, S. X. Huang, I. Chen, T. F. Walsh, R. J. DeVita, M. J. Wyvratt, M. T. Goulet, N. Ren, J. Lo, Y. T. Yang, J. B. Yudkovitz, K. Cheng, R. G. Smith, *Bioorg. Med. Chem. Lett.* **2000,** *10*, 1723–1727.

[19] J. C. Danilewicz, S. M. Abel, A. D. Brown, P. V. Fish, E. Hawkeswood, S. J. Holland, K. James, A. B. McElroy, J. Overington, M. J. Powling, D. J. Rance, *J. Med. Chem.* **2002**, *45*, 2432–2453.

[20] K. Paruch, M. P. Dwyer, C. Alvarez, C. Brown, T. Chan, R. J. Doll, K. Keertikar, C. Knutson, B. McKittrick, J. Rivera, R. Rossman, G. Tucker, T. Fischmann, A. Hruza, V. Madison, A. A. Nomeir, Y. Wang, P. Kirschmeier, E. Lees, D. Parry, N. Sgambellone, W. Seghezzi, L. Schultz, F. Shanahan, D. Wiswell, X. Xu, Q. Zhou, R. A. James, V. M. Paradkar, H. Park, L. R. Rokosz, T. M. Stauffer, T. J. Guzi, *ACS Med. Chem. Lett.* **2010**, *1*, 204–208.

[21] S. Paul, A. K. Ghoshal, B. Mandal, *Ind. Eng. Chem. Res.* **2009**, *48*, 1414–1419.

[22] L. Zhang, Y. Fang, *PCT Int. Appl. Patent* WO 2013063464, 2 May 2013.

1.2.1 Enantiopure 2-Piperidine ethanol: synthesis or resolution

To access the enantiomerically pure forms of 2-piperidine ethanol, two strategies can be considered: the enantioselective synthesis of the desired enantiomer or the resolution of the racemate.[23]

The main drawback of the first approach lies in the necessity of several synthetic steps just to obtain the required **1**-enantiomer, that is usually a precursor in a complex synthesis. On the other hand, racemate resolution takes advantage of the availability and the low cost of racemic 2-piperidine ethanol and should lead to both the enantiomers. This could be an advantage in a DOS approach starting from **1**.

Enantioselective synthesis of 2-piperidine ethanol enantiomers.

In this paragraph some stereoselective strategies for the synthesis of 2-piperidine ethanol (**1**) or of the corresponding *N*-protected aldehyde are reported. From this list is possible to appreciate the variety of approaches that could be exploited to control the configuration of the stereocenter in α-position to the piperidinic nitrogen.

One of the first reported enantioselective syntheses involved an intermolecular cyclisation between a hexa-cyclic nitrone and a chiral allylether. This reaction occurred with *erythro*-selectivity. The enantioselectivity depended on the size of the substituent attached to the allylether stereocenter. The obtained bicyclic compound was then converted into the *N*-Cbz protected 2-piperidineacetaldehyde that was used as fundamental building block for the synthesis of (-)-coniine[24] and (-)-oncinotine,[25] as reported in Scheme 1a. An alternative protocol took advantage of an asymmetric allylation, exploiting a chiral auxiliary, to achieve the total synthesis of the natural product (-)-Stellettamide B.[26]

(*R*)-2-piperidine ethanol was a key intermediate in this synthesis and was obtained in seven steps from glutaric anhydride. The anhydride was converted into a glutarimide, incorporating (*R*)- 2-(1-aminoethyl)phenol as chiral auxiliary. Upon reductive treatment, followed by acidification, a tricyclic *N,O*-acetal was obtained as single diastereomer and was then allylated in the presence of allyltrimethylsilane and titanium tetrachloride. The stereoselective allylation favoured the formation of the desired (*R*)-isomer, with a 6:1 ratio over the (*S*)-one. Methylation of the phenolic hydroxyl group, followed by oxidative cleavage of the double bond to aldehyde, gave

[23] D. Perdicchia, M. Christodoulou, G. Fumagalli, F. Calogero, C. Marucci, D. Passarella, *Int. J. Mol. Sci.* **2016**, *17*, 17.
[24] M. Ito, M. Maeda, C. Kibayashi, *Tetrahedron Lett.* **1992**, *33*, 3765–3768.
[25] H. Ina, M. Ito, C. Kibayashi, *J. Org. Chem.* **1996**, *61*, 1023–1029.
[26] N. Yamazaki, W. Dokoshi, C. Kibayashi, *Org. Lett.* **2001**, *3*, 193–196.

and intermediate that was converted into **(*R*)-1** though hydrogenation. The general synthetic route is reported in Scheme 1b.

An analogous strategy was employed for the synthesis of tetraponerines T3 and T4, in which a diastereoselective allylation in the presence of (S_S)- tert-butanesulfinamide as chiral auxiliary, gave the fundamental (*R*)-*N*-Cbz protected 2-piperidineacetaldehyde building block (Scheme 1c).[27]

A Marouka asymmetric allylation was the key step in the stereoselective synthesis of several piperidine-based alkaloids, such as (+)-coniine, (+)-pseudoconhydrine, and (+)-sedamine. This reaction took advantage of a chiral binol-based titanium catalyst, instead of a chiral auxiliary, and gave an homoallylic alcohol with 96% e.e., that was converted in few steps into (*S*)-*N*-Boc- piperidineacetaldehyde. Form this intermediate the three alkaloids were easily accessed with high enantiopurity (Scheme 1d).[28]

A more concise strategy to afford *N*-Boc- and *N*-Cbz-protected 2-piperdine ethanol involved an intramolecular aza-Michael reaction of carbamates bearing an α,β-unsaturated aldehyde. The reaction was catalysed by Jørgensen's catalyst and gave aldehydes that were reduced to the corresponding *N*-protected versions of 2-piperdine ethanol, with good yield and excellent e.e. (94%, Scheme 1e). These scaffolds were used as precursor for the syntheses of three natural piperidine-alkaloids: (+)-sedamine, (+)-allosedamine, and (+)-coniine.[29] The same reactivity was exploited to synthesize pelletierine and homopipecolic acid.[30] Finally, *N*-Boc-2-piperidineacetaldehyde was obtained taking advantage of the chiral pool concept, starting from a commercially available scaffold directly bearing the stereocenters in the proper configuration. This was the case of *N*-Boc-(*S*)-pipecolic acid, that was converted into the desired aldehyde in four steps, involving the reduction of the carboxylic acid to alcohol, followed by oxidation to aldehyde, Wittig olefination and acid hydrolysis of the enol ether, as reported in Scheme 1f.[31]

[27] I. Bosque, J. C. Gonzalez-Gomez, A. Guijarro, F. Foubelo, M. Yus, *J. Org. Chem.* **2012**, *77*, 10340–10346.
[28] G. Satyalakshmi, K. Suneel, D. B. Shinde, B. Das, *Tetrahedron Asymmetry* **2011**, *22*, 1000–1005.
[29] S. Fustero, D. Jimenez, J. Moscardo, S. Catalan, C. del Pozo, *Org. Lett.* **2007**, *9*, 5283–5286.
[30] E. C. Carlson, L. K. Rathbone, H. Yang, N. D. Collett, R. G. Carter, *J. Org. Chem.* **2008**, *73*, 5155–5158.
[31] R. Singh, G. Panda, *RSC Adv.* **2013**, *3*, 19533–19544.

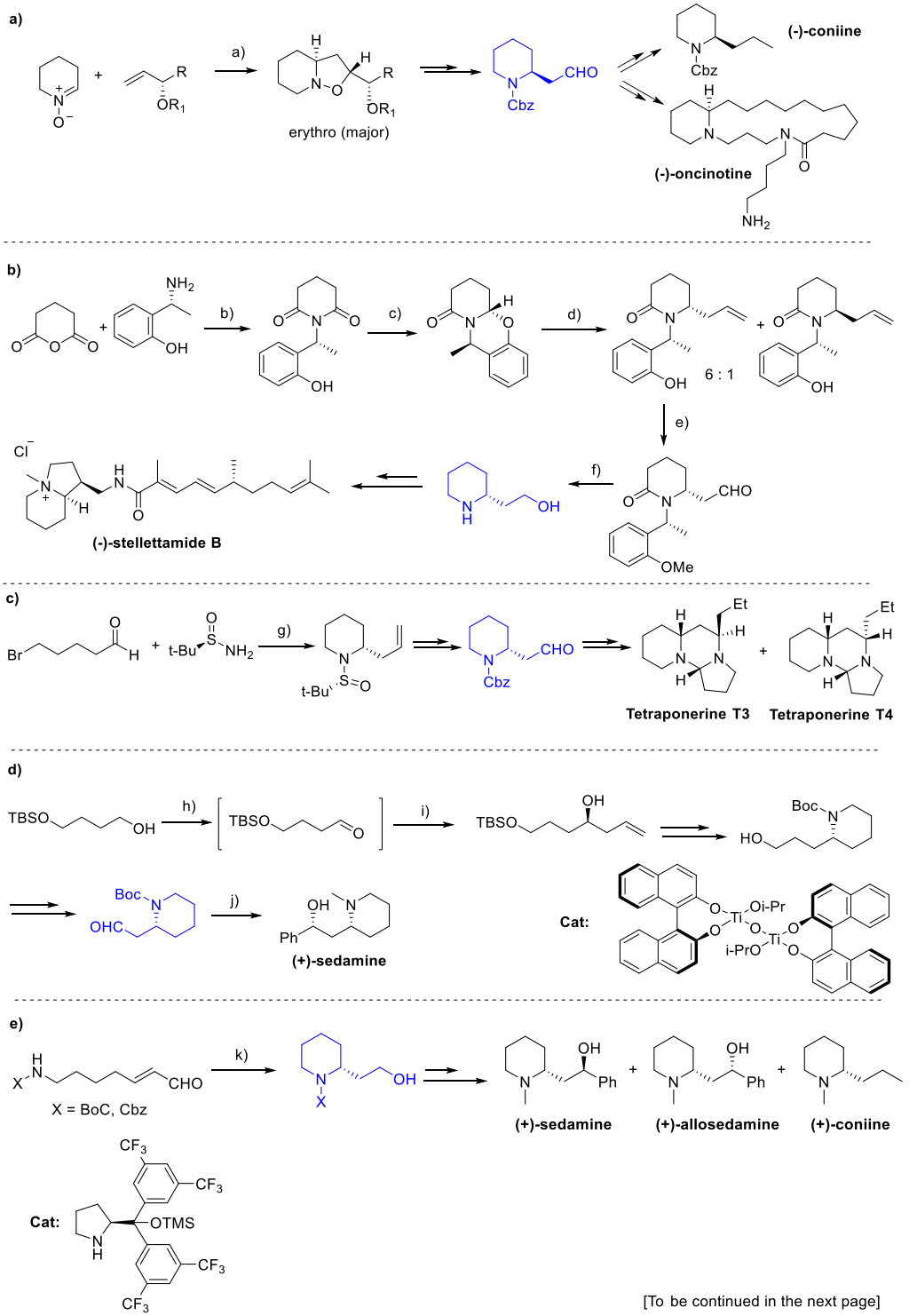

[To be continued in the next page]

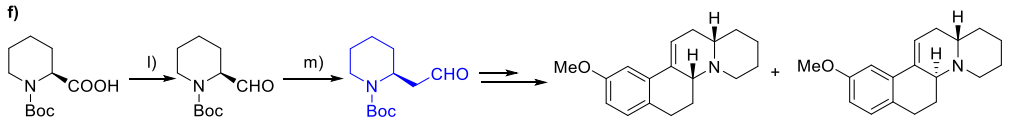

Scheme 1. Summary of the synthetic strategies leading to enantiopure 2-piperdine ethanol or 2-piperidine acetaldehyde. *Reagents and conditions*. a) Toluene, reflux; b) AcCl, toluene, reflux; c) Vitride, toluene, -78 °C, then HCl; d) allyltrimethylsilane, $TiCl_4$, toluene, 50 °C; e) MeI, K_2CO_3, acetone, then OsO_4-$NaIO_4$, dioxane-H_2O; f) $LiAlH_4$, Et_2O, reflux, then H_2/Pd-C, MeOH; g) $Ti(OEt)_4$, In(0), THF, r.t., then allylbromide, KHMDS; h) PCC, CH_2Cl_2, 0°C to rt, 0.5 h, i) Cat, Allyl-$SnBu_3$; CH_2Cl_2, -15°C to 0°C, 72h, j) PhMgBr, THF,-78°C, then $LiAlH_4$, THF, r.t., 8 h; k) Cat., PhCOOH, $CHCl_3$, -50°c, 20h, then $NaBH_4$, MeOH; l) BH_3·THF, THF, 3h, then Swen oxidation; m) $Ph_3P^+CH_2(OMe)Cl^-$, $(Me_3Si)_2NK$, THF, -78°C to r.t., 5h, then HCl, acetone, r.t., 10 min.

Resolution of the racemic mixture.

Chiral resolution of the **1-**racemic mixture was the first method through which one of the two enantiomers was isolated. The protocol involves the formation of diastereomeric salts, from the interaction of the racemate with a chiral acid.

The first attempt to be reported, exploited the recrystallisation of D-10-camphorsulfonate-based diastereomeric salts.[32] However, this resolution proved to be quite challenging, because the racemic salt displayed a strong tendency to separated, rather than the diastereomeric forms. Thus, really slow crystallisation was required, to grow diastereomeric salts large enough to be separated by hand. Moreover, several sequential recrystallisations were required to achieve a satisfactory enantiomeric excess.

This protocol was improved changing the type of resolving agent. Few years ago, two procedures, based on *N*-acetyl-L-leucine[33] and *N*-sulphonyl pyroglutamic acid[34] were patented. In both of the cases, a single crystallisation of the obtained diastereomeric salt afforded good enantiomeric excess (95% and 86%, respectively), further improvable simply with a second crystallisation (to 98% and 99%).

An interesting alternative is constituted by enzymatic kinetic resolution of racemates. This approach has been used to a great extent in the past years, for the resolution of several racemates, and it is based on the ability of enzymes to react preferentially with one of the two enantiomers, usually with high selectivity.[35] However, only few

[32] M. S. Toy, C. C. Price, *J. Am. Chem. Soc.* **1960**, *82*, 2613–2616.
[33] F. X. Chen, M. M. Tamarez, J. Xie, *PCT Int. Appl. Patent* WO 2008021509, 21 February 2008.
[34] R. Callens, R. Gire, C. Pousset, *PCT Int. Appl. Patent* WO 2009080708, 2 July 2009.
[35] a) G. Carrea, S. Riva, *Angew. Chem. Int. Ed.* **2000**, *39*, 2226–2254; b) K. M. Koeller, C. H. Wong, *Nature* **2001**, *409*, 232–240.

procedures are reported on 2-piperidine ethanol, all of them based on the reactivity of the hydroxyl group.

The reason why is related to the high conformational flexibility of the scaffold, that renders the two enantiomers less distinguishable for the enzyme. Moreover, the differentiation involves modification of the primary alcohol, quite fare away from the stereocenter.

Pig liver esterases (PLE) was one of the first enzymes to be exploited for the resolution of racemic piperidines bearing a stereocenter in 2 or 3 position.[36] The enzyme was able to hydrolyse two different racemic esters, **2** and **3,** reported in Scheme 2a.

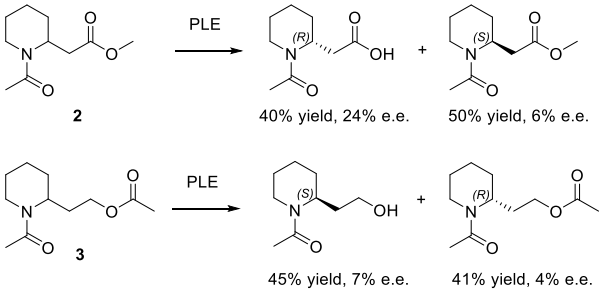

Scheme 2. Enzymatic kinetic resolutions of racemic ester **2** and **3**.

Enzymatic reaction was stopped at 50% conversion, giving enantiomers characterised by low e.e.%.

Few years later, the use of a different enzyme, the so-called porcine pancreas lipase (PPL), was patented by a Japanese group for the resolution of racemic *N*-Fmoc-2-piperdine ethanol (**4**), involving an enzymatic esterification with vinyl acetate (Scheme 3). Unfortunately, the abstract in English tongue didn't report any e.e.% value.

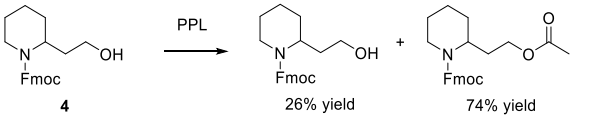

Scheme 3. Enzymatic kinetic resolution of **4**.

Finally, in 2003, an efficient protocol for the obtainment of both the enantiomers with high enantioselectivity was reported by Danieli and co-workers.[37] This work was the result of a systematic screening of 20 different lipases on *N*-protected piperidine ethanol, varying the protecting group (Fmoc, Boc and Cbz).

[36] E. J. Toone, J. B. Jones, *Can. J. Chem.* **1987**, *65*, 2722–2726

[37] M. Angoli, A. Barilli, G. Lesma, D. Passarella, S. Riva, A. Silvani, B. Danieli, *J. Org. Chem.* **2003**, *68*, 9525–9527.

The best results were obtained with Boc, performing the enzymatic reaction at 45°C in an organic solvent such as methyl tert-butyl ether and hexane.

Interestingly two enzymes, lipase PS and porcine pancreatic lipases (PLL) displayed a complementary enantioselectivity, favouring the (*R*)- and (*S*)- enantiomers, respectively.

Therefore, the optimised protocol reported in Scheme 4 was developed, to resolved 2-piperidine ethanol in its two enantiomers, with final 90% e.e. for the (*R*)-one and 95% e.e. for the (*S*)-one.

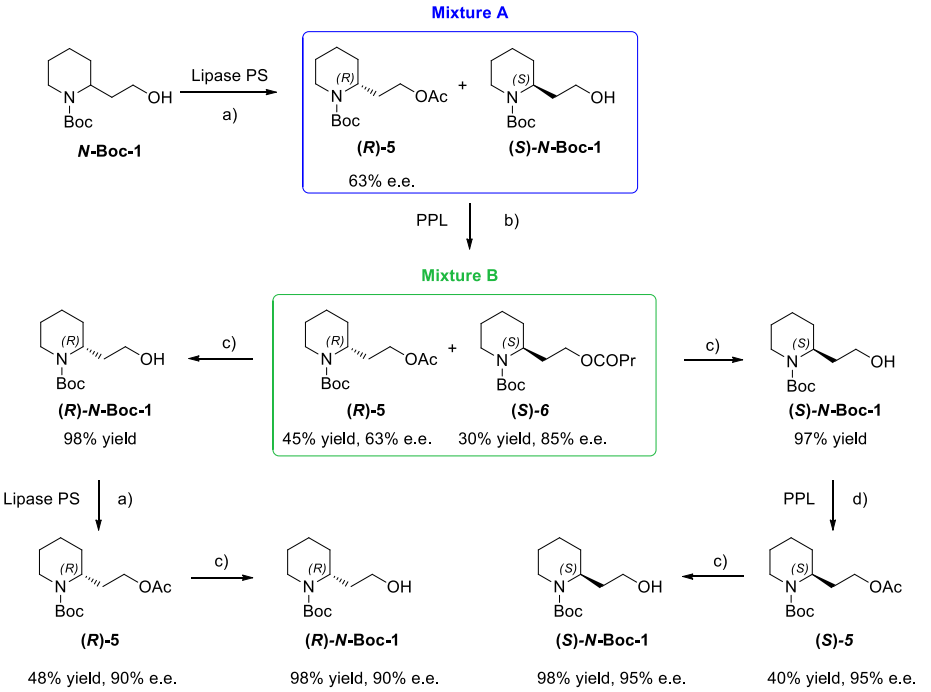

Scheme 4. Optimised protocol for 2-piperidine ethanol enzymatic kinetic resolution. (a) $AcOCH{=}CH_2$, hexane, 20°C, 190 min (45%); (b) $PrCOOCH{=}CH_2$, MTBE, 20°C, 11.5 h (30%), flash chromatography (AcOEt-hexane 1:9); (c) CH_3OH, Na_2CO_3; and (d) $AcOCH{=}CH_2$, MTBE, 20 °C, 46 h (48%).

The racemic *N*-Boc-2-piperidine ethanol was acetylated in the presence of Lipase PS and vinylacetate, stopping the reaction at 50% conversion, to give a mixture (**A**), in which the (*R*)-enantiomer was esterified to **(*R*)-5** and (*S*)-one remained unreacted. Crude mixture **A** was butanoylated by the PPL enzyme, selective toward (*S*)-enantiomer. In this way, mixture **B**, composed by **(*R*)-5** (63% e.e.) and **(*S*)-6** (85% e.e.) and unreacted, almost racemic *N*-Boc-**1** was obtained. The three compounds were easily separated by flash chromatography. Esters **(*R*)-5** and **(*S*)-6** were hydrolysed to

(*R*)-1 and **(*S*)-1**. To enhance the quite low enantioselectivity given by the two enzymes, the two compounds underwent independently a second sequence of enzymatic acetylations, in which **(*R*)-1** reacted with lipase PS and **(*S*)-1** with PPL. Hydrolyses of the two esters **(*R*)-6** and **(*S*)-6** afforded the two desired enantiomers of 2-piperidine ethanol in high enantiopurity (90% and 95% e.e. respectively).
Notably, the protocol is scalable on gram-scale.

1.2.2 Diversity-oriented synthesis from 2-piperidine ethanol.

With both of *N*-Boc-2-piperidine ethanol enantiomers accessible in high enantiopurity and considerable amount, several syntheses of natural and synthetic products were completed in the last years in the Passarella's research groups, demonstrating the versatility of 2-piperidine ethanol to achieve high chemical diversity.
The amine and hydroxyl functionalities can be efficiently elaborated in different ways, and the molecule contains a piperidine moiety that is a common motif in medicinal chemistry. These features render the 2-piperidine ethanol an ideal precursor for a diversity-oriented approach aimed at synthesizing potential bioactive compounds.
In this field, two particular derivatives of **1** proved to be highly versatile: the *N*-Boc-protected *2*-piperidineacetaldehyde **7** and the *N*-Boc-protected 2-allyl-piperidine **8**. **7** derives by the oxidation of *N*-Boc-**1**, under Swern conditions or using Dess-Martin Periodinane (DMP). Wittig olefination of aldehyde **7**, gave the allyl-derivative **8**. Thus, **1**, **7** and **8** appeared as the good starting points for a diversity-oriented approach aimed at the synthesis of piperidine-based compounds. In this context, the results achieved in the last years are summarised in Scheme 5 and illustrated in detail in the next paragraphs.

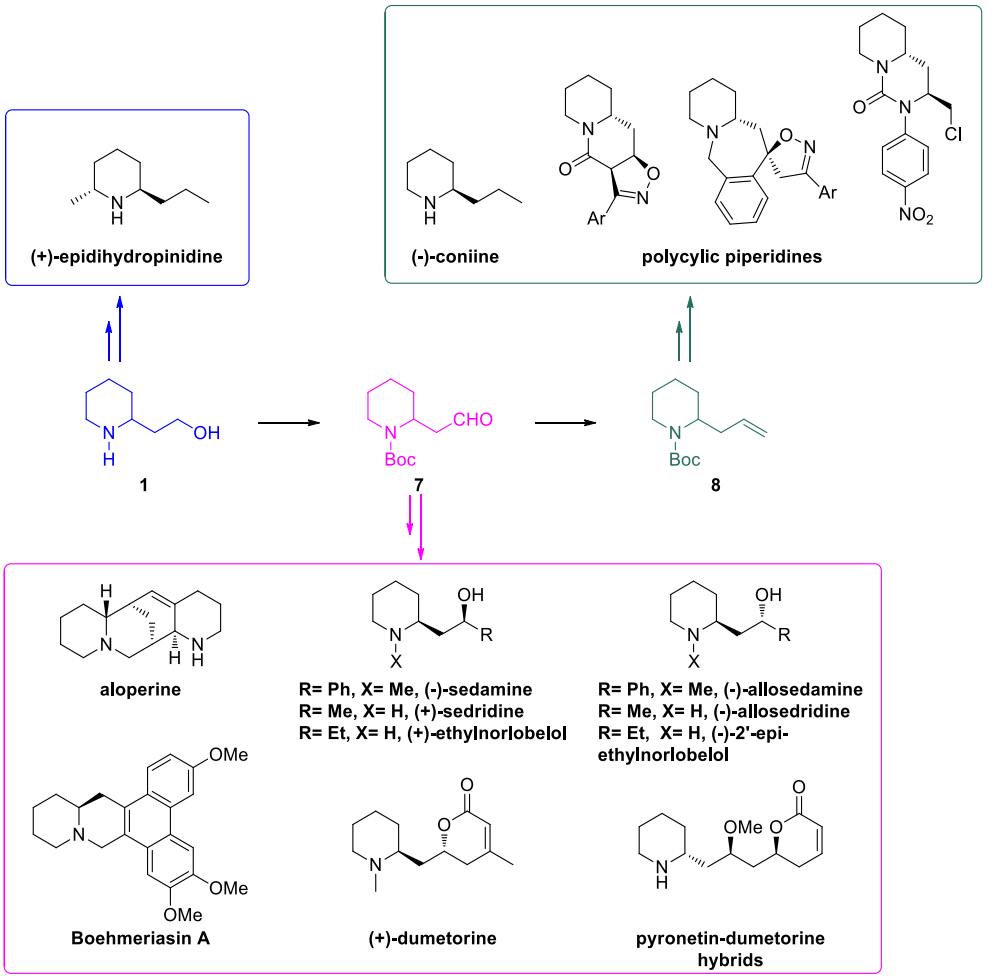

Scheme 5. Summary of the piperidine-based derivatives previously synthesised in our research group.

Overview of the previously synthesised derivatives from 2-piperidine ethanol 1.

- Synthesis of (-)- and (+)-epidihydropinidine

(+)-epidihydropinidine is the major alkaloid present in the Norwegian spruce *Picea abiens* Karsten. The (-)-enantiomer is rarer in nature, but both these compounds are found in several *Pinus* species. Their common scaffold is characterised by a *trans*-2,6-disubstituted piperidine core, in which the two substituents are a methyl and a propyl groups. Thus, while the latter could derive from the side chain of 2-piperidine ethanol, exploiting an oxidation-Wittig olefination-hydrogenation sequence, the methyl substituent should be introduced *ex-novo*. To this extent, a Beak's α-

lithiation/alkylation of *N*-Boc-**1** was envisaged. The choice of the proper *N*-Boc-**1** enantiomer, obtained accordingly the enzymatic kinetic resolution protocol (Scheme 4), allowed the synthesis of both epidihydropinidine enantiomers. As reported in Scheme 6, after protection of the hydroxyl group of *N*-Boc-**1**, the introduction of the methyl group was prioritised over the elaboration of the side chain. The precursor underwent a selective α –deprotonation, in the presence of s-BuLi and TMEDA. Treatment with dimethylsulfate provide the desired methylated product. NMR analysis confirmed the trans-configuration of the two stereocenters, coherently with a transition state in which the Boc-protecting group chelate the lithium cation. Notably, the presence of a bulky silylether on the side chain, prevented interference with this reaction. After silylether cleavage, the hydroxyl group was oxidised to aldehyde. The side chain was extended of one carbon atom through a Wittig olefination, affording an alkene that was reduced under catalytic hydrogenation conditions. Removal of the Boc protecting group provided the final compound.

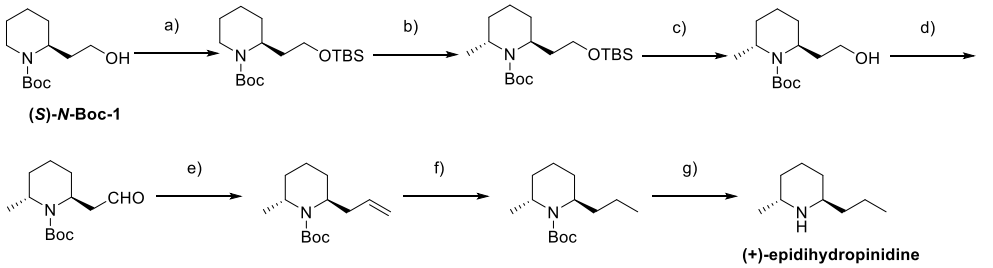

Scheme 6. *Reagents and conditions*: a) TBSCl, imidazole, CH_2Cl_2; b) TMEDA, s-BuLi, Et_2O, -78 °C, $MeSO_4$; c) Na_2CO_3, MeOH; (d) Dess–Martin Periodinane (DMP), CH_2Cl_2; e) $Ph_3P{=}CH_2$, THF; f) Pd/C 10%wt., H_2, MeOH; g) TFA, CH_2Cl_2.

Overview of the previously synthesised derivatives from aldehyde 7.

- Synthesis of (±)-aloperine and (±)-6-*epi*-aloperine from racemic **7.**

Aloperine is a natural lupinine-alkaloid, isolated for the first time in 1935 form *Sophora* and *Leptorhabdos parviflor* Benth. These plants are exploited in the traditional Chinese medicine, on the basis of cardiovascular, anti-inflammatory and antiallergic properties.

To achieve the total synthesis of the racemic form of aloperine, a protocol based on an efficient intramolecular Diels-Alder reaction and an aza-annulation was developed, as reported in Scheme **7a**.

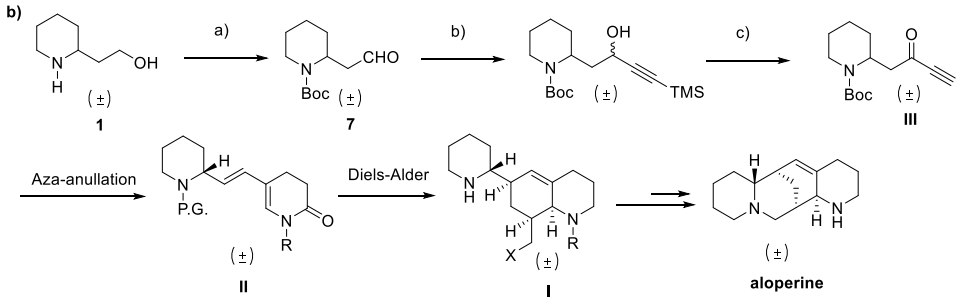

Scheme 7. Synthetic approach giving racemic aloperine (a). Synthetic route converting **7** into key intermediate **III** (b). *Reagent and conditions*. a) $(Boc)_2O$, NaOH, t-BuOH (86%); Dess-Martin periodinane, CH_2Cl_2 (89%); (b) $BrMgCCSiMe_3$, -78 °C, THF (86%); (c) $(COCl)_2$, DMSO, TEA (87%); TBAF, THF (84%).

The key intermediate of this synthesis was **III**, obtained from aldehyde **7** in two steps, involving alkylation and oxidation of the alcohol. An aza-annulation of the acetylenic ketone **III**, in the presence of acryloyl chloride and benzyl-amine led to compound **II.** An intermolecular Diels-Alder reaction of **II** with methyl acrylate gave the octahydroquinoline compound **I**, that was finally converted in the racemic aloperine, *via* nucleophilic substitution.

It is noteworthy that the Diels-Alder reaction gave two diastereomers, epimers at the stereocenter in α-position to the piperidinic nitrogen. The same synthetic route was applied also to the second epimer, affording racemic 6-*epi*-aloperine.

Moreover, few years later, the synthesis of enantiopure (+)-aloperine (the natural occurring product) was completed, taking advantage of the (*R*)-*N*-Boc-**1**, obtained through the enzymatic kinetic resolution, reported in Scheme 4.[38]

- Enantioselective synthesis of *Sedum* alkaloids, boehmeriasin A, dumetorine and pironetin-dumetorine hybrids.

Enantiopure aldehyde **7** was exploited to a great extent, for the synthesis of several natural products, such as *Sedum*-alkaloids, Boehmeriasin A, dumetorine and pironetin-dumetorine hybrids compounds. As appreciable in Scheme 8, all these syntheses involved as key step the alkylation of **7**, using a Grignard reagent or a stereoselective allylating agent. *Sedum alkaloids* are family of natural products, found in several plants. One example is *Lobelia inflata*, whose extract has been used in traditional medicine, for the treatment of respiratory diseases. Among the members of this family, sedamine, allosedamine, sedridine, allosedridine, ethylnorlobelol and

[38] A. Barilli, F. Belinghieri, D. Passarella, G. Lesma, S. Riva, A. Silvani, B. Danieli, *Tetrahedron Asymmetry* **2004**, *15*, 2921–2925.

20-epi-ethylnorlobelol, shares a piperidinic core. Thus, their syntheses (including the different enantiomers) could be envisaged starting from the proper enantiomer of **7**, obtained through enzymatic kinetic resolution (Scheme 4).[39]

Each enantiomer of aldehyde **7** underwent the same synthetic pathway, leading to the formation of enantiomeric final products. Alkylation of **7** with phenylmagnesium bromide afforded two diastereomers. They were separated through column chromatography, and each one was treated with $LiAlH_4$, to directly converted the Boc protecting group to methyl. In this way, (-)-sedamine and (-)-allosedamine were obtained from (*S*)-aldehyde and (+)-enantiomers from (*R*)-aldehyde.

On the other hand, alkylation of **(*S*)- 7** with methylmagnesium bromide afforded (+)-sedridine and (-)-allosedridine, after cleavage of the Boc-protecting group in the presence of TFA. The corresponding enantiomers were synthesised from (*R*)-aldehyde. The same procedure, but using ethylmagnesium bromide and **(*S*)- 7**, gave (+)-ethylnorlobelol and (-)-20-e pi-ethylnorlobelol.

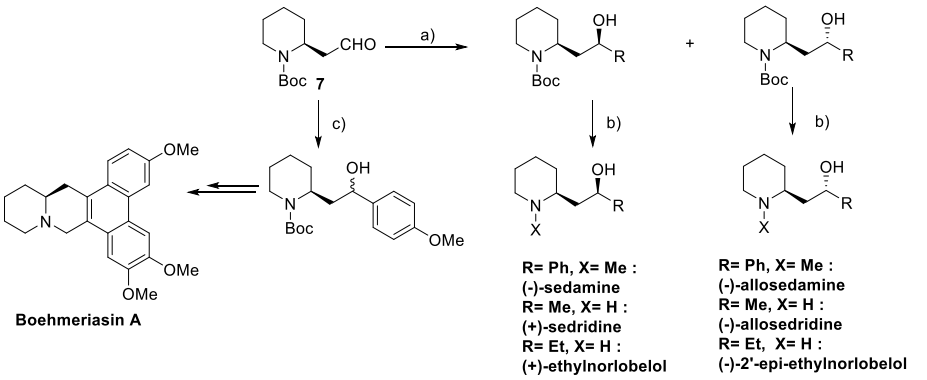

Scheme 8. *Reagents and conditions*. a) Grignard reagent, THF, -20 °C; b) $LiAlH_4$, THF, reflux (for (-)-sedamine and (-)-allosedamine); TFA, CH_2Cl_2 for (+)-sedridine, (-)-allosedridine, (+)-ethylnorlobelol and (-)-2'-epi-ethylnorlobelol (the same synthetic route, performed on (*R*)-*N*-Boc-**1**, gave the corresponding enantiomers). c) p-methoxyphenylmagnesium bromide, THF.

A similar strategy was applied to the total synthesis of Boehmeriasin A, a phenanthroquinolizidine alkaloid extracted from *Boehmeria siamensis* Craib, characterised by interesting cytotoxic activity against different cancer cells lines.[40]

[39] D. Passarella, A. Barilli, F. Belinghieri, P. Fassi, S. Riva, A. Sacchetti, A. Silvani, B. Danieli, *Tetrahedron Asymmetry* **2005**, *16*, 2225–2229.

[40] M. S. Christodoulou, F. Calogero, M. Baumann, A. N. García-Argáez, S. Pieraccini, M. Sironi, F. Dapiaggi, R. Bucci, G. Broggini, S. Gazzola, et al., *Eur. J. Med. Chem.* **2015**, *92*, 766–775.

Also in this case aldehyde **(*S*)-7** was alkylated with a Grignard reagent (p-methoxyphenylmagnesium bromide), affording two diastereomeric alcohols that were oxidised to the corresponding ketone. After the cleavage of the Boc protecting group the amine was condensed with 2-bromo-4,5- dimethoxyphenylacetic acid. An intramolecular aldol- type condensation of the obtained intermediate, in the presence of KOH, furnished a 1:1 mixture of atropisomers. A palladium-catalysed coupling afforded the fundamental phenanthroquinolizidine scaffold and reduction of the lactam in the presence of $LiAlH_4$ led to the desired natural product, as reported in Scheme 9.

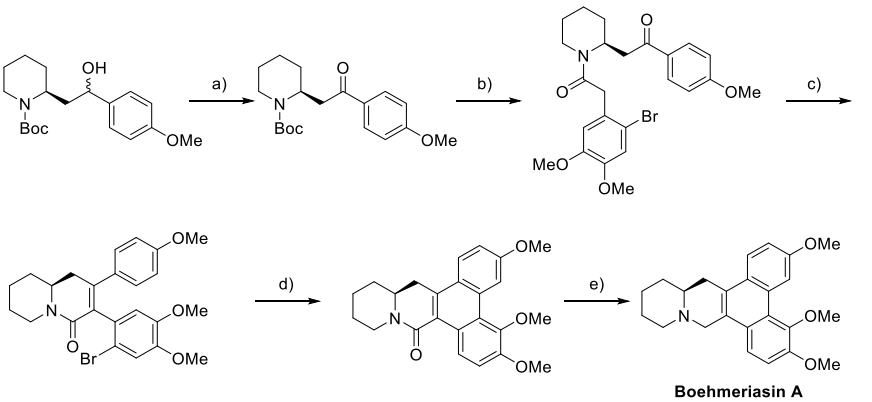

Scheme 9. *Reagents and conditions*. a) DMP, CH_2Cl_2; b) i. TMSCl, MeOH; ii. 2-bromo-4,5-dimethoxyphenylacetic acid, DIPEA, HATU, THF; c) KOH, EtOH; d) $Pd(OAc)_2$, K_2CO_3, 2'-(diphenylphosphino)-*N,N'*-dimethyl- (1,1'-biphenyl)-2-amine, DMA; e) $LiAlH_4$, THF.

Finally, aldehyde **7** proved to be the perfect precursor for the synthesis of dumetorines, including the natural alkaloid (+)-dumetorine, its enantiomer[41] and a family of pironetin-dumetorine hybrids.[42]

For what concern the synthesis of (+)-dumetorine, (*S*)-aldehyde was alkylated in a stereoselective fashion, through an asymmetric allylboration reaction with B-allyl-diisopinocampheylborane (obtained from (+)-B -methoxydiisopinocampheylborane and methylallyl-magnesium bromide). The desired homoallylic alcohol was obtained with high selectivity (*d.e.* >95%) and was acylated with the commercially available acryloyl chloride. Ring closing metathesis afforded the desired lactone. Cleavage of the Boc protecting group gave the desired amine in low yield, and the formation of

[41] D. Passarella, S. Riva, G. Grieco, F. Cavallo, B. Checa, F. Arioli, E. Riva, D. Comi, B. Danieli, *Tetrahedron Asymmetry* **2009**, *20*, 192–197.

[42] C. Marucci, M. S. Christodoulou, S. Pieraccini, M. Sironi, F. Dapiaggi, D. Cartelli, A. M. Calogero, G. Cappelletti, C. Vilanova, S. Gazzola, G. Broggini, D. Passarella, *European J. Org. Chem.* **2016**, *2016*, 2029–2036.

the tricyclic compound resulting from the Michael addition on the α,β-unsaturated carbonyl resulted to be favoured. However, the obtained free amide underwent a reductive amination in the presence of formaldehyde and $NaBH_3CN$, leading to the natural (+)-dumetorine, albeit in low yield. The inconvenient of the competitive Michael addition was avoided adapting the synthetic sequence to flow-chemistry.[43] (-)-dumetorine was obtained in the same way, starting from (*R*)-aldehyde (Scheme 10).

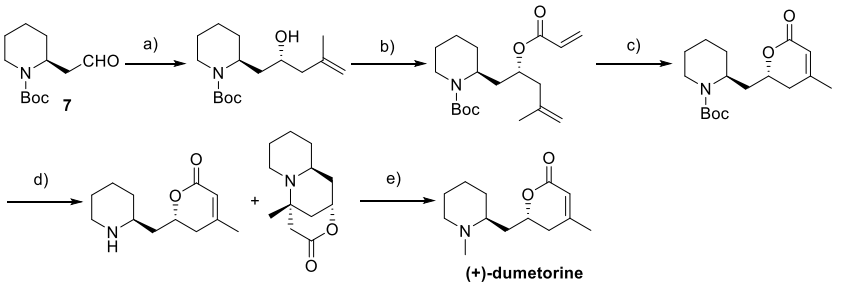

Scheme 10. *Reagents and conditions*. a) (+)-B -methoxydiisopinocampheylborane, methylallyl-magnesium bromide, THF, -78°C; b) acryloyl chloride, DIPEA, CH_2Cl_2, c) 2nd generation Grubbs cat., CH_2Cl_2 40 °C; (d) TFA, CH_2Cl_2; (e) CH_2O, $NaBH_3CN$, CH_3CN.

Then, a similar approach was exploited for the synthesis of hybrids compounds, combination the structure of the natural products (+)-dumetorine and (-)-pironetin. The idea was to develop a class of possible α-tubulin binders, considering that pironetin is one of the few known compounds able to bind α-tubulin. In this case, aldehyde **7** was used in its racemic form. In fact, the general aim was to synthesize all the eight possible stereoisomeric hybrids: to this extent, the control over the stereochemical outcome through an asymmetric Brown's allylation resulted to be more convenient than the use of an enantiopure aldehyde.

The resulting diastereomeric homoallylic alcohols were separated and all of them underwent the same synthetic route, involving methylation and oxidative cleavage, to obtain another aldehyde, that was allylated in the same way. At this point, the synthesis reflected the protocol exploited for (+)-dumetorine: the alcohol was acylated in the presence of acryloyl chloride and a ring closing metathesis afforded the α,β-unsaturated lactone typical of pironetin. The Boc-protecting group was cleaved in the presence of TFA (Scheme 11). In this case no competitive Michael addition occurred, considering that the formation of a less favoured 8-membered ring

[43] E. Riva, A. Rencurosi, S. Gagliardi, D. Passarella, M. Martinelli, *Chem. - A Eur. J.* **2011**, *17*, 6221–6226.

would have been involved. The choice of the chiral allylating agent allowed the obtainment of all the eight possible stereoisomers.

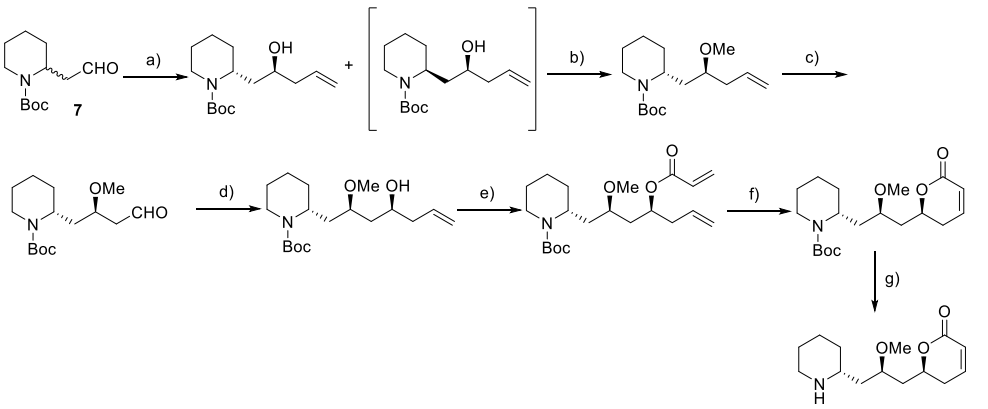

Scheme 11. *Reagents and conditions*. a) allyl-BIpc$_2$ [from (–)-DIP-Cl and allylmagnesium bromide], THF; b) MeI, NaH, THF; c) O_3, CH_2Cl_2, PPh_3; d) allyl-BIpc$_2$ [from (–)-DIP-Cl and allylmagnesium bromide], THF; e) acryloyl chloride, TEA, CH_2Cl_2; f) 2nd generation Grubbs cat., CH_2Cl_2 40 °C; g) TFA, CH_2Cl_2.

Biological tests revealed that the eight hybrid stereoisomers influenced tubulin polymerisation, albeit with modest inhibition properties. However, the presence of the piperidine moiety, suggested the possibility of use it as an anchor point, for the synthesis of bivalent compounds. The efforts in this field are reported in Chapter 5.

Overview of the previously synthesised derivatives from 2-allyl-piperidine 8.

- Synthesis of (-)-coniine and polycyclic piperidine derivatives.

Finally, starting from 2-allyl-piperidine **8,** the syntheses of the natural alkaloid (-)-coniine and of three polycyclic scaffolds, characterised by increased structural complexity, were successfully accomplished (Scheme 12). The synthesis of (-)-coniine required only two steps, namely the hydrogenation of the double bond, followed by cleavage of the protecting group.[37]

For the obtainment of the polycyclic compounds, Boc-protecting group was cleaved, and the piperidinic nitrogen was functionalised with aryl or alkenyl moiety, then, exploiting the allyl handle already present in intermediate **8**, structural diversification was achieved through coupling or metathesis reactions.[44]

[44] E. Borsini, G. Broggini, F. Colombo, M. Khansaa, A. Fasana, S. Galli, D. Passarella, E. Riva, S. Riva, *Tetrahedron Asymmetry* **2011**, *22*, 264–269.

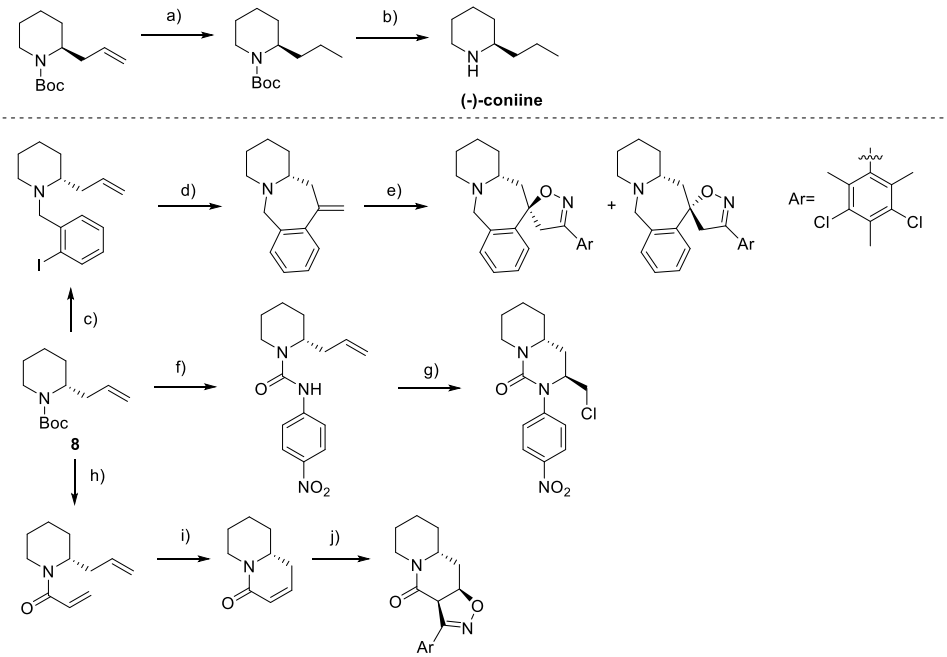

Scheme 12. *Reagents and conditions*. a) H_2, $Pd(OH)_2$; b) TFA, CH_2Cl_2, c) i. TFA, CH_2Cl_2; ii. 2-iodobenzyl bromide, K_2CO_3, toluene, 70°C; d) $Pd(PPh_3)_4$ 10%, TEA, CH_3CN, reflux; e) 3,5-dichloro-2,4,6-trimethylbenzonitriloxide, toluene, reflux; f) i. TFA, CH_2Cl_2; ii. 4-NO_2-phenyl isocyanate, toluene, reflux; g) $Pd(CH_3CN)_2Cl_2$ 5%, $CuCl_2$, DMF, 100°C; h) i. TFA, CH_2Cl_2; ii. acryloyl chloride, TEA, CH_2Cl_2; i) 2nd generation Grubbs cat., CH_2Cl_2 40 °C; j) 4-NO_2-phenyl isocyanate, toluene, reflux.

1.3. DOS from 2-piperidine ethanol: exploration of new portions of the chemical space.

The demonstrated versatility of 2-piperidine ethanol and its derivatives **7** and **8**, prompted us to consider the exploration of new regions of the surrounding chemical space. As already mentioned, piperidine is a common structural motif in nature and in several bioactive compounds. Thus, the further diversification of 2-piperidine ethanol assumes an importance non only from a pure synthetic point of view, but also as a tool to access compounds that could present interesting biological activities.

Scaffolds **9** and **10**, already exploited for the synthesis of the hybrid compounds cited in the previous paragraph,[42] appeared as new promising starting points to achieve structural diversification. As appreciable in Scheme 13, they were used to a great extent for the synthesis of four new classes of piperidine-derivatives, that were the focus of this thesis.

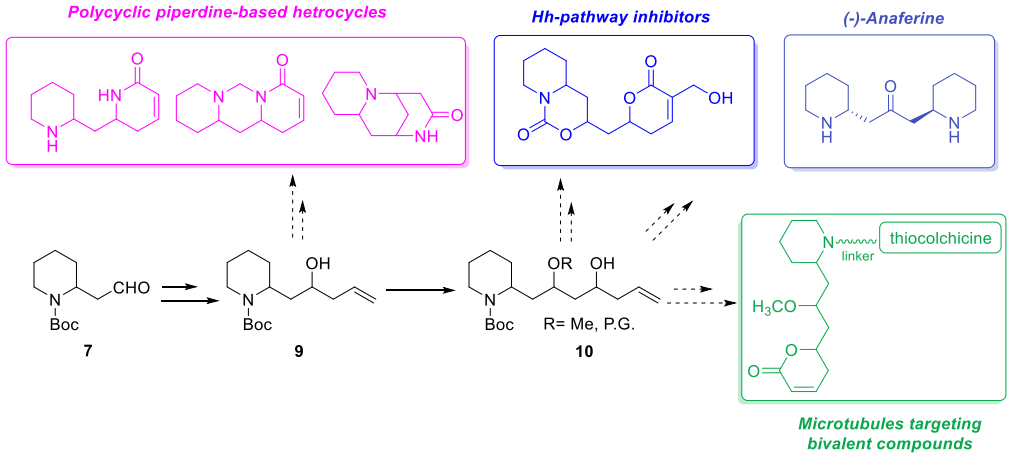

Scheme 13. Structures of the new compounds resulting from the expansion of the DOS-approach from 2-piperidine ethanol.

1.3.1 Planning of library expansion

A small library of novel polycyclic piperidine-based heterocycles, characterised by three different scaffolds, was afforded from **9**, upon interconversion of the homo-allylic alcohol into the corresponding amine through a Mitsunobu-Staudinger reduction sequence. The amine would be elaborated into a fundamental key lactam, reported in Scheme 14A, that should be converted into highly differentiated scaffolds under acidic or Eschweiler-Clarke conditions, depending on lactam the stereochemistry.

Scaffold **10** derives from **9**, through oxidative cleavage of the double bond, followed by allylation of the resulting aldehyde. In this way, a new homoallylic alcohol, connected to the piperidine through a 2-hydroxylpropane linker, was obtained.

As reported in the synthesis of pironetin-dumetorine hybrids, homoallylic alcohol **10** can be converted into an α,β-unsaturated lactone, which is a key element in several bioactive compounds. Thus, this prompted us to envisage the synthesis of a new class of Hedgehog signalling pathway inhibitors, for applications in anticancer therapy. To this extent, the structure of the lactone was slightly modified, and the piperdine moiety was elaborated into a bicyclic carbamate, through intramolecular condensation with the hydroxyl group on the propane linker (Scheme 14B).

Interconversion of scaffold **10** into an homoallylic amine, exploiting the same Mitsunobu-Staudinger approach envisaged for the synthesis of the polycyclic piperidine-based heterocycles, would provide an interesting amine-containing intermediate, that could be converted into a lactam, as reported in Scheme 14A. A scaffold like that, containing two six membered nitrogen-containing rings, connected by a 2-hydroxypropane linker, sounded quite familiar to us. We realised that our DOS approach led us to a known natural product, (-)-anaferine, that can be obtained reducing the unsaturated lactam and oxidizing the hydroxyl group to ketone (Scheme 14C).

Finally, the pironetin-dumetorine hybrids previously synthesised in our laboratory from 2-piperidine ethanol, were considered as building blocks for the synthesis of microtubules-targeting bivalent compounds. In fact, we realised that the piperidinic nitrogen could have been exploited as a good anchor point, for the attachment of a linker and another tubulin binder. In this way two families of bivalent compound, bearing two different type of linkers were accessed (Scheme 14D).

The syntheses of all the four classes of derivatives will be disclosed in detail in the next chapters.

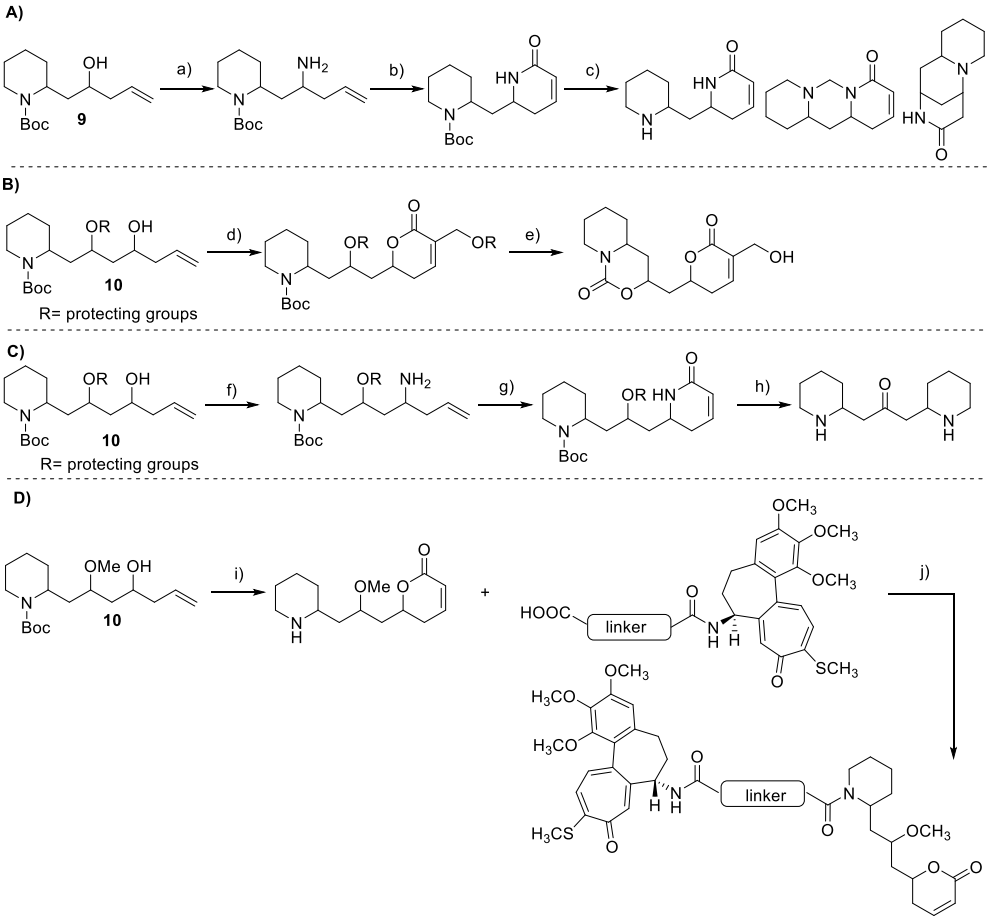

Scheme 14. Forward synthetic approach leading to the four new classes of pipeperidine-based derivatives. a) Mitsunobu/Staudinger red.; b) acylation, ring closing metathesis (RCM); c) H^+ or Eschweiler-Clarke; d) esterification, RCM; e) protecting groups cleavage, carbamate formation; f) Mitsunobu/Staudinger red.; g) acylation, RCM; h) lactam reduction, alcohol oxidation, protecting groups cleavage; i) acylation, RCM; j) coupling.

2. Synthesis of new piperidine-based heterocycles

2.1 Planning of the synthesis

The first efforts in the synthesis of new piperidine derivatives, starting from 2-piperidine ethanol, were focused on the obtainment of polyheterocyclic compounds, presenting scaffolds resembling some classes of natural products, such as some lupin and lycopodium alkaloids.[45]

A detailed forward-synthetic pathway is depicted in Scheme 15.

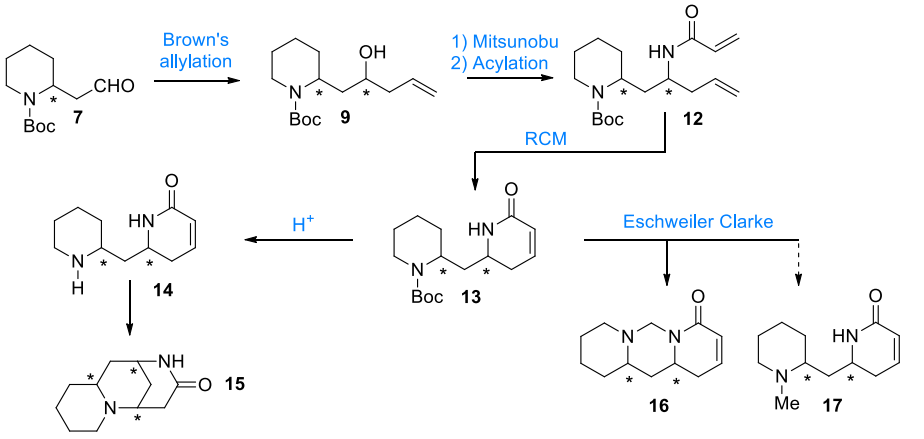

Scheme 15. Forward-synthetic pathway for the obtainment of four new heterocyclic scaffolds.

The element of novelty compared with the previously reported syntheses was a functional group interconversion from alcohol to amine. In fact, we planned to convert the homoallylic alcohol **9** into the corresponding azide, taking advantage of a Mitsunobu reaction in the presence of diphenylphosphoryl azide, followed by a Staudinger reduction. Then, an acylation, followed by a ring closing metathesis would convert the amine into the cyclic lactam **13**. Intermediate **13** appeared as an appealing starting point to achieve a further structural diversification, exploring in this way new portions of the chemical space.

In fact, the cleavage of the Boc protecting group in acid environment, would lead to intermediate **14**, that could eventually undergo a collateral intramolecular aza-Michael addition, leading to a thermodynamically stable 6-membered ring in scaffold **15**. On the other hand, an Eschweiler-Clarke reaction, performed directly on **13**, would give an iminium intermediate, that could be transformed into two different scaffolds: a reduction by hydride transfer, as in the "classic" Eschweiler-Clarke reaction, should lead to the *N*-methyl derivative **17**. However, the nucleophilic lactam hydrogen could

[45] E. Bonandi, P. Marzullo, F. Foschi, D. Perdicchia, L. Lo Presti, M. Sironi, S. Pieraccini, G. Gambacorta, J. Saupe, L. Dalla Via, D. Passarella. *European J. Org. Chem.* **2019**, 5–12.

attack the iminium salt as well, in an intramolecular fashion, affording the octahydrodipyrido pyrimidone **16**.

It is noteworthy that the fundamental building block **13** contains two stereocenters and hence can exist as four stereoisomers. Considering that a protocol for the stereoselective synthesis of all the stereoisomers of alcohol **9** was previously developed in our laboratory,[42] the stereodivergent synthesis of all the possible stereoisomers of scaffolds (**14-16**) was envisaged.

2.2 Synthetic efforts

In detail, the synthesis started with the racemic aldehyde **7**, obtained from the 2-piperidine ethanol as reported previously.[44] Through a highly stereoselective Brown's asymmetric allylboration,[46,47] performed using both the enantiomers of *B*-allyl di-isopinocampheylborane, all the four stereoisomers of the homo- allylic alcohol **9** were accessed. In particular, the diastereomeric alcohols **9a** and **9b** were obtained reacting the aldehyde with (–)- *B* -allyl diisopinocampheylborane (generated in situ by the reaction between (-)-di-isopinocampheylboron chloride (DIP-Cl) and allylmagnesium bromide), and were separated through column chromatography (*d.r.* ≈ 1:1).

Alcohols **9c** and **9d** were obtained in the same conditions and in similar diastereomeric ratio, simply using (+)-*B* -allyl diisopinocampheylborane. (Scheme 16).

Considering the aim of obtaining all the possible stereoisomers, the employment of an asymmetric allylation protocol on a racemic aldehyde, was the optimal solution. In this way, performing two parallel reactions on racemic **7**, with the two enantiomeric with *B* -allyl diisopinocampheylboranes, compounds **9a-d** were accessed, simply separating the two diastereomeric alcohols in each reaction. On the other hand, the use of enantiopure aldehydes, obtained after the enzymatic kinetic resolution of 2-piperidine ethanol, would have required four parallel Brown's allylations to give compounds **9a-d**.

[46] H. C. Brown, P. K. Jadhav, *J. Am. Chem. Soc.* **1983**, *105*, 2092-2093.

[47] V. Ramachandran, G. M. Chen, H. C. Brown, *Tetrahedron Lett.* **1997***, 38,* 2417–2420.

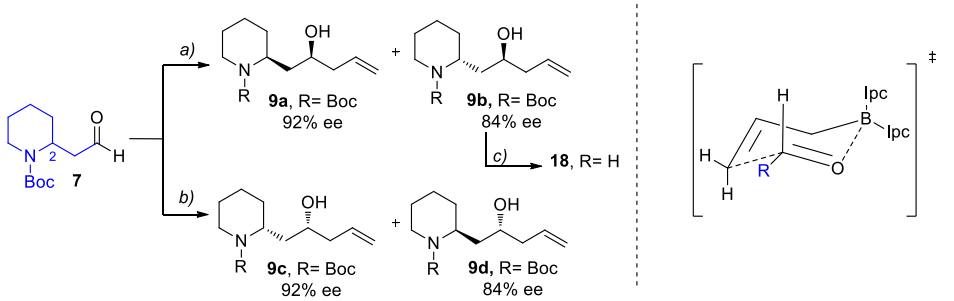

Scheme 16. *Reagent and conditions*. a) (–)-allyl-BIpc$_2$ (from (–)-DIP-Cl and allyl- magnesium bromide), THF, –78 °C to r.t., 4 h, 90 % overall yield; b) (+)-allyl-BIpc$_2$ (from (+)-DIP-Cl and allylmagnesium bromide), THF, –78 °C to r.t., 4 h, 88 % overall yield; c) TFA, CH_2Cl_2, 0 °C to r.t., 18 h, yield: 90 %. On the right, the chair like transition state, in which the aldehyde bulkier substituent occupies a pseudo-equatorial position, is represented. The intrinsic chirality of the Ipc substitutents determines on which of the aldehyde faces the alkylation occurs.

The relative *syn*/*anti* configuration was assigned on the basis of X-rays analysis, performed on one of the anti-isomers, after the cleavage of the Boc protecting group, leading to **18** (Scheme 16). In this way the relative (*S, R*) configuration was secured (Figure 3).

CCDC 1891130 contains the supplementary crystallographic data. These data can be obtained free of charge from The Cambridge Crystallographic Data Centre via www.ccdc.cam.ac.uk/structures.

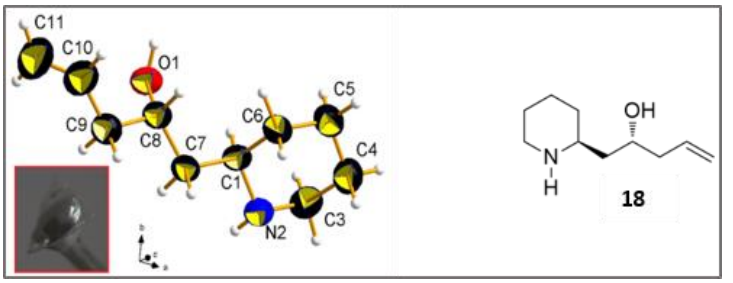

Figure 3. Asymmetric unit of **18** at room temperature as determined from the X-ray diffraction experiment, with the atom-numbering scheme. Thermal ellipsoids of non-H atoms were drawn at the 50 % probability level. Inset: crystal of **18** (dimensions: 875 x 700 x 75 μm) used for the present analysis.

The absolute configuration depends on the stereochemistry of the employed DIP-Cl isomer. The stereoselectivity arises from the formation of a chair-like transition state, in which the aldehyde bulky substituent occupies a pseudo-equatorial position, to minimize steric 1,3-diaxial interactions with the isopinocampheyl (Ipc) group (see

scheme 16). The choice of the Ipc enantiomer determines on which of the aldehyde faces the allylation occurs.

To confirm the absolute configuration, a stereoselective allylation with (+)-DIP-Cl was performed on small scale on the enantiopure aldehyde 2-(*R*), [23,37] confirming the obtainment of **9c**.

The enantiopurity of our alcohols was determined through chiral HPLC on reverse phase. *Syn*-isomers (**9a** and **9c**), were obtained with a 92 % e.e. while the *anti*-alcohols (**9b** and **9d**), were accessed with 84 % e.e. This result could be explained considering the influence of the existing stereocenter that, despite being in β-position, bears a bulky piperidine ring as substituent. The HPLC chromatograms of compound are reported as an example in Figure 4.

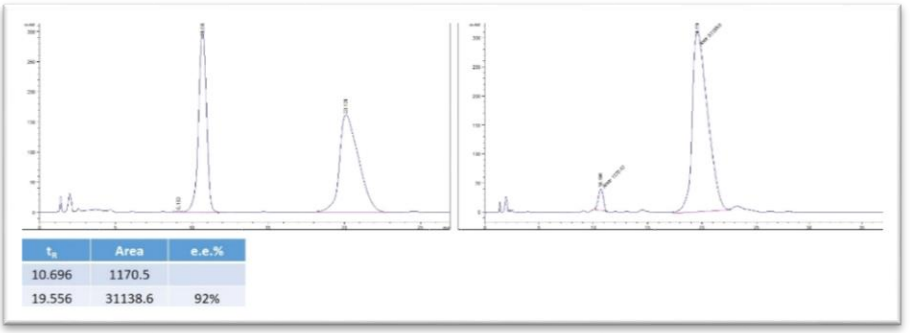

Figure 4. HPLC chromatograms for the determination of the e.e. in sample **9a**, chosen as an example. On the left the analysis of the racemic mixture is reported, while on the left the one of the enantiopure compound is appreciable. HPLC conditions: chiralcel AD-RH RP column, 1 mL/min, CH_3CN:H_2O = 35:65, 96 bar, λ: 204 nm.

In the attempt to improve the enantiomeric excesses, in particular for the *anti*-compounds, a different method based on Leighton's strained silacyles was tested[48]. Aldehyde **7** was reacted with (4*S*,5*S*)-2-Allyl-2-chloro-3,4-dimethyl-5-phenyl-1-oxa-3-aza-2-silacyclopentane, already available in our laboratory, as reported in Scheme 17.

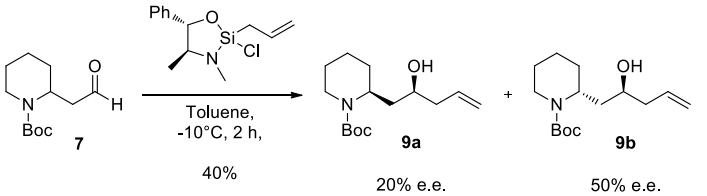

Scheme 17. Alternative Leighton's allylation of aldehyde 7.

[48] J. W. A. Kinnaird, P. Y. Ng, K. Kubota, X. Wang, J. L. Leighton, *J. Am. Chem. Soc.* **2002**, *124*, 7920–7921.

Mechanistically, the aldehyde complexation with the silane, giving a trigonal bipyramidal intermediate, seems to be followed by allyl transfer.

It emerged that this (4*S*,5*S*)-2-Allyl-*2*-chloro-3,4-dimethyl-5-phenyl-1-oxa-3-aza-2-silacyclopentane behaved in the same way of (–)-allylBIpc$_2$, favouring majorly the formation of alcohols **9a** and **9b**, but with low yield and poor enantiomeric excesses of 20% and 50% respectively.

Thus, Brown's chemistry proved to be the most solid option on this kind of substrates and was used extensively also in the other projects reported in this thesis.

All the alcohol **9a-d** underwent the same synthetic pathway, reported in Scheme 18 on products **a**, as an example. A Mitsunobu reaction in the presence of diphenylphosphoryl azide (DPPA) allowed the interconversion of the hydroxyl group into the corresponding azide, with inversion of configuration.[49] The azides were immediately reduced under Staudinger conditions, giving amines **11-d**.[50]

Acylation of the amines with the commercially available acryloyl chloride, followed by a ring closing methatesis (RCM), led to the obtainment of the fundamental building block **13**.

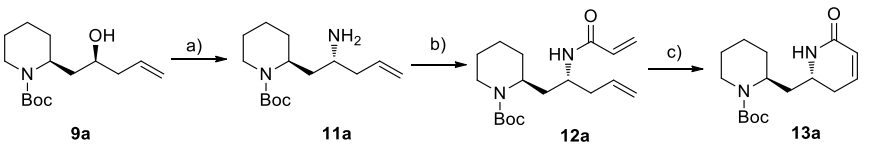

Catalysts sceening for RCM step

Catalyst	Loading	Time	Yield
H G	10 mol %	7h	54-60%
M73 SIMes	1 mol %	2h	73-80%

Scheme 18. *Reagent and conditions*: a) i. PPh_3, DIAD, DPPA, THF, 0 °C to r.t., 4 h; ii. PPh_3, THF/H_2O 10:1, 5 h, 40 °C, yield: 62 % over two steps; b) TEA, acryloyl chloride, CH_2Cl_2, 0 °C to r.t., 2 h, yield: 63 %; c) Ru-catalyst, CH_2Cl_2, 50 °C, 1.5–7 h, yield: 73 %. (Reported on compounds **a** as example).

For the last step, two different catalysts were tested: the 2nd generation Hoveyda–Grubbs (HG-II) (yields 54–60 %) and the Umicore M73 SIMes (yields 73–80 %).

The latter resulted to be our catalyst of choice, because it proved to be more efficient, affording the desired lactams with higher yields, more rapidly and using a lower amount of catalyst. [51] Moreover, M73 SIMes catalyst displayed a higher affinity for silica, facilitating the purification through column chromatography.

[49] K. C. Kumara Swamy, N. N. Bhuvan Kumar, N. N., E. Balaraman, K. V. P. Pavan Kumar, *Chem. Rev.* **2009**, *109*, 2551-2651.

[50] A. Takada, K. Uda, T. Ohtani, S. Tsukamoto, D. Takahashi, K. Toshima, *J. Antibiot.* **2013**, *66*, 155–159.

[51] D. Rix, F. Caijo, I. Laurent, F. Boeda, H. Clavier, S. P. Nolan, M. Mauduit, *J. Org. Chem.* **2008**, *73*, 4225-4228.

Chiral HPLC analysis of products **13a-d** confirmed the maintenance of the previously observed enantiomeric excesses.

At this stage, the first "branch" of the ramification of our synthesis was explored. Products **13a-d** were treated with trifluoroacetic acid (TFA), to cleave the Boc protecting group.

It was observed that while *syn*-compounds gave the expected deprotected amines **14b** and **14d**, the *anti*-substrates underwent directly the intramolecular aza-Michael addition on the α,β -unsaturated lactam, giving the tricyclic compounds **15a** and **15c**. The configuration of the newly formed stereocenter was defined by the configuration of the already present stereocenters (Scheme 19).

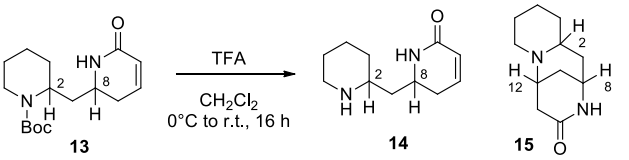

	Starting material			Product				
		H-2	*H-8*		*H-2*	*H-8*	*H-12*	Yield
Syn	**13b**(2*R*, 8*R*)	β	β	**14b***(2R,8R)*	β	β	-	66%
	13d(2*S*,8*S*)	α	α	**14d***(2S,8S)*	α	α	-	70%
Anti	**13a***(2S, 8R)*	α	β	**15a***(2S,8S,12R)*	α	α	α	>95%
	13c(2*R*, 8*S*)	β	α	**15c**(2*R*,8*R,12S*)	β	β	β	>95%

Scheme 19. Outcome of compounds **13** Boc cleavage.

To justify the different outcome of compounds **13** deprotection, the 3D structures and energies of the different transition states leading to tricyclic products **15** were examined, as reported in Figure 5.

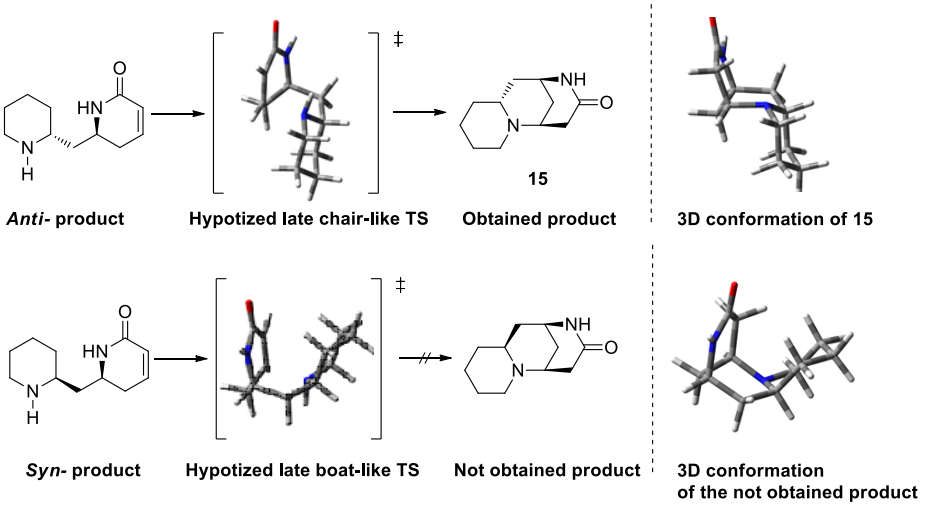

Figure 5. Hypothetic transition states leading to the formation of the Michael adducts.

According to Hammond's postulate, a late transition state (TS), similar in energy to the final products, was assumed. The reactant and TS structures have been optimised with semi-empirical calculations, using the PM6 model.[52] The intrinsic reaction coordinate pathways, connecting reactants to the corresponding transition states, were calculated for both the diastereomers. 3D models suggested that *anti*-compounds are converted in **15** assuming a favoured chair-like transition state, while *syn*-ones should adopt a disfavoured boat-like transition state. These assumptions were supported by calculations, that demonstrated that *syn*- compounds presented a higher activation energy with respect to the *anti*-ones. In detail, the activation energies resulted to be of 9.28 kcal/mol for the *anti*-compounds, and of 11.54 kcal/mol for the *syn*-ones. The calculated activation energy difference of 2.26 kcal/mol is in qualitative agreement with experimental results, justifying why *syn*-products **13b** and **13d** can be effectively deprotected, without undergoing conjugate additions, while *anti*-products tend to cyclize, producing **15a** and **15c**.

To complete the planned exploration of the chemical space, an Eschweiler–Clarke reaction[53,54,55] was performed on compounds **13a-d**.

Considering the mechanism of Eschweiler–Clarke reaction (Scheme 20), that involves the cleavage of the Boc-protecting group, followed by the formation of an iminium intermediate, two different scaffolds could be formed.

[52] J. J. P. Stewart, *J. Mol. Model.* **2007**, *13*, 1173-1213.
[53] H. T. Clarke, H. B. Gillespie, S. Z. J. Weisshaus, *J. Am. Chem. Soc.* **1933**, *55*, 4571–4587.
[54] S. Torchy, D. J. Barbry, *Chem. Research.* **2001**, *2001,* 292–293.
[55] G. Bobowski, *J. Org. Chem.* **1985**, *50*, 929–931.

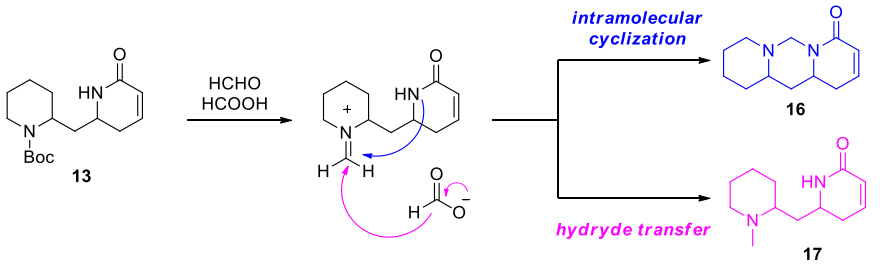

Scheme 20. Possible outcomes of the Eschweiler-Clarke reaction on products **13**.

The expected hydride transfer by the formate anion, should reduce the iminium salt, giving the *N*-methyl derivative **17**. However, an intramolecular nucleophilic attack by the lactam nitrogen could occur as competitive reaction, leading to the formation of a new thermodynamically favoured 6-memebered ring (compound **16**).
In all the cases, the formation of the octahydrodipyrido pyrimidinones **16** was observed, as reported in Scheme **21**.

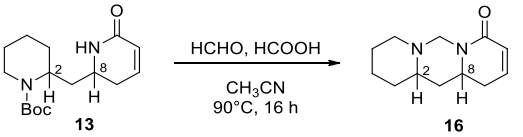

	Starting material			Product			
		H-2	*H-8*		*H-2*	*H-8*	Yield
Syn	**13b**(2*R*, 8*R*)	β	β	**16b**(2*R*, 8*R*)	α	β	80%
	13d(2*S*,8*S*)	α	α	**16d**(2*S*, 8*S*)	β	α	77%
Anti	**13a***(2S, 8R)*	α	β	**16a**(2*S*, 8*R*)	β	β	68%
	13c(2*R*, 8*S*)	β	α	**16c**(2*R*, 8*S*)	α	α	65%

Scheme 21. Outcome of Eschweiler-Clarke reaction on compound **6**.

To obtain scaffold **17**, a reduction of the iminium salt with a stronger reducing agent, such as $NMe_3 \cdot BH_3$ complex, was attempted. Unfortunately, this reaction resulted in a complex mixture of products, impossible to purify.
Thus, eight compounds, presenting three new scaffolds, were obtained through this DOS approach. It is noteworthy that this strategy opens the possibility of synthesizing scaffolds resembling natural products, in a stereoselective fashion. In fact, compounds **15** presents the isomeric scaffold of some lupin alkaloids, such as (-)-cytisine, (-)-

sparteine and (-)-anagyrine,[56,57,58,59] while products **16** are characterised by a simplified structure of several Lycopodium alkaloids, like lycocernuine and cernuine (Figure 6).[60,61]

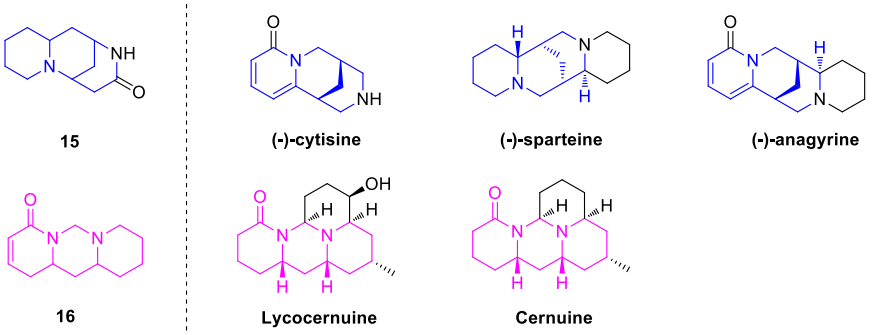

Figure 6. Comparison between the general structures of scaffolds **15** and **16** and similar natural products.

It is interesting that scaffolds **14-16** contains two possible pharmacophores: a piperidine ring and a bioisoster of an α,β-unsaturated lactone.[62,63,64,65]

Thus, despite the purely synthetic nature of this work, preliminary biological tests were performed on three different cancer cell lines, including A-2780 (human ovarian carcinoma), A-2780cis (resistant human ovarian carcinoma) and HT-29 colon adenocarcinoma. None of the tested compounds was particularly active. However, this project led to a small library of three diversified piperidine-based scaffolds, obtained in a stereoselective fashion. Considering the importance of diversified libraries in the drug discovery and development process, our compounds are currently being tested on other cancer cell lines and will be also considered for *in silico* studies for fragment-based drug discovery.

[56] I. Philipova, G. Stavrakov, N. Vassilev, R. Nikolova, B. Shivachev, V. Dimitrov, *J. Organomet. Chem.* **2015**, *778*, 10-20.
[57] B. Danieli, G. Lesma, D. Passarella, A. Sacchetti, A. Silvani, A. Virdis, *Org. Lett.* **2004**, *6*, 493-496.
[58] S. Okuda, H. Kataoka, K. Tsuda, Chem. Pharm. Bull. **1965**, 13, 491-500.
[59] J. D. Firth, S. J. Canipa, L. Ferris, P. O'Brien, *Angew. Chem. Int. Ed.* **2018**, *57*, 223 –226.
[60] Q. Yang, Y. Zhu, R. Zhan, Y. A. Chen, *Chem. Nat. Compd*. **2018**, *54,* 729-731.
[61] N. Veerasamy, R. G. Carter, *Tetrahedron* **2016**, *72*, 4989-5001.
[62] P. Goel, O. Alam, M. J. Naim, F. Nawaz, M. Iqbal, M. I. Alam, *Eur. J. Med. Chem.* **2018**, *157*, 480–502.
[63] S. B. Buck, C. Hardouin, S. Ichikawa, D. R. Soenen, C.-M. Gauss, I. Hwang, M. R. Swingle, K. M. Bonness, R. E. Honkanen, D. L. Boger, *J. Am. Chem. Soc.* **2003**, *125*, 15694–15695.
[64] P. Kumar, S. V. Naidu, *J. Org. Chem.* **2006**, *71*, 3935–3941.
[65] Z. Tian, S. Chen, Y. Zhang, M. Huang, L. Shi, F. Huang, C. Fong, M. Yang, P. Xiao, *Phytomedicine* **2006**, *13*, 181–186.

2.3 Experimental part

General

Unless otherwise stated, reagents and solvents were purchased from Sigma Aldrich, Fluorochem or TCI and used without further purification. All reactions were carried out in oven-dried glassware and dry solvents, under nitrogen atmosphere and were monitored by thin layer chromatography (TLC) on silica gel (Merck precoated 60F254 plates), with detection by UV light (254 nm) or by solutions of potassium permanganate stain or ninhydrin.

Flash chromatography was performed using silica gel (240-400 mesh, Merck) as stationary phase.

^{1}H-NMR spectra were recorded on a Bruker Avance Spectrometer (400 MHz) and are reported relative to residual $CDCl_3$ or CD_3OD. ^{13}C-NMR spectra were recorded on the same instruments (100 MHz) and are reported relative to residual $CDCl_3$ or CD_3OD. All 1D and 2D NMR spectra were collected using the standard pulse sequences available with Bruker Topspin 1.3. Chemical shifts (δ) for proton and carbon resonances are quoted in parts per million (ppm) relative to tetramethylsilane (TMS), used as an internal standard. Data for ^{1}H-NMR are reported as follows: chemical shift (δ/ppm) (multiplicity, coupling constant (Hz), integration). Multiplicities are reported as follows: s = singlet, d = doublet, t = triplet, m = multiplet, bs = broad singlet. Data for ^{13}C-NMR are reported in terms of chemical shift (δ/ppm).

Mass spectra were registered exploiting the electrospray ionisation (ESI) technique, on a Q-Tof micro mass spectrometer.

Specific rotation values were measured on a P-1030 Jasco polarimeter, using 1 mL cells, with path length of 10 cm. Measures were collected at 20-25°C, using sodium D line wavelength λ=589 nm. HPLC analysis were performed using a 15 cm X 4.6 mm Chiralcel® AD-RH RP column at 35°C. Detection occurred at two different wavelengths (254 nm and 204 nm).

General procedure for the synthesis of compounds 10. *Errore. Il segnalibro non è definito.*

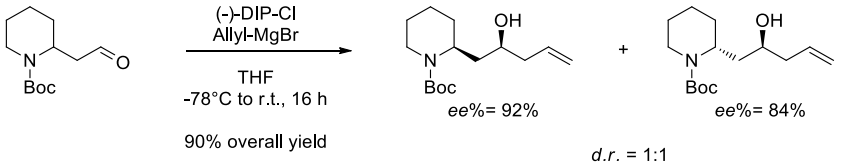

Allylmagnesium bromide (1 M solution in Et_2O, 2.86 mL, 2.86 mmol) was added dropwise to a solution of (–)-DIP-Cl (1.06 g, 3.30 mmol) in anhydrous THF (13.5 mL), previously cooled at –78 °C. The reaction mixture was warmed to 0 °C and stirred at this temperature for 1 h. The solution was allowed to stand until magnesium chloride precipitated. The supernatant solution was carefully transferred to another flask and cooled at -78°C.Then, a solution of aldehyde **7** (0.500 g, 2.20 mmol) in anhydrous THF (6.5 mL) was added dropwise. The resulting solution was stirred at -78°C for 1 h and then 16 h at room temperature. The reaction was quenched with NaH_2PO_4 buffer solution at pH 7 (13.5 mL), MeOH (13.5 mL) and 30 % H_2O_2 (6.7 mL). After stirring for 30 min, the mixture was washed with saturated aqueous $NaHCO_3$ and extracted with Et_2O. The combined organic phases were dried over Na_2SO_4 and filtered. The solvent was evaporated under vacuum, and the residue was purified by column chromatography on silica gel (hexane/EtOAc, 8:2) to give **9a** and **9b** as yellow oils (90% overall yield). In order to obtain the other couple of diastereomers (**9c** and **9d**), the reaction was performed in the same way, using the (+)-DIP-Cl.

(S)-tert-butyl 2-((S)-2-hydroxypent-4-enyl)piperidine-1-carboxylate (9a).

Yield: 44%.

^{1}H NMR (400 MHz, $CDCl_3$): δ = 5.81–5.91 (m, 1H), 5.08 (d, J = 17.4 Hz, 1H), 5.05 (d, J =9.7 Hz, 1H), 4.47 (bs, 1H), 3.95 (bs, 1H), 3.39 (bs, 1H), 2.66 (dt, J = 12.7, 2.0 Hz, 1H), 2.27–2.33 (m, 1H), 2.16–2.23 (m, 1H), 2.01 (dt, J = 12.5, 1.8 Hz, 1H), 1.73–1.76 (m, 1H), 1.42 (s, 9H), 1.35–1.59 (m, 6H).

^{13}C NMR (100 MHz, $CDCl_3$): δ = 167.1, 135.5, 116.6, 80.2, 67.1, 46.2, 41.1, 39.3, 36.9, 29.2, 28.6, 25.3, 19.4.

MS (ESI) m/z $[M + H]^+$ calcd. for $C_{15}H_{28}NO_3$: 270.2069, found: 270.2072.

HPLC analysis: Chiralcel AD-RH RP column, 1 mL/min, $CH_3CN:H_2O$ = 35:65, 96 bar, λ: 204 nm, t_R: 21.342 min, *e.e.*%: 92%.

$[\alpha]_D^{20}$: –33 (*c* = 1, $CHCl_3$).

(R)-tert-butyl 2-((R)-2-hydroxypent-4-enyl)piperidine-1-carboxylate (3c).

Yield: 42%

MS (ESI) m/z $[M + H]^+$ calcd. for $C_{15}H_{28}NO_3$: 270.2069, found: 270.2073.

HPLC analysis: Chiralcel AD-RH RP column, 1 mL/min, $CH_3CN:H_2O$ = 35:65, 96 bar, λ: 204 nm, t_R: 11.05 min, *e.e.*%: 92%.

$[\alpha]_D^{20}$: +35 (*c* = 0.8, $CHCl_3$).

(R)-tert-butyl 2-((S)-2-hydroxypent-4-enyl)piperidine-1-carboxylate (9b).

Yield: 46%.

^{1}H NMR (400 MHz, $CDCl_3$): δ= 5.85–5.75 (m, 1H), 5.10 (d, J = 17.3 Hz, 1H), 5.08 (d, J = 9.8 Hz, 1H), 4.32 (br. s, 1H), 3.88–3.93 (m, 1H), 3.88–3.93 (m, 1H), 3.65 (tt, J = 7.5, 2.4 Hz,1H), 2.79 (dt, J = 12.8, 0.2 Hz,1 H), 2.27–2.32 (m, 1H), 2.14–2.21 (m, 1H), 1.77–1.82 (m, 1H), 1.42 (s,9 H), 1.35–1.59 (m, 6H) ppm.

^{13}C NMR (100 MHz, $CDCl_3$): δ= 155.29, 135.06, 117.4, 79.6, 71.3, 48.0, 41.8, 38.8, 37.0, 28.9, 28.4, 25.5, 18.9 ppm.

MS (ESI) m/z $[M+ H]^+$ calcd. for $C_{15}H_{28}NO_3$: 270.2069, found: 270.2071.

HPLC analysis: Chiralcel AD-RH RP column, 1 mL/min, $CH_3CN:H_2O$ = 35:65, 96 bar, λ: 204 nm, t_R: 8.12 min, *e.e.*%: 84%.

$[\alpha]_D^{20}$: +15 (*c* = 0.9, $CHCl_3$).

(S)-tert-butyl 2-((R)-2-hydroxypent-4-enyl)piperidine-1-carboxylate, (9d).

Yield: 46%.

ESIMS m/z $[M +H]^+$ calcd. for $C_{15}H_{28}NO_3$: 270.2069, found: 270.2068.

HPLC analysis: Chiralcel AD-RH RP column, 1 mL/min, $CH_3CN:H_2O$ = 35:65, 96 bar, λ: 204 nm, t_R: 9.24 min, *e.e.*%: 84%.

$[\alpha]_D^{20}$: –14 (*c* = 1.3, $CHCl_3$).

General procedure for the synthesis of compounds 11.

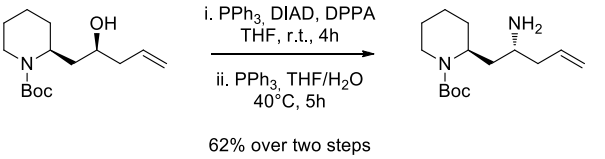

62% over two steps

PPh_3 (0.277 g, 1.06 mmol) was added to a solution of **9** (0.237 g, 0.88 mmol) in anhydrous THF (7.5 mL) at room temperature. The reaction mixture was cooled at 0°C and diisopropylazodicarboxylate (DIAD) (209 µL, 1.06 mmol) was carefully added dropwise. After 10 minutes, diphenylphosphorylazide (DPPA) (228 µL, 1.06 mmol) was slowly added as well. The reaction mixture was warmed to room temperature and stirred for 4 h. The solvent was evaporated under vacuum and the residue was purified by column chromatography on silica gel (Hexane/EtOAc, 95:5), to give the azide as a light yellow oil, which was immediately used in the next step. The azide (0.194 g, 0.66 mmol), was dissolved in THF (11.5 mL) and treated with PPh_3 (0.346 g, 1.32 mmol) and water (1.2 mL). The reaction mixture was warmed to 40°C and stirred at that temperature for 5 h. The reaction mixture was cooled to room temperature and water (5 mL) was added carefully. The layers were separated and the aqueous one was extracted with Et_2O. The collected organic phases were washed with brine (5 mL), dried over Na_2SO_4, filtered and concentrated under vacuum. The crude product was purified by column chromatography on silica gel (CH_2Cl_2/MeOH, 9:1) to give **11** as a light yellow oil.

(S)-tert-butyl 2-((R)-2-aminopent-4-enyl)piperidine-1-carboxylate (11a).

Yield: 62% over two steps.

^{1}H NMR (400 MHz, $CDCl_3$) δ 5.87 – 5.73 (m, 1H), 5.20 – 5.10 (m, 2H), 4.37 (m, 1H), 3.96-3.94 (m, 1H), 3.30 (bs, 2H), 2.86-2.80 (m, 2H), 2.48 – 2.37 (dt, J = 13.5, 5.3 Hz, 1H), 2.15 (dt, J = 13.3, 6.4 Hz, 1H), 1.97 – 1.86 (m, 1H), 1.67 – 1.49 (m, 6H), 1.45 (s, 9H), 1.41-1.35 (m, 1H) ppm.

^{13}C NMR (100 MHz, $CDCl_3$) δ 154.97, 134.67, 118.38, 79.50, 48.76, 47.80, 40.86, 38.99, 36.20, 29.02, 28.49 (3 CH_3), 25.56, 19.07 ppm.

MS (ESI) m/z $[M + Na]^+$ calcd. for $C_{15}H_{28}N_2O_2Na$: 291.2048, found: 291.2051.

$[\alpha]_D^{20}$: -30 (*c* = 1.02, $CHCl_3$).

(R)-tert-butyl 2-((S)-2-aminopent-4-enyl)piperidine-1-carboxylate (11c).

Yield: 65% over two steps.

MS (ESI) m/z $[M + Na]^+$ calcd. for $C_{15}H_{28}N_2O_2Na$: 291.2048, found: 291.2049.

$[\alpha]_D^{20}$: +33 (*c* = 0.98, $CHCl_3$).

(R)-tert-butyl 2-((R)-2-aminopent-4-enyl)piperidine-1-carboxylate (11b).

Yield: 67% over two steps.

^{1}H NMR (400 MHz, $CDCl_3$) δ 5.79 (ddt, J = 17.3, 10.1, 7.1 Hz, 1H), 5.15 (m, 2H), 4.43 (m, 1H), 4.09 (bs, 2H), 3.96 (m, 1H), 2.81 – 2.62 (m, 2H), 2.58 – 2.39 (m, 1H), 2.38-2.23 (m, 1H), 2.17 – 1.98 (m, 1H), 1.72 (m, 1H), 1.63 – 1.50 (m, 4H), 1.47 (s, 9H), 1.43 – 1.32 (m, 2H) ppm.

^{13}C NMR (100 MHz, $CDCl_3$) δ 135.16, 118.90, 80.78, 48.43, 46.96, 40.66, 39.70, 35.73, 30.01, 29.11 ($3CH_3$), 26.15, 19.73 ppm (detected signals).

MS (ESI) m/z $[M + Na]^+$ calcd. for $C_{15}H_{28}N_2O_2Na$: 291.2048, found: 291.2052.

$[\alpha]_D^{20}$: +14 (*c* = 0.72, $CHCl_3$).

(S)-tert-butyl 2-((S)-2-aminopent-4-enyl)piperidine-1-carboxylate (11d).

Yield: 64% over two steps.

MS (ESI) m/z $[M + Na]^+$ calcd. for $C_{15}H_{28}N_2O_2Na$: 291.2048, found: 291.2050.

$[\alpha]_D^{20}$: -11 (*c* = 0.85, $CHCl_3$).

General procedure for the synthesis of compounds 12.

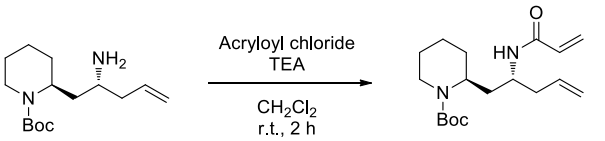

Anhydrous TEA (0.311 mL, 2.24mmol) was added to a solution of **11** (0.272 g, 1.02 mmol) in anhydrous CH_2Cl_2 (3.2 mL) cooled at 0°C. After 10 minutes, acryloyl chloride (0.124 mL, 1.52 mmol) was slowly added dropwise. The reaction mixture was stirred for 2 h at room temperature, then a saturated aqueous solution of NH_4Cl was added and the reaction mixture was extracted with CH_2Cl_2. The collected organic phases were washed twice with brine, dried over Na_2SO_4, filtered and concentrated under vacuum. The crude was purified by column chromatography on silica gel (CH_2Cl_2/MeOH, 9:1) to give **12** as a light yellow oil.

(S)-tert-butyl 2-((R)-2-acrylamidopent-4-enyl)piperidine-1-carboxylate (12a).
Yield: 63%.
^{1}H NMR (400 MHz, $CDCl_3$) δ 6.30 (dd, J = 17.0, 1.2 Hz, 1H), 6.13 (dd, J = 17.0, 10.3 Hz, 1H), 5.86 – 5.69 (m, 1H), 5.64 (dd, J = 10.3, 1.2 Hz, 1H), 5.20 – 4.96 (m, 2H), 4.28 (m, 1H), 4.07 (m, 1H), 3.96 (m, 1H), 2.85 (t, 1H), 2.38 – 2.16 (m, 2H), 1.83 – 1.64 (m, 2H), 1.63 – 1.63 (m, 5H), 1.47 (s, 9H), 1.38-1.32 (m, 1H) ppm.
^{13}C NMR (100 MHz, $CDCl_3$) δ 165.96, 155.84, 135.23, 131.93, 126.65, 118.40, 80.26, 47.80, 47.13, 40.32, 39.55, 34.21, 29.18 ($3CH_3$), 28.81, 26.09, 19.63 ppm.
MS (ESI) m/z $[M + Na]^+$ calcd. for $C_{18}H_{30}N_2O_3Na$: 345.2154, found: 345.2153.
$[\alpha]_D^{20}$: -26 (*c* = 0.88, $CHCl_3$).

(R)-tert-butyl 2-((S)-2-acrylamidopent-4-enyl)piperidine-1-carboxylate (12c).
Yield: 61%.
MS (ESI) m/z $[M + Na]^+$ calcd. for $C_{18}H_{30}N_2O_3Na$: 345.2154, found: 345.2156.
$[\alpha]_D^{20}$: +28 (*c* = 0.91, $CHCl_3$).

(R)-tert-butyl 2-((R)-2-acrylamidopent-4-enyl)piperidine-1-carboxylate (12b).
Yield: 66%.
^{1}H NMR (400 MHz, $CDCl_3$) δ 6.24 (dd, J = 17.0, 1.6 Hz, 1H), 6.06 (dd, J = 17.0, 10.2 Hz, 1H), 5.85 – 5.70 (ddt, J = 17.2, 10.2, 7.1 Hz, 1H), 5.58 (dd, J = 10.2, 1.5 Hz, 1H), 5.15 – 5.01 (m, 2H), 4.35 (m, 1H), 4.01 – 3.85 (m, 2H), 2.73 (td, J = 13.2, 2.2 Hz, 1H), 2.42 (m, 1H), 2.36 (m, 1H), 1.87 (ddd, J = 14.0, 8.0, 5.5 Hz, 1H),1.71 (dt, J = 14.0, 5.8 Hz, 1H), 1.67 – 1.50 (m, 5H), 1.45 (s, 9H), 1.43 – 1.32 (m, 1H) ppm.

^{13}C NMR (100 MHz, $CDCl_3$) δ 165.02, 155.07, 134.71, 131.40, 125.80, 117.70, 79.67, 47.32 (2 CH), 39.27, 37.83, 33.45, 29.62, 28.49 ($3CH_3$), 25.51, 19.06 ppm.
MS (ESI) m/z $[M + Na]^+$ calcd. for $C_{18}H_{30}N_2O_3Na$: 345.2154, found: 345.2155.
$[\alpha]_D^{20}$: -23 (*c* = 1.17, $CHCl_3$).

(S)-tert-butyl 2-((S)-2-acrylamidopent-4-enyl)piperidine-1-carboxylate (12d).
Yield: 64%.
MS (ESI) m/z $[M + Na]^+$ calcd. for $C_{18}H_{30}N_2O_3Na$: 345.2154, found: 345.2157.
$[\alpha]_D^{20}$: +20 (*c* = 0.97, $CHCl_3$).

General procedure for the synthesis of compounds 13.

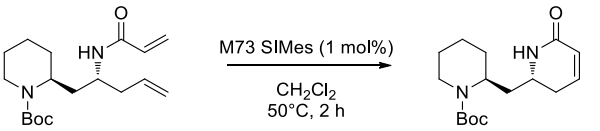

73%

A solution of Umicore M73 SIMes catalyst (4.2 mg, 0.0057 mmol) in anhydrous CH_2Cl_2 (8 mL) was added dropwise to a solution of **12** (0.183 g, 0.57mmol) in anhydrous CH_2Cl_2 (24 mL). The reaction mixture was stirred for 2 h at 50°C, then the solvent was removed under vacuum. The residue was purified by column chromatography on silica gel (CH_2Cl_2/MeOH, 95:5) to give **13** as a white amorphous solid.

(S)-tert-butyl 2-(((R)-6-oxo-1,2,3,6-tetrahydropyridin-2-yl)methyl)piperidine-1-carboxylate (13a).

Yield: 73%.

^{1}H NMR (400 MHz, $CDCl_3$) δ 6.66 – 6.52 (m, 1H), 5.91 (d, J = 9.9 Hz, 1H), 4.33 (m, 1H), 3.98 (m, 1H), 3.59 – 3.47 (m, 1H), 2.76 (t, J = 12.9 Hz,1H), 2.56 (dt, J = 17.6, 5.0 Hz, 1H), 2.27 – 2.08 (m, 1H), 2.08 – 1.93 (m, 2H), 1.76 – 1.51 (m, 5H), 1.47 (s, 9H), 1.44-1.36 (m, 1H) ppm.

^{13}C NMR (100 MHz, $CDCl_3$) δ 167.08, 155.61, 141.10, 125.31, 80.61, 49.79, 47.99, 39.81, 36.85, 30.57, 29.91, 29.11 ($3CH_3$), 26.06, 19.68 ppm.

MS (ESI) m/z $[M + Na]^+$ calcd. for $C_{16}H_{26}N_2O_3Na$: 317.1841, found: 317.1845.

HPLC analysis: Chiralcel AD-RH RP column, 1 mL/min, $CH_3CN:H_2O$ = 35:65, 96 bar, λ: 254 nm, t_R: 7.70 min, *e.e.*%: 92%.

$[\alpha]_D^{20}$: +13 (*c* = 0.91, $CHCl_3$).

(R)-tert-butyl 2-(((S)-6-oxo-1,2,3,6-tetrahydropyridin-2-yl)methyl)piperidine-1-carboxylate (13c).

Yield: 77%

MS (ESI) m/z $[M + Na]^+$ calcd. for $C_{16}H_{26}N_2O_3Na$: 317.1841, found: 317.1842.

HPLC analysis: Chiralcel AD-RH RP column, 1 mL/min, $CH_3CN:H_2O$ = 35:65, 96 bar, λ: 254 nm, t_R: 10.17 min, *e.e.*%: 92%.

$[\alpha]_D^{20}$: -13 (*c* = 1.2, $CHCl_3$).

(R)-tert-butyl 2-(((R)-6-oxo-1,2,3,6-tetrahydropyridin-2-yl)methyl)piperidine-1-carboxylate (13b).

Yield: 80%.

^{1}H NMR (400 MHz, $CDCl_3$) δ 6.62 – 6.44 (m, 1H), 5.89 (dd, J = 9.9, 1.4 Hz, 1H), 4.41 (m, 1H), 3.99 (m, 1H), 3.36 (m, 1H), 2.65 (t, J = 12.5 Hz, 1H), 2.59 - 2.48 (m, 1H), 2.14 (dt, J = 17.8, 4.7 Hz, 1H), 1.90 (m, 1H), 1.81 – 1.66 (m, 1H), 1.59 (m, 4H), 1.54 – 1.39 (m, 11H).
^{13}C NMR (100 MHz, $CDCl_3$) δ 165.69, 139.68, 124.66, 47.34 (2CH), 38.70, 35.74, 30.04, 29.45, 28.56 ($3CH_3$), 25.61, 19.28 ppm (detected signals).
MS (ESI) m/z $[M + Na]^+$ calcd. for $C_{16}H_{26}N_2O_3Na$: 317.1841, found: 317.1840.
HPLC analysis: Chiralcel AD-RH RP column, 1 mL/min, $CH_3CN:H_2O$ = 35:65, 96 bar, λ: 254 nm, t_R: 8.71 min, *e.e.*%: 83%.
$[\alpha]_D^{20}$: -66 (*c* = 0.85, $CHCl_3$).

(S)-tert-butyl 2-(((S)-6-oxo-1,2,3,6-tetrahydropyridin-2-yl)methyl)piperidine-1-carboxylate (13d).
Yield: 78%.
MS (ESI) m/z $[M + Na]^+$ calcd. for $C_{16}H_{26}N_2O_3Na$: 317.1841, found: 317.1843.
HPLC analysis: Chiralcel AD-RH RP column, 1 mL/min, $CH_3CN:H_2O$ = 35:65, 96 bar, λ: 254 nm, t_R: 11.15 min, *e.e.*%: 82%.
$[\alpha]_D^{20}$: +60 (*c*= 0.94, $CHCl_3$).

General procedure for the synthesis of compounds 14.

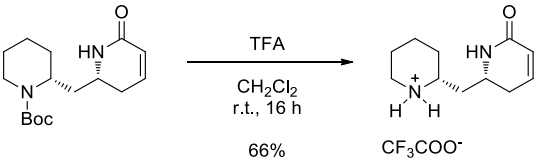

TFA (65 µL, 0.85 mmol) was added to a solution of **13** (0.031 g, 0.11mmol) in anhydrous CH_2Cl_2 (17 mL), cooled at 0°C. The reaction mixture was stirred at room temperature for 18 h, then the solvent was removed under vacuum, affording **14** as CF_3COOH salt (white amorphous solid).

(R)-6-((R)-piperidin-2-ylmethyl)-5,6-dihydropyridin-2(1H)-one (14b) CF_3COOH salt.
Yield: 66%.
^{1}H NMR (400 MHz, $CDCl_3$) δ 9.06 – 8.56 (m, 2H), 7.86 (bs, 1H), 6.67 (m, 1H), 5.90 (d, J = 9.3 Hz, 1H), 3.89 (m, 1H), 3.50 – 3.36 (m, 1H), 3.36 – 3.21 (m, 1H), 2.91 (m, 1H), 2.65 – 2.47 (m, 1H), 2.30 – 2.17 (m, 1H), 2.05 – 1.79 (m, 5H), 1.79 – 1.67 (m, 1H), 1.67 – 1.58 (m, 1H), 1.54 (m, 1H).
^{13}C NMR (100 MHz, $CDCl_3$) δ 168.69, 167.18, 161.33 (q), 142.50, 123.13, 53.36, 46.06, 45,03, 38.53, 29.51, 28.87, 22.30, 22.09.
MS (ESI) m/z calcd. for $[C_{11}H_{19}N_2O]^+$: 195.1497, found: 195.1501.
$[\alpha]_D^{20}$: -25 (*c*=0.62, MeOH).

(S)-6-((S)-piperidin-2-ylmethyl)-5,6-dihydropyridin-2(1H)-one (14d) CF_3COOH salt.
Yield: 70%.
MS (ESI) m/z calcd. for $[C_{11}H_{19}N_2O]^+$: 195.1497, found: 195.1499.
$[\alpha]_D^{20}$: +20 (*c*=0.70, MeOH).

General procedure for the synthesis of compounds 15.

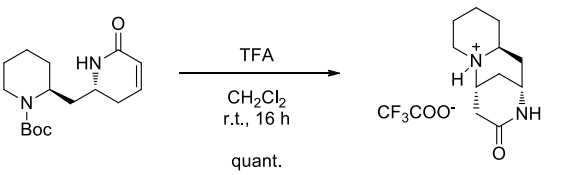

TFA (120 µL, 1.25 mmol) was added to a solution of **13** (0.023 g, 0.08 mmol) in anhydrous CH_2Cl_2 (13 mL), cooled at 0°C. The reaction mixture was stirred at room temperature for 16 h, then the solvent was removed under vacuum. The residue was purified by column chromatography on silica gel (CH_2Cl_2/MeOH, 95:5 to 85:15), to give the **15** (0.024 g, quant.) as CF_3COOH salt (white amorphous solid).

(2S,6R,11aS)-decahydro-4H-2,6-methanopyrido[1,2-a][1,5]diazocin-4-one (15a)
CF_3COOH salt.
Yield: 95%.
^{1}H NMR (400 MHz, CD_3OD) δ 3.65 (bs, 1H), 3.33 – 3.19 (m, 1H), 2.71 (m, 3H), 2.54 (m, 1H), 2.36 (dd, *J* = 19.1, 5.8 Hz, 1H), 2.18 – 1.90 (m, 2H), 1.87 – 1.50 (m, 5H), 1.48 – 1.30 (m, 3H).
^{13}C NMR (100 MHz, CD_3OD) δ 174.41, 163.05 (q), 55.00, 53.30, 53.02, 46.56, 39.88, 33.16, 31.51, 30.29, 26.21, 24.98 (detected signals).
MS (ESI) m/z calcd. for $[C_{11}H_{19}N_2O]^+$: 195.1497, found: 195.1498.
$[\alpha]_D^{20}$:+30 (*c*= 1.18, MeOH).

(2R,6S,11aR)-decahydro-4H-2,6-methanopyrido[1,2-a][1,5]diazocin-4-one (15c)
CF_3COOH salt.
Yield: >95%.
MS (ESI) m/z calcd. for $[C_{11}H_{19}N_2O]^+$: 195.1497, found: 195.1499.
$[\alpha]_D^{20}$:-29 (*c*= 1.20, MeOH).

General procedure for the synthesis of compounds 16.

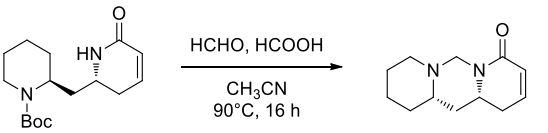

A 37% aqueous solution of formaldehyde (20µL, 0.28 mmol) and formic acid (11 µL, 0.28 mmol) were added to a solution of **13** (0.050 g, 0.16 mmol) in CH_3CN (0.9 mL). The reaction mixture was stirred for 2 h at 90°C, then other 20µL of formaldehyde solution and 11 µL of formic acid were added. The reaction mixture was stirred at 90°C for 12 h. The solvent was removed under vacuum and the residue was dissolved in CH_2Cl_2 and washed with a saturated aqueous $NaHCO_3$. The aqueous layer was extracted with CH_2Cl_2 and the combined organic phases were dried over Na_2SO_4, filtered and concentrated under vacuum. The crude product was purified by column chromatography on silica gel (CH_2Cl_2/MeOH, 98:2 to 95:5), to give **16** as a yellow amorphous solid.

(11aS,12aR)-6,8,9,10,11,11a,12,12a-octahydrodipyrido[1,2-c:1',2'-f]pyrimidin-4(1H)-one (16a).

Yield: 68%.

^{1}H NMR (400 MHz, $CDCl_3$) δ 6.50 (ddd, J = 10.0, 5.3, 3.0 Hz, 1H), 5.89 (dd, J = 10.0, 1.6 Hz, 1H), 5.18 (d, J = 11.0 Hz, 1H), 3.65 – 3.44 (m, 1H), 3.03 (d, J = 11.0 Hz, 1H), 2.94 (d, J = 10.6 Hz, 1H), 2.50 (dt, J = 18.0, 5.8 Hz, 1H), 2.26 (ddt, J = 16.4, 10.5, 2.7 Hz, 1H), 2.18 – 1.98 (m, 2H), 1.81 – 1.51 (m, 6H), 1.42-1.29 (m, 2H).

^{13}C NMR (100 MHz, $CDCl_3$) δ 164.56, 138.70, 124.33, 65.23, 60.49, 53.17, 51.64, 39.14, 31.69, 29,65, 24.87, 23.55.

MS (ESI) m/z $[M + Na]^+$calcd. for $C_{12}H_{18}N_2ONa$: 229.1317, found: 229.1319.

$[\alpha]_D^{20}$: +46 (*c*= 0.60, $CHCl_3$).

(11aR,12aS)-6,8,9,10,11,11a,12,12a-octahydrodipyrido[1,2-c:1',2'-f]pyrimidin-4(1H)-one (16c).

Yield: 65%.

MS (ESI) m/z $[M + Na]^+$ calcd. for $C_{12}H_{18}N_2ONa$: 229.1317, found: 229.1318.

$[\alpha]_D^{20}$: -47 (*c*= 0.55, $CHCl_3$).

(11aR,12aR)-6,8,9,10,11,11a,12,12a-octahydrodipyrido[1,2-c:1',2'-f]pyrimidin-4(1H)-one (16b).

Yield: 80%.

^{1}H NMR (400 MHz, $CDCl_3$) δ 6.54 – 6.43 (m, 1H), 5.90 (dd, J = 9.8, 2.5 Hz, 1H), 4.63 (d, J = 10.5 Hz, 1H), 3.92 (m, 1H), 3.84 (d, J = 10.5 Hz, 1H), 2.90 (d, J = 11.6 Hz, 1H), 2.42 (m, 1H), 2.37 – 2.25 (m, 2H), 2.18 – 2.04 (m, 1H), 1.92 (ddd, J = 13.6, 11.7, 8.7 Hz, 1H), 1.78 (d, J = 12.9 Hz, 1H), 1.63 – 1.53 (m, 3H), 1.52 – 1.46 (m, 2H), 1.37-1.29 (m, 1H).
^{13}C NMR (100 MHz, $CDCl_3$) δ 164.50, 138.62, 125.84, 62.63, 58.43, 54.22, 48.10, 37.11, 32.18, 31.26, 25.21($2CH_2$).
MS (ESI) m/z $[M + Na]^+$ calcd. for $C_{12}H_{18}N_2ONa$: 229.1317, found: 229.1320.
$[\alpha]_D^{20}$: +16 (*c*= 0.62, $CHCl_3$).

(11aS,12aS)-6,8,9,10,11,11a,12,12a-octahydrodipyrido[1,2-c:1',2'-f]pyrimidin-4(1H)-one (16d).
Yield: 77%
$[\alpha]_D^{20}$: -13 (*c*= 0.70, $CHCl_3$)
MS (ESI) m/z $[M + Na]^+$ calcd. for $C_{12}H_{18}N_2ONa$: 229.1317, found: 229.1321.

Synthesis of racemic mixture of (S)-2-((R)-2-hydroxypent-4-en-1-yl)piperidin-1-ium 2,2,2-trifluoroacetate and (R)-2-((S)-2-hydroxypent-4-en-1-yl)piperidin-1-ium 2,2,2-trifluoroacetate (18).

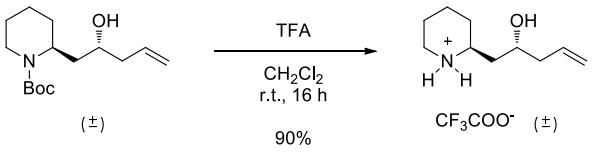

TFA (2.2 mL. 28.0 mmol) was added to a solution of ***anti*-9** (0.500 g, 1.84 mmol, racemic) in anhydrous CH_2Cl_2 (20 mL), cooled at 0°C. The reaction mixture was stirred at room temperature for 16 h, then the solvent was removed under vacuum. The product (light yellow wax) didn't require further purification.

Yield: 90%.

^{1}H NMR (400 MHz, $CDCl_3$) δ 8.36 (bs, 1H), 7.83 (bs, 1H), 5.87 – 5.57 (m, 1H), 5.27 – 5.00 (m, 2H), 4.11 – 3.83 (m, 1H), 3.46 (m, 1H), 3.23 (m, 1H), 3.03 – 2.80 (m, 1H), 2.25 (m, 2H), 2.13 – 1.62 (m, 7H), 1.62 – 1.43 (m, 1H).

^{13}C NMR (100 MHz, $CDCl_3$) δ 161.34, 133.07, 119.19, 71.44, 58.56, 45.05, 42.62, 38.44, 29.68, 22.20 ($2CH_2$) (detected signals).

MS (ESI) m/z calcd. for $[C_{10}H_{20}NO]^+$: 170.1545, found: 170.1544.

Computational Studies

Compounds *syn*- and *anti*-structures (see Figure 5) were optimised at the semiempirical level with the PM6 method.[53] Transition states were built assuming a late transition state, similar in energy to the final products, according to Hammond's postulate. TS and minima were identified through frequency calculation.

Intrinsic reaction coordinate pathway connecting the reactants to the transition state was also computed at the semiempirical PM6 level. All calculations were performed with the Gaussian 2016 package Gaussian 16, Revision B.01.[66]

[66] M. J. Frisch, G. W. Trucks, H. B. Schlegel, G. E. Scuseria, M. A. Robb, J. R. Cheeseman, G. Scalmani, V. Barone, G. A. Petersson, H. Nakatsuji, X. Li, M. Caricato, A. V. Marenich, J. Bloino, B. G. Janesko, R. Gomperts, B. Mennucci, H. P. Hratchian, J. V. Ortiz, A. F. Izmaylov, J. L. Sonnenberg, D. Williams-Young, F. Ding, F. Lipparini, F. Egidi, J. Goings, B. Peng, A. Petrone, T. Henderson, D. Ranasinghe, V. G. Zakrzewski, J. Gao, N. Rega, G. Zheng, W. Liang, M. Hada, M. Ehara, K. Toyota, R. Fukuda, J. Hasegawa, M. Ishida, T. Nakajima, Y. Honda, O. Kitao, H. Nakai, T. Vreven, K. Throssell, J. A. Montgomery, Jr., J. E. Peralta, F. Ogliaro, M. J. Bearpark, J. J. Heyd, E. N. Brothers, K. N. Kudin, V. N. Staroverov, T. A. Keith, R. Kobayashi, J. Normand, K. Raghavachari, A. P. Rendell, J. C. Burant, S. S. Iyengar, J. Tomasi, M. Cossi, J. M. Millam, M. Klene, C. Adamo, R. Cammi, J. W. Ochterski, R. L. Martin, K. Morokuma, O. Farkas, J. B. Foresman, and D. J. Fox, Gaussian, Inc., Wallingford CT, **2016.**

3. Hedgehog signalling pathway as target

3.1 Hedgehog signalling pathway: physiological conditions

Since their isolation in the early 1990s, members of the Hedgehog (Hh) family of intercellular signalling proteins have been identified as fundamental mediators during embryonic development. In fact, Hh signalling pathway is involved in the growth, patterning, and morphogenesis of the different components of vertebrates and invertebrates bodies.[67]

Several studies demonstrated that, during embryogenesis, interactions between cells are fundamental for the regulation of invertebrate and vertebrate development.

It is noteworthy that, despite the different morphological outcome (for example considering a fly and a mammalian), there is a high conservation in the deployment of members of the same signalling families, to regulate the development of these different organisms. Hedgehog pathway is a clear example of this phenomenon.

Hh pathway was initially discovered as a segment polarity gene in *Drosophila melanogaster* embryonic development, thanks to the pioneering work of Nüsslein-Volhard and Wieschaus.[68] During the screening of the possible mutations that could disrupt the Drosophila larval body conformation, it emerged that several of them caused the duplication of denticles (spiky cuticular appendix that are present on the anterior half of each body segment of the larva), as well as the loss of naked cuticle, present on the posterior half of each segment. These malformations result in an ensemble of denticles protruding from the larval cuticle, originating a sort of hedgehog shape that inspired the name of the signalling pathway that, once mutated, was responsible of the abnormal development of the larva.

Further studies demonstrated that Hh pathway is responsible of the patterning of Drosophila wings, legs and eye discs, and that it is involved in the regulation of other processes, such as germ-cell migration, development of the optic lamina, gonad, abdomen, gut and trachea.

Hedgehog genes were identified in also in other invertebrates (e.g. leech, sea urchin, cephalochordate amphioxus); in 1993 vertebrate hedgehog genes were reported in fish, chick and mouse.

It is noteworthy that while in Drosophila only one hh gene was identified, three of them were found in mouse and generally speaking in mammalians: Desert hedgehog

[67] P. W. Ingham, A.P. McMahon, *Genes Dev.* **2001**, *15*, 3059–3087.
[68] E. Christiane Nüsslein-Volhard, Wieschaus, *Nature* **1980**, *287*, 795–801.

(Dhh), Indian hedgehog (Ihh), and Sonic hedgehog (Shh).[69] The first one is the most similar to the Drosophila hedgehog, while the other two are more related to each other and probably represent a more recent gene duplication event.
Sonic hedgehog is of fundamental importance in vertebrate, because its expression appears to be related with the patterning of the neural tube and limb as well as in the formation of the spinal cord.
Further studies confirmed that Hh genes are involved in the embryo development in several organisms. As can be appreciated in Table 1, that summarizes hedgehog pathway functions in vertebrates, the most parts of their body plan are somehow influenced by this signalling.

Table 1[67]

Tissue/organ	Hh signalling	Role
Angiogenesis	Ihh	Stimulate endothelial cells production in yolk sac
Blood cells	Shh Ihh	Stem cells proliferation Activation of hematopoiesis
Bones and cartilages	Shh	Differentiation in endochondral skeleton
Eye	Shh (Ihh, Dhh)	Retinal neurogenesis, astrocyte proliferation in optical nerve
Gut	Shh	Mesenchyme proliferation/inhibition, radial patterning of gut tube, separation of trachea and esophagus
Gonads	Dhh	Testes maturation, male germ line development
Heart	Shh or Ihh	Cardiac morphogenesis
Limbs	Shh	Skeleton patterning, growth of limbs-bud
Lung	Shh	Branching epithelium
Muscle	Shh	Proliferation of muscle precursors
Neurons	Shh	Neural precursors proliferation, survival and death
Pancreas	Shh	Insulin production, inhibition of pancreatic analgem formation
Hair/feather	Shh	Follicle/feathers formation
Tooth	Shh	Growth, morphogenesis, polarity
Olfactory	Shh	Olfactory pathway formation

[69] Y. Echelard, D. J. Epstein, B. St-Jacques, L. Shen, J. Mohler, J. A. McMahon, A. P. McMahon, *Cell.* **1993**, *75*, 1417-1430.

3.1.1 Hedgehog signal transduction: physiological mechanism.

The general signalling mechanism for Hh pathway is conserved from fly to mammal, although in the second case additional components are obviously present.[70] The most important difference concerns the presence of three hedgehog genes instead of one. The key components in mammal Hh signalling molecules are:

- three HH ligands, named after the corresponding genes (Sonic hedgehog—Shh, Indian hedgehog—Ihh and Desert hedgehog—Dhh);
- A Patched receptor (Ptch1 and Ptch2, less common than Ptch1). Ptch 1 is a twelve-pass transmembrane protein;
- A key signal transducer, the so called Smoothened (Smo) protein. Smo is a seven-pass transmembrane domain receptor of the G-protein-coupled receptor (GPCR) superfamily;
- Different zinc-finger transcription factors (GLI). In vertebrates, three different factors exist: Gli1, Gli2 and Gli3. The expression of the corresponding genes is regulated by the ratio of Gli activators (GliA) and Gli repressor (GliR).

In the absence of HH ligands, Smo is inhibited by Ptch1, preventing in this way its migration to the primary cilia (PC). In this situation, the signal transduction is turned off; Smo is present as inactive internalised dimer, composed by two monomers that stay in a close configuration, thanks to electrostatic interactions between arginine and asparagine clusters at the C-terminus. When Smo is inactivated, the Glioma-associated transcriptional mediators (Gli1, Gli2 and Gli3) are retained at the ciliary tip, in complex with a negative regulator, called suppressor of fused (Sufu). In "OFF" condition, Gli2 and Gli3 are present in a phosphorylated form, mediated by protein kinase A (PKA) and glycogen synthase kinase 3β (GSK3β). When Gli2 and Gli3 are phosphorylated they can bind with an adaptor protein, called β-transducin repeat-containing protein (β-TrCP), giving a Gli/β-TrCP complex that is subsequently ubiquinated by the Cul1-based E3 ligase. Ubiquination results in partial proteasomal degradation, that leads to the formation of Gli-transcriptional repressors (Gli2R and Gli3R).[71] These repressors migrate in the nucleus and block Hh target genes expression. A simplified representation of "OFF- Hh pathway" is reported in Figure 7A.[72]

[70] Y. Jia, Y. Wang, J. Xie, *Arch. Toxicol.* **2015**, *89*, 179–191.
[71] E. Y. C. Hsia, Y. Gui, X. Zheng, *Front. Biol.* **2015**, *10*, 203–220.
[72] C. R. Cochrane, A. Szczepny, D. N. Watkins, J. E. Cain, *Cancers* **2015**, *7*, 1554–1585.

The Hh signalling cascade (ON- Hh pathway) is initiated by the binding of one of the HH ligands to Ptch1. This process is facilitated by co-receptors, that form multimolecular complexes with Ptch1, characterised by and increased affinity for the proper HH ligand. Examples of co-receptors are Cdon, Boc and Gas1. The three different HH ligands control the signalling outcome, in a concentration- and duration-dependent manner. For this reason, the reception and signal Hh transduction system should be able to convert different signals into specific outputs.[73]

Upon binding of HH ligands to Ptch1, the inhibition of Smo protein is relieved. The complete mechanisms by which Ptch1 represses or activates Smo hasn't been completely elucidated yet. However, the final result is that Smo is phosphorylated by two kinases (CK1 and Grk2), in an adjacent domain to the C-terminus. The phosphorylation neutralised the electrostatic interactions that previously kept the Smo protein in its closed-inactivated form, promoting an opened-activated conformation. Smo interacts with β-Arrestin (Arrb2) and with a Kif kinesin protein, then is translocated to the primary cilia (PC). Simultaneously, Ptch1 becomes internalised and degraded by lysosomes. The degradation mechanism is still not fully understood.

The presence of an activated Smo form in the primary cilia facilitates the release of full-length Gli activators (GliA) from Sufu, bypassing in this way the proteolytic cleavage leading to the formation of Gli repressors (Gli2R and Gli3R). Gli activators translocate to the nucleus, where Hh target genes are finally activated. These expressed Hh genes include *Gli1, Ptch1 and Hhip*, which are positive and negative regulators of Hh signalling[72,73]. A simplified representation of the activated Hh transduction is reported in Figure 7B.

[73] E. Pak, R. A. Segal, *Dev. Cell* **2016**, *38*, 333–344.

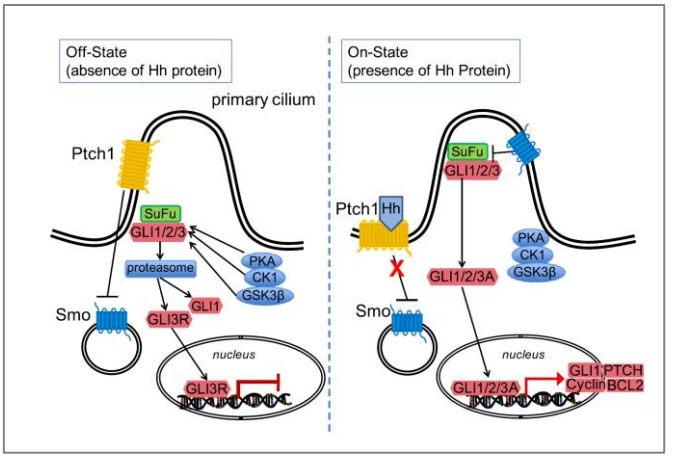

Figure 7. Generic scheme for Hh pathway transduction mechanism, showing the inhibited and activated situations. Adapted from "T. Yoneyama, M. A. Arai, S. K. Sadhu, F. Ahmed, M. Ishibashi, Bioorganic Med. Chem. Lett. 2015, 25, 3541–3544", Copyright 2015, with permission from Elsevier.

As already mentioned, Hh signalling pathway is responsible of several processes involved in the embryonic development in invertebrates and vertebrates, but then is physiologically silenced for the most part of the adult age in different tissue.

However, Hh pathway can be reactivated to promote regeneration processes,[74] for example after an injury, or in the case of stem cells. Stem cells are characterised by self-renewal properties, as well as by the possibility to generates differentiated daughter-cells that will constitute adult organs. It emerged that several Hh components, such as Ptch1, Gli1, and Gli2 are highly expressed in stem-progenitor cells compared with differentiated cells. Moreover, Hh activation promotes stem cells proliferation in several adult tissues, such as skin, blood, gut, prostate, muscle and the nervous system.[75,76,77]

Furthermore, it has been demonstrated that an aberrant activation is involved several diseases, such as Gorlin syndrome[78] and cancer. In these cases, it is also possible that the activation of the gene expression does not occur through the mechanism described above, but Gli transcription factors can be activated by other

[74] A. Beachy Philip, S. Karhadkar Sunil, M. Berman David, *Nature* **2004**, *432*, 324–331.
[75] S. Liu, G. Dontu, I. D. Mantle, S. Patel, N. S. Ahn, K. W. Jackson, P. Suri, M. S. Wicha, *Cancer Res.* **2006**, *66*, 6063–6071.
[76] R. Petrova, A. L. Joyner, *Development* **2014**, *141*, 3445–3457.
[77] J. Jiang, C. chung Hui, *Dev. Cell* **2008**, *15*, 801–812.
[78] L. Pastorino, P. Ghiorzo, S. Nasti, L. Battistuzzi, R. Cusano, C. Marzocchi, M. L. Garré, M. Clementi, G. Bianchi Scarrá, *Am. J. Med. Genet. Part A* **2009**, *149*, 1539–1543.

molecules/signalling, which are independent from HH ligands and Smo. This process is known as a "non-canonical" activation of Hh pathway.
The role of Hh signalling pathway in in cancer development (including non-canonical activations) will be the central topic of the next paragraph.

3.2. Aberrant activation of Hh pathway in cancer.

The first hint that an aberrant activation of Hh signalling pathway could have been involved in carcinogenesis was suggested by studies on Gorlin syndrome. This disease is an autosomal dominant disorder, which results in skeleton and craniofacial malformations. An increased risk in the development of medulloblastoma and advanced basal cell carcinoma (BCC) is evident in patients affected by this syndrome.[79,80]
Different studies demonstrated that a Ptch1 mutation is responsible of Gorlin syndrome and that mutations of Smo, Ptch1 and SUFU were involved in medulloblastomas and BCC. These findings were finally confirmed through experiments performed on transgenic mice, demonstrating that mice presenting mutations in the genes that encode components of the Hh signalling pathway tend to develop BCC, or similar skin tumours.[81]
These findings suggested that may be other tumours type could derive from Hh pathway dysregulations.
This hypothesis was later confirmed by the discovery that rhabdomyosarcoma[82] and meningiomas[83] are related to Ptch1 and Smo mutations; moreover, several other types of cancer appeared to be associated with aberrant Hh signalling. However, in each tumour type, the mechanism underlying the abnormal activation could be quite different.

[79] R. McMillan, W. Matsui, *Clin. Cancer Res.* **2012**, *18*, 4883–4888.
[80] R. L. Johnson, A. L Rothman, J. Xie, L. V. Goodrich, J. W. Bare, J. M. Bonifas, A. G. Quinn, R. M. Myers, D. R. Cox, et. al. *Science* **1996**, *272*, 1668 - 1671.
[81] E. H. Epstein, *Nat. Rev. Cancer* **2008**, *8*, 743–754.
[82] U. Tostar, C. J. Malm, J. M. Meis-Kindblom, L. G. Kindblom, R. Toftgard, A. B. Unden*, J. Pathol.* **2006**, *208*, 17–25.
[83] V. E. Clark, E. Z. Erson-Omay, A. Serin, J. Yin, J. Cotney, K. Özduman, T. Avsar, J. Li, P. B. Murray, O. Henegariu, S. Yilmaz, J. Moliterno Günel, G. Carrión-Grant, B. Yilmaz, C. Grady, B. Tanrikulu, M. Bakircioglu, H. Kaymakçalan, A. O. Caglayan, L. Sencar, E. Ceyhun, A. F. Atik, Y. Bayri, H. Bai, L. E. Kolb, R. M. Hebert, S. B. Omay, K. Mishra-Gorur, M. Choi, J. D. Overton, E. C. Holland, S. Mane, M. W. State, K. Bilgüvar, J. M. Baehring, P. H. Gutin, J. M. Piepmeier, A. Vortmeyer, C. W. Brennan, M. N. Pamir, T. Kiliç, R. P. Lifton, J. P. Noonan, K. Yasuno, M. Günel, *Science*, **2013**, *339*, 1077–1080.

In particular, Hh pathway seems to play three different roles in cancer development: a tumour driving effect, a tumour promoting role and a regulator effect for residual cancer cells.[84]

- Tumour driving effect.

It has been demonstrated that in the development of some types of cancer, such as the aforementioned BCCs, medulloblastomas, rhabdomyosarcoma, and in Barrett's esophagus tumour and some gastrointestinal stomal tumours, the Hh signalling plays a driving function, in the sense that its aberration is the direct cause of cancer.

- Tumour promoting role.

A hedgehog - tumour promoting role was observed in the mouse model of small cell lung cancer (SCLC). Further studies demonstrated that a constitutive activation of Smo protein contributes to aggravate the tumour severity, promoting the clonogenicity of human SCLC in vitro.[85] However, Hh dysregulations are not able to promote cancer development by themselves. For this reason, it is said that in this situation Hh pathway plays only a tumour promoting role.

- Regulator effect for residual cancer cells.

Finally, it could happen that, although Hh pathway is not directly involved in carcinogenesis, it promotes the metastatic process, as occurs in some types of pancreatic cancers.[86] Moreover, Hh signalling appears to be involved in the maintenance of residual cancer cells. These cells survive chemotherapy and are responsible of the relapse in different tumours. A typical example involves the case of cancer stem cells (CSCs), that will be extensively treated in the next chapter.

Considering the strict correlation between cancer and the aberrant activation of Hh pathway, it's evident that the targeting of this signalling is really appealing for applications in anticancer therapy. In fact, in the last decade huge efforts were oriented at the identification and development of potential Hh-inhibitors. Unfortunately, the major pitfall in Hh signalling pathway targeting is that the

[84] D. Gu, J. Xie, *Cancers.* **2015**, *7*, 1684–1698.
[85] K. S. Park, L. G. Martelotto, M. Peifer, M. L. Sos, A. N. Karnezis, M. R. Mahjoub, K. Bernard, J. F. Conklin, A. Szczepny, J. Yuan, R. Guo, B. Ospina, J. Falzon, S. Bennett, T. J. Brown, A. Markovic, W. L. Devereux, C. A. Ocasio, J. K. Chen, T. Stearns, R. K. Thomas, M. Dorsch, S. Buonamici, N. D Watkins, C. D. Peacock, J. Sage, *Nat. Med.* **2011**, *17*, 1504–1508.
[86] G. Feldmann, S. Dhara, V. Fendrich, D. Bedja, R. Beaty, M. Mullendore, C. Karikari, H. Alvarez, C. Iacobuzio-Donahue, A. Jimeno, K. L. Gabrielson, W. Matsui, A. Maitra, *Cancer Res.* **2007**, *67*, 2187–2196.

abnormal activation occurs through different independent mechanisms, that are reported in Figure 8.

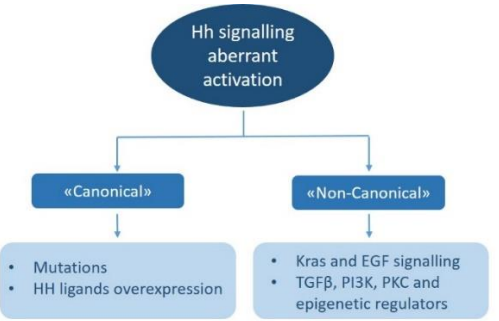

Figure 8. Schematic representation of the possible mechanisms of aberrant activation of Hh signalling.

In humans, one of the most common activation mechanisms involves somatic gene mutations at some of the key players in Hh signalling, such as Ptch1, Smo or Sufu, that finally result in the aberration of the whole pathway.

On the other hand, a different mode of activation involves the over-expression of hedgehog ligands, resulting either in autocrine or paracrine Hh signalling. In the first case, found for example in SCLC, colorectal and prostate carcinomas, tumour cells simultaneously secrete and respond to the overexpressed HH ligands.[87] However, Hh signalling is often a reciprocal paracrine process, in which the overexpressed HH ligands secreted by tumour cells interact with stromal cells in the tumour microenvironment, inducing these cells to enhance the production of factors that stimulate the growth of the tumour. This mechanism is present in several lymphomas and multiple myeloma.[79,88]

The aforementioned modes of action belong to the so-called “canonical activations”. This means that, despite the aberrations concerning mutations or overexpression of HH ligands, the signal transduction follows the “canonical” activation scheme depicted in the previous paragraph.

However, Hh signalling may be activated in a non-canonical fashion, when Gli transcription factors are activated independently of the presence of an HH ligand bound to Ptch. In these cases, the activation is induced by other molecules or signalling pathways.

[87] D. N. Watkins, D. M. Berman, S. G. Burkholder, B. Wang, P. A. Beachy, S. B. Baylin, *Nature* **2003**, *422*, 313–317.

[88] C. Dierks, J. Grbic, K. Zirlik, R. Beigi, N. P. Englund, G. R. Guo, H. Veelken, M. Engelhardt, R. Mertelsmann, J. F. Kelleher, P. Schultz, M. Warmuth, *Nat. Med.* **2007**, *13*, 944–951.

Among the entities that can escape the strict ligand-Ptch1 receptor promoted signalling, Kras and EGF signalling, TGFβ, PI3K, PKC and epigenetic regulators are the most important.[84]

3.2.1 The role in CSCs proliferation

The proved role of Hh signalling in stem cells self-renewal and proliferation, as well as in cancer development, clearly suggests that a similar influence could be exerted on cancer stem cells.

Cancer stem cells are a subpopulation of cancer cells, characterised by the ability to indefinitely regenerate themselves and to originate differentiated daughter tumour cells, a behavior typical of all the stem cells. [89]

Since their identification in human acute myeloid leukemia in 1994,[90] CSCs appeared to be responsible of carcinogenesis, tumour growth, and relapse. This theory has been then confirmed and several CSCs populations where found in different human tumours, such as brain, breast, colon, pancreatic and prostate cancers, as well as in melanoma.[91]

As represented in Figure 9, CSCs are unaffected by traditional anticancer therapies (namely chemotherapy and radiation). Therefore, after a certain period of time since the apparent successful treatment, the survived CSCs core begins to self-regenerate and, more importantly, to differentiate themselves into new tumour-bulk cells. This mechanism results in tumour recurrence and drug resistance.[92]

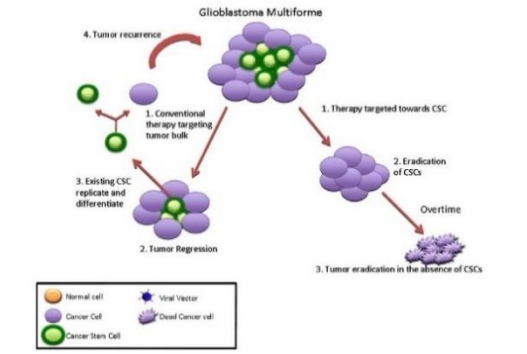

Figure 9. Representation of the cancer stems cells hypothesis. Adapted from ref [93]. Copyright (2009), with permission from Elsevier.

[89] B. T. Tan, C. Y. Park, L. E. Ailles, I. L. Weissman, *Lab. Investig.* **2006**, *86*, 1203–1207.
[90] T. Lapidot, C. Sirard, J. Vormoor, B. Murdoch, T. Hoang, J. Caceres-Cortes, M. Minden, B. Paterson, M. A. Caligiuri, J. E. Dick, *Nature* **1994**, *367*, 645–648.
[91] J. Koury, L. Zhong, J. Hao, *Stem Cells Int.* **2017**, *2017*, 1–10.
[92] C. Delude, *Nature*, **2011**, *480*, S43–S45.
[93] M. Dey, I. V. Ulasov, M. S. Lesniak, *Cancer Lett.* **2010**, *289*, 1–10.

But why CSCs are unaffected by traditional therapies?
Generally speaking, conventional anticancer drugs are able to discriminate between healthy and cancer cells on the basis of the proliferation rate. In fact, cancer cells undergo a very rapid division and, for this reason are targeted by anticancer therapies. However, CSCs are slow dividing cells and can remain in a quiescent state for a long time, appearing more similar to the healthy cells that should escape the drug treatment. Moreover, CSCs are apoptosis-resistant cancer cells and they overexpress some specific transporter belonging to the ATP binding cassette (ABC) family, that are able to pump the drug outside the cell.[94] The resistance against radiotherapy could derive from efficient DNA repair mechanisms and from hypoxia, that is beneficial to contrast the reactive oxygen species.[95] The mechanisms responsible of drug resistance are summarised in Figure 10.

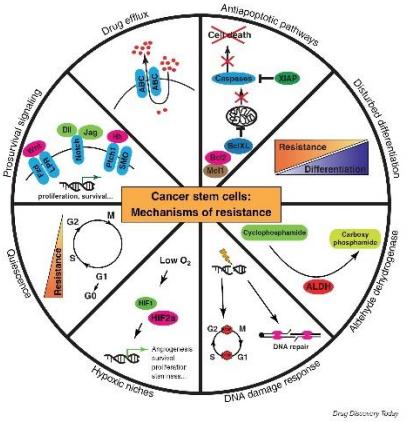

Figure 10. Molecular mechanisms of CSCs resistance to anticancer therapy.[96]

As result of these mechanisms, traditional therapies fail to recognize the differences in gene expression of different cells within individual tumours.
For this reason, the eradication of the CSCs core from the tumour bulk, exploiting a proper CSCs-targeted therapy, should be an optimal way to achieve a durable response in the cure of cancer.
Nowadays, the most common approaches available to contrast CSCs proliferation are the administration of oncolytic viruses and the targeting of the signalling pathways responsible of their maintenance.

[94] M. Dean, T. Fojo, S. Bates, *Nat. Rev. Cancer* **2005**, *5*, 275–284.
[95] M. Diehn, R. W. Cho, N. A. Lobo, T. Kalisky, M. J. Dorie, A. N. Kulp, D. Qian, J. S. Lam, L. E. Ailles, M. Wong, B. Joshua,M. J. Kaplan , I. Wapnir, F. M. Dirbas, G. Somlo, C. Garberoglio, B. Paz, J. Shen, S. K. Lau, S. R. Quake, J. M. Brown, I. L. Weissman, M. F. Clarke, *Nature* **2009**, *458*, 780–783.
[96] P. A. Sotiropoulou, M. S. Christodoulou, A. Silvani, C. Herold-Mende, D. Passarella, *Drug Discov. Today* **2014**, *19*, 1547–1562.

Oncolytic viruses are particular viruses that replicate selectively in cancer cells, spreading within the tumour and killing these cells without harming normal tissues. Their action is based on the fact that the properties that allow cancer cells to proliferate, also make them better host for the viruses. For example, cancer cells often lack proper immune defence mechanisms, because they have to escape the detection by the immune system of the host organism. However, this makes cancer cells more sensible to virus invasion. Moreover, the deregulation of the physiological apoptosis mechanism, which is at the basis of cancer cells proliferation, results in a sort of "double-edge blade", because the tumour can't eliminate the infected cancer cells, allowing the diffusion of the virus through its bulk.[97,98]

The targeting of the prosurvival signalling pathways underlying the self-renewal and differentiation mechanisms is another efficient strategy to contrast CSCs. In the last years, several efforts were oriented at identifying drugs acting on these signalling pathways. Among them, Hedgehog, Wnt, Notch, insulin growth factor (IGF), nuclear factor (NF)-kB, Janus kinase/signal transducers and activators of transcription (JAK/STAT) pathways and bone morphogenetic proteins are preferentially activated in CSCs, and therefore constitute promising targets for anticancer treatment.[96]

Data inferred from several human tumours (i.e. glioblastoma, breast and pancreatic cancer, chronic myeloid leukemia, multiple myeloma), suggest a prominent role of Hh pathway in CSCs, as demonstrated by the higher levels of signalling in these type of cells than in the tumour bulk.[99] Hh pathway appears to be involved in CSCs proliferation, regulating the production of stemness-determining genes, similarly to the physiological role in healthy stem cells. Hh signalling appears to be involved in both the self-renewal and differentiation processes. [72,100]

This assumption is supported by several experimental proves. Some examples are reported below.

Experiments performed on mice models of chronic myeloid leukemia, demonstrated that the loss of Hh signalling by genetic modification of Smo protein led to the inhibition of leukemic stem cells, accompanied by a prolonged beneficial effect. [101]

Inhibition of Hh signalling in breast cancer, through the administration of cyclopamine (a well-known Smo binder), or siRNA resulted in the alteration of the expression of

[97] S. Chaurasiya, N. G. Chen, S. G. Warner, *Cancers* **2018**, *10*, 124.
[98] G. Y. Gillespie, J. Roth, G. Friedman, T. Smith, *Oncolytic Virotherapy* **2014**, *3*, 21–33.
[99] C. D. Peacock, Q. Wang, G. S. Gesell, I. M. Corcoran-Schwartz, E. Jones, J. Kim, W. L. Devereux, J. T. Rhodes, C. A. Huff, P. A. Beachy, D. N. Watkins, W. Matsui, *Proc. Natl. Acad. Sci.* **2007**, *104*, 4048–4053.
[100] A. A. Merchant, W. Matsui, *Clin. Cancer Res.* **2010**, *16*, 3130–3140.
[101] C. Zhao, A. Chen, C. H. Jamieson, M. Fereshteh, A. Abrahamsson, J. Blum, H. Y. Kwon, J. Kim, J. P. Chute, D. Rizzieri, M. Munchhof, T. VanArsdale, P. A. Beachy, T. Reya, *Nature* **2009**, *458*, 776–779.

BMI-1, which is a key player in the self-renewal mechanism of normal stem cells.[75] These two Hh inhibitors also led to the loss of tumourigenic potential in glioblastoma CSCs.[102] On the other hand, other experiments proved that Hh pathway activation was beneficial to CSC self-renewal and proliferation.

These findings indicate that Hh signalling contributes to the determination of CSCs fate, regulating self-renewal and differentiation processes as well as the interactions between CSCs and differentiated tumour cells.

3.3 Inhibition of Hedgehog pathway in anticancer therapy.

The strict relation between Hh pathway aberrant activation and carcinogenesis processes, including CSCs maintenance, attracted the interest of the scientific community in the last decade and Hh inhibition emerged as a really promising strategy exploitable in anticancer therapy.

The inhibition can occur at different levels of the signalling mechanism. Generally speaking, three are the main possibilities, summarised also in Figure 11:

- Upstream Smo protein inhibition.
- Direct inhibition of Smo protein.
- Inhibition of Gli-mediated transcription or Gli factors.

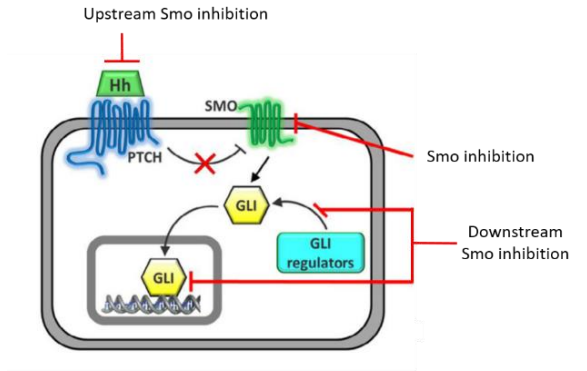

Figure 11. Schematic representation of the possible inhibition strategies of Hh pathway. Adapted from ref [103], Copyright (2018), with permission from Elsevier.[103]

[102] V. Clement, P. Sanchez, N. de Tribolet, I. Radovanovic, A. Altaba, *Curr Biol.* **2007**, *17*, 165– 172.
[103] F. Ghirga, M. Mori, P. Infante, *Bioorganic Med. Chem. Lett.* **2018**, *28*, 3131–3140.

Upstream inhibition of Smo protein

The first strategy consists in the targeting of "players" involved in the earliest stages of Hh signalling, before Smo protein activation. Examples of this type of targets include Sonic HH ligands, Hh acyl transferase (Hhat), an enzyme involved in the release of the activating HH ligands in the cell, and Liver X receptors (LXRs), which are negative regulator of the active HH ligands. However, the upstream targeting of Smo protein isn't a really effective method to inhibit Hh pathway.[104] In fact, despite the achieved inhibition of one of the aforementioned targets, Hh pathway can be activated at a downstream level, rendering this strategy ineffective. Moreover, reported binders of SHH, Hhat and LXRs displayed only a limited inhibitory activity on Hh pathway.

Inhibition of Smo protein

So far, the direct inhibition of Smo protein proved to be the most investigated technique. As a proof, several potent Smo inhibitors have been developed in the last years (and will be reported in paragraph 3.3.1) and some of them recently entered the clinical trials. Three of them, vismodegib (Erivedge®), sonidegib (Odomzo®) and glasdegib (Daurismo)™ were approved by the FDA for the treatment of metastatic and locally advanced basal cell carcinoma and myeloid leukemia, in 2012, 2015 and 2018, respectively.[105,106,107] The success of this strategy is probably due to the elucidation of Smo receptor X-ray structure,[108] also in complex with small ligands, that allows a more rational design of potential inhibitors, exploiting *in-silico* techniques. The most relevant information about the structure are reported in the box below.

Structural elucidation of Smo protein: X-rays studies

The characterizing structural features of Smo protein were identified on the basis of X-rays analysis of the protein itself complexed with different small ligands. One of the first crystal structures was elucidated by Wang *et. al.* and in that case Smo protein was complexed with the agonist Taladegib.[108] This study demonstrated that SMO protein receptor presents the stereotypical seven-pass α-helix trasmembrane bundle domain (TMD) of class A GPCRs, while the other conserved motifs typical of A GPCRs are absent. Smo protein presents two additional domains. The first one is the so called

[104] M. Xin, X. Ji, L. K. De La Cruz, S. Thareja, B. Wang, *Med. Res. Rev.* **2018**, *38*, 870–913.
[105] S. Berardozzi, F. Bernardi, P. Infante, C. Ingallina, S. Toscano, E. De Paolis, R. Alfonsi, M. Caimano, B. Botta, M. Mori, L. Di Marcotullio, F. Ghirga, *Eur. J. Med. Chem.* **2018**, *156*, 554–562.
[106] T. Rimkus, R. Carpenter, S. Qasem, M. Chan, H.-W. Lo, *Cancers* **2016**, *8*, 22.
[107] K. K. Chahal, M. Parle, R. Abagyan, *Anticancer. Drugs* **2018**, *29*, 387–401.
[108] C. Wang, H. Wu, V. Katritch, G. W. Han, X.-P. Huang, W. Liu, F. Y. Siu, B. L. Roth, V. Cherezov, R. C. Stevens, *Nature* **2013**, *497*, 338–343.

extracellular domain (ECD), constituted by a complex arrangement of long extracellular loops stabilised by four disulphide bonds. This complex domain is organised in two different parts: the extracellular cysteine-rich domain (CRD) and the ECD linker domain. The second additional domain is the intracellular carboxy-terminal domain. Considering these differences with A GPCRs, Smo protein is classified as a Frizzled-class GPCR.[109] The generic structure of Smo, presenting the division into the different domain is reported in Figure 12.

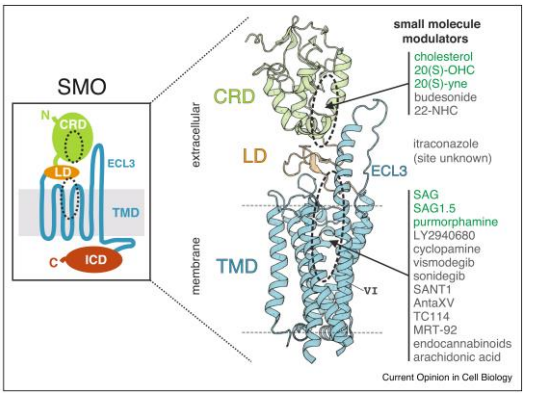

Figure 12. Overall structure of SMO, displaying the extracellular region, constituted by the cysteine rich domain CRD (green) and the extracellular linker domain LD (orange), the seven-pass a-helical transmembrane domain (TMD, blue) and the intracellular domain (ICD, red). This picture indicates also the two binding sites of Smo (dashed circles), together with some examples of binders (agonists in green, antagonists in grey). Adapted from ref [109], Copyright (2017), with permission from Elsevier.

Smo modulation involves at least two binding sites. The first one is located between the TMD and the ECLs. This site is characterised by a long and narrow conformation and it connected to the extracellular environment through a small orifice, formed by the ECD linker domain. It seems that this opening allows the access of small molecules in the binding site.

The TMD site is targeted by Taladegib (LY2940680 in the Figures), cyclopamine, vismodegib, sonidegib, and other agonists and antagonists reported in Figure 12.[109,110] In Wang's work, the binding of taladegib in this TMD site was reported. Notably, the receptor crystallised as a parallel dimer (Figure 13), with helices IV and V at the interface between the two units. This finding is coherent with the dimeric structure that Smo seems to possess in cellular membrane.

[109] E. F. Byrne, G. Luchetti, R. Rohatgi, C. Siebold, *Curr. Opin. Cell Biol.* **2018**, *51*, 81–88.

[110] C. Wang, H. Wu, T. Evron, E. Vardy, G. W. Han, X.-P. Huang, S. J. Hufeisen, T. J. Mangano, D. J. Urban, V. Katritch, V. Cherezov, M. G. Caron, B. L. Roth, R. C. Stevens, *Nat. Commun.* **2014**, *5*, 4355.

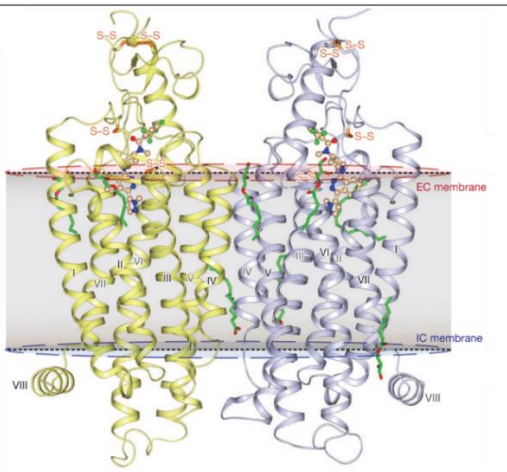

Figure 13. Dimeric structure of Smo, complexed with Taladegib. Adapted by permission from Nature/Springer, according to ref 108, copyright 2013.

The second Smo binding site is located on the CRD, and is characterised by a shallow hydrophobic cavity. This groove can harbor well cholesterol and oxysterols in general (Figure 12). TMD and CRD binding sites are located in different domains, but they seem to be allosterically linked. CRD binding site is quite important for Smo activation. In fact, it has been demonstrated that cholesterol is a Smo agonist, that binds to CRD contributing to Smo conformational transition from the inactive form to the active one, disrupting a π-cation interaction. Recent studies revealed that cholesterol can activate Hh signalling, also in the absence of HH ligands.[111]

The comparison between two X-ray structures of active SMO, bound to cholesterol and cyclopamine, respectively, demonstrated that the CRD undergoes a drastic reorientation. This could be a proof of the allosteric relationship between the two binding sites in Smo. The binding of cholesterol to CRD activates also the TMD, that assumes the proper shape to host small molecule binders, proving the allosteric communication between the binding sites.[112] Notably, cholesterol could be a mediator of the interaction between Ptch1 and Smo: in fact, Ptch1 exerts its inhibitory activity toward Smo forbidding the interaction between cholesterol and Smo.

[111] P. Huang, D. Nedelcu, M. Watanabe, C. Jao, Y. Kim, J. Liu, A. Salic, *Cell* **2016**, *166*, 1176-1187.
[112] P. Huang, S. Zheng, B. M., Y. Kim, D. Nedelcu, L. Aravena, J. Liu, A. C. Kruse, A. Salic, *Cell* **2018**, *174*, 312–324.

Unfortunately, the use of Smo inhibtors in anticancer therapy is limited by two factors: the development of drug resistance as consequence of mutations in Smo protein, and the possibility of a downstream activation of Hh pathway at the level of Gli transcriptional regulators. [103,107,113,]

The first evidence of resistance to a Smo inhibitor was found in a medulloblastoma patient, that had been treated with vismodegib. After a good initial response to the therapy, this patient developed a relapse and died. Sequencing of the tumour DNA showed a mutation of Smo protein, arising from the replacing of an aspartic acid with a histidine residue.[114] Moreover, this mutated Smo activated the Hh signalling, similarly to the wild type version, and also in the absence of Ptch1 activity. Thus, an apparent minimal modification in Smo residues appears to drastically reduce the affinity of a potent binder such as vismodegib for the binding site. The effect is more marked if these mutations are located nearby the antagonist site.

An analogous situation emerged with sonidegib, leading to the identification of five distinct mutantions, and other studies demonstrated that this kind of drug-resistance mechanism was developed for several other not-approved Smo inhibitors.[115, 116,117]

In addition, Smo inhibition can be frustrated by genetic downstream modifications, such as Smo-independent hyperactivation of Gli transcriptional factors, Sufu modification or the already mentioned non-canonical Hh activations. These modifications were responsible of the displayed resistance in medulloblastoma and basal cell carcinomas.[84]

For this reason, Hh signalling pathway inhibition at Gli level could appear as a most reliable approach to escape drug resistance. However, also this strategy presents some drawbacks, as reported in the following section.

[113] E. Peer, S. Tesanovic, F. Aberger, *Cancers* **2019**, *11*, 538.

[114] R. L. Yauch, G. J. P. Dijkgraaf, B. Alicke, T. Januario, C. P. Ahn, T. Holcomb, K. Pujara, J. Stinson, C. A. Callahan, T. Tang, J. F. Bazan, Z. Kan, S. Seshagiri, C. L. Hann, S. E. Gould, J. A. Low, C. M. Rudin, F. J. de Sauvage, *Science* **2009**, *326*, 572–574.

[115] S. X. Atwood, K. Y. Sarin, R. J. Whitson, J. R. Li, G. Kim, M. Rezaee, M. S. Ally, J. Kim, C. Yao, A. L. S. Chang, A. E. Oro, J. Y. Tang, *Cancer Cell* **2015**, *27*, 342–353.

[116] S. Buonamici, J. Williams, M. Morrissey, A. Wang, R. Guo, A. Vattay, K. Hsiao, J. Yuan, J. Green, B. Ospina, Q. Yu, L. Ostrom, P. Fordjour, D. L. Anderson, J. E. Monahan, J. F. Kelleher, S. Peukert, S. Pan, X. Wu, S. Maira, C. García-Echeverría, K. J. Briggs, D. N. Watkins, Y. Yao, C. Lengauer, M. Warmuth, W. R. Sellers, M. Dorsch, *Sci. Transl. Med.* **2010**, *2*, 51ra70.

[117] C. Wang, H. Wu, T. Evron, E. Vardy, G. W. Han, X.-P. Huang, S. J. Hufeisen, T. J. Mangano, D. J. Urban, V. Katritch, V. Cherezov, M.G. Caron, B.L. Roth, R.C. Stevens, *Nat. Commun.* **2014**, *5*, 4355.

Inhibition of Gli-mediated transcription or Gli factors

The pharmacological modulation of Gli transcriptional regulators is probably considered the most promising strategy to block Hh signalling. Considering that Gli factors are involved in the final stage of the signalling, it's clear that their inhibition could escape downstream activations.

In particular, chemical entities able to target Gli1 or the post- translational modifications that control Gli functions, should be good candidates to inhibit the expression of Gli-target genes.[118,119] However, the lack of a completely elucidated structure of the possible binding sites made the development of this strategy really challenging. Nowadays, only a quite limited number of inhibitors has been disclosed and for most of them the mechanism of action hasn't been totally elucidated.

So far, only few of them entered the clinical trials and arsenic trioxide (Trisenox®) is the only Gli1 binder that gained FDA approval for the treatment of acute promyelocytic leukemia.[120]

Thus, despite the great potentiality of this approach, the inhibition of Hh signalling through Smo targeting is still the most common strategy and the aforementioned drawbacks could be overcame exploiting a combined approach.[121]

The administration of a drugs cocktail is increasingly becoming a paradigm in anticancer therapy, to obtain an enhanced efficacy –given by the simultaneous action on multiple targets- and to prevent the induction of drug resistance by the single components.

In this context, several studies reported the combined use of vismodegib or sonidegib with other anticancer agents,[106,122] as well as the combination of GANT-61, a Gli-inhibtor with rapamycin,[123] to treat a wide range of malignancies. Moreover, a really interesting study reported the simultaneous targeting of Smo and Gli factors, through the administration of itraconazole and ATO, with promising *in vivo* results for the treatment of medulloblastoma and basal cells carcinoma.[124]

Thus, in particular in the field of combined therapy, the search for new potent Smo inhibitors is still of great importance: this will be the goal of the work presented in this

[118] E. Peer, S. Tesanovic, F. Aberger, *Cancers.* **2019**, *11*, 538.
[119] P. Infante, R. Alfonsi, B. Botta, M. Mori, L. Di Marcotullio, *Trends Pharmacol. Sci.* **2015**, *36*, 547–558.
[120] A. List, M. Beran, J. Di Persio, J. Slack, N. Vey, C. S. Rosenfeld, P. Greenberg, *Leukemia* **2003**, *17*, 1499–1507.
[121] B. Al-Lazikani, U. Banerji, P. Workman, *Nat Biotechnol.* **2012**, *30*, 679-692.
[122] B. Biehs, G. J. P. Dijkgraaf, R. Piskol, B. Alicke, S. Boumahdi, F. Peale, S. E. Gould, F. J. A. de Sauvage, F.J. A, *Nature* **2018**, *562*, 429–433.
[123] D. Pan, Y. Li, Z. Li, Y. Wang, P. Wang, Y. Liang, *Leuk Res.* **2012**, *36*, 742-748.
[124] J. Kim, B. T. Aftab, J. Y.Tang, D. Kim, A. H.Lee, M. Rezaee, J. Kim, B. Chen, E. M. King, A. Borodovsky, G. J. Riggins, E. H. Epstein Jr, P. A. Beachy, C. M.Rudin, *Cancer Cell*. **2013**, *23*, 23-34.

chapter. But before entering in the details of the design and synthesis of our potential Smo inhibitors, a brief summary of the known most important member of this family will be given in the following paragraph.

3.3.1 Smo inhibitors: a brief overview.

In this section, some important Smo inhibitors, approved by FDA or currently in the clinical trials, will be presented. This preference is justified considering our aim to design new potential Smo inhibitors.

As already mentioned, the development of Smo inhibitors has been a hot topic in the last decade and the vastness of the identified Smo-binders preclude the possibility to be exhaustive in their description. For this reason, only few characteristic examples will be reported. However, several reviews are available on this topic.[103,106,125]

The idea of targeting Hh signalling pathway began with the discovery of the SMO-inhibitory activity of Cyclopamine, a steroidal alkaloid extracted from *Veratrum californicum*.[126] This compound was used to a great extent as a model to study Hh signalling inhibition in cells. Unfortunately, despite the high potential as Smo binder, its clinical applications were limited by the severe off-target side effects, including weight loss, muscle spasm, nausea, fatigue and diarrhea. Moreover, cyclopamine is a teratogen compound. The origin of its name is quite curious and it is related to "cyclopia", a malformation observed in some lambs born in the West U.S.A., back in 1950's. The cyclopia was caused by the teratogenic effect of *Veratrum californicum*, that was accidentally eaten by pregnant sheep.[127] However, the elucidation of the Smo-related activity of cyclopamine, prompted the scientific community to develop new inhibitors, characterised by a better therapeutic profile.

This is the case of Vismodegib, the first Shh pathway inhibitor to gain the approval of FDA, in 2012, for the treatment of metastatic or recurrent BCC in adult patients that can not be cured with surgery or radiotherapy. Unfortunately, further studies demonstrated that vismodegib use can induce drug resistance, due to a mutation in Smo protein. Currently, vismodegib is studied in several clinical trials, on a wide range of tumours, as monotherapy and also in combination with other drugs.

Another approved Smo inhibitor for the treatment of cancer patients is Sonidegib. This orally bioavailable compound appears to induce cellular apoptosis in several cancer cell lines affecting both tumour epithelial cells and CSCs. The applications in anticancer therapy are quite similar to Vismodegib, in fact it is currently employed to

[125] H. J. Sharpe, W. Wang, R. N. Hannoush, F. J. De Sauvage, *Nat. Chem. Biol.* **2015**, *11*, 246–255.
[126] J. K. Chen, J. Taipale, M. K. Cooper, P. A. Beachy, *Genes Dev.* **2002**, *16*, 2743–2748.
[127] J. K. Chen, *Nat Prod Rep.* **2016**, *33*, 595–601.

treat locally advance BCC in adult, when surgery and radiotherapy are useless. Further phase I/II trials are in progress on solid and hematological tumours.

A different class of Smo binders include phthalazine derivatives, such as Anta XV and Taladegib. The former is a potent Hh inhibitor with marked affinity for SMO protein, but characterised by poor water solubility and inhibition of hERG (a protein that constitutes part of potassium ion channels) as side effects. The latter is currently in phase II trials, in combination with taxol, carboplatin, and radiation for the treatment of esophagus adenocarcinoma. It is noteworthy that Taladegib overcomes the D473H SMO mutation, responsible of drug resistance. For this reason, it can be used as a first line treatment, in all of the cases in which that mutation limits the employment of other Smo-antagonists.

Another compound that recently obtained FDA approval (November 2018) is Glasdegib, a Smo inhibitor able to interfere with leukemia-initiation and with leukemia stem cell dormancy. In fact, nowadays it is used in combination with cytarabine for the treatment of acute myeloid leukemia in over 75 years old patients that cannot be cured with intensive chemotherapy. Some studies suggest that Glasdegib also inhibit GLI2 factor. Further clinical trials are in progress.[128]

A quite particular case is represented by Itraconazole. This compound is a licensed antifungal agent, used for the treatment of several fungal infections, such as aspergillosis, coccidioidomycosis and candidiasis. In a screening of drugs already tested on human it emerged as a potent Hh-pathway inhibitor. However, differently from other Smo-inhibitors, it elicits its action forbidding the migration of Smo protein in the primary cilium during the aberrant activation of Hh signalling. Despite limitation given by adverse effects (typical of similar antifungal compounds) and drug-drug interactions, Phase II clinical trials are ongoing for the treatment of BCC. [129]

The structures of all the mentioned Smo inhibitors are reported in Figure 14.

[128] S. M. Hoy, *Drugs* **2019**, *79*, 207-213.

[129] J. Kim, J. Y. Tang, R. Gong, J. Kim, J. J. Lee, K. V. Clemons, C. R. Chong, K. S. Chang, M. Fereshteh, D. Gardner, T. Reya, J. O. Liu, E. H. Epstein, D. A. Stevens, P. A. Beachy, *Cancer Cell* **2010**, *17*, 388–399.

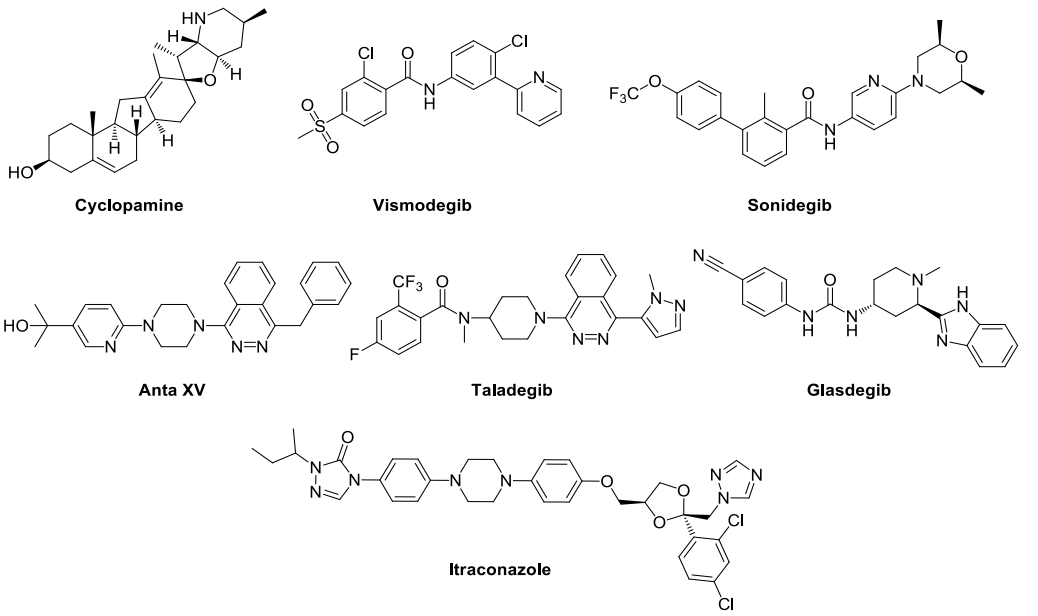

Figure 14. Structures of approved or in clinical trials Smo inhibitors.

3.3.2. Withanolides and withanolide-like compounds as Hh pathway inhibitors

The list of the Hh-inhibitors reported in the previous section can be enriched considering the class of withanolides. Withanolides are a wide family of natural products (more than 300 members), present as secondary metabolites in plant belonging majorly to the genera of the solanaceae family. Whitanolides share a common scaffold, characterised by two fundamental moieties: an ergostane-like steroid part and a lactone (or a lactone derivative). They are well-known for their pharmacological potential, based on a wide range of bioactivities, including adaptogenic, diuretic, cytotoxic, sedative, anti- inflammatory and immunomodulatory.[130] The ability of these compounds to cross the blood brain barrier justifies also their neuroprotective properties.[131]

Whitaferin A (Figure 15) was the first member of this family to be isolated from *Withania Somnifera*, in 1965. In addition to the aforementioned pharmacological activities, Withaferin A displays interesting anticancer properties, depending on the simultaneous targeting of different signalling pathways, including Hedgehog. In this

[130] P. T. White, C. Subramanian, H. F. Motiwala, M. S. Cohen, *Anti-Inflammatory Nutraceuticals and Chronic Diseases*, Springer International Publishing, Cham, **2016**, 329-371.
[131] G. Kumar, R. Patnaik, *Med. Hypotheses* **2016**, *92*, 35–43.

context the mechanism of action has not be completely elucidated, but it Withaferin A and other naturally occurring structurally related withanolides such as 27-deoxywithaferin A, 24-5,6-deoxywithaferin A or 2,3-dihydro-3-b-O-sulfatewithaferin A appear to suppress the expression of Hh signalling pathway target proteins. The inhibition involved GLI1, Ptch, BCL-2 (another Hh target protein) and the formation of GLI1-DNA complex.[132]

In 2015, Waldmann *et. al.* published an innovative study, based on the Biology-oriented synthesis (BIOS) of withanolides-inspired modulators of Hh signalling.[133] BIOS aims at exploiting the intrinsic biological relevance of natural products and their structural characteristics to guide the design of new collection of derivatives, that should be enriched in in diverse biological effects. In this case, a common motif was searched in several active withanolides (including Withaferin A) and the fundamental scaffold that emerged (**IV**) was characterised by the presence of an unsaturated lactone, connected by a methylene linker to a *trans*-hydrindane bicycle, which is a simplification of the steroid portion typical of withanolides (Figure 15). This scaffold was used as starting point for the design and synthesis of a library on withanolides-inspired analogs, characterised by different substitution patterns. The validity of this approach was confirmed by the results of biological test: some compounds of this library inhibited Smo protein efficiently. The best result was obtained for compound **V** (structure reported in Figure 14), that competed with cyclopamine for the binding, giving a K_i = (57 ± 10) nM.

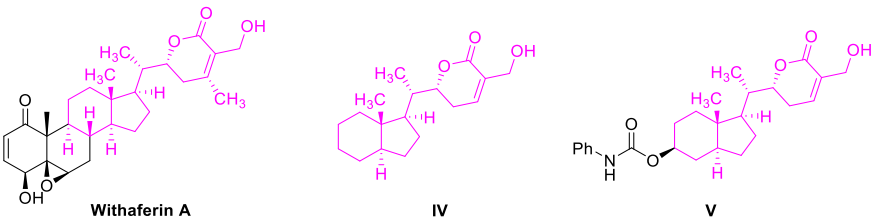

Figure 15. Structures of: Withaferin A, chosen as representative example of withanolides; **IV**, the simplified fundamental scaffold; **V**, the best Smo inhibitor emerged by Waldmann's studies.

[132] T. Yoneyama, M. A. Arai, S. K. Sadhu, F. Ahmed, M. Ishibashi, *Bioorganic Med. Chem. Lett.* **2015**, *25*, 3541–3544.

[133] J. Švenda, M. Sheremet, L. Kremer, L. Maier, J. O. Bauer, C. Strohmann, S. Ziegler, K. Kumar, H. Waldmann, *Angew. Chemie - Int. Ed.* **2015**, *54*, 5596–5602.

3.4 Rational design and synthesis of new inhibitors

Since 2015, when in the Passarella's laboratories a small library of triazole bioisosteres of Vismodegib was successfully synthesised,[134] our interest in the targeting of Hh signalling pathway in anticancer therapy (and in particular against CSCs) has increasingly growth.

This prompted us to develop a new potential inhibitor.

When we began to plan its design, we considered several factors.

First of all, we decided to take inspiration from nature. Natural products are still one of the most important sources for drug discovery and the structural modification of an already active compound is usually a good starting point to obtain new derivatives characterised by a certain biological effect.[135,136]

In particular, we were attracted by withanolides, that appear to inhibit Hh pathway at different levels.[132]

Waldmann's work demonstrated the importance of the withanolides α,β-unsaturated lactone, and the structure of his most active analog **V** suggested that a carbamate could be beneficial for the bioactivity. These data gave us the idea of combining the fundamental lactone with a carbamate generated on 2-piperidine ethanol, in order to explore another branch or our diversification approach (Scheme 21).

To rationally decide how to connect together these two moieties, we took advantage of docking simulations, performed in Smo protein binding site.

The result is compound **19**, reported in Figure 16, together with Withaferin A and Waldmann's simplified scaffold **IV**.

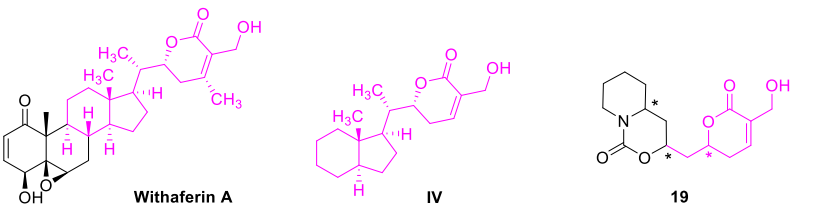

Figure 16. comparison between our scaffold **19** and withaferin A and **IV**. The common portion are coloured in pink.

Docking studies confirmed the intrinsic importance of the α,β-unsaturated lactone for the interaction with Smo protein binding site and for this reason it was maintained

[134] M. S. Christodoulou, M. Mori, R. Pantano, R. Alfonsi, P. Infante, M. Botta, G. Damia, F. Ricci, P. A. Sotiropoulou, S. Liekens, B. Botta, D. Passarella, *ChemPlusChem* **2015**, *80*, 938-943.

[135] D. J. Newman, G. M. Cragg, *J. Nat. Prod.* **2016**, *79*, 629–661.

[136] F. E. Koehn, G. T. Carter, *Nat. Rev. Drug Discov.* **2005**, *4*, 206–20.

unchanged. It was then connected with a rigid bicyclic carbamate, that replaced the steroid moiety of Withaferin A, or the *trans*- hydrindane bicycle of **IV**.
As reported in Figure 17, our scaffold fits well in Smo trasmembrane bundle domain (TMD) binding site and the carbonyl group of the carbamate could give a favourable interaction with the Arg400 residue. The superimposition of **19** with Taladegib showed that they adopt more or less the same spatial disposition in Smo binding site.

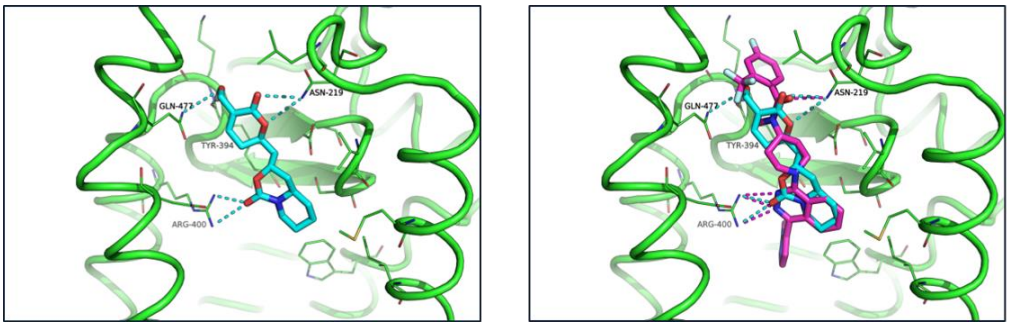

Figure 17. Docking simulation of **19** in Smo protein TMD binding site, showing the fundamental interaction with Arg400 (left). Superimposition of **19** (cyan) with Taladegib (pink), displaying a similar binding mode.

Compound **19** should be obtained as another branch of our DOS library, starting from 2-piperidine ethanol and exploiting the key intermediate **9**. In Scheme 22 the final forward synthetic route, that was the result of several failed attempts, is summarised. In this case an oxidative cleavage of the double bond, afforded an aldehyde that was allylated as in the case of product **7**. The obtained homoallylic alcohol, appeared to be an interesting intermediate, because the lacton could be built on it, exploiting an esterification followed by a ring closing metathesis. On the other hand, the piperidinic nitrogen and the other secondary alcohol of **10** would react to originate the cyclic carbamate.

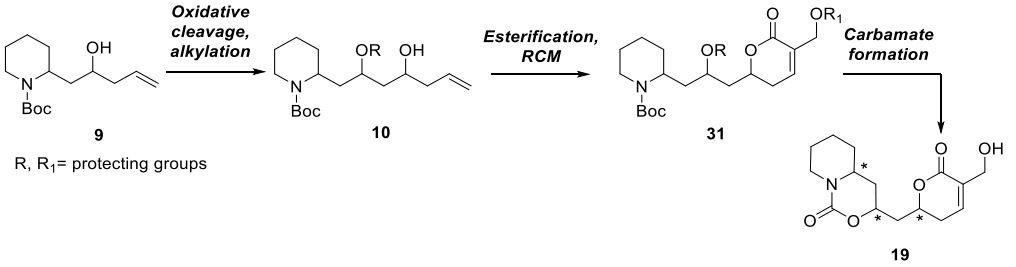

Scheme 22. Simplified forward synthetic pathway, leading to the formation of the new compound 19. a) oxidative cleavage/allylation; b) esterification, RCM; c) protecting groups cleavage, carbamate formation.

Notably, **19** present three different stereocenters and so exists as eight possible stereoisomers. Also in this case we took advantage of molecular modeling, to identifiy the most promising stereoisomer, characterised by a *R,S,R* configuration of the streoenters, to prioritize its synthesis.

Before proceeding with the description of the first explorative studies for the synthesis of compound **19**, is important to stress out that we were aware of the aforementioned limitations associated with the targeting of Smo protein, but we wanted to exploit molecular modeling to develop a rational scaffold, with the aim of test it also on GLI. In fact, our target molecule is a simplified version of Withaferin A, that seems to be active also on GLI factors. However, the obtainment of a new Smo inhibitor could be a starting point for further studies, aimed at the overcoming of the drug resistance problem (i.e. the use of this compound in combined therapy).

3.4.1 Preliminary synthetic efforts

The first synthetic pathway to be developed, foresaw the formation of the carbamate at an early stage of the route and the formation of the lactone as one of the last steps. Two stereoselective Brown's allylation, performed in the same conditions reported in Scheme 16, chapter 2, should allow the control over the stereochemical outcome of the synthesis. In fact, using the proper combination of the two enantiomer of allyl-$BIpc_2$, all the eight stereoisomers of **19** could be obtained. However, the first explorative studies were performed in not-stereoselective conditions, to check the feasibility of our synthetic strategy and to perform a preliminary biological evaluation on the racemic compounds.

The forward synthetic approach, starting from homoallylic alcohol **9,** can be appreciated in Scheme 23.

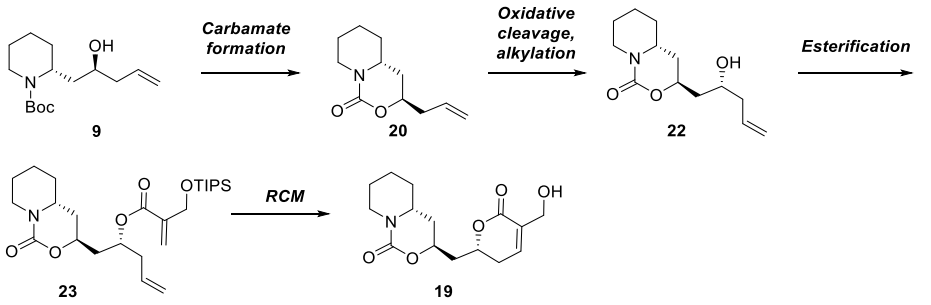

Scheme 23. Forward leading to formation of the most promising stereoisomer of **19**, on the basis of the docking studies.

Thus, our first attempt started from the *anti*-diastereomer of the homoallylic alcohol **9**, required to obtain the most promising isomer of the final compound **19**, on the basis of docking simulation. Generally speaking, two different methods could be ideally employed to covert **anti-9** in a cyclic carbamate, and are reported in Scheme 24. The most intuitive one is the cleavage of the Boc protecting group, followed by a cyclisation in the presence of carbonyldiimidazole (CDI).[137] The second possibility is a one pot reaction in the presence of methanesulfonyl chloride (MsCl) and a base, such as pyridine.[138] The hydroxyl group is converted into a good leaving group and, after the elimination of a unit of isobutene, the carbonyl group of Boc displaces the mesylated hydroxyl group, giving the cyclic carbamate **20**. The fundamental difference between the two mechanisms is that the second one occurs with inversion of configuration, involving a nucleophilic substitution. Thus, ***anti*-9** can be converted into the ***syn*-20** through the first procedure and into the ***anti*-20** through the second one. The relative stereochemical configuration of the two carbamates was confirmed by ^{1}H-NOESY NMR experiments, that evidenced a cross-peak between protons H_2 and H_8 in the carbamate generated through the CDI-mediated reaction, while no cross-peaks were appreciable in the case of the one-pot procedure. Both the reactions were completely diastereoselective, because in both of the cases no formation of the other diastereomer was appreciable.

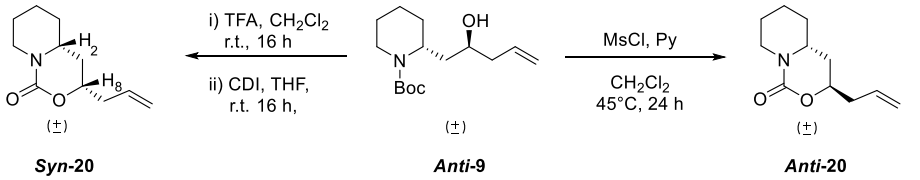

Scheme 24. Different sterochemical outcome of the diastereoselective cyclisation affording carbamates **20**.

Considering the relative stereochemistry of the desired final product, the *anti*-carbamate was required and so we employed the one-pot method. However, the possibility of control the stereochemical outcome of this cyclisation choosing the proper strategy could be really useful, finding application in the synthesis of the eight enantiopure stereoisomers.

The double bond of ***anti*-20** was oxidatively cleaved to the corresponding aldehyde ***anti*-21**, that, should have been successfully allylated in racemic conditions, leading to the formation of the two diastereomeric alcohols **22**.

[137] R. W. Bates, J. Boonsombat, *Org. Biomol. Chem.* **2005**, *3*, 520–523.
[138] S. Mill, C. Hootelé, *Can. J. Chem.* **1996**, *74*, 2434–2443.

For the oxidative step, several oxidative conditions were tested. First of all, ozonolysis in the presence of PPh_3 as reducing agent was performed, accordingly to similar procedures applied in our laboratory.[42] The aldehyde was actually formed, as demonstrated by mass spectroscopy of the crude mixture, but proved to be extremely unstable, beginning to decompose even before reaction completion. The crude product was conserved at -20°C overnight and the day after the aldehyde was completely degraded (Table 2, Entry 1). Then, the reaction was repeated in the same conditions, but purification through column chromatography immediately followed the work-up. Unfortunately, the aldehyde resulted to be unstable on silica. (Table 2, Entry 2)

To avoid the purification of the reaction mixture, Me_2S was used instead of PPh_3 and, at the same time, the period of time under ozone atmosphere was shortened, to prevent as much as possible the degradation. The allylation step was performed immediately after the work-up, on the crude product. In that case, a mixture of the diastereomers of compound **22** was obtained, but with a low yield (10% over ozonolysis and allylation step, Table 2, Entry 3). Therefore, we changed the oxidant, testing catalytic OsO_4 and $NaIO_4$, in the presence of 2,6-lutidine, hoping that milder conditions could have been beneficial for aldehyde stability.[139] Also in that case, the allylation step was performed as soon as possible on crude **21**. Unfortunately, we obtained only a slightly improvement of the yield over the two steps (20%, Table 2, Entry 4). Finally, we tried to condense the two steps in one-pot, performing an ozonolysis and adding the Grignard's reagent in the reaction mixture, as soon as the disappearance of the alkene spot was observed on TLC analysis.[140] Also in this case the yield was unsatisfactory (23%, Table 2, Entry 5).

[139] W. Yu, Y. Mei, Y. Kang, Z. Hua, Z. Jin, *Org. Lett.* 2004, *6*, 3217-3219.
[140] R. Willand-Charnley, P. H. Dussault, *J. Org. Chem.* **2013**, *78*, 42-47.

Table 2.

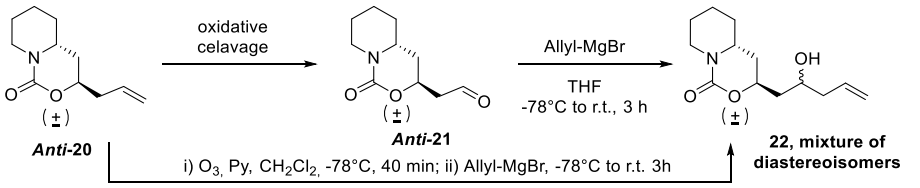

Entry	Oxidizing agent	Time	Allylation step	Yield for 22*
1	O_3 (then PPh_3)	1h under O_3, 2h with PPh_3	-	- (crude ***anti*-21** decomposed overnight at -20°C)
2	O_3 (then PPh_3)	1h under O_3, 2h with PPh_3	-	- (***anti*-21** decomposed during column chromatography)
3	O_3 (then Me_2S)	0.5 h under O_3, 2h with Me_2S	Allyl-MgBr on ***anti*-21** crude	10%
4	OsO_4, $NaIO_4$	2 h	Allyl-MgBr on ***anti*-21** crude	20%
5	O_3, Py	40 min	Allyl-MgBr, **one pot**	23%

*Yield calculated over the sum of the two diastereomers of **22**.

The impossibility of obtaining satisfactory yields in the oxidative cleavage / allylation sequence prompted us to change our synthetic strategy.
Aldehyde instability appeared to be the major pitfall of our first approach. The natural consequence was to try to obtain alcohol **22** avoiding the formation of the aldehyde. Thus, we developed the forward synthetic pathway reported below (Scheme 25).

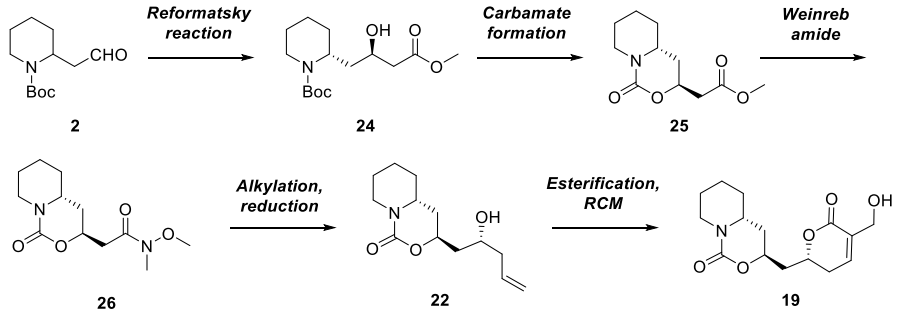

Scheme 25. Second synthetic approach, based on a Reformatsky reaction. The pathway is reported on the best inhibitor on the basis of docking simulations.

In this case, instead of allylating the aldehyde **7**, leading to intermediate **9**, a Reformatsky reaction in the presence of methylbormo acetate and zinc was exploited, in order to introduce a C-2 fragment instead of a C-3.[141] In this way, the oxidative cleavage, shortening the carbon chain of one carbon atom, should be avoided. Then, the diastereoselective cyclisation would lead to carbamate **25**, and after a sequence involving the formation of a Weinreb amide, alkylation and reduction of the formed keton, alcohol **22** should be afforded. The synthetic pathway is reported in Scheme 26.

Also in this case we worked in racemic conditions, and the first step of the new synthesis was the Reformatsky reaction. Aldehyde **7** was treated with the Reformatsky reagent, previously synthesised reacting methylbromo acetate and zinc. To our delight, this reaction gave an almost equimolar mixture of diastereomeric β-hydroxyesters ***anti*-24** and ***syn*-24** easily separable through column chromatography (88% yield on the two diasteroisomers). The relative configurations were assigned through ^{1}H-NMR NOESY experiment, after the conversion of each diastereomer into the corresponding cyclic carbamate ***anti*-25** and ***syn*-25**, exploiting the one-pot procedure in the presence of MsCl and Py. The anti- one was selected and different procedures were considered to transform it into a Weinreb amide.[142] Attempts aimed at the direct conversion of the methylester into the amide failed. In particular *N,O*-dimethyl hydroxylamine hydrochloride, in the presence of trimethylamine or $AlCl_3$, was tested. In the first case the product completely degraded, in the second case only a halo of a new product was appreciable on TLC. The starting material was recovered and the new product was isolated. Unfortunately, this product wasn't the desired one. Its structure remained not-elucidated due to the low amount of product that rendered impossible a complete characterisation.

Therefore, we decided to hydrolyze the methyl ester to the corresponding carboxylic acid, in order to insert the Weinreb amide through a simple coupling between the carboxylic acid and *N,O*-dimethyl hydroxylamine hydrochloride, promoted by 1-Ethyl-3-(3-dimethylaminopropyl)carbodiimide hydrochloride (EDC·HCl). Unfortunately, the carbamate proved to be unstable also during the basic hydrolysis.

[141] K. K. Pasunooti, R. Yang, S. Vedachalam, B. K. Gorityala, C.-F. Liu, X.-W. Liu, *Bioorg. Med. Chem. Lett.* **2009**, *19*, 6268–6271.

[142] S. Ueno, R. Shimizu, R. Kuwano, *Angew. Chemie - Int. Ed.* **2009**, *48*, 4543-4545.

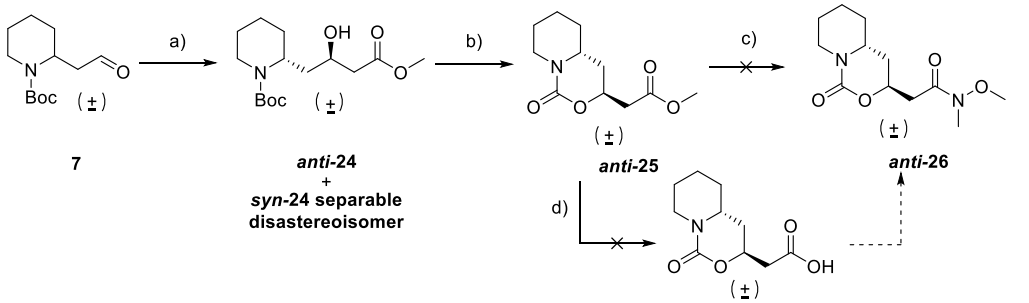

Scheme 26. Failed synthetic pathway leading to ***anti*-26** formation. *Reagents and conditions*. a) methylbromo acetate, Zn powder, THF, 0°C to r.t., 2h, 88%; b) MsCl, Py, CH_2Cl_2, 45°C, 24h, 70%; c) $CH_3ONHMe{\cdot}HCl$, TEA or $AlCl_3$, CH_2Cl_2, 0°C to r.t., 16h; d) LiOH, THF/H_2O, r.t., 16h.

This prompted us to rearrange our synthetic pathway, postponing the formation of the carbamate in a late stage of the synthesis. This proved to be the best choice, and allowed us to complete the synthesis of our target molecule.

3.4.2 Final synthetic route

The final synthetic strategy is reported in Scheme 27. We decided to perform the challenging cyclisation at the end of the synthesis and to take advantage once again of the key intermediate **10.** The other fundamental steps of the new route remained two allylations and the ring closing metathesis to build the α,β-unsaturated lactone.

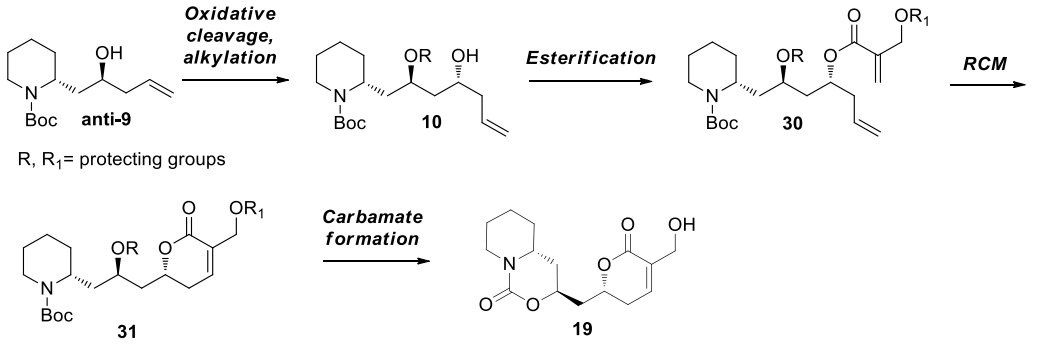

Scheme 27. Final forward synthetic pathway, leading to the formation of the best inhibitor **19,** on the basis of docking simulations.

The complete synthetic route is reported in Scheme 28.

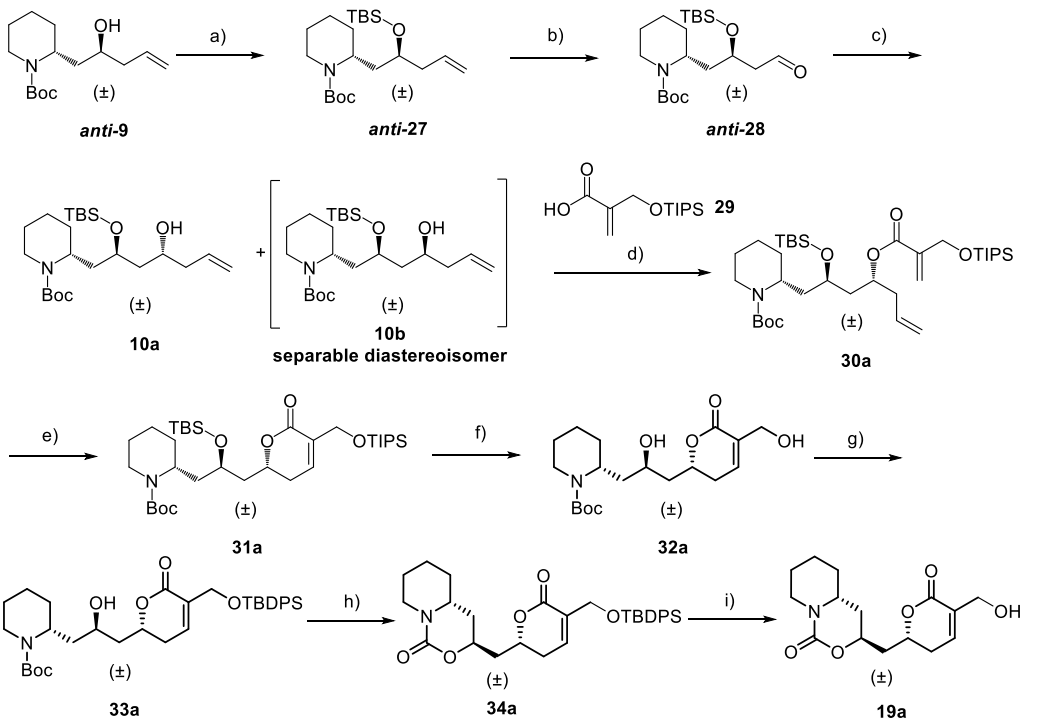

Scheme 28. Final synthetic pathway leading to compound **19**. The reactions are reported on stereoisomers "a" as an example. Reaction and conditions. a) TBSCl, imidazole, CH_2Cl_2, r.t., 4h, 91%; O3, PPh3, CH_2Cl_2, -78°C to r.t., 3h, 62%; c) Allylmagnesium bromide 1.0 M in THF, THF, -78°C to r.t., 4h, 80%; d) DCC, DMAP, CH_2Cl_2, r.t., 0°C to r.t., 18h, 87%; e) Stewart-Grubbs catalyst 45 mol%, toluene, 80°C, 8h, 75%; f) TBAF 1.0 M in THF; THF, -20°C to -10°C, 6h, 67%; g) TBDPSCl, imidazole, CH_2Cl_2, -10°C, 4h, 65%; h) MsCl, Py, CH_2Cl_2, 45°C, 24h, 50%; i) TBAF 1.0 M in THF; THF, -20°C, 3h, 60%.

The first step was the protection the hydroxyl group of intermediate ***anti*-9** as *tert*-butyldimethylsylil ether (***anti*-27**). Being convinced that the problems found during the oxidative cleavage of ***anti*-20** were connected with the instability of the carbamate under oxidative conditions, we tried to perform an ozonolysis on ***anti*- 27**. To our delight, this time the aldehyde ***anti*- 28** was stable even during column chromatography. The yield wasn't particularly high (62%), but perfectly comparable with other ozonolysis performed in our laboratory on similar substrates.[42] ***anti*-28** was allylated with allylmagnesium bromide, giving two separable racemic diastereomers, in almost 1 : 1 ratio. The relative configuration of the newly formed sterocenter was

assigned through a comparison with a parallel study aimed at the total synthesis of (-)-anaferine, in which the same reaction was performed in a stereoselective fashion, through a Brown's asymmetric allylation. More details are reported in paragraph 4.3 The diastereomer with the relative (*R, R, R*)-configuration, required for the synthesis of the most promising **19**-stereoisomer, will be indicated as **10a,** and the same nomenclature will be used also for the following intermediates of the synthetic pathway. The other diastereomer, characterised by the relative (R, R, S)-configuration, and the would be indicated as **10b.** With **10a** and **10b** in our hands, we proceed in parallel with the synthetic route on both of them. **10** compounds were condensed with carboxylic acid **29**, synthesised according literature,[133] giving esters **30a-b**. For the subsequent ring closing metathesis (RCM), a small screening of catalyst was performed on compound **30a**, as reported in Table 3.

The first tested catalyst was the M73-SIMes that gave us impressive r esults in the synthesis of the piperidine-containing polycycles in Chapter 2. The only difference was the higher reaction temperature (80°C): this is a common expedient to thermodynamically favour the RCM of hindered olefins. Unfortunately, in this case an almost 3 : 1 mixture of the desired product **31a** and the dimer originated by the cross methatesis (CM) on the less hindered double bond was obtained, as reported in Table 3, entry 1. The formation of the CM product was probably due to the steric hindrance of the TIPS protecting group, that made the formation of the dimer more accessible than the ring enclosure. Therefore, we tested a less bulky catalyst, the 2nd generation Hoveyda-Grubbs (entry 2), and a 10-fold dilution. In this case, only traces of CM product were appreciable. However, the reaction time was prolonged and different additions of fresh catalyst were necessary to reach the reaction completion, considering that the catalyst progressively degraded at high temperatures. Finally, we exploited a Stewart-Grubbs catalyst (entry 3), which is a less hindered version of the 2nd generation Hoveyda-Grubbs, particularly suitable for RCM reactions on bulky alkenes.[133] In this case **31a** was obtained with a satisfactory 75% yield, although using the same sub-stoichiometric amount of catalyst of entry 2. The optimised procedure was applied to **30b**, giving **31b** with comparable yield.

Table 3. Screening of catalysts for RCM reaction on **30a**.

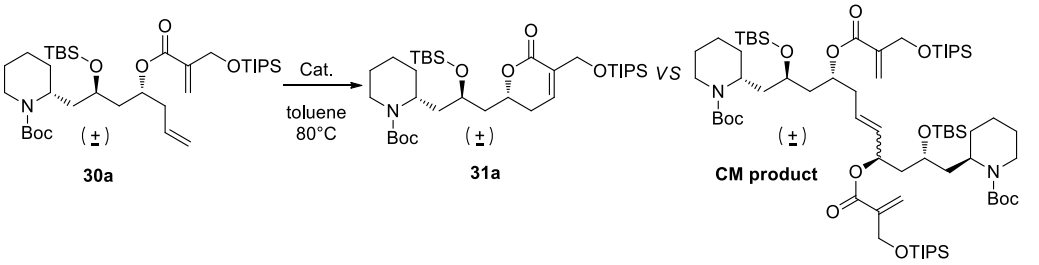

Entry	Catalyst	Loading %	Time (h)	Ratio RCM/CM	Yield % for **31a**
1	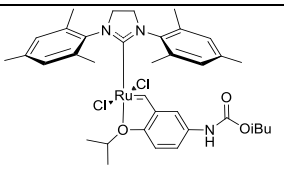 M73-SIMes	5 mol%	2 h	3 : 1	35 %
2	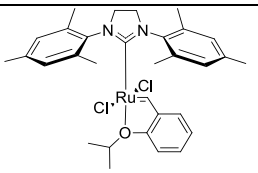 2nd generation Hoveyda-Grubbs	45 mol%	8 h	9 : 1	57 %
3	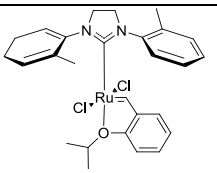 Stewart-Grubbs	45 mol%	8 h	Only **31a**	75 %

Reaction conditions. Entry 1: the catalyst was added as a 0.003 M solution in toluene, to a 0.02 M solution of **30a** in toluene, heated at 80°C. Entries 2 and 3: the catalyst (15 mol%) was added as a 0.003 M solution in toluene, to a 0.002 M solution of **30a** in toluene, heated at 80°C. Other two aliquots of catalyst (15 mol%, 0.003 M solution in toluene for each one) were added every two hours.

Once obtained compounds **31a-b**, the general idea was to deprotect the secondary alcohol, to perform the diastereoselective cyclisation leading to the cyclic carbamate and finally to cleave the protecting group on the primary alcohols. However, in this case the best strategy proved to be the cleavage of both the silylethers, followed by the regioselective protection of the primary alcohol with a bulky silyl protecting group. In fact, previous attempts involving the use of an orthogonal protecting group on the

primary alcohol of **29**, led to several problems about stability and purification during the following synthetic steps.

Thus, compounds **31a-b** were treated with tetra-n-butylammonium fluoride (TBAF). The use of two distinct silylethers allowed a better monitoring over the reaction, that resulted to be quite challenging. In fact, a first attempted, performed at r.t. and with only a slight excess of TBAF, led to the complete degradation of **31a-b**. The temperature was lowered to -20°C. In that case, only the primary alcohol was cleaved, even in the presence of excess of TBAF. After several attempts, we realised that the optimal reaction conditions to avoid product degradation involved the addition of several aliquots of TBAF (every hour), increasing the temperature progressively over seven hours, from -20°C to -10°C. The final amount of TBAF, after the repeated additions, was about 5 equivalents. Also in this conditions, the reaction didn't reach the completion and a halo of the mono-deprotected product was visible in TLC. However, the further addition of TBAF, as well as the increasing of the temperature began to promote the degradation of the residual mono-deprotected compound. The best obtained result for this reaction was a 66% yield, that was quite satisfactory considering the type of reaction.

Then the primary alcohols of **33a-b** were selectively protected with a bulky silylether, such as *tert*-butyldiphenylsilyl ether (TBDPS). Despite the presence of two hindered six-membered rings around the secondary alcohols, it tended to be partially protected as well, so the use of a sub-stoichiometric amount of TBDPS-Cl (0.9 eq) and of a low temperature (-20 °C) were essential requirements to gain a good selection over the primary alcohol. Compounds **33a-b** underwent the diastereoselective cyclisation in the presence of MsCl and pyridine, affording the bicyclic carbamates **34a-b**. After the cleavage of the protecting group with TBAF at -20°C, the final racemic compounds **19a-b** were finally obtained.

The synthesis of the other two members of the racemic library, obtainable using ***syn*-9** as starting material, is still in progress in our laboratory.

In the meantime, a preliminary biological evaluation of the accessed compounds was considered.

Preliminary biological evaluation

Thus, **19a** and **19b,** as well as some of the previous intermediates of the synthesis (**31a-b - -34a-b**), underwent a quite simple preliminary biological test, aimed at evaluating their inhibitory activity toward Hh signalling pathway.

To this extent, a Hh-dependent luciferase reporter assay on Shh-light II cells was performed. This is a generic test, typically used to characterize Hh antagonists and

their ability to inhibit the signalling, but it doesn't permit to establish which protein involved in the signalling has been targeted by a certain compound. However, this is usually the first biological test to be performed, because the direct evaluation of Smo protein inhibition is not sufficient to deduce the effective inhibition of the whole signalling, considering the possibility of downstream activations of Hh pathway.

In this test Shh-LIGHT II cells were used. These cells belong to a clonal NIH 3T3 cell line, which stably incorporates Gli-dependent firefly luciferase reporter and the pRL-TK Renilla as normalisation control. These cells are able to produce luminescence only if the Hh pathway is activated, while it's inhibition results in a decreasing of the luminescence. Thus, Shh-light II cells were treated with a mixture of SAG (a chlorobenzothiophene-containing Smo agonist) and the tested Smo inhibitors, to determine the inhibitory effected on Hh signalling. These data could be inferred indirectly, monitoring the suppression of luciferase activity.[105]

Luciferse and renilla values were determined using the dual-luciferase assay system kit (Biotium Inc). The results were expressed as the ratio between the luciferase and renilla values, and represented the mean of three independent experiments, each one as triplicate.

From this first screening, two intermediates, **33b** and **34b**, emerged as the most promising compounds, inhibiting Hh signalling in a dose-dependent manner, with IC_{50} values of 7.44 µM and 12.95 µM, respectively (Figure 18a).

On the other hand, the final compounds **19a** and **19b** proved to be inactive.

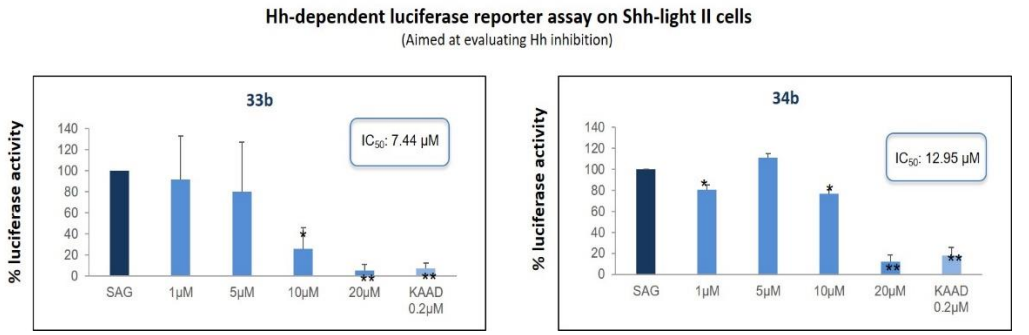

Figure 18. Results of the Hh-dependent luciferase reporter assay on **33b and 34b**, showing the dose-response curve in NIH3T3 Shh-Light II cells, treated with SAG or a mixture of SAG and increasing dosages of the tested compounds (1-5-10-20 µM) the tested compounds. KAAD was considered as positive control. The reported data represent the mean ± SD of three independent experiments. (*) $P < 0.05$ vs SAG; (**) $P < 0.01$ vs SAG.

The activity of compound **34b** seems to be in agreement with the rational design of our scaffold through computational studies. The fact that compounds **19a-b**, in which the key primary alcohol on the lactone moiety (fundamental for the interaction with Smo) was deprotected, could be the result of a poor pharmacokinetic profile, resulting from the polarity of **19**, that could prevent its migration through the cellular membrane of Shh-light II cells.

In silico simulations for the binding mode of active compounds **33b** and **34b** revealed that they can still fit in Smo binding site, despite the presence of the TBDPS protecting group on the key lactone moiety.

The stability of this protecting group in the medium of the Hh-dependent luciferase reporter assay is currently under investigation.

Stereoselective synthesis of 33b and 34b enantiomers.

With the two active compounds in our hand, we envisaged their stereoselective synthesis, to obtain the two enantiomers of each racemate, to test them independently. To this extent, Brown's conditions were exploited in both of the two allylation steps. The first enantiomer was obtained exploiting a combination of (-)-DIP-Cl / (-)-DIP-Cl for the two allylations, while the second enantiomer required the use of a (+)-DIP-Cl / (+)-DIP-Cl combination. The synthesis started with enantiopure ***anti-9*** compounds, synthesised accordingly to the procedure reported in Chapter 2. After the protection of the hydroxyl group, followed by oxidative cleavage of the double bond, the two enantiopure aldehydes ***(R,R)*-28b** and ***(S,S)*-28b** were obtained. Then, alkylation in the presence of the proper enantiomer of allyl-$BIpc_2$ was performed, leading to alcohols ***(R,R,S)*-10b** and ***(S,S,R)*-10b**, as reported in Scheme 29.

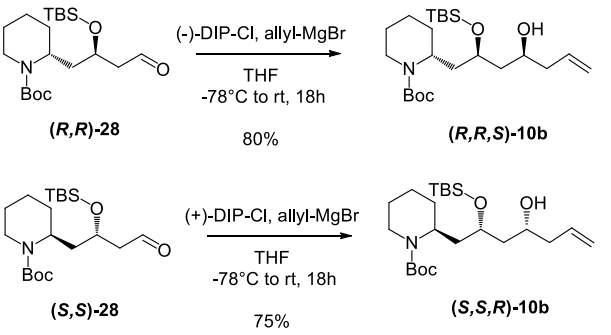

Scheme 29. Stereoselective synthesis of alcohols **10b** enantiomers.

The diastereomeric ratio was determined through ^{1}H-NMR, as reported in Figure 19.

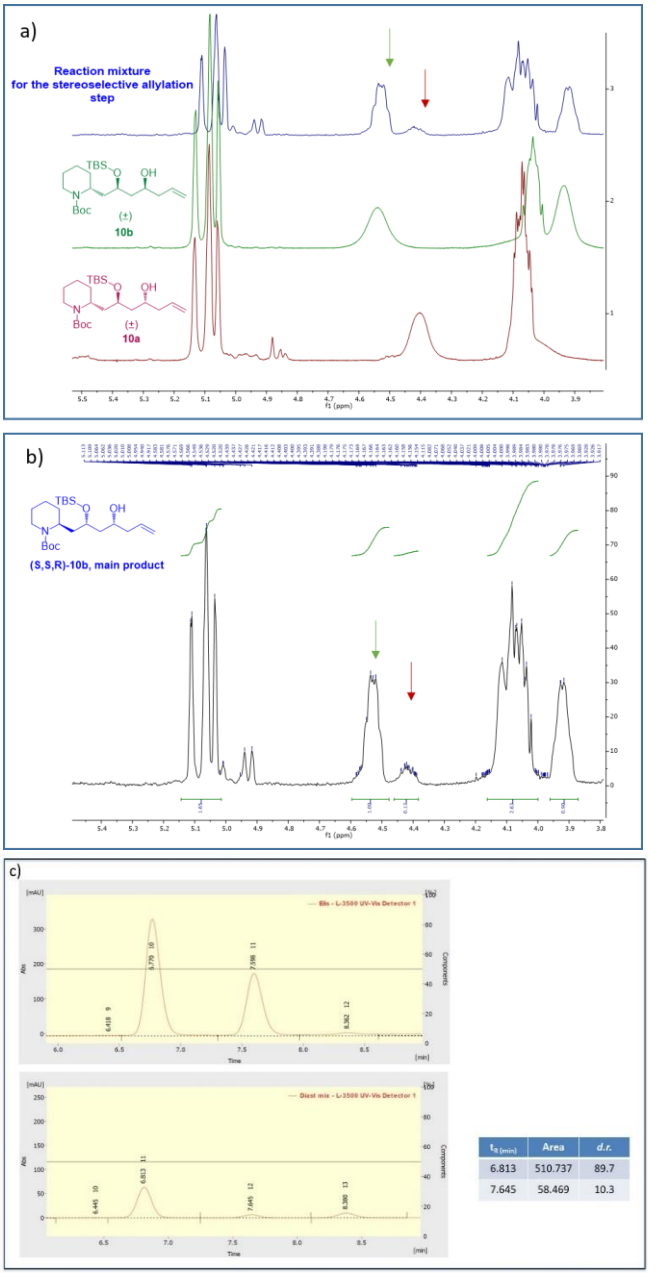

t_R (min)	Area	d.r.
6.813	510.737	89.7
7.645	58.469	10.3

Figure 19. Determination of the *d.r.* for the asymmetric synthesis of alcohols **10b**, by ^{1}H-NMR in C_6D_6 and HPLC a) Comparison between the ^{1}H-NMR spectrum of allylation reaction mixture (blue) and the spectra of the separated diastereomers **10a** and **10b**. The different chemical shift of the C-H signal around 4.5 ppm was exploited for the *d.r.* determination. b) Zoom of the blue spectra, highlighting the areas used for the *d.r.* determination. c) HPLC chromatogram of the mixture of diastereomers **10a** and **10b** (top) and of **(*S,S,R*)-10b**, reported as an example. Column: Zorbax SB-C18 5micronm 4.6x250 mm, 100% CH3CN, flux: 1 mL/min, λ= 205 nm.

^{1}H-NMR spectra of diastereomeric alcohols **10a** and **10b**, registered in $CDCl_3$, were almost completely superimposable, rendering the *d.r.* determination impossible.
To our delight, changing the solvent with deuterated benzene, the signals shift led to the separation of a C-H signal, as appreciable from Figure 19a (green and red spectra). Therefore, the ^{1}H-NMR spectra of the allylation reaction mixtures were recorded at 75°C, for both the enantiomers. The heating was mandatory to improve the spectra resolution. In Figure 19a the spectrum of the reaction mixture containing the **(*S, S, R*)-30b** enantiomer as main product (given by the use of the (+)-DIP-Cl / (+)-DIP-Cl combination) is reported in blue as example. As can be appreciated from the red arrow, a small peak corresponding to the undesired diastereomer was appreciable. The comparison between the area of these signals, highlighted also in Figure 19b, gave a *d.r.* = 85:15. The same value was detected for **(*R, R, S*)-30b** enantiomer.
Recently we were also able to find proper HPLC conditions for the determination of the diastereomeric ratio. As reported in Figure 19c, this technique gave an almost 90:10 ratio.
Once purified, the enantiomeric alcohols **30b** were converted into the corresponding products **33b** and **34b**, through the same synthetic route depicted in Scheme 28.
Products (*R, R, S*)-33b, (*S, S, R*)-33b, (*R, S, S*)-34b and (*S, R, R*)-34b are currently under biological evaluation.

3.5 Synthesis of 2nd generation inhibitors

After the development of a feasible synthetic route for the synthesis of scaffold **19**, the syntheses of two different classes of second generation Hh signalling pathway inhibitors, inspired by the same scaffold, were considered. The general structures of the new derivatives are reported in Figure 20. The first scaffold is an analog of **19**, bearing a bicyclic urea instead of the carbamate. The second one is a modification of **19**, in which an aryl group has been inserted in α-position to the carbamate nitrogen.

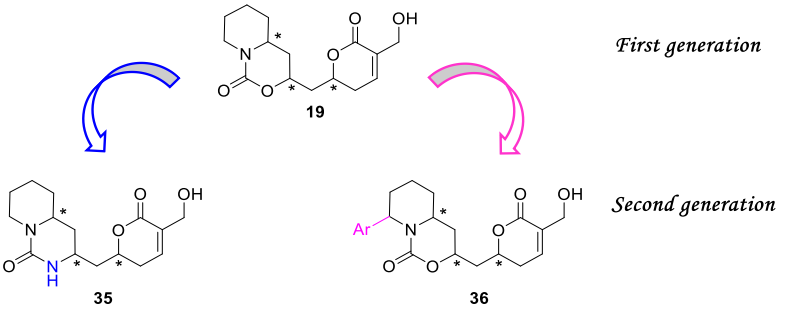

Figure 20. Structure of the 2nd generation potential Smo inhibitors.

Synthesis of scaffold 35.

For the synthesis of scaffold **35**, the carbamate of **19** was replaced with the corresponding urea. Our idea was to adapt the first proposed synthesis of **19** (Scheme 23) to this new compound. In fact, that synthesis was the shortest to be developed, considering the number of synthetic steps. As aforementioned, that strategy was abandoned due to the instability of the carbamate during the oxidative cleavage of the double bond of **20**. However, we reasoned that the urea could have been more stable, and in that case a library of urea-based potential Hh-inhibitors could have been synthesised in an easier and faster way, compared with the corresponding carbamate. But before starting with the synthesis of scaffold **35**, we took advantage once again of docking simulation, to evaluate the impact of the replacement of the carbamate with a urea. As reported in Figure 21, **35** fits well in Smo protein binding site, and maintains the fundamental interaction with the Arg400 residue. The presence of a new HBD doesn't negatively impact the interaction with Smo. Also in this case, the binding mode of **35** was compared with Taladegib. As appreciable in Figure 21, right panel, the two compounds presented a comparable spacial disposition in Smo binding site.

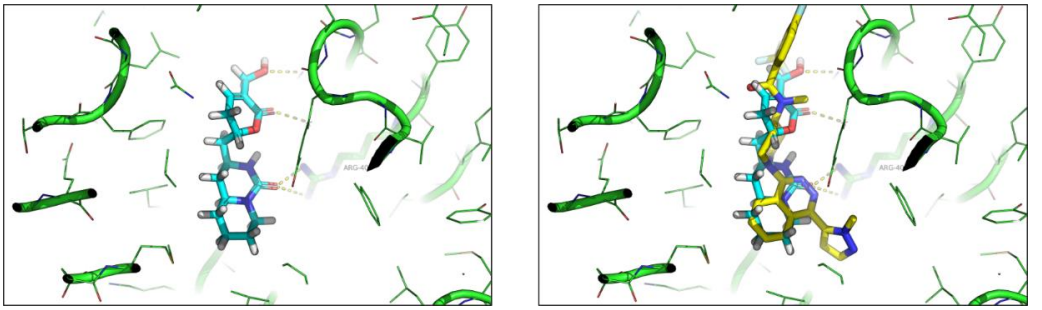

Figure 21. Docking simulation of **35** in Smo protein binding site, showing the maintenance of the interaction with Arg400 (left). Superimposition of **35** (cyan) with Taladegib (yellow), displaying a similar binding mode.

Encouraged from the positive results of molecular modelling simulations, we planned the synthesis of analog **35**, according to the first synthetic strategy that was planned for compound **19** (Scheme 23). In that case the instability of the carbamate, and in particular of aldehyde **21**, prompted us to change the synthetic protocol. However, we reasoned that a urea could have been more stable in the same reaction conditions, leading to the development of the forward synthetic pathway depicted in Scheme 30. The key step in this synthesis should be the functional group interconversion (FGI) from alcohol to amine, to build the urea on this moiety. Thus, this synthesis could be an additional ramification of the general DOS approach, starting from the amine **11**, exploited in the synthesis of the piperidinic polycyclic derivatives of Chapter 2.
Similarly, to **19**, also scaffold **35** bears three stereocenters. For the explorative studies, we decided to prioritize the synthesis of only one of them, to check if the shorter synthetic approach was feasible on the urea derivative. In particular, we exploited the racemic *syn*-diastereomer of the key intermediate **9**, as starting material. This isomer was available in a large amount in our laboratory, because it was obtained as side product in the synthesis of the most precious ***anti*-9**, and has remained unused until that moment.

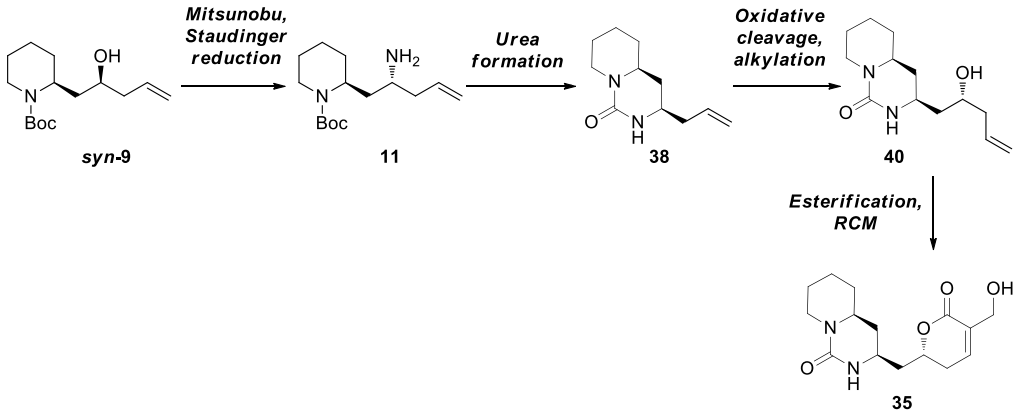

Scheme 30. Forward synthetic pathway leading to the formation of **35**.

The synthesis started with the interconversion of ***syn*-9** into the corresponding amine **11**, through the Mitsunobu/Stuaudinger reduction protocol already employed in Chapter 2. After the cleavage of the Boc protecting group, diamine **37** was reacted with CDI (carbonyldiimidazole), giving the bicyclic urea **38**, in a diastereoselective fashion, through a mechanism characterised by configuration retention. For the oxidative cleavage, a standard ozonolysis reaction in the presence of PPh_3 was attempted. Unfortunately, also in that case, a complex reaction mixture, impossible to purify due to the presence of several degradation products, was obtained. Thus, a different approach was attempted. A combination of $RuCl_3$ and $NaIO_4$, generating *in situ* RuO_4, was used as an alternative to the more toxic OsO_4, as reported in literature.[143] To our delight, the desired aldehyde **39** was obtained, with an acceptable yield, considering the challenging reaction. The same procedure wasn't applied to the synthesis of carbamate based-scaffold **19**, because the ruthenium oxides in combination with $NaIO_4$, is used to oxidize the α-position of *N*-Boc piperidines to the corresponding lactams, and we wanted to avoid collateral reactions. [144]

39 was alkylated with the proper Grignard reagent, but the two diastereomers resulted inseparable through column chromatography. The subsequent esterification with carboxylic acid **29** was attempted on the mixture of the two diastereomers, hoping to obtain separable esters. Unfortunately, that was not the case and **41** isomers remained inseparable. To avoid proceeding in the synthetic pathway with complex mixtures, we were forced to employ a stereoselective approach also during the preliminary studies, as reported in Scheme 31.

[143] A. Pinto, M. Piccichè, R. Griera, E. Molins, J. Bosch, M. Amat, *J. Org. Chem.* **2018**, *83*, 8364–8375.
[144] M. Piccichè, A. Pinto, R. Griera, J. Bosch, M. Amat, *Org. Lett.* **2017**, *19*, 6654–6657.

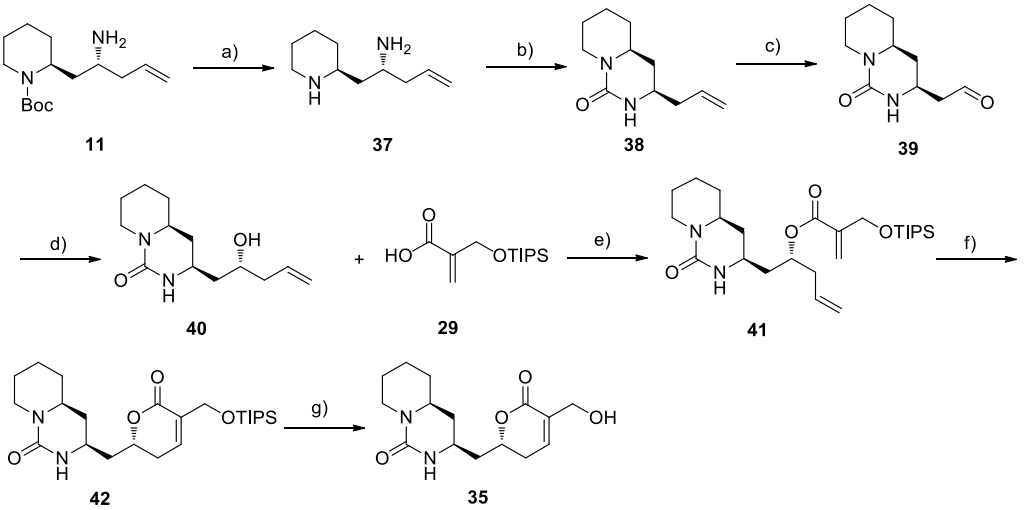

Scheme 31 Synthesis of enantiopure **35**. *Reagents and conditions*. a) HCl in dioxane, CH_2Cl_2, 0°C to r.t., 5h, 90%; b) CDI, DMAP, THF, 0°C to 35°C, 18h, 73%; c) $RuCl_3 \cdot nH_2O$, CH_3CN, r.t., 5h, 60%; d) (+)-allyl-$BIpc_2$ (from (+)-DIP-Cl and allylmagnesium bromide), THF, –78 °C to r.t., 16 h, 65%; e) DCC, DMAP, CH_2Cl_2, 0°C to r.t., 18h, 75%; f) Stewart-Grubbs catalyst 45 mol%, toluene, 80°C, 8h, 45%; g) TBAF 1.0 M in THF, THF, -20°C, 4h, 68%.

Enantiopure **11** was synthesised according to our previous works,[45] and was converted into the corresponding aldehyde **39** as reported in Scheme 31. A stereoselective Brown's allylation in the presence of (+)-DIP-Cl led to the formation of the homoallylic alcohol **40**. The configuration of the newly formed stereocenter was determined by the chirality of the pinene substituents on the borane, and the desired product **40** was obtained with a diastereomeric ratio of 80:20 over the other diastereomer. The *d.r.* was determined through ^{1}H-NMR, as reported in Figure 22.

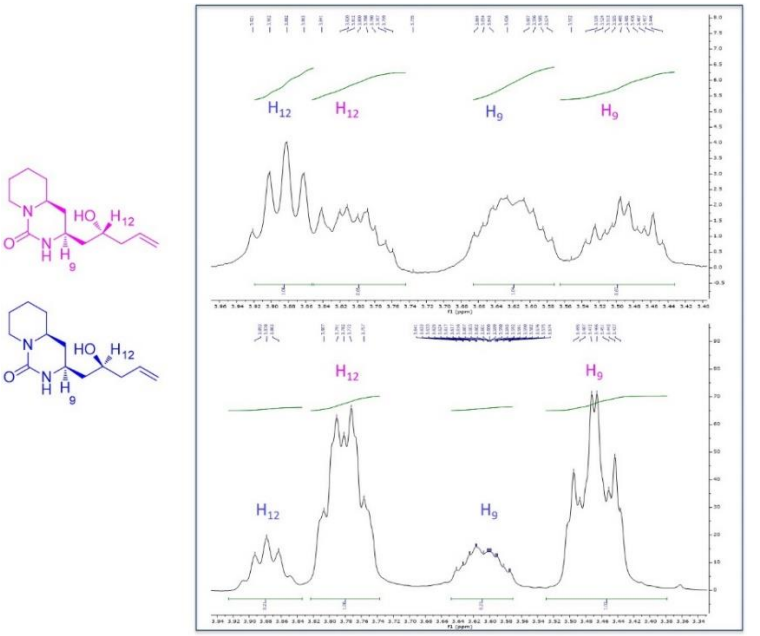

Figure 22. Determination of the *d.r.* for the allylation step, exploiting ^{1}H-NMR in $CDCl_3$. The top spectrum represents the inseparable mixture of the two diastereomers, obtained under non-stereoselective allylation conditions. The bottom spectrum represents the diastereomeric mixture afforded after Brown asymmetric allylation.

Condensation of **41** with **29** gave ester **41**, that underwent RCM, using the optimised procedure based on the use of the Stewart-Grubbs catalyst. Comparably with the synthesis of lactone **31**, no formation of the cross metathesis product was observed, but **42** resulted more difficult to purify. Finally, cleavage of the TIPS protecting group in the presence of TBAF, afforded the desired final product **35**.

The possibility of exploiting a short pathway for the obtainment of this new class of potential Hh-inhibitors, is really intriguing and the synthesis of the other stereoisomers will continue in our laboratory. The biological evaluation of enantiopure compound **35** is currently ongoing and the results will better orient the future development of the synthesis of potential Hh inhibitors characterised by this urea-based scaffold.

Synthesis of scaffold 36.

In the attempt of enhancing the affinity of our carbamate scaffold **19** for Smo binding site, the introduction of an aryl group in α-position to the piperidinic nitrogen was considered, on the basis of computational studies. In Figure 23, the docking simulations performed on compound **19** are reported again, together with the structure of the arylated-scaffold **36**.

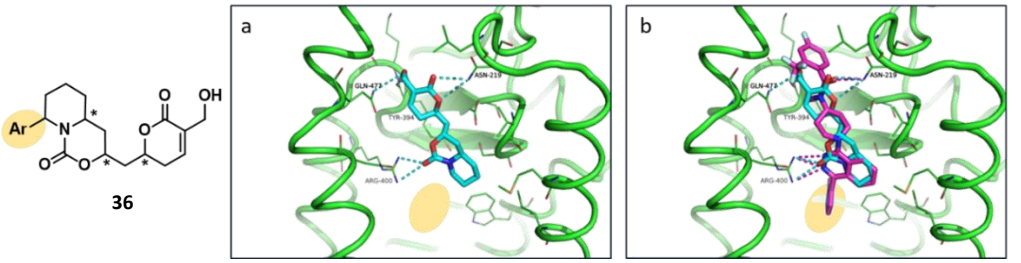

Figure 23. a. Docking simulation of **19** (cyan) in Smo protein binding site, showing the empty space (yellow oval) that could be occupied by an aryl moiety. b. Superimposition of **19** (cyan) with Taladegib (pink), displaying that the pyrazole moiety occupies the empty pocket (yellow oval).

As it is inferable from Figure 23a, representing **19** in Smo active site, an aryl group in the proper position, would occupy an empty pocket in the binding site and this should further stabilize the binding. Moreover, observing Figure **23b**, **36**-aryl group would occupy the same position of the pyrazole ring of taladegib.

However, the direct introduction of the aryl group on **19** seemed unfeasible, considering the proved instability of the bicyclic carbamate during the early stages of this work. For this reason, the synthesis of a new 2-piperdine ethanol-like precursor, directly bearing the aryl group in the proper position, appeared to be the best option. Thus, the first goal became the obtainment of this new starting material **48.** A possible synthetic strategy is reported in Scheme 32.

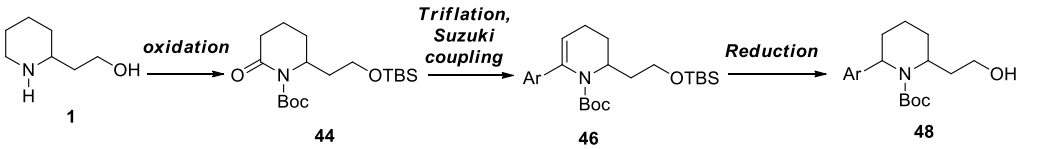

Scheme 32. Forward synthetic pathway leading to **48** formation.

As reported in a worked by Piccichè *et al.*,[144] a piperidine ring could be easily converted into a triflate that, after a cross coupling reaction, should allow the insertion of an aryl moiety in α-position to the piperidinic nitrogen.

Thus, *N*-Boc -2-piperidine ethanol was protected as *tert*-butlydimethylsilyl ether at the hydroxyl group. The piperidine was transformed into the corresponding lactam **44**, through a ruthenium mediated oxidation ($RuO_2 \cdot nH_2O$, $NaIO_4$), as reported by Piccichè. In basic conditions and in the presence of *N*-phenyl bis-trifluoromethane sulfonamide, the lactam was converted into a triflate **45**, that underwent a Suzuki coupling with an aryl boronic acid. For our first precursor, we used the simple phenylboronic acid, but of course different aryl-derivatives could be synthesised simply choosing the proper boronic acid. The obtained compound **46** proved to be unstable and so the next step, namely the reduction of the double bond, was performed immediately. Considering that racemic 2-piperidine ethanol was exploited as starting material, and that the reduction can occur on both the faces of the piperidine ring, two possible racemic diastereomers (*syn*- and *anti*-) could be potentially expected. We decided to perform a simple hydrogenation in the presence of Pd/C catalyst. In fact, we wanted to isolate the two diastereomeric compounds (each one as racemate) and, after complete characterisation, use them as reference compounds in a screening of conditions for stereoselective reductions. However, the hydrogenation didn't proceed as expected, because the reduction of the double bond was accompanied by the cleavage of the TBS protecting group, affording directly the final scaffold **48** and not the expected products **47** (Scheme 33).

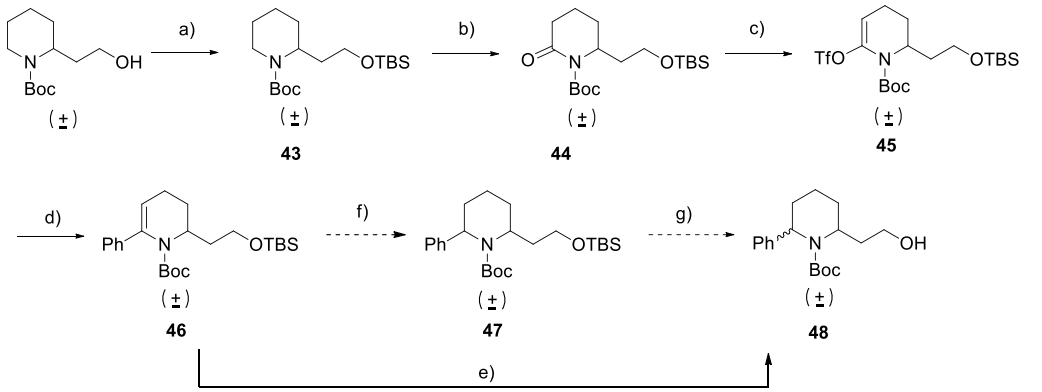

Scheme 33. Synthesis of the new precursor **48**. *Reagents and conditions*. a) TBSCl, CH_2Cl_2, r.t., 2h, quant; b) $RuO_2 \cdot nH_2O$, $NaIO_4$, EtOAc, r.t., 5h, 90%; c) LiHMDS, *N*-Ph-bis(trifluorosulfonimide), -78°C to r.t., 16h, 81%; d) $Pd(PPh_3)_4$, phenylboronic acid, THF/H_2O, 50°C, 8h, 94%; e) H_2, Pd/C, MeOH, r.t., 16h, 91%; f) H_2, Pd/C, MeOH; g) TBAF 1.0 M in THF, THF.

TLC analysis of the reaction mixture gave a single spot as product, that was isolated through column chromatography. This prompted us to hypothesise that the two formed diastereomers could possess the same R_f. In fact, NMR analysis revealed a

mixture of diastereomers, resulting from the addition of hydrogen on both the faces of the double bond. So far, diastereomers separation proved to be impossible.
Therefore, we will try to differentiate them in the following steps of the synthesis. An alternative could be the derivatization of the hydroxyl or nitrogen groups, leading to the separation of the two diastereomers.
A stereoselective reduction of the double bond of compound **45** will be considered as well. Once separated, the two diastereomeric precursors will be employed for the synthesis of compounds bearing **36** scaffold, taking advantage of the protocol developed for the synthesis of scaffold **19**.

In conclusion, after several attempts, a feasible synthetic route for the synthesis of scaffold **19** has been established and two out of the four stereoisomeric members of the racemic library have been successfully obtained. Preliminary biological evaluation of these compounds and of some previous synthetic intermediates led to the individuation of two promising Hh inhibitor. The two enantiomers of these compounds were synthesised, and their biological evaluation is currently in progress.
In parallel, preliminary studies aimed at the synthesis of two classes of 2nd generation inhibitors were made. A synthetic protocol for the enantioselective synthesis of urea-based inhibitors **35** has been successfully developed and it could be easily tuned to obtain all the possible stereoisomers. The biological evaluation of the obtained stereoisomer is currently ongoing; the results will orient the future development of this project.
On the other hand, the synthesis of a new arylated precursor (**48**), exploitable for the synthesis of scaffold **36** has been accomplished. The clarification of the diastereomeric composition of compound **48** is in progress. In future the stereoselective synthesis of the most favourable precursor **48** (on the basis of docking simulation) will be considered and this isomer will be exploited as starting material for the total synthesis of scaffold **36**, through the same protocol developed for the obtainment of **19.**

3.6 Experimental part

General

Unless otherwise stated, reagents and solvents were purchased from Sigma Aldrich, Fluorochem or TCI and used without further purification. Unless otherwise stated, all reactions were carried out in oven-dried glassware and dry solvents, under nitrogen atmosphere and were monitored by thin layer chromatography (TLC) on silica gel (Merck precoated 60F254 plates), with detection by UV light (254 nm) or by solutions of potassium permanganate stain or ninhydrin.
Flash chromatography was performed using silica gel (240-400 mesh, Merck) as stationary phase.
^{1}H-NMR spectra were recorded on a Bruker Avance Spectrometer (400 MHz) and are reported relative to residual $CDCl_3$ or CD_3OD. ^{13}C-NMR spectra were recorded on the same instruments (100 MHz) and are reported relative to residual $CDCl_3$ or CD_3OD. All 1D and 2D NMR spectra were collected using the standard pulse sequences available with Bruker Topspin 1.3. Chemical shifts (δ) for proton and carbon resonances are quoted in parts per million (ppm) relative to tetramethylsilane (TMS), used as an internal standard. Data for ^{1}H-NMR are reported as follows: chemical shift (δ/ppm) (multiplicity, coupling constant (Hz), integration). Multiplicities are reported as follows: s = singlet, d = doublet, t = triplet, m = multiplet, bs = broad singlet. Data for ^{13}C-NMR are reported in terms of chemical shift (δ/ppm).
Mass spectra were registered exploiting the electrospray ionisation (ESI) technique, on a Q-Tof micro mass spectrometer.
Specific rotation values were measured on a P-1030 Jasco polarimeter, using 1 mL cells, with path length of 10 cm. Measures were collected at 20-25°C, using sodium D line wavelength λ=589 nm.

General procedure for the synthesis of carbamates with inversion of configuration.
Pyridine (4.45 mmol) and methanesulfonyl chloride (0.59 mmol) were added to a solution of substrate (0.15 mmol) in 3 mL of CH_2Cl_2, cooled at 0°C. The reaction mixture was refluxed at 45°C for 24 h, then the solvent was removed under vacuum, and heptane was used to remove pyridine. The residue was dissolved again in CH_2Cl_2 and water. The aqueous layer was extracted with CH_2Cl_2 and the combined organic phases were dried over Na_2SO_4, filtered and concentrated under vacuum. The crude product was purified by column chromatography on silica gel.

General procedure for the synthesis of carbamates with retention of configuration.

To a solution of substrate (0.93 mmol) in anhydrous THF, CDI (1.39 mmol) and DMAP (0.093 mmol) were added at 0°C. The reaction was stirred at 35°C for 48h. Eventually, another equivalent of CDI was added to force the reaction to reach the completion. The solvent was removed under vacuum and the residue was partitioned in EtOAC and water (10 mL). The aqueous layer was extracted with EtOAc. The combined organic phases were washed with brine, dried over Na_2SO_4 and concentrated under vacuum. The residue was purified by column chromatography on silica gel.

Synthesis of racemic (3R,4aR)-3-allylhexahydropyrido[1,2-c][1,3]oxazin-1(3H)-one (anti-20)

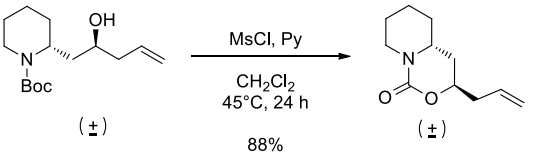

Synthesised according the general procedure for the synthesis of carbamates with inversion of configuration, starting from alcohol **9**.

Yield: 88%, light yellow oil.
^{1}H NMR (400 MHz, $CDCl_3$) δ 5.89 – 5.75 (m, 1H), 5.20 – 5.10 (m, 2H), 4.45 – 4.36 (m, 1H), 4.28 (dtd, *J* = 9.1, 6.4, 2.5 Hz, 1H), 3.34 – 3.22 (m, 1H), 2.75 – 2.62 (m, 1H), 2.56 – 2.45 (dt, *J* = 13.9, 6.3 Hz, 1H), 2.39 – 2.25 (dt, *J* = 14.3, 7.2 Hz, 1H), 2.01 – 1.95 (m, 1H), 1.95 – 1.88 (m, 1H), 1.74 (m, 1H), 1.72 – 1.68 (m, 1H), 1.63 – 1.55 (m, 1H), 1.47 (m, 3H).
^{13}C NMR (100 MHz, $CDCl_3$) δ 153.70, 132.74, 118.66, 73.11, 53.28, 45.97, 39.04, 33.27, 32.59, 25.62, 24.68.
MS (ESI) m/z $[M + Na]^+$ calcd. for $C_{11}H_{17}NO_2Na$: 218.11, found: 218.78

Synthesis of racemic (3R,4aS)-3-allylhexahydropyrido[1,2-c][1,3]oxazin-1(3H)-one (syn-20)

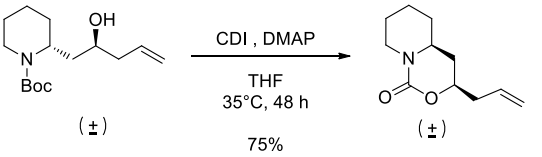

Synthesised according the general procedure for the synthesis of carbamates with inversion of configuration, starting from alcohol **9**.

Yield: 75%, light yellow wax.
^{1}H NMR (400 MHz, $CDCl_3$) δ 5.84 (ddt, *J* = 17.2, 10.3, 7.1 Hz, 1H), 5.20 – 5.10 (m, 2H), 4.52 – 4.41 (m, 1H), 4.24 – 4.14 (m, 1H), 3.28 (tdd, *J* = 11.1, 5.4, 2.6 Hz, 1H), 2.67 (td, *J* = 12.9, 2.9 Hz, 1H), 2.55 – 2.44 (m, 1H), 2.35 (m, 1H), 2.08 (ddd, *J* = 13.8, 5.5, 1.8 Hz, 1H), 1.91 – 1.79 (m, 3H), 1.76 – 1.67 (m, 1H), 1.57 (m, 1H), 1.51 – 1.36 (m, 1H), 1.24 – 1.12 (m, 1H).

^{13}C NMR (100 MHz, $CDCl_3$) δ 153.80 , 132.60 , 118.69 , 74.42 , 54.09 , 44.84 , 39.33 , 35.24 , 33.73 , 25.10 , 23.77 .
MS (ESI) m/z $[M + Na]^+$ calcd. for $C_{11}H_{17}NO_2Na$: 218.11, found: 218.50

Oxidative cleavage for the synthesis of diastereomeric mixture of 3-(2-hydroxypent -4-en-1-yl)hexahydropyrido[1,2-c][1,3]oxazin-1(3H)-one (22).

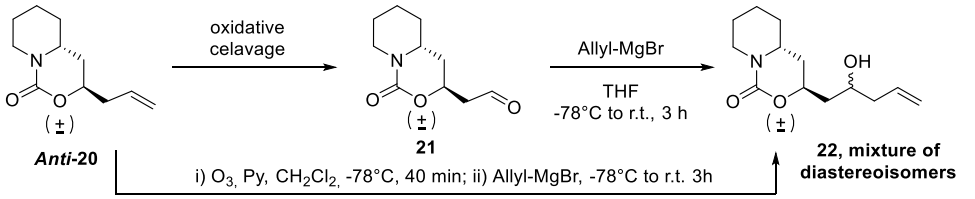

Method 1: ozonolysis, followed by allylation.

Ozone was fluxed through a solution of ***Anti*-20** (0.156 g, 0.80 mmol) in CH_2Cl_2 (13 mL), cooled at -78°C. After the disappearing of the alkene spot in TLC (0.5 h), the residual ozone was remove from the solution fluxing nitrogen for 10 minutes. Me_2S (240 µL, 3.19 mmol) was added at -78°C, then the reaction mixture was stirred for 2 h at r.t.. The solvent was removed under vacuum and the residue was immediately dissolved in anhydrous THF (6 mL) and cooled at -78°C. A solution of allylmagnesium bromide 1.0 M in THF (0.9 mL, 0.90 mmol) was added dropwise. The reaction mixture was stirred at -78°C for 1 h, and for 2 h at r.t.. The reaction was quenched adding a saturated aqueous solution of NH_4Cl. The layers were separated and the aqueous one was extracted with Et_2O. The combined organic phases were washed with brine, dried over dried over Na_2SO_4 and concentrated under vacuum. The residue was purified by column chromatography on silica gel (CH_2Cl_2 : MeOH =97:3), affording **22** (0.019 g, 10%) as a mixture of inseparable diastereomers.

Method 2: Oxidation with OsO_4 / $NaIO_4$, followed by allylation.

***Anti*-20** (0.129 g, 0.66 mmol) was dissolved in a mixture of dioxane : H_2O (5.25 mL : 1.75 mL), then OsO_4 (0.017 mg, 0.066 mmol) and 2,6-lutidine (0.142 mg, 1.33 mmol) were added at r.t.. The reaction mixture was stirred at r.t. for 10 min, then $NaIO_4$ (0.496 g, 2.32 mmol) was added portion-wise over 20 min. The reaction mixture was stirred at r.t. for 2 h, then the reaction was diluted with water and extracted with CH_2Cl_2. The combined organic phases were washed with brine, dried over dried over Na_2SO_4 and concentrated under vacuum.

The residue underwent allylation process as reported in the previous procedure. After column chromatography, **22** (0.032 g, 20%) as a mixture of inseparable diastereomers.

Method 3: one-pot ozonolysis and allylation

Ozone was fluxed through a solution of ***Anti*-20** (0.120 g, 0.61 mmol) in anhydrous CH_2Cl_2 (8 mL) and anhydrous pyridine (150 µL, 1.85 mmol), cooled at -78°C. After 40

min, nitrogen is fluxed for 15 minutes through the solution, to remove the residual ozone. Then, a 1.0 M solution of allylmagnesium bromide in THF (670 µL,0.67 mmol) was added dropwise and the reaction mixture was stirred 4 h at r.t. The reaction mixture was quenched with a saturated aqueous solution of NH_4Cl, that was extracted with CH_2Cl_2. The combined organic phases were washed with brine, dried over Na_2SO_4 and concentrated under vacuum. The residue was purified by column chromatography on silica gel (CH_2Cl_2 : MeOH =97:3), affording 22 (0.033 g, 23%) as a mixture of inseparable diastereomers.

Diastereomeric mixture of 3-(2-hydroxypent -4-en-1-yl)hexahydropyrido[1,2-c][1,3]oxazin-1(3H)-one (22)

^{1}H NMR (400 MHz, $CDCl_3$) δ 5.91- 5.68 (m, 2H), 5.23 – 5.07 (m, 4H), 4.68- 4.49 (m, 2H), 4.47-4.38 (m, 2H), 4.11 – 4.01 (m, 1H), 3.90-3.81 (m, 1H), 3.38 – 3.20 (m, 2H), 2.77 – 2.63 (m, 2H), 2.47- 2.36 (m, 2H), 2.35-2.12 (m, 2H), 2.07- 1.94 (m, 2H), 1.91-1.82 (m, 4H), 1.79 – 1.07 (m, 16H). (mixture of diastereomers).

MS (ESI) m/z $[2M + Na]^+$ calcd. for $C_{13}H_{21}NO_3Na$: 501.29, found 501.90

Synthesis of compounds anti-24 and syn-24.

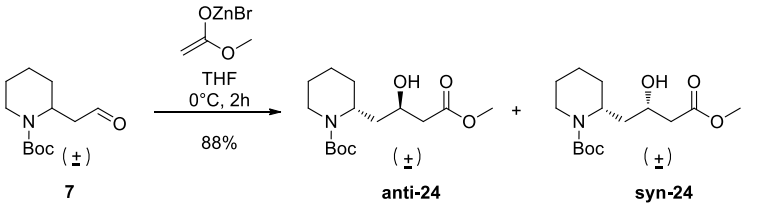

3 mL of a 1.0 M solution of Reformatsky reagent in anhydrous THF were prepared as follows. TMSCl (50 µL, 0.38 mmol) was added dropwise to a suspension of powder of zinc (0.182 g, 2.78 mmol) in anhydrous THF (1.5 mL). The suspension was refluxed for 15 min, to favour zinc activation. The reaction was cooled at r.t, then a solution of methylbormo acetate in anhydrous THF (1.5 mL) was added dropwise, at a rate that maintain a gentle reflux. When the reaction mixture became green, the Reformatsky reagent has been formed. The reaction mixture was stirred for 5 min, then it was allowed to decant.

In parallel aldehyde **7** (0.160 g, 0.70 mmol) was dissolved in anhydrous THF (3 mL) and cooled at 0°C. Then, 1.8 mL of the 1.0 M solution of Reformatsky reactive was added dropwise over 15 minutes. The reaction mixture was stirred at 0°C for 2 h, then a saturated aqueous solution of NH_4Cl was added. The layers were separated and the aqueous one was extracted with EtOAc. The combined organic phases were washed with a saturated aqueous solution of $NaHCO_3$ and brine, then were dried over Na_2SO_4 and concentrated under vacuum. The residue was purified by column chromatography on silica gel (Hex : EtOAc =8:2), affording *syn*-**24** and ***anti*-24** (0.084 g and 0.104 g respectively, 88% overall yield) as uncoloured oils.

Racemic mixture of tert-butyl (2R)-2-[(2S)-2-hydroxy-4-methoxy-4-oxobutyl] piperidine-1-carboxylate and tert-butyl (2S)-2-[(2R)-2-hydroxy-4-methoxy-4-oxobutyl]piperidine-1-carboxylate (Syn-24)

^{1}H NMR: (400 MHz, $CDCl_3$) δ 4.53 – 4.38 (m, 1H), 3.99 – 3.87 (m, 1H), 3.85 – 3.72 (m, 1H), 3.67 (s, 3H), 2.74 – 2.64 (m, 1H), 2.57 (dd, *J* = 15.2, 7.3 Hz, 1H), 2.40 (dd, *J* = 15.6, 5.4 Hz, 1H), 2.04 (t, *J* = 12.8 Hz, 1H), 1.78 – 1.65 (m, 1H), 1.64 – 1.56 (m, 2H), 1.55-1.49 (m, 2H), 1.45 (s, 9H), 1.40 – 1.32 (m, 1H), 1.31-1.24 (m, 1H).

^{13}C NMR: (100 MHz, $CDCl_3$) δ 172.46 , 156.64 , 80.40 , 64.58 , 51.69 , 46.37 , 41.39 , 39.64 , 37.11 , 29.32 , 28.49 (3 CH_3), 25.56 , 19.30.

MS (ESI) m/z $[M + Na]^+$ calcd. for $C_{15}H_{27}NO_5Na$: 324.18, found: 324.27

***Racemic mixture of (2R)-2-[(2R)-2-hydroxy-4-methoxy-4- oxobutyl] piperidine-1-carboxylate and (2S)-2-[(2S)-2-hydroxy-4-methoxy-4- oxobutyl] piperidine-1-carboxylate (Anti-*24)**

^{1}H NMR (400 MHz, $CDCl_3$) δ 4.40 – 4.24 (m, 1H), 4.03 – 3.84 (m, 2H), 3.66 (s, 3H), 2.76 (m, 1H), 2.61 (dd, *J* = 16.0, 3.3 Hz, 1H), 2.43 (dd, *J* = 16.0, 8.5 Hz, 1H), 1.93 (dt, *J* = 14.6, 7.9 Hz, 1H), 1.65 – 1.47 (m, 6H), 1.40 (s, 9H), 1.37 (m, 1H).
^{13}C NMR: (100 MHz, $CDCl_3$) δ 173.11, 155.98, 79.80, 66.38, 51.71, 47.76, 41.16, 39.72, 37.00, 29.21, 28.47 (3 CH_3), 25.54, 19.09.
MS (ESI) m/z $[M + Na]^+$ calcd. for $C_{15}H_{27}NO_5Na$: 324.18, found: 324.30.

Synthesis of racemic mixture of methyl 2-[(3S,4aR)-1-oxo-octahydropyrido[1,2-c][1,3]oxazin-3-yl]acetate and methyl 2-[(3R,4aS)-1-oxo-octahydropyrido[1,2-c][1,3]oxazin-3-yl]acetate (anti-25).

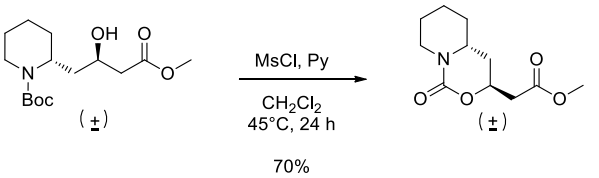

Synthesised according the general procedure for the synthesis of carbamates with inversion of configuration, starting from ***anti*-24**.

Yield: 70%, white wax.
^{1}H NMR (400 MHz, $CDCl_3$) δ 4.75 – 4.63 (m, 1H), 4.37 (m, 1H), 3.69 (s, 3H), 3.33 – 3.25 (m, 1H), 2.79 (dd, *J* = 16.1, 6.4 Hz, 1H), 2.68 (t, *J* = 12.4 Hz, 1H), 2.53 (dd, *J* = 16.1, 6.6 Hz, 1H), 2.03 (m, 1H), 1.97 – 1.88 (m, 1H), 1.84 (m, 1H), 1.68 (m, 1H), 1.64 – 1.59 (m, 1H), 1.58 – 1.42 (m, 3H).
^{13}C NMR (100 MHz, $CDCl_3$) δ 170.27, 153.12, 70.07, 53.20, 52.10, 46.00, 39.32, 33.03, 32.89, 25.50, 24.54.
MS (ESI) m/z $[M + Na]^+$ calcd. for $C_{11}H_{17}NO_4Na$: 250.10, found: 250.77.

Synthesis of tert-butyl (2R)-2-[(2S)-2-[(tert-butyldimethylsilyl)oxy]pent-4-en-1-yl]piperidine-1-carboxylate and (2S)-2-[(2R)-2-[(tert-butyldimethylsilyl)oxy]pent-4-en-1-yl]piperidine-1-carboxylate (27)

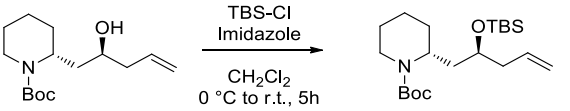

90%

TBSCl (0.574 g, 3.81 mmol) was added to a solution of ***anti*-9** (0.790 g, 2.93 mmol) and imidazole (0.400 g, 5.86 mmol) in anhydrous CH_2Cl_2 (15 mL), previously cooled at 0°C. The reaction mixture was then diluted with CH_2Cl_2 and washed with brine. The aqueous layer was extracted with CH_2Cl_2 and the collected organic phases were dried over Na_2SO_4, filtered and concentrated under vacuum.
The crude product was purified by column chromatography on silica gel (Hex: EtOAc = 9:1), to give **27** (1.010 g, 90%) as a yellow oil.

^{1}H NMR (400 MHz, $CDCl_3$) δ 5.95 – 5.65 (m, 1H), 5.14 – 4.94 (m, 2H), 4.36 – 4.16 (m, 1H), 4.07 – 3.87 (m, 1H), 3.67 (dq, *J* = 7.6, 5.2 Hz, 1H), 2.86 – 2.63 (m, 1H), 2.50 – 2.31 (m, 1H), 2.31 – 2.16 (m, 1H), 1.83 (m, 1H), 1.75 – 1.47 (m, 7H), 1.46 (s, 9H), 0.98 – 0.79 (m, 9H), 0.07 (s, 3H), 0.06 (s, 3H).
^{13}C NMR (100 MHz, $CDCl_3$) δ 155.02, 135.26, 117.13 ,79.36, 69.54 , 47.54, 41.23 , 39.01, 36.06, 36.84 , 29.07 , 28.68 (3 CH_3) , 26.04 , 25.84 (3 CH_3) , 19.27 , -4.34 (2 CH_3).
MS (ESI) m/z $[M + Na]^+$ calcd. for $C_{21}H_{41}NO_3SiNa$: 406.27, found:406.31

Stereoselective synthesis
Enantiopure **(*R, S*)-27** and **(*S, R*)-27** isomers were obtained performing the reaction on enantiopure ***anti*-9** isomers.

(*S, R*)-27: $[\alpha]_D^{20}$ **:** +16.9 (*c*= 0.62, $CHCl_3$).
(*S,R*)-27: $[\alpha]_D^{20}$ **:** -18.8 (*c*= 0.55, $CHCl_3$).

Synthesis of tert-butyl (2R)-2-[(2R)-2-[(tert-butyldimethylsilyl)oxy]-4-oxobutyl]piperidine-1-carboxylate and tert-butyl (2S)-2-[(2S)-2-[(tert-butyldimethylsilyl)oxy]-4-oxobutyl]piperidine-1-carboxylate (28)

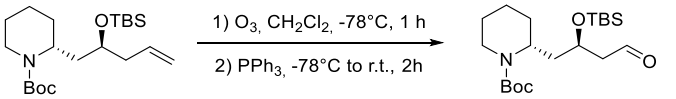

Ozone was fluxed through a solution of **27** (0.329 g, 0.86 mmol) in CH_2Cl_2 (10 mL), cooled at -78°C. After 1 h, the residual ozone was remove from the solution fluxing nitrogen for 10 minutes. PPh_3 (0.337 g, 1.29 mmol) was added at -78°C, then the reaction mixture was stirred for 2 h at r.t.. The solvent was removed under vacuum and the residue was purified
by column chromatography on silica gel (Hex: EtOAc = 9:1), affording **28** (0.198 g, 60%) as a yellow oil.

^{1}H NMR (400 MHz, $CDCl_3$) δ 9.77 (s, 1H), 4.36 – 4.23 (m, 1H), 4.13 (d. quint., *J* = 11.5, 4.2 Hz, 1H), 4.07 – 3.95 (m, 1H), 2.76 (t, *J* = 12.2 Hz, 2H), 2.53 (ddd, *J* = 15.6, 7.0, 3.2 Hz, 1H), 2.14 – 1.97 (m, 1H), 1.56 (dd, *J* = 29.8, 11.2 Hz, 6H), 1.44 (s, 9H), 1.41 – 1.32 (m, 1H), 0.86 (s, 9H), 0.07 (s, 3H), 0.04 (s, 3H).
^{13}C NMR (100 MHz, $CDCl_3$) δ 202.30, 154.99, 79.72, 66.21, 50.38, 47.42, 41.52, 38.16, 29.52, 28.64 (3 CH_3), 25.90 (3 CH_3), 25.76, 19.36, 18.07, -4.19, -4.60.
MS (ESI) m/z $[M + Na]^+$ calcd. for $C_{20}H_{39}NO_4SiNa$: 408.25, found: 408.38.

Stereoselective synthesis
Enantiopure **(*R, R*)-28** and **(*S, S*)-28** isomers were obtained performing the reaction on enantiopure precursors.

(*R, R*)-28: $[\alpha]_D^{20}$ **:** +22.2 (*c*= 0.52, $CHCl_3$).
(*S, S*)-28: $[\alpha]_D^{20}$ **:** -20.8 (*c*= 0.89, $CHCl_3$).

Racemic procedure for the synthesis of 10a and 10b

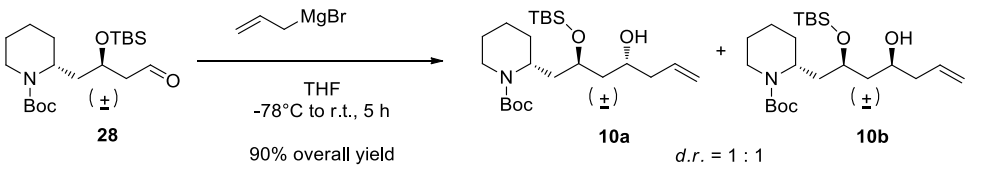

Allylmagnesium bromide (1.0 M solution, 1.37 mL, 1.37 mmol) was added dropwise to a solution of **28** in anhydrous THF (10 mL), previously cooled at -78°C. the reaction mixture was stirred for 1 h at -78°C and then allowed to warm to r.t. After 5 h, the reaction was quenched with a saturated aqueous solution of NH_4Cl. The layers were separated and the aqueous one was extracted with Et_2O. The combined organic layers were washed with brine, dried over Na_2SO_4, filtered and concentrated under vacuum. The crude product was purified by column chromatography on silica gel (Hex: EtOAc = 9:1), to give **10a** and **10b** (0.289 g and 0.235 g respectively, 90% overall yield) as light yellow oils.

Racemic mixture of (R)-tert-butyl 2-((2R,4R)-2-((tert-butyldimethylsilyl)oxy)-4-hydroxyhept-6-en-1-yl)piperidine-1-carboxylate and (S)-tert-butyl 2-((2S,4S)-2-((tert-butyldimethylsilyl)oxy)-4-hydroxyhept-6-en-1-yl)piperidine-1-carboxylate (10a)

^{1}H NMR (400 MHz, $CDCl_3$) δ 5.86 (ddt, *J* = 17.2, 10.2, 7.0 Hz, 1H), 5.13 – 5.04 (m, 2H), 4.20 (m 1H), 3.99 (m, 1H), 3.89 (m, 2H), 2.81 (t, *J* = 10.6 Hz, 1H), 2.23 (dh, *J* = 20.5, 6.7 Hz, 2H), 2.12 – 2.02 (m, 1H), 1.75 – 1.47 (m, 8 H), 1.45 (s, 9H), 1.39 (m, 1H), 0.89 (s, 9H), 0.08 (s, 3H), 0.07 (s, 3H).
^{13}C NMR (100 MHz, $CDCl_3$) δ 135.32, 117.13, 79.77, 67.95 (2 CH), 47.46, 42.87, 41.37, 30.06, 29.86, 28.68 (3 CH_3), 26.01 (3 CH_3), 25.82, 19.43, 17.91, -4.33, -4.69. (detected signals)
MS (ESI) m/z $[M + Na]^+$ calcd. for $C_{23}H_{45}NO_4SiNa$: 450.30, found: 450.59

Racemic mixture of (R)-tert-butyl 2-((2R,4S)-2-((tert-butyldimethylsilyl)oxy)-4-hydroxyhept-6-en-1-yl)piperidine-1-carboxylate and (S)-tert-butyl 2-((2S,4R)-2-((tert-butyldimethylsilyl)oxy)-4-hydroxyhept-6-en-1-yl)piperidine-1-carboxylate (10b)

^{1}H NMR (400 MHz, $CDCl_3$) δ 5.86 (m, 1H), 5.17 – 5.02 (m, 2H), 4.36 – 4.20 (m, 1H), 4.15 – 3.91 (m, 1H), 3.91 – 3.76 (m, 2H), 2.78 (t, *J* = 12.7 Hz, 1H), 2.23 (m, 2H), 2.12 – 1.98 (m, 1H), 1.98 – 1.77 (m, 1H), 1.72 – 1.48 (m, 7H), 1.45 (s, 9H), 1.43 – 1.38 (m, 1H), 0.89 (s, 9H), 0.10 (s, 6H).
^{13}C NMR (100 MHz, $CDCl_3$) δ 155.11, 135.19, 117.43, 79.61, 70.72, 70.07, 47.43, 43.65, 42.36, 39.18 (2 CH_2), 29.8, 28.67 (3CH_3), 26.01 (3CH_3), 25.83, 19.39, 18.45, -3.89, -4.46.
MS (ESI) m/z $[M + Na]^+$ calcd. for $C_{23}H_{45}NO_4SiNa$: 450.30, found: 450.79

Stereoselective Procedure for the synthesis of (R)-tert-butyl 2-((2R,4S)-2-((tert-butyldimethylsilyl)oxy)-4-hydroxyhept-6-en-1-yl)piperidine-1-carboxylate ((R,R,S)-10b) and (S)-tert-butyl 2-((2S,4R)-2-((tert-butyldimethylsilyl)oxy)-4-hydroxyhept-6-en-1-yl)piperidine-1-carboxylate ((S,S,R)-10b).

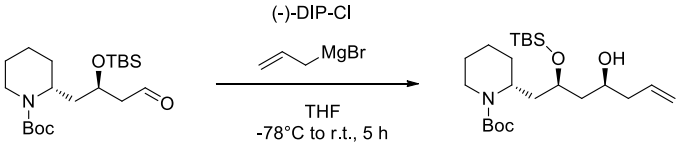

(-)-DIP-Cl (1.292 g, 4.03 mmol) was dissolved in anhydrous THF (16 mL) and cooled at -78°C. Allylmagnesium bromide (1.0 M solution, 4.14 mL, 4.14 mmol) was added dropwise. The reaction mixture was stirred for 1 h at -5°C and then the white solid was allowed to precipitate. **(*R, R*)-28** (0.914 g, 2.37 mmol) was dissolved in anhydrous THF (8 mL) and was added to the supernatant of the previous mixture cooled at -78°C. After 1 h, the reaction was warmed to r.t. and stirred overnight. The mixture was concentrated, a saturated solution of NaH_2PO_4 (14mL), MeOH (14 mL) and H_2O_2 35% (7mL) were added. The mixture was stirred for 30 min; a saturated solution of $NaHCO_3$ was added. The layers were separated and the aqueous one was extracted with Et_2O. The combined organic layers were washed with brine, dried over Na_2SO_4, filtered and concentrated under vacuum.
The crude product was purified by column chromatography on silica gel (Hex: EtOAc = 8:2, second column CH_2Cl_2, the CH_2Cl_2 : MeOH= 95:5), to give **(*R, R, S*)-10b** (0.932 g, 92%) as light yellow oil.

(*R, R, S*)-10b: $[\alpha]_D^{20}$ **:** +3.1 (*c*= 0.63, $CHCl_3$).

The opposite enantiomer **(*S, S, R*)-10b** was obtained exploiting the same procedure, but using (+)-DIP-Cl enantiomer and **(*S, S*)-28** aldehyde.

(*S, S, R*)-10b $[\alpha]_D^{20}$: -2.1 (*c*=1.1, $CHCl_3$).

HPLC conditions: Column: Zorbax SB-C18 5micronm 4.6x250 mm, 100% CH_3CN, flux: 1 mL/min, λ= 205 nm.
t_R for compounds 10b: 6.81 min.

General procedure for the synthesis of 30a and 30b

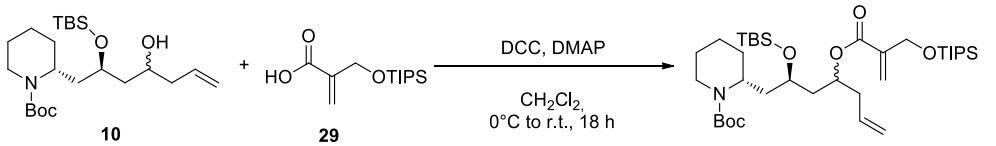

DCC (0.110 g, 0.87 mmol) and DMAP (0.020 g, 0.38 mmol) were added to a solution of **10** (0.233 g, 0.54 mmol) and **29** (0.212 g, 0.82 mmol) in anhydrous CH_2Cl_2 (7 mL), previously cooled at 0°C. The reaction mixture was stirred at 0°C for 3. minutes and then at r.t. overnight. The reaction mixture was diluted in CH_2Cl_2 and washed with a saturated aqueous solution of $NaHCO_3$. The organic layer was dried over Na_2SO_4, filtered and concentrated under vacuum. The residue was dissolver in cool ethyl acetate and filtered through a plug of celite, to remove DCC. After concentration, the crude product was purified by column chromatography on silica gel (Hex : EtOAC = 97:3), to give **30** as a uncoloured oil.

Racemic mixture of (R)-tert-butyl 2-((2R,4R)-2-((tert-butyldimethylsilyl)oxy)-4-((2-(((triisopropylsilyl)oxy)methyl)acryloyl)oxy)hept-6-en-1-yl)piperidine-1-carboxylate and (S)-tert-butyl 2-((2S,4S)-2-((tert-butyldimethylsilyl)oxy)-4-((2-(((triisopropyl silyl)oxy)methyl)acryloyl)oxy)hept-6-en-1-yl)piperidine-1-carboxylate (30a)

Yield: 92%

^{1}H NMR (400 MHz, $CDCl_3$) δ 6.19 (s, 1H), 5.92 – 5.89 (m, 1H), 5.68 (ddt, *J* = 14.3, 10.2, 7.1 Hz, 1H), 5.03 – 4.94 (m, 3H), 4.40 – 4.36 (m, 2H), 4.32 – 4.23 (m, 1H), 3.99 – 3.87 (m, 1H), 3.69 (m, 1H), 2.68 (m, 1H), 2.32 (t, *J* = 6.4 Hz, 2H), 1.95 – 1.80 (m, 2H), 1.63 – 1.42 (m, 7H), 1.39 (s, 9H), 1.35 – 1.25 (m, 1H), 1.13 – 1.04 (m, 3H), 1.00 (m, 18H), 0.81 (s, 9H), -0.03 (s, 3H), -0.10 (s, 3H).

^{13}C NMR (100 MHz, $CDCl_3$) δ 165.40, 154.67, 139.97, 133.41, 123.20, 117.82, 79.14, 70.97, 66.86, 61.68, 47.18, 40.48, 39.32, 29.25, 28.52 ($3CH_3$), 25.91 ($3CH_3$), 25.69 (2 CH_2), 19.26 (2 CH_2), 17.99 (6 CH_3), 17.32, 11.99 (3 CH), -4.07, -4.92.

MS (ESI) m/z $[M + Na]^+$ calcd. for $C_{36}H_{69}NO_6Si_2Na$: 690.46, found: 690.53.

Racemic mixture of (R)-tert-butyl 2-((2R,4S)-2-((tert-butyldimethylsilyl)oxy)-4-((2-(((triisopropylsilyl)oxy)methyl)acryloyl)oxy)hept-6-en-1-yl)piperidine-1-carboxylate and (S)-tert-butyl 2-((2S,4R)-2-((tert-butyldimethylsilyl)oxy)-4-((2-(((triisopropyl silyl)oxy)methyl)acryloyl)oxy)hept-6-en-1-yl)piperidine-1-carboxylate (30b)

Yield: 82%
^{1}H NMR (400 MHz, $CDCl_3$) δ 6.24 (d, *J* = 2.0 Hz, 1H), 5.96 (d, *J* = 2.1 Hz, 1H), 5.73 (ddt, *J* = 17.3, 10.4, 7.1 Hz, 1H), 5.25 – 5.10 (m, 1H), 5.08 – 4.98 (m, 2H), 4.43 (t, *J* = 2.1 Hz, 2H), 4.34 (bs, 1H), 4.06 – 3.85 (m, 1H), 3.67 (quint., *J* = 6.0 Hz, 1H), 2.76 (t, *J* = 12.6 Hz, 1H), 2.44 – 2.35 (m, 1H), 2.29 (dt, *J* = 14.3, 7.1 Hz, 1H), 2.00 – 1.87 (m, 1H), 1.87 – 1.70 (m, 2H), 1.72 – 1.59 (m, 1H), 1.51 (m, 5H), 1.44 (s, 9H), 1.38 – 1.31 (m, 1H), 1.18 – 1.09 (m, 3H), (m, 18H), 0.88 (s, 9H), 0.03 (s, 6H).
^{13}C NMR (100 MHz, $CDCl_3$) δ 165.32, 154.93, 140.12, 133.62, 123.39, 117.97, 79.29, 70.68, 67.22, 61.75, 47.07, 40.53, 39.29, 29.82, 28.67 ($3CH_3$), 25.99 ($3CH_3$), 25.80 (2 CH_2), 19.15 (2 CH_2), 18.11 (6 CH_3), 17.22, 12.11 (3 CH), -4.30, -4.43.
MS (ESI) m/z $[M + Na]^+$ calcd. for $C_{36}H_{69}NO_6Si_2Na$: 690.46, found: 690.61.

The two enantiomers of **30b** were synthesised from enantiopure **(*R, R, S*)-10b** and **(*S, S, R*)-10b** isomers.

***(R)-tert-butyl 2-((2R,4S)-2-((tert-butyldimethylsilyl)oxy)-4-((2-(((triisopropylsilyl)oxy)methyl)acryloyl)oxy)hept-6-en-1-yl)piperidine-1-carboxylate* (*R, R, S*)-30b**
$[\alpha]_D^{20}$: +9.1 (*c*= 0.74, $CHCl_3$).

***(S)-tert-butyl 2-((2S,4R)-2-((tert-butyldimethylsilyl)oxy)-4-((2-(((triisopropyl silyl)oxy)methyl)acryloyl)oxy)hept-6-en-1-yl)piperidine-1-carboxylate* (*S, S, R*)-30b**
$[\alpha]_D^{20}$: -13.9 (*c*= 0.694, $CHCl_3$).

General procedure for the synthesis of 31a and 31b

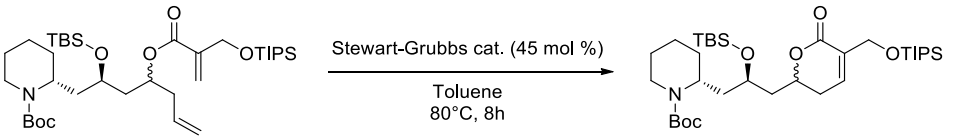

A solution of SG cat (0.020 g, 0.03 mmol) in 10 mL of toluene was added dropwise to a solution of **30** (0.150 g, 0.022 mmol) in degassed, anhydrouos toluene (80 mL), heated at 80°C. The reaction mixture was stirred at 80°C for 8 hours. During that range of time, other two additions of SG cat (0.020 g, 0.03 mmol for each of them) were performed. The solvent was removed under vacuum and the residue was purified by column chromatography on silica gel (Hex: EtOAc = 9:1), to give **31** as a yellow oil.

Racemic mixture of (R)-tert-butyl 2-((R)-2-((tert-butyldimethylsilyl)oxy)-3-((R)-6-oxo-5-(((triisopropylsilyl)oxy)methyl)-3,6-dihydro-2H-pyran-2-yl)propyl)piperidine-1-carboxylate and (S)-tert-butyl 2-((S)-2-((tert-butyldimethylsilyl)oxy)-3-((S)-6-oxo-5-(((triisopropylsilyl)oxy)methyl)-3,6-dihydro-2H-pyran-2-yl)propyl)piperidine-1-carboxylate (31a)

Yield: 75%.

^{1}H NMR (400 MHz, $CDCl_3$) δ 6.94 – 6.82 (bs, 1H), 4.58 – 4.47 (m, 2H), 4.42 (d, *J* = 2.2 Hz, 1H), 4.37 (m, 1H), 4.07 – 3.94 (m, 2H), 2.76 (t, *J* = 12.8 Hz, 1H), 2.39 – 2.29 (m, 2H), 2.18 – 2.05 (m, 1H), 2.02 – 1.90 (m, 1H), 1.57 (m, 7H), 1.44 (s, 9H), 1.40 – 1.30 (m, 1H), 1.19 – 1.08 (m, 3H), 1.05 (m, 18H), 0.85 (s, 9H), 0.07 (s, 3H), 0.03 (s, 3H).

^{13}C NMR (100 MHz, $CDCl_3$) δ 164.36, 154.75, 137.49, 131.91, 79.56, 74.51, 65.83, 60.90, 46.87, 41.87, 38.49 (2 CH_2), 30.23 (2 CH_2), 28.62 (3 CH_3), 26.00 (3 CH_3), 25.83, 19.39, 18.10 (6 CH_2), 17.51. 12.05 (3 CH), -4.10, -4.66.

MS (ESI) m/z $[M + Na]^+$ calcd. for $C_{34}H_{65}NO_6Si_2Na$: 662.42, found: 662.81.

Racemic mixture of (R)-tert-butyl 2-((R)-2-((tert-butyldimethylsilyl)oxy)-3-((S)-6-oxo-5-(((triisopropylsilyl)oxy)methyl)-3,6-dihydro-2H-pyran-2-yl)propyl)piperidine-1-carboxylate and (S)-tert-butyl 2-((S)-2-((tert-butyldimethylsilyl)oxy)-3-((R)-6-oxo-5-(((triisopropylsilyl)oxy)methyl)-3,6-dihydro-2H-pyran-2-yl)propyl)piperidine-1-carboxylate (31b).

Yield: 79%

^{1}H NMR (400 MHz, $CDCl_3$) δ 6.95 – 6.79 (bs, 1H), 4.54 (m, 1H), 4.49 (s, 1H), 4.42 – 4.38 (s, 1H), 4.35 – 4.25 (m, 1H), 4.03 – 3.90 (m, 1H), 3.86 – 3.78 (m, 1H), 2.79 – 2.67 (m, 1H), 2.40 – 2.31 (m, 2H), 2.12 – 2.02 (m, 1H), 1.96 – 1.84 (m, 2H), 1.69 – 1.51 (m, 6H),

1.41 (s, 9H), 1.37 – 1.31 (m, 1H), 1.15 – 1.07 (m, 3H), 1.03 (m, 18H), 0.84 (s, 9H), 0.03 (s, 3H), 0.00 (s, 3H).

^{13}C NMR (100 MHz, $CDCl_3$) δ 164.54, 154.87, 137.27, 131.74, 79.32, 75.22, 66.87, 60.78, 46.88, 41.01 , 39.18, 36. 56, 29.75, 29.47, 28.60 (3 CH_3), 25.89 (3 CH_3), 25.75, 19.27, 18.05 (6 CH_3), 17.35, 12.0 (3 CH), -4.23, -4.61.

MS (ESI) m/z $[M + Na]^+$ calcd. for $C_{34}H_{65}NO_6Si_2Na$: 662.42, found: 662.62.

The two enantiomers of **31b** were synthesised from enantiopure **(*R, R, S*)-30b** and **(*S, S, R*)-30b** isomers.

***(R)-tert-butyl 2-((R)-2-((tert-butyldimethylsilyl)oxy)-3-((S)-6-oxo-5-(((triisopropylsilyl)oxy)methyl)-3,6-dihydro-2H-pyran-2-yl)propyl)piperidine-1-carboxylate* (*R, R, S*)-31b.**

$[\alpha]_D^{20}$: -3.6 (*c*= 0.55, $CHCl_3$).

***(S)-tert-butyl 2-((S)-2-((tert-butyldimethylsilyl)oxy)-3-((R)-6-oxo-5-(((triisopropylsilyl)oxy)methyl)-3,6-dihydro-2H-pyran-2-yl)propyl)piperidine-1-carboxylate* (*S, S, R*)-31b.**

$[\alpha]_D^{20}$: +7.0 (*c*= 0.54, $CHCl_3$).

General procedure for the synthesis of compounds 32a and 32b

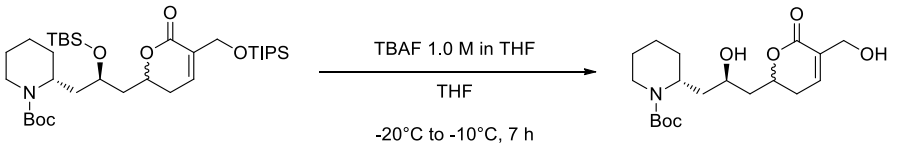

A solution of TBAF 1.0 M in THF (400 µL, 0.41 mmol) was added dropwise to a solution of **31** (0.105 g, 0.16 mmol) in anhydrous THF (5 mL), cooled at -20°C. The reaction mixture was stirred for 1 h at -20°C. Then, other three aliquots of 400 µL of TBAF were added every hour, and the temperature of the reaction mixture was raised of 5 °C every time, to reach -10°C. A final addition of TBAF (150 µL) was performed at that temperature and, after 1 h, the reaction mixture was quenched with an aqueous saturated solution of NH_4Cl. The aqueous layer was extracted with Et_2O and the combined organic phases were dried over Na_2SO_4, filtered and concentrated under vacuum. The residue was purified by column chromatography on silica gel (EtOAc 100%), affording **32** as an uncoloured viscous oil.

Racemic mixture of (R)-tert-butyl 2-((R)-2-hydroxy-3-((R)-5-(hydroxymethyl)-6-oxo-3,6-dihydro-2H-pyran-2-yl)propyl)piperidine-1-carboxylate and (S)-tert-butyl 2-((S)-2-hydroxy-3-((S)-5-(hydroxymethyl)-6-oxo-3,6-dihydro-2H-pyran-2-yl)propyl) piperidine-1-carboxylate (32a)

Yield: 60%.

^{1}H NMR (400 MHz, $CDCl_3$) δ 6.90 – 6.66 (m, 1H), 4.80 – 4.67 (m, 1H), 4.34 – 4.24 (m, 3H), 4.07 – 3.97 (m, 1H), 3.96 – 3.85 (m, 1H), 2.80 (t, *J* = 12.3 Hz, 1H), 2.40 (m, 2H), 1.90 (dd, *J* = 13.7, 9.6 Hz, 1H), 1.77 (dt, *J* = 15.3, 8.0 Hz, 1H), 1.70 – 1.53 (m, 7H), 1.44 (s, 9H), 1.36 – 1.30 (m, 1H).

^{13}C NMR (100 MHz, $CDCl_3$) δ 165.53, 154.26, 140.45, 131.66, 80.24, 75.56, 66.40, 61.70, 48.75, 42.60, 39.94, 39.21, 30.18, 29.82, 28.61 ($3CH_3$), 25.55, 19.23.

MS (ESI) m/z $[M + Na]^+$ calcd. for $C_{19}H_{31}NO_6Na$: 392.2049, found: 392.2053.

Racemic mixture of (R)-tert-butyl 2-((R)-2-hydroxy-3-((S)-5-(hydroxymethyl)-6-oxo-3,6-dihydro-2H-pyran-2-yl)propyl)piperidine-1-carboxylate and of (S)-tert-butyl 2-((S)-2-hydroxy-3-((R)-5-(hydroxymethyl)-6-oxo-3,6-dihydro-2H-pyran-2-yl)propyl)piperidine-1-carboxylate (32b).

Yield: 66%

^{1}H NMR (400 MHz, $CDCl_3$) δ 6.90 – 6.57 (m, 1H), 4.75 – 4.55 (m, 1H), 4.35 – 4.19 (m, 3H), 3.99 – 3.86 (m, 1H), 3.86 – 3.73 (m, 1H), 2.88 – 2.75 (m, 1H), 2.58 – 2.29 (m, 2H), 2.00 – 1.80 (m, 3H), 1.72 – 1.49 (m, 6H), 1.42 (s, 9H), 1.37 – 1.27 (m, 1H).

^{13}C NMR (100 MHz, $CDCl_3$) δ 140.33, 131.49, 80.14, 76.72, 67.16, 61.42, 48.35, 41.55, 39.74, 38.61, 29.77, 29.17, 28.57 (3 CH_3), 25.53, 19.17. (detected signals).

MS (ESI) m/z $[M + Na]^+$ calcd. for $C_{19}H_{31}NO_6Na$: 392.20, found: 392.56.

The two enantiomers of **32b** were synthesised from enantiopure **(*R, R, S*)-31b** and **(*S, S, R*)-31b** isomers

***(R)-tert-butyl 2-((R)-2-hydroxy-3-((S)-5-(hydroxymethyl)-6-oxo-3,6-dihydro-2H-pyran-2-yl)propyl)piperidine-1-carboxylate* (*R, R, S*)-32b**

$[\alpha]_D^{20}$: -2.8 (*c*= 1.02, $CHCl_3$).

(S)-tert-butyl 2-((S)-2-hydroxy-3-((R)-5-(hydroxymethyl)-6-oxo-3,6-dihydro-2H-pyran-2-yl)propyl)piperidine-1-carboxylate (S, S, R)-32b

$[\alpha]_D^{20}$: +3.8 (*c*= 0.57, $CHCl_3$).

General procedure for the synthesis of compounds 33a and 33b

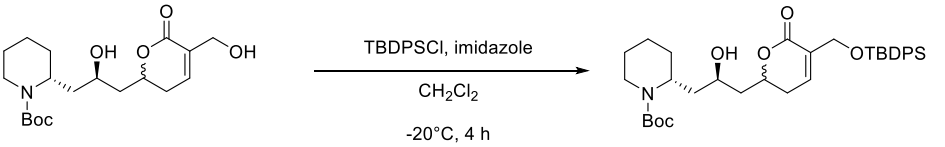

Imidazole (0.007 g, 0.094 mmol) and TBDPSCl (0.024 g, 0.089 mmol) were added dropwise to a solution of **32** (0.035 g, 0.094 mmol) in 2 mL of anhydrous CH_2Cl_2, cooled at -20°C. The reaction mixture was stirred at the same temperature for 4 h, then water was added. The aqueous layer was extracted with CH_2Cl_2. The combined organic phases were washed with brine, dried over Na_2SO_4, filtered and concentrated under vacuum. For what concern purification, compound **33a** proved to be unstable in column chromatography and was used without further purification in the following step. On the other hand, **33b** was successfully purified by column chromatography on silica gel (Hex : EtOAc= 7 : 3), affording the clean product as an uncoloured oil.

Racemic mixture of (R)-tert-butyl 2-((R)-3-((R)-5-(((tert-butyldiphenylsilyl) oxy)methyl)-6-oxo-3,6-dihydro-2H-pyran-2-yl)-2-hydroxypropyl)piperidine-1-carboxylate and (S)-tert-butyl 2-((S)-3-((S)-5-(((tert-butyldiphenylsilyl)oxy)methyl)-6-oxo-3,6-dihydro-2H-pyran-2-yl)-2-hydroxypropyl)piperidine-1-carboxylate (33a)

MS (ESI) m/z $[M + Na]^+$ calcd. for $C_{35}H_{49}NO_6SiNa$: 630.32, found: 630.81.

Racemic mixture of (R)-tert-butyl 2-((R)-3-((S)-5-(((tert-butyldiphenylsilyl) oxy)methyl)-6-oxo-3,6-dihydro-2H-pyran-2-yl)-2-hydroxypropyl)piperidine-1-carboxylate and (S)-tert-butyl 2-((S)-3-((R)-5-(((tert-butyldiphenylsilyl)oxy)methyl)-6-oxo-3,6-dihydro-2H-pyran-2-yl)-2-hydroxypropyl)piperidine-1-carboxylate (33b)

Yield: 65%

^{1}H NMR (400 MHz, $CDCl_3$) δ 7.66 – 7.61 (m, 4H), 7.39 (m, 6H), 7.04 – 6.98 (bs, 1H), 4.59 (dq, *J* = 10.9, 6.3 Hz, 1H), 4.51 (d, *J* = 15.7 Hz, 1H), 4.43 – 4.29 (m, 2H), 4.00 – 3.90 (m, 1H), 3.90 – 3.83 (m, 1H), 2.89 – 2.78 (m, 1H), 2.59 – 2.47 (m, 1H), 2.47 – 2.36 (m, 1H), 2.01 – 1.90 (m, 2H), 1.90 – 1.82 (m, 2H), 1.71 – 1.51 (m, 5H), 1.46 (s, 9H), 1.43 – 1.39 (m, 1H), 1.09 (s, 9H).

^{13}C NMR (100 MHz, $CDCl_3$) δ 164.36, 155.71, 138.00, 135.59 (4 CH), 133.24 (2 Cq), 131.28 , 129.98 (2 CH), 127.92 (4 CH), 80.19 , 76.68 , 67.56 , 61.46 , 48.54 , 41.64 , 36.14 , 33.56, 29.84 , 29.22 , 28.63 (3 CH_3), 27.04 (3 CH_3), 25.59, 20.73, 19.27.

MS (ESI) m/z $[M + Na]^+$ calcd. for $C_{35}H_{49}NO_6SiNa$: 630.32, found: 630.55.

The two enantiomers of **33b** were synthesised from enantiopure **(*R, R, S*)-32b** and **(*S, S, R*)-32b** isomers.

***(R)-tert-butyl 2-((R)-3-((S)-5-(((tert-butyldiphenylsilyl) oxy)methyl)-6- oxo- 3,6-dihydro -2H-pyran-2-yl)-2-hydroxypropyl)piperidine-1-carboxylate* (*R, R, S*)-33b.**
$[\alpha]_D^{20}$: +1.6 (*c*= 0.22, $CHCl_3$).

***(S)-tert-butyl 2-((S)-3-((R)-5-(((tert-butyldiphenylsilyl)oxy)methyl)-6- oxo -3,6-dihydro-2H-pyran-2-yl)-2-hydroxypropyl)piperidine-1-carboxylate (S, S, R*)-33b.**
$[\alpha]_D^{20}$: -2.8 (*c*= 1.12, $CHCl_3$).

General procedure for the synthesis of compounds 34a and 34b

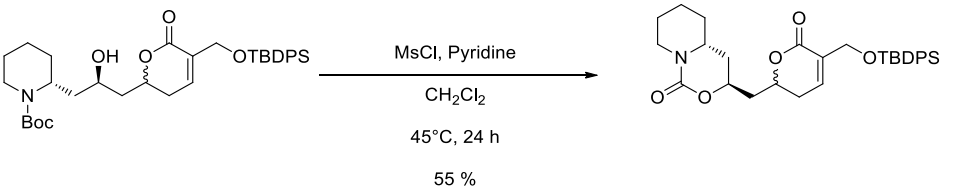

Pyridine (360 µL, 4.45 mmol) and methanesulfonyl chloride (46 µL, 0.59 mmol) were added to a solution of **33** (0.090 g, 0.15 mmol) in 3 mL of CH_2Cl_2, cooled at 0°C. The reaction mixture was refluxed at 45°C for 24 h, then the solvent was removed under vacuum, and hexane was used to remove pyridine. The residue was dissolved again in CH_2Cl_2 and water. The aqueous layer was extracted with CH_2Cl_2 and the combined organic phases were dried over Na_2SO_4, filtered and concentrated under vacuum. The crude product was purified by column chromatography on silica gel (Hex: EtOAc = 1:1), affording **34** as a white wax.

Racemic mixture of (3S,4aR)-3-(((R)-5-(((tert-butyldiphenylsilyl)oxy)methyl)-6-oxo-3,6-dihydro-2H-pyran-2-yl)methyl)hexahydropyrido[1,2-c][1,3]oxazin-1(3H)-one and (3R,4aS)-3-(((S)-5-(((tert-butyldiphenylsilyl)oxy)methyl)-6-oxo-3,6-dihydro-2H-pyran-2-yl)methyl)hexahydropyrido[1,2-c][1,3]oxazin-1(3H)-one (34a).

Yield: 68%.

^{1}H NMR (400 MHz, $CDCl_3$) δ 7.64 (m, 4H), 7.40 (m, 6H), 7.0.2 (bs, 1H), 4.74 – 4.58 (m, 1H), 4.58 – 4.44 (m, 2H), 4.38 (m, 2H), 3.30 (m, 1H), 2.83 – 2.63 (m, 1H), 2.63 – 2.42 (m, 2H), 2.24 – 2.05 (m, 2H), 2.05 – 1.89 (m, 2H), 1.78 (m, 1H), 1.74 – 1.65 (m, 1H), 1.65 – 1.42 (m, 4H), 1.09 (s, 9H).

^{13}C NMR (100 MHz, $CDCl_3$) δ 164.11, 153.33, 137.96, 135.56 (4 CH), 134.78, 133.17, 131.38, 129.99 (2 CH), 127.93 (4 CH), 74.14, 69.77, 61.36, 53.37, 46.08, 38.95, 33.17, 33.13, 29.18, 27.02 (3 CH_3), 25.57, 24.61, 19.43.

MS (ESI) m/z $[M + Na]^+$ calcd. for $C_{31}H_{39}NO_5SiNa$: 556.25 found: 556.36.

Racemic mixture of (3S,4aR)-3-(((S)-5-(((tert-butyldiphenylsilyl)oxy)methyl)-6-oxo-3,6-dihydro-2H-pyran-2-yl)methyl)hexahydropyrido[1,2-c][1,3]oxazin-1(3H)-one and (3R,4aS)-3-(((R)-5-(((tert-butyldiphenylsilyl)oxy)methyl)-6-oxo-3,6-dihydro-2H-pyran-2-yl)methyl)hexahydropyrido[1,2-c][1,3]oxazin-1(3H)-one (34b).

Yield: 80%

^{1}H NMR (400 MHz, $CDCl_3$) δ 7.64 (m, 4H), 7.47 – 7.32 (m, 6H), 7.02 (bs, 1H), 4.78 (t, *J* = 9.1 Hz, 1H), 4.61 (t, *J* = 9.2 Hz, 1H), 4.51 (m, 1H), 4.37 (m, 2H), 3.29 (m, 1H), 2.68 (t,

J = 11.4 Hz, 1H), 2.39 (m, 2H), 2.09 – 1.95 (m, 2H), 1.90 (m, 2H), 1.78 – 1.64 (m, 2H), 1.58 (m, 2H), 1.53 – 1.43 (m, 2H), 1.08 (s, 9H).
^{13}C NMR (100 MHz, $CDCl_3$) δ 164.05, 153.29, 137.56, 135.51 (4 CH), 133.21, 133.05, 131.59, 129.98 (2 CH), 127.94 (4 CH), 73.70, 69.47, 61.35, 53.48, 46.11, 40.62, 33.72, 33.13, 29.92, 27.01 (3 CH_3), 25.55, 24.64, 19.41.
MS (ESI) m/z $[M + Na]^+$ calcd. for $C_{31}H_{39}NO_5SiNa$: 556.25, found: 556.63.

The two enantiomers of **34b** were synthesised from enantiopure **(*R, R, S*)-33b** and **(*S, S, R*)-33b** isomers.

(3S,4aR)-3-(((S)-5-(((tert-butyldiphenylsilyl)oxy)methyl)-6-oxo-3,6-dihydro-2H-pyran-2-yl)methyl)hexahydropyrido[1,2-c][1,3]oxazin-1(3H)-one ((R, S, S)-34b).

$[\alpha]_D^{20}$: +10.4, (*c*= 0.91, $CHCl_3$).

(3R,4aS)-3-(((R)-5-(((tert-butyldiphenylsilyl)oxy)methyl)-6-oxo-3,6-dihydro-2H-pyran-2-yl)methyl)hexahydropyrido[1,2-c][1,3]oxazin-1(3H)-one ((S, R, R)-34b).

$[\alpha]_D^{20}$: -12.9 (*c*= 0.69, $CHCl_3$).

General procedure for the synthesis of compounds 19a and 19b

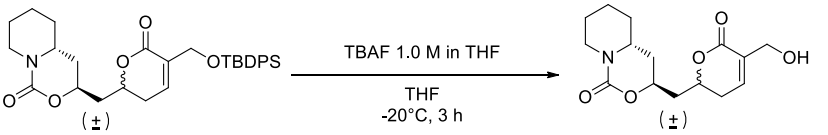

A solution of TBAF 1.0 M (160 µL, 0.16 mmol) in THF was added dropwise to a solution of **34** (0.041 g, 0.08 mmol) in 2 mL of anhydrous THF, cooled at -20°C. The reaction mixture was stirred at -20°C for 3 h, then the reaction was quenched adding a saturated aqueous solution of NH_4Cl. The layers were separated and the aqueous one was extracted with EtOAc. The combined organic phases were dried over Na_2SO_4, filtered and concentrated under vacuum. The crude product was purified by column chromatography on silica gel (gradient from EtOAc 100% to EtOAc : MeOH = 97 :3), giving **19** as a white wax.

Raceimic mixture of (3S,4aR)-3-(((R)-5-(hydroxymethyl)-6-oxo-3,6-dihydro-2H-pyran-2-yl)methyl)hexahydropyrido[1,2-c][1,3]oxazin-1(3H)-one and (3R,4aS)-3-(((S)-5-(hydroxymethyl)-6-oxo-3,6-dihydro-2H-pyran-2-yl)methyl)hexahydropyrido [1,2-c][1,3]oxazin-1(3H)-one (19a)

Yield: 44%.

^{1}H NMR (400 MHz, $CDCl_3$) δ 6.85 (bd, 1H), 4.74 – 4.67 (m, 1H), 4.57 – 4.49 (m, 1H), 4.42 – 4.34 (m, 1H), 4.31 (m, 2H), 3.36 – 3.28 (m, 1H), 2.69 (t, *J* = 12.7 Hz, 1H), 2.62 – 2.55 (m, 1H), 2.48 (dt, *J* = 18.1, 4.8 Hz, 1H), 2.19 (dt, *J* = 13.9, 6.7 Hz, 1H), 2.15 – 2.10 (m, 1H), 2.07 – 1.91 (m, 2H), 1.79 (bd,*J* = 14.0 Hz, 1H), 1.70 (m, 1H), 1.64 – 1.58 (m, 2H), 1.51 (m, 2H).

^{13}C NMR (100 MHz, $CDCl_3$) δ 165.15, 153.29, 140.34, 131.62, 74.42, 69.69, 61.65, 53.39, 46.11, 38.92, 33.18, 33.14, 29.24, 25.57, 24.62.

MS (ESI) m/z $[M + Na]^+$ calcd. for $C_{15}H_{21}NO_5Na$: 318.1317, found: 318.1318.

Racemic mixture of (3S,4aR)-3-(((S)-5-(hydroxymethyl)-6-oxo-3,6-dihydro-2H-pyran-2-yl)methyl)hexahydropyrido[1,2-c][1,3]oxazin-1(3H)-oneand (3R,4aS)-3-(((R)-5-(hydroxymethyl)-6-oxo-3,6-dihydro-2H-pyran-2-yl)methyl)hexahydropyrido [1,2-c][1,3]oxazin-1(3H)-one (19b).

Yield: 60%

^{1}H NMR (400 MHz, $CDCl_3$) δ 6.92 – 6.75 (bs, 1H), 4.91 – 4.75 (m, 1H), 4.67 – 4.53 (m, 1H), 4.47 – 4.30 (m, 2H), 4.26 (d, *J* = 13.7 Hz, 1H), 3.30 (q, *J* = 6.1, 5.6 Hz, 1H), 2.68 (td, *J* = 12.8, 2.8 Hz, 1H), 2.44 – 2.36 (m, 2H), 2.07 – 1.97 (m, 1H), 1.97 – 1.92 (m, 2H), 1.86 (ddd, *J* = 14.7, 10.0, 2.6 Hz, 1H), 1.78 – 1.65 (m, 2H), 1.58 (m, 2H), 1.54 – 1.44 (m, 2H).

^{13}C NMR (100 MHz, $CDCl_3$) δ 165.13, 153.30, 139.92, 131.83, 73.96, 69.39, 61.56, 53.50, 46.14, 40.53, 33.69, 33.15, 29.94, 25.56, 24.65.
MS (ESI) m/z $[M + Na]^+$ calcd. for $C_{15}H_{21}NO_5Na$: 318.13, found: 318.16.

Synthesis of (R)-1-((S)-piperidin-2-yl)pent-4-en-2-amine (37)

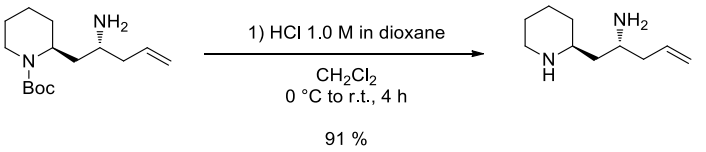

A 4M solution of HCl in dioxane (1.13 mL, 4.43 mmol) was added to a solution of **11** (0.595 g, 2.22 mmol) in CH_2Cl_2, previously cooled to 0 °C. The mixture was stirred at room temperature for 2 hours, then another aliquot of HCl in dioxane (2.26 mL, 8.85 mmol) was added, and the solution was stirred for additional 2 hours.
The solvent was evaporated, the residue was dissolved in CH_2Cl_2 and washed with a saturated aqueous solution of $NaHCO_3$, then the layers were separated. The aqueous phase was basified with NaOH 10 % and extracted with EtOAc. The collected organic phases were washed with brine, dried over Na_2SO_4, filtered and concentrated under vacuum to obtain **37** (0.340g, 91%), that was used in the following step without further purification.

^{1}H-NMR (400 MHz, CD_3OD): δ = 5.84 – 5.78 (m, 1H), 5.28 – 5.23 (m, 2H), 3.47 – 3.44 (m, 1H), 3.32 – 3.27 (m, 2H), 2.92 – 3.03 (m, 1H), 2.47 – 2.40 (m, 2H), 2.06 – 2.00 (m, 2H), 1.88 – 1.85 (m, 4H), 1.78 – 1.54 (m, 2H), 1.52 – 1.45 (m, 1H).
^{13}C-NMR (100 MHz, CD_3OD): δ = 131.53, 119.75, 53.00, 47.83, 44.67, 37.51, 36.33, 28.34, 21.88, 21.54.
$[\alpha]_D^{20}$: -3.8 (*c* = 1.0, MeOH).
MS (ESI) m/z $[M + H]^+$ calcd. for $C_{10}H_{21}N_2$: 168.16, found: 169.02.

Synthesis of (3R,4aS)-3-allyloctahydro-1H-pyrido[1,2-c]pyrimidin-1-one (38)

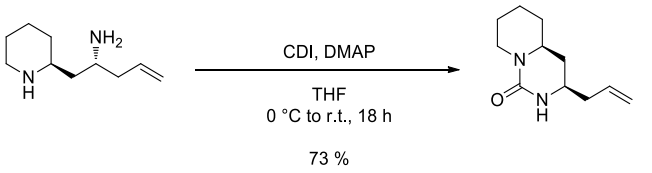

Carbonyldiimidazole (0.248 g, 1.53 mmol) and dimethylaminopyridine (0.019 g, 0.15 mmol) were added to a stirred solution of **37** (0.257 g, 1.53 mmol) in anhydrous THF, previously cooled at 0 °C. The reaction mixture was warmed to room temperature and stirred overnight.

The solution is diluted with EtOAc and washed with H_2O. The phases were separated and the aqueous one was extracted with Et_2O. The collected organic phases were washed with brine, dried over Na_2SO_4, filtered and concentrated under vacuum.

The crude product was purified by column chromatography on silica gel (CH_2Cl_2 : MeOH = 95:5), affording **38** (0.217 g, 73%) as a white wax.

^{1}H-NMR (400 MHz, $CDCl_3$): δ = 5.76 – 5.60 (m, 1H), 5.17 – 5.05 (m, 2H), 4.66 (bs, 1H), 4.50 – 4.36 (d, 1H), 3.34 (m, 1H), 3.10 (m, 1H), 2.47 (td, J = 12.8, 2.7 Hz, 1H), 2.28 – 2.19 (m, 1H), 2.04 (m, 1H), 1.97 – 1.88 (m, 1H), 1.81 – 1.70 (m, 2H), 1.70 – 1.62 (m, 1H),), 1.50 – 1.36 (m, 1H), 1.33 (dq, *J* = 9.5, 3.9, 3.4 Hz, 2H), 1.30 – 1.20 (m, 1H), 1.20 – 1.08 (m, 1H).

^{13}C-NMR (100 MHz, $CDCl_3$): δ = 156.78, 133.33, 119.02, 53.91, 48.28, 42.85, 40.70, 37.07, 33.53, 25.30, 24.00.

$[\alpha]_D^{20}$: -0.8 (*c* = 0.85, $CHCl_3$).

MS (ESI) m/z $[M + Na]^+$ calcd. for $C_{11}H_{18}N_2ONa$: 217.13, found: 217.00.

Synthesis of 2-((3S,4aS)-1-oxooctahydro-1H-pyrido[1,2-c]pyrimidin-3-yl) acetaldehyde (39).

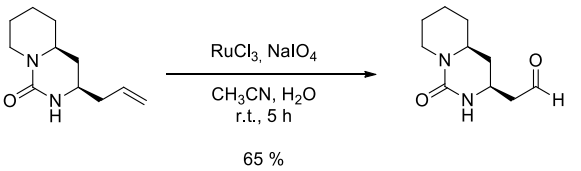

A solution of $RuCl_3$ (0.010 g, 0.04 mmol) in H_2O (1.5 mL) was added to a stirred solution of **38** (0.274 g, 1.41 mmol) in CH_3CN, then $NaIO_4$ (0.605 g, 2.82 mmol) was added in portions. The reaction mixture was stirred for 5 h.

The reaction was quenched with a saturated solution of $Na_2S_2O_3$, and diluted with EtOAc. The layers were separated and the aqueous one was extracted with EtOAc. The collected organic phases were washed with brine, dried over Na_2SO_4, filtered and concentrated under vacuum.

The crude product was purified by column chromatography on silica gel (CH_2Cl_2 : MeOH = 93:7), affording **39** (0.180 g, 65%) as an uncoloured oil, that was characterised only by ^{1}H-NMR and immediately reacted in the following step, due to aldehyde instability.

^{1}H-NMR (400 MHz, $CDCl_3$): δ 9.78 (s, 1H), 5.24 – 5.00 (m, 1H), 4.55 – 4.36 (m, 1H), 3.97 – 3.75 (m, 1H), 3.18 (tt, *J* = 11.0, 3.5 Hz, 1H), 2.63 (t, *J* = 6.8 Hz, 2H), 2.56 – 2.45 (m, 1H), 2.01 (dt, *J* = 13.1, 3.6 Hz, 1H), 1.84 – 1.68 (m, 3H), 1.35 (m, *2*H), 1.29 – 1.09 (m, 2H).

Synthesis of (3S,4aS)-3-((R)-2-hydroxypent-4-en-1-yl)octahydro-1H-pyrido[1,2-c] pyrimidin-1-one (40).

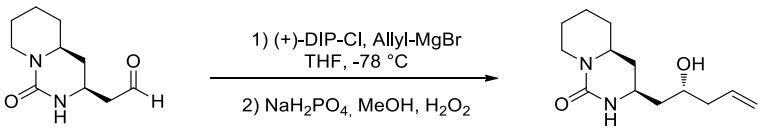

Allylmagnesium bromide (1 M solution in Et_2O, 0.610 mL) was added dropwise to a solution of (+)-DIP-Cl (0.222 g, 0.690 mmol) in anhydrous THF (3 mL), previously cooled at -78 °C. The reaction mixture was warmed to 0 °C and stirred at this temperature for one hour. The solution was allowed to stand until magnesium chloride precipitated. The supernatant solution was transferred to another flask and cooled at -78 °C, then a solution of **39** (0.080 g, 0.41 mmol) in anhydrous THF (2 mL) was added dropwise. The resulting solution was stirred at -78°C for one hour and then 16 hours at room temperature.

The reaction was quenched with NaH_2PO_4 buffer solution at pH 7 (3 mL), MeOH (3 mL) and 30 % H_2O_2 (1.5 mL). After stirring for 30 min, a saturated aqueous $NaHCO_3$ was added, and the mixture was extracted with Et_2O. The combined organic phases were dried over Na_2SO_4 and filtered, then the solvent was evaporated under vacuum.

The residue was purified by column chromatography on silica gel (CH_2Cl_2 : MeOH = 95:5), affording **40** (0.050 g, 52%) as an uncoloured oil.

^{1}H-NMR (400 MHz, $CDCl_3$): δ 6.22 (s, 1H), 5.84 – 5.72 (m, 1H), 5.13 – 5.00 (m, 2H), 4.40 (d, *J* = 13.2 Hz, 1H), 3.83 – 3.74 (m, 1H), 3.46 (m, 1H), 3.13 – 3.04 (m, 1H), 2.48 – 2.40 (m, 1H), 2.23 (qt, *J* = 13.7, 6.7 Hz, 2H), 1.86 (m, 1H), 1.73 (m, 2H), 1.67 – 1.61 (m, 1H), 1.56 – 1.49 (m, 1H), 1.47 – 1.39 (m, 2H), 1.39 – 1.28 (m, 2H), 1.16 – 1.07 (m, 1H).

^{13}C-NMR (100 MHz, $CDCl_3$): δ = 157.00, 134.69, 117.76, 70.91 , 53.76 , 49.55 , 43.48 , 42.78, 41.78 , 37.81 , 33.47 , 25.33 , 23.98.

$[\alpha]_D^{20}$: +5.6 (*c* = 0.99, $CHCl_3$).

MS (ESI) m/z $[M + Na]^+$ calcd. for $C_{13}H_{22}N_2O_2Na$: 261.17, found: 261.72.

Synthesis of (R)-1-((3S,4aS)-1-oxooctahydro-1H-pyrido[1,2-c]pyrimidin-3-yl)pent-4-en-2-yl 2-(((triisopropylsilyl)oxy)methyl)acrylate (41).

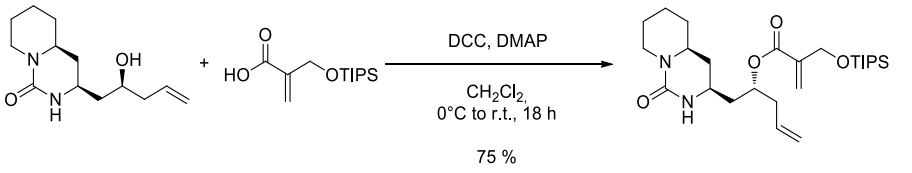

Dimethylaminopyridine (0.020 g, 0.16 mmol) and dicyclohexylcarbodiimide (0.080 g, 0.31 mmol) were added to a stirred solution of **40** (0.049 g, 0.20 mmol) and **29** (0.080 g, 0.31 mmol) in anhydrous CH_2Cl_2, previously cooled at 0 °C. The reaction mixture was stirred for 30 minutes at 0 °C, then for 4 hours at room temperature.

The reaction mixture was diluted with CH_2Cl_2 and washed with saturated aqueous $NaHCO_3$. The layers were separated and the aqueous one was extracted with Et_2O. The collected organic phases were washed with brine, dried over Na_2SO_4, filtered and concentrated under vacuum.

The crude product was purified by column chromatography on silica gel (CH_2Cl_2 : MeOH = 97:3), giving **41** (0.074 g, 75 %) as a light yellow oil.

^{1}H NMR (400 MHz, Chloroform-*d*) δ 6.37 – 6.16 (m, 1H), 6.13 – 5.89 (m, 1H), 5.78 – 5.58 (m, 1H), 5.18 – 5.02 (m, 2H), 4.82 – 4.68 (m, 1H), 4.47 – 4.34 (m, 3H), 3.44 – 3.25 (m, 1H), 3.15 – 2.98 (m, 1H), 2.45 (t, *J* = 12.5 Hz, 1H), 2.39 – 2.27 (m, 2H), 2.13 – 1.98 (m, 1H), 1.85 - 1.71 (m, 2H), 1.69 – 1.55 (m, 2H), 1.45- 1.27 (m, 5H), 1.18 – 1.07 (m, H), 1.05 (m, 18H).

^{13}C-NMR (100 MHz, $CDCl_3$): δ = 165.52, 156.72, 139.71, 132.79, 124.33, 118.72, 70.43, 61.73, 53.81, 46.75, 42.82, 40.47, 39.36, 36.88, 33.49, 25.27, 23.96, 18.07 (6 CH_3), 12.06 (3 CH).

$[\alpha]_D^{20}$: -15.4 (*c* = 1.13, $CHCl_3$).

MS (ESI) m/z $[M + Na]^+$ calcd. for $C_{26}H_{46}N_2O_4SiNa$: 501.31, found: 501.48.

Synthesis of compound of (3S,4aS)-3-(((R)-6-oxo-5-(((triisopropylsilyl)oxy)methyl)-3,6-dihydro-2H-pyran-2-yl)methyl)octahydro-1H-pyrido[1,2-c]pyrimidin-1-one (42).

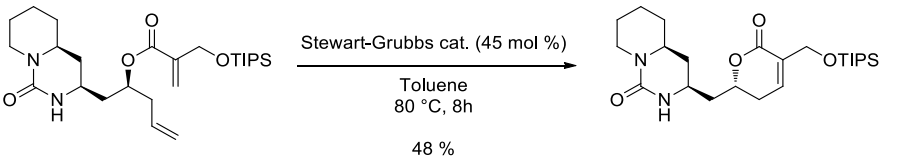

A solution of Stewart-Grubbs 2nd generation catalyst (0.008 g, 0.014 mmol) in anhydrous, degassed toluene (3.0 mL) was added dropwise to a stirred solution of **41** (0.043 g, 0.090 mmol) in anhydrous, degassed toluene, previously heated at 80 °C. An equivalent amount of catalyst in solution is then added after 2 and 4 hours. The reaction mixture is stirred at 80 °C for overall 8 hours.
The solvent was evaporated under vacuum and the residue was purified by column chromatography on silica gel (Hex : EtOAc= 8 : 2), giving **42** (0.020 g, 48%) as a brown oil.

^{1}H-NMR (400 MHz, $CDCl_3$): δ 6.93 (bs, 1H), 5.15 (bs, 1H), 4.67 – 4.51 (m, 2H), 4.51 – 4.35 (m, 2H), 3.83 – 3.47 (m, 1H), 3.15 (tt, *J* = 10.9, 3.1 Hz, 1H), 2.58 – 2.43 (m, 1H), 2.40 (dq, *J* = 7.9, 2.8 Hz, 2H), 2.36 – 2.23 (m, 1H), 2.03 (tt, *J* = 8.1, 4.8 Hz, 2H), 1.97 (dt, *J* = 9.4, 5.5 Hz, 2H), 1.85 – 1.74 (m, 2H), 1.74 – 1.65 (m, 2H), 1.65 – 1.56 (m, 1H), 1.20-1.11 (m, 3H), 1.08 (s, 18H).
^{13}C-NMR (100 MHz, $CDCl_3$): δ = 156.91, 136.94, 131.77, 119.08, 74.82, 60.62, 53.58, 45.72, 41.04, 36.53, 34.52, 33.69, 26.70, 25.14, 23.81, 17.96 (6 CH_3), 11.91 (3 CH).
$[\alpha]_D^{20}$: +8.53 (*c* = 0.4525, $CHCl_3$).
MS (ESI) m/z $[M + Na]^+$ calcd. for $C_{24}H_{42}N_2O_4SiNa$: 473.28, found: 473.55.

Synthesis of (3S,4aS)-3-(((R)-5-(hydroxymethyl)-6-oxo-3,6-dihydro-2H-pyran-2-yl)methyl)octahydro-1H-pyrido[1,2-c]pyrimidin-1-one (35).

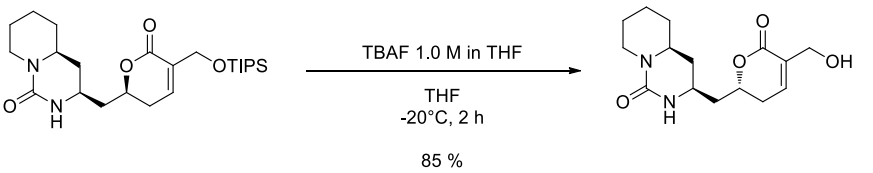

85 %

Tetrabutylammonium fluoride (1 M solution in THF, 0.05 mL, 0.05 mmol) was added dropwise to a solution of **42** (0.014 g, 0.03 mmol) in anhydrous THF, previously cooled at -20 °C. The reaction mixture was stirred at -20 °C for 2 hours.

The reaction was quenched with a saturated aqueous solution of NH_4Cl. The layers were separated and the aqueous one was extracted with EtOAc. The collected organic phases were washed with brine, dried over Na_2SO_4, filtered and concentrated under vacuum.

The crude product was purified by column chromatography on silica gel (EtOAc : MeOH = 9:1), affording **35** (0.008 g, 85%) as a yellow oil.

^{1}H-NMR (400 MHz, $CDCl_3$): δ = 6.84 (bs, 1H), 5.24 (bs, 1H), 4.60 (m, 1H), 4.43 (m, 1H), 4.30 (s, 2H), 3.65 (m, 1H), 3.16 (t, *J* = 10.7 Hz, 1H), 2.50 (t, *J* = 12.0 Hz, 1H), 2.40 (m, 2H), 2.00 (m, 3H), 1.77 (m, 2H), 1.69 (m, 2H), 1.51 (m, 4H).

^{13}C-NMR (100 MHz, $CDCl_3$): δ = 164.64, 157.32, 139.81, 131.81, 75.46, 61.51, 53.71, 46.73, 42.91, 40.37, 36.74, 33.52, 32.07, 25.29, 23.95.

$[\alpha]_D^{20}$: +12.92 (c = 0.77, $CHCl_3$).

MS (ESI) m/z $[M + Na]^+$ calcd. for $C_{15}H_{22}N_2O_4Na$: 317.15, found: 317.06.

Synthesis of racemic tert-butyl 2-{2-[(tert-butyldimethylsilyl)oxy]ethyl}piperidine-1-carboxylate (43).

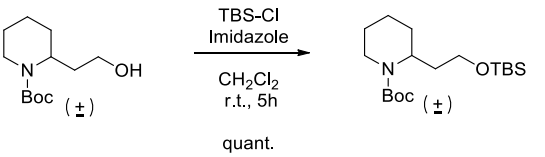

TBSCl (0.433 g, 2.88 mmol) was added to a solution of *N*-Boc-piperidine ethanol (0.550 g, 2.40 mmol) and imidazole (0.327 g, 4.80 mmol) in anhydrous CH_2Cl_2 (8 mL). The reaction mixture was stirred at r.t. for 5 hours, then diluted with CH_2Cl_2 and washed with brine. The aqueous layer was extracted with CH_2Cl_2 and the collected organic phases were dried over Na_2SO_4, filtered and concentrated under vacuum.
The crude product was purified by column chromatography on silica gel (Hex: EtOAc = 8:2), to give **43** (0.826 g, quant.) as a yellow oil.

^{1}H NMR (400 MHz, $CDCl_3$) δ 4.22–4.31 (m, 1H), 3.95 (bd, 1H),3.51–3.86 (m, 2H), 2.76 (td, *J* = 13.5, 3 Hz, 1H), 1.84–2.02 (m, 1H), 1.52–1.71 (m, 7H), 1.42 (s, 9H), 0.86 (s, 9H), 0.05 (s, 6H).
^{13}C NMR (100 MHz, $CDCl_3$) 154.9, 79.0, 61.1, 48.0, 38.8, 33.2, 28.7, 28.4 ($3CH_3$), 25.9 ($3CH_3$), 25.6, 19.1, 18.3, 5.3 ($2CH_3$).

MS (ESI) *m/z* $[M + Na]^+$ calcd. for $C_{18}H_{37}NO_3SiNa$: 366.24, found: 366.71.

Synthesis of racemic tert-butyl 2-{2-[(tert-butyldimethylsilyl)oxy]ethyl}-6-oxopiperidine-1-carboxylate (44)

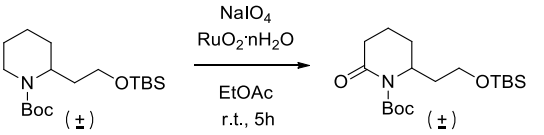

A 10% wt $NaIO_4$ aqueous solution (0.811 g, 3.90 mmol) and $RuO_2 \cdot nH_2O$ were added to a solution of **43** (0.584 g, 1.70 mmol) in EtOAc (3.3 mL). The reaction mixture was stirred at r.t. for 5 hours, then diluted with EtOAc. The layers were separated and the aqueous one was extracted with EtOAc. iprOH was added to the collected organic phases and the solution was filtered over celite. The recovered organic phases were dried over Na_2SO_4, filtered and concentrated under vacuum.
The crude product was purified by column chromatography on silica gel (Hex: EtOAc = 85:15), to give **44** (0.546 g, 90%) as a yellow oil.

^{1}H NMR (400 MHz, $CDCl_3$) δ 4.34 – 4.10 (m, 1H), 3.60 (m, 2H), 2.48 – 2.32 (m, 2H), 1.94 – 1.75 (m, 4H), 1.70 (m, 2H), 1.45 (s, 9H), 0.82 (s, 9H), 0.01 (s, 6H).
^{13}C NMR (100 MHz, $CDCl_3$ δ 171.48, 152.66, 82.63, 60.38, 53.81, 36.63, 34.10, 27.94 (3 CH_3), 26.19 (3 CH_3), 25.85, 18.17, 17.07, -5.46 (2 CH_2).
MS (ESI) m/z $[M + Na]^+$ calcd. for $C_{18}H_{35}NO_4SiNa$: 380.22, found: 380.45

Synthesis of racemic tert-butyl 2-{2-[(tert-butyldimethylsilyl)oxy]ethyl}-6-(trifluoromethanesulfonyloxy)-1,2,3,4-tetrahydropyridine-1-carboxylate (45).

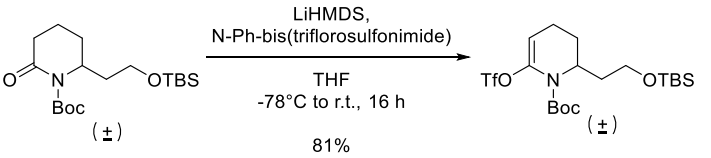

A 1.0M solution of LiHMDS in THF (2.3 mL, 2.29 mmol was added to a solution of **44** (0.546 g, 1.53 mmol) in anhydrous THF (7 mL) cooled to -78°C. The reaction mixture was stirred for 2 hours, then (1.091 g, 3.06 mmol) was added. The mixture was warmed to r.t. and stirred overnight. The reaction mixture was quenched with an aqueous 10% wt NaOH solution; the layers were separated and the aqueous one was extracted with Et_2O. The collected organic phases were dried over Na_2SO_4, filtered and concentrated under vacuum.

The crude product was purified by column chromatography on silica gel (Hex: CH_2Cl_2 = 6:4), to give **45** (0.605 g, 81%) as a yellow oil.

^{1}H NMR (400 MHz, $CDCl_3$) δ 5.25 (t, *J* = 3.8 Hz, 1H), 4.71 – 4.63 (m, 1H), 3.67 (dd, *J* = 6.7, 5.5 Hz, 2H), 2.26 – 2.18 (m, 2H), 1.85 (ddt, *J* = 14.2, 8.9, 5.4 Hz, 1H), 1.74 (m, 2H), 1.58 – 1.54 (m, 1H), 1.49 (s, 9H), 0.89 (s, 9H), 0.05 (s, 3H), 0.04 (s, 3H).

^{13}C NMR (100 MHz, $CDCl_3$) δ 152.95, 138.97, 116.99 (q), 106.10, 82.85, 60.22 , 52.00 , 32.46 , 28.14 (3 CH_3), 26.11 (3 CH_3) , 25.61 , 19.54 , -5.27 , -5.36. detected signals.

MS (ESI) m/z $[M + Na]^+$ calcd. for $C_{19}H_{34}F_3NO_6SSiNa$: 512.17, found: 512.15.

Synthesis of racemic tert-butyl 2-{2-[(tert-butyldimethylsilyl)oxy]ethyl}-6-phenyl-1,2,3,4-tetrahydropyridine-1-carboxylate (46).

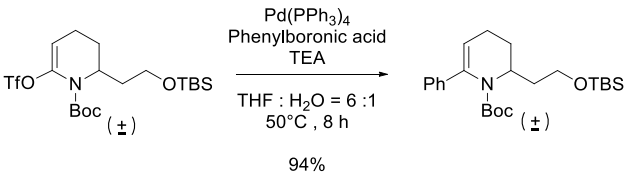

$Pd(PPh_3)_4$ (45.4 mg, 0.04 mmol) was added to a solution of **45** (0.385 g, 0.79 mmol), phenylboronic acid (0.192 g, 1.57 mmol), and anhydrous TEA (2.5 mL, 17.90 mmol) in a 6:1 mixture of anhydrous THF and H_2O (16 mL). The reaction mixture was stirred at 50°C until reaction completion. The reaction mixture was diluted with EtOAc, washed with a saturated solution of NH_4Cl. The layers were separated and the aqueous one was extracted with EtOAc. The collected organic phases were dried over Na_2SO_4, filtered and concentrated under vacuum.
The crude product was purified by column chromatography on silica gel (Hex: EtOAc = 98:2), to give **46** (0.308 g, 94%) as a yellow oil, that was used immediately in the following step due to its instablity.

^{1}H NMR (400 MHz, $CDCl_3$) δ 7.28-7.17 (m, 5H), 5.39-5.15 (m, 1H), 4.71-4.61 (m, 1H), 3.89-3.75 (m, 2H), 2.28- 2.15 (m, 2H), 2.01-1.72 (m, 2H), 2.00-1.87 (m, 2H), 1.05 (s, 9H), 0.83 (s, 9H), 0.04 (s, 6H).
MS (ESI) m/z $[M + Na]^+$ calcd. for $C_{24}H_{39}NO_3SiNa$: 440.26, found 440.37.

Synthesis of racemic tert-butyl 2-(2-hydroxyethyl)-6-phenylpiperidine-1-carboxylate (48).

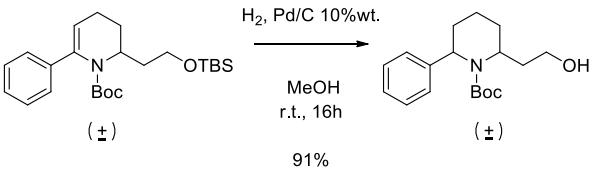

46 (0.040 g, 0.10 mmol) and Pd/C 10% wt (0.040 g) were dissolved in MeOH (2.2 mL). The reaction mixture was put under H_2 atmosphere and stirred overnight at r.t. The mixture was filtered over celite, washed with MeOH and CH_2Cl_2 and concentrated to give a mixture of **48** diastereomers (0.027 g, 91%) as a white amorphous solid.

^{1}H NMR (400 MHz, $CDCl_3$) δ 7.30 – 7.14 (m, 5H), 4.38 (m, 1H), 3.83 – 3.69 (m, 1H), 3.67 – 3.57 (m, 2H), 2.62 (t, J = 7.7 Hz, 2H), 1.87 – 1.77 (m, 1H), 1.71 – 1.56 (m, 2H), 1.58 – 1.47 (m, 2H), 1.48 – 1.43 (m, 13 H), 1.33 – 1.24 (m, 1H). (diastereomeric mixture)
^{13}C NMR (100 MHz, $CDCl_3$) δ 157.27, 142.50, 129.022 (2 CH), 128.45 (2 CH), 127.67, 79.89, 59.08, 47.28 (2 CH), 39.19, 35.93, 31.31, 28.47 (3 CH_3), 25.93. (diastereomeric mixture)
MS (ESI) m/z $[M + Na]^+$ calcd. for $C_{18}H_{27}NO_3Na$: 328.19, found 328.88.

Biology

Shh-Light II were cultured in DMEM plus 10% FBS, antibiotics and L-glutamine.

The luciferase assay was performed in Shh-Light II cells, stably incorporating a Gli-responsive luciferase reporter and the pRL-TK Renilla (Normaliza- tion control), treated for 48 h with SAG (200 nM) and the studied compounds. Luciferase and Renilla activity were assayed with a dual-luciferase assay system according to the manufacturer's in- struction (Biotium Inc., Hayward, CA, USA). Results are expressed as Luciferase/Renilla ratios and represent the mean ±SD of three independent experiments, each performed in triplicate.

4. (-)-anaferine: an unexpected encounter

4.1 *Withania somnifera*: source of piperidinic alkaloids.

Withania somnifera is a green shrub belonging to *Solanaceae*, that can reach a height of 0.5 - 2 meters (Figure 24). It is also known with the names of Indian ginseng, winter cherry and 'Ashwagandha', in Sanskrit language. This plant is widely diffused in drier regions of tropical and subtropical zones, and grows majorly in Middle East, India, Sri Lanka, China and in some parts of South Africa. It can be cultivated in the warmer regions of Europe, including insular Italy, and in India is growth as a medicinal plant. In fact, *Withania somnifera* has been used for centuries in the traditional Ayurvedic medicine, on the basis of an extremely wide range of bioactivities, including anti-inflammatory, anti-stress, immunomodulatory, adaptogenic, anticancer and neuroprotective activities.[145] Notably, *Withania somnifera* seems to be the only plant, among the 23 species belonging to *withania* genre, to displays pharmacological properties.
In Ayurvedic medicine, this plant is classified as an herbal Rasayana, namely a physical and mental health promoting substance. Roots are the part of the plant most used for therapeutic applications. However, leaves, seeds, flowers and fruits are employed to contrast fever, swelling, ulcers, tumours and as aphrodisiac and diuretic agents.

Figure 24. *Withania somnifera* shrub and its berries.

In the last decades, *Withania somnifera* properties attracted the attention of the scientific communities, and several studies were aimed at the scientific validation of its employment as multi-purpose drug in traditional medicine. The results of these pharmacological tests have been reviewed by different groups.[145,146,147]
Withania somnifera proved to modulate oxidative stress markers and to reduce lipid peroxidation, acting as a free radical scavenger. In fact, this plant is a rich source of antioxidant compounds, that could be involved in the reported anti-stress, anti-ageing

[145] N. J. Dar, A. Hamid, M. Ahmad, *Cell. Mol. Life Sci.* **2015**, *72*, 4445–4460.
[146] S. K. Kulkarni, A. Dhir, *Prog. Neuro-Psychopharmacology Biol. Psychiatry* **2008**, *32*, 1093–1105.
[147] L. C. Mishra, B. B. Singh, S. Dagenais, *Altern. Med. Rev.* **2000**, *5*, 334–346.

and cognition facilitating properties. The anticancer, anti-angiogenetic, anti-inflammatory, anti-diabetic, anti-arthritic, cardio and neuroprotective activities were confirmed as well.

Notably, this plant proved to attenuate Parkinson's diseases symptoms in rats,[148] to prevent fibril formation in Alzheimer's disease[149] and to modulate signalling pathways involved in cancer development.[132,150]

Interestingly, these impressive pharmacological properties are accompanied by an extremely low toxicity. In fact, the hydroalcoholic extract of *Withania Somnifera* underwent wde-range toxicity tests on rats and even during pregnancy. No remarkable toxic effects were appreciable, even when the extract was administered at high concentrations and for prolonged time.[151,152,]

Withania somnifera also appears to be safe when administered to humans, considering that its extract is currently marketed as food supplement.

Obviously, the pharmacological properties depend on the compounds contained in the extract.

Withania somnifera is a rich source of natural products, mostly withanolides, already treated in the previous chapter, and alkaloids. It contains also a significative amount of iron.

So far, several sitoindosides (e.g. sitoindoside VII and sitoindoside VIII), 40 withanolides, including the aforementioned Withaferin A, and different alkaloids have been isolated.

The list of the alkaloids, present in different parts of the plant, includes: withananine, withanine, pseudo-withanine, somnine, somniferine, somniferinine, tropine, psuedo-tropine, 3-α-gloyloxytropane, choline, cuscohygrine, isopelletierine, anahydrine and anaferine.

The fact that more than a half of these compounds are piperidine-alkaloids was interesting, considering the importance of these kind of products in our research group. Some representative examples are reported in Figure 25.

[148] S. Rajasankar, T. Manivasagam, S. Surendran, *Neurosci Lett* **2009**, *454*, 11–15.
[149] B. Jayaprakasam, K. Padmanabhan, M. G. Nair, *Phytother Res,* **2010,** *24*, 859–863.
[150] D. L. Palliyaguru, S. V. Singh, T. W. Kensler, *Mol. Nutr. Food Res.* **2016**, *60*, 1342–1353.
[151] P. C. Prabu, S. Panchapakesan, C. D. Raj, *Phytother Res* **2013,** *27*, 1169–1178.
[152] P. C. Prabu, S. Panchapakesan, *Drug Chem Toxicol* **2015**, *38*, 50–56.

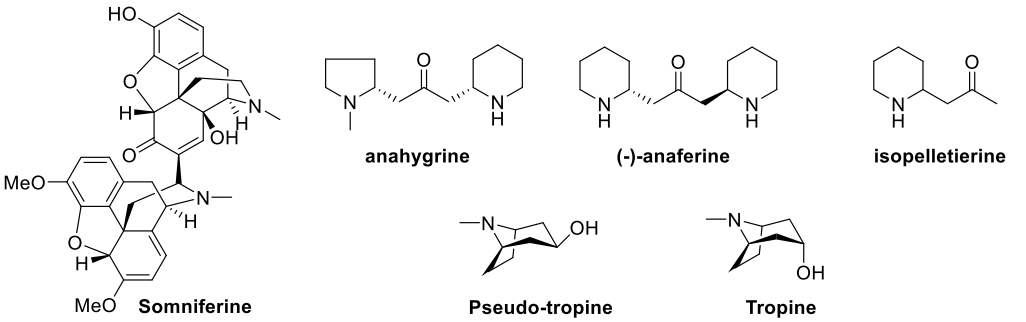

Figure 25. Structural representation of some piperidine alkaloids present in *Withania somnifera*.

4.2 Anaferines

The focus of this chapter is (-)-anaferine, an alkaloid containing two piperidine rings, connected by a 2-propanone moiety. This molecule is C2-symmetrical, and so exists as two enantiomers and a meso form. The mixture of these diastereomers was isolated for the first time in 1962, from the root extract of *Withania Somnifera*.[153] The racemate was resolved independently by Schwarting[154] and Moreman,[155] few years later. To this extent, diastereomeric salts were generated and separated, exploiting mandelic acid and (*R*)-6,6′-dinitrobiphenyl-2,2′-dicarboxylic acid, respectively. In both the works, ORD (optical rotary dispersion) analysis was exploited to assign the absolute configuration to the two anaferine enantiomers. The result was the same: (-)-anaferine proved to be the (*R,R*)- enantiomer, and (+)-anaferine the (*S,S*)-enantiomer.[154,155,156] Nowadays, the general name "anaferine" generally indicates the (*R,R*)-enantiomer.

The pure enantiomers are quite labile in neutral or basic environment and tend to epimerize through a Michael - Michael sequence. On the contrary, their salts are configurationally stable, and that's the reason why anaferines are generally synthesised as dihydrochloride salts.

Most of the studies and the synthetic efforts concerning (-)-anaferine, date back to the 70's. Nevertheless, in the last years, this alkaloid attracted once again the interest of the scientific community, considering that some recent studies suggested that it could find application in neurodegenerative diseases treatment. This idea is not

[153] A. Rother, J. M. Bobbitt, A. E. Schwarting, *Chem. Ind.* **1962***,* 654-655.
[154] M. M. El-Olemy, A. E. Schwarting, *J. Org. Chem.* **1969**, *34*, 1352–1354.
[155] H. C. Beyerman, L. Maat, C. A. Moerman, *Recl. Trav. Chim. Pays-Bas* **1971**, *90*, 1326-1330.
[156] J. C. Craig, S. Y. C. Lee, S. K. Roy, *J. Org. Chem.* **1978**, *43*, 347–349.

surprising, considering that *Withania somnifera*, the natural source of (-)-anaferine, is used in Ayurvedic medicine to improve memory and cognitive abilities, on the basis of neuroprotective properties. In particular, *in silico* simulations suggested that (-)-anaferine could behave as an inhibitor of GluN2B-containing *N*-methyl-D-aspartate receptors (NMDARs)[131] and as nicotinic acetylcholine receptor (nAChR) agonist.[157]
Some details about these two studies will follow below.

- ✓ ***Anaferine as GluN2B-NMDARs inhibitor.***

NMDARs receptors are essential proteins for the function of mammals' central nervous system (CNS). However, the overactivation of GluN2B-containing NMDARs induces excitotoxic neuronal death[158] and is related to several neurodegenerative diseases, including Alzheimer's, Huntington's and Parkinson's diseases and multiple sclerosis.
Thus, the inhibition of GluN2B-containing NMDARs constitutes a therapeutic strategy to contrast neurodegeneration. In the study reported by Patnaik and Kumar,[131] several *Withania somnifera* phytochemicals were tested *in silico*, to check their possible inhibitory activity.
(-)-anaferine gave good results: *in silico* simulation identified it as a promising allosteric GluN2B - NMDARs inhibitor, and its drug-likeness was confirmed by the respecting of Lipinski's rule of five and blood brain barrier permeability. It is noteworthy that, among the 25 tested compounds, only anaferine and other five *withania* phytochemicals displayed high affinity for GluN2B – NMDARs and could be considered for the treatment of neurodegenerative diseases.

- ✓ ***Anaferine as nAChR agonist***

nAChR receptors are members of the ligand-gated ion channel family. In particular, α7- nAChR receptor is widely diffused in the brain and when it is not properly expressed or it is not functioning correctly, diseases such as Alzheimer, schizophrenia and epilepsy.[159,160] In particular, agonists of α7- nAChR appear to play a neuroprotective action against nerve growth factor depletion and β-amyloid fibrils formation.
This prompted Sadasivan and co-workes to evaluate some *Withania somnifera* metabolites as possible agonists or antagonists of nAChR, exploiting an *in silico*

[157] C. Remya, K. V. Dileep, E. J. Variayr, C. Sadasivan, *Front. Life Sci.* **2016**, *9*, 201–213.
[158] Y. Liu, T. P. Wong, M. Aarts, A. Rooyakkers, L. Liu, T. W. Lai, D. C. Wu, J. Lu, M. Tymianski. A. M. Craig, Y. T. Wang*, J. Neurosci.* **2007**, *27,* 2846–2857.
[159] A: A. Jensen, B. Frolund, T. Liljefors, P. Krogsgaard-Larsen, *J Med Chem.* **2005**, *48*, 4707–4745.
[160] M. R. D'Andrea, R. G. Nagele, *Curr Pharm Des.* **2006**, *12*, 677–684.

approach.[157] Docking simulations allowed the prediction of the binding affinity of the candidates for the receptor, while further simulations were exploited to determine their drug-likeness (Lipinski rule of five, CNS activity, ADME analysis and blood brain barrier (BBB) permeability).
Among the tested compounds, only four of them gave promising results: anaferine, anahygrine, cuscohygrine and isopelletierine. On the basis of these simulations, anaferine possesses interesting CNS activity, and should behave as nAChR receptors agonist. As reported also by the work of Patnaik,[131] this alkaloid appeared to respect Lipinski's rule of five and to be able to cross the BBB. Interestingly, (-)-anaferine gave the best binding affinity for nAChR, compared with its enantiomer and meso-form.

Thus, the possible applications in the treatment of neurodegenerative diseases makes anaferines as promising bioactive candidates. A clear sign of the renewed interest in this alkaloid is the recently reported enantioselective total synthesis of (+)-anaferine.[161] This is the first synthesis to be published since 2002, when Blechert and Stapper accomplished the synthesis of the corresponding (-)-enantiomer.[162]
These two strategies will be briefly presented in the next paragraph.

4.2.1 Previous enantioselective total synthesis of anaferines

The first enantioselective synthesis of (-)-anaferine was published in 2002. The key step was a tandem ring rearrangement metathesis, consisting in a ring-opening metathesis, followed by two ring-closing metatheses, as reported in Scheme 34. The synthesis started from an enantiopure cycloheptene derivative, that can be obtained in five steps from the commercially available tropone. Form this compound, the chirality was transferred into the two piperidine rings, through the tandem rearrangement.

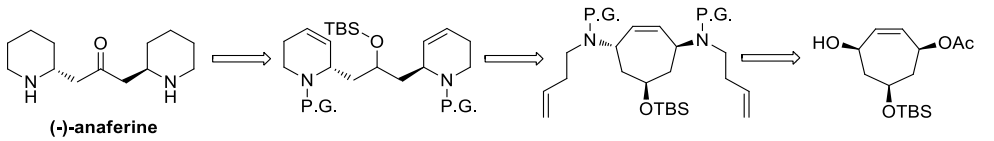

Scheme 34. Retrosynthetic approach for the synthesis of (-)-anaferine, by Stapper and Blechert.

[161] J. Torres, M. Escolano, F. Rabasa-Alcañiz, A. Sanz-Vidal, M. Sánchez-Roselló, C. del Pozo, *Org. Chem. Front.* **2019**, *6*, 3210-3214.
[162] S. Blechert, C. Stapper, *European J. Org. Chem.* **2002**, 2855–2858.

The first step of the synthesis was a Mitsunobu reaction, to convert the free hydroxyl group into an amine, with inversion of configuration. After the cleavage of the acetyl moiety, the hydroxyl group was converted into the corresponding chloride, with inversion of configuration. The subsequent nucleophilic substitution in the presence of but-3-enylamine, afforded the desired diamine, with a global retention of configuration.

After a cleavage/reprotection sequence, the tandem ring opening – ring closing metathesis was performed in the presence of Grubbs catalyst. The heptacycle was broken at the double bond, and the two piperidine rings were formed through RCM, affording the bis-tetrahydropyridine derivative. The two double bonds were reduced through hydrogenation, and the two Cbz protecting groups were cleaved as well. The silylether was removed in acid environment and the two piperidinic nitrogens were protected again, as Boc. Oxidation of the hydroxyl group to the corresponding ketone, followed by cleavage of the protecting groups on the piperdines, afforded (-)-anaferine dihydrochloride, with a 23% overall yield over eleven steps. The synthetic route is summarised in Scheme 35.

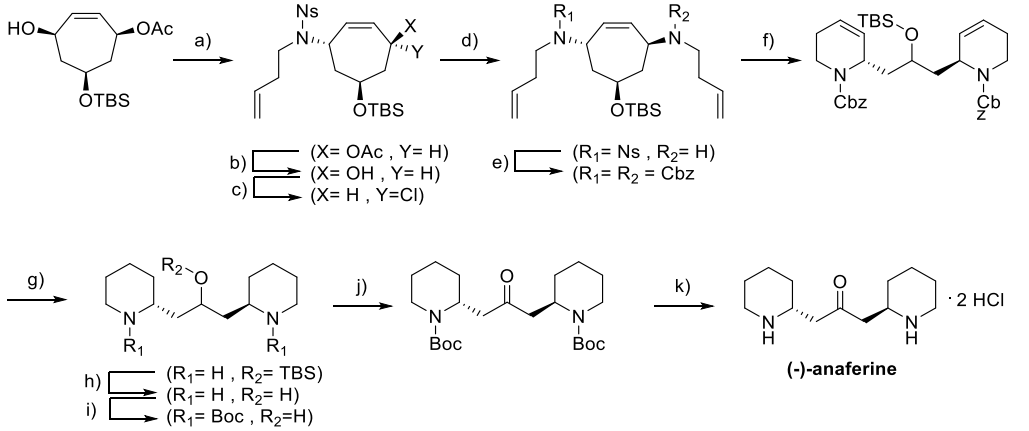

Scheme 35. *Reaction and conditions.* a) *N*-nosyl-*N*-but-3-enylamine, PPh_3, DEAD, THF, r.t., 89%; b) KCN, MeOH, r.t., 86%; c) MsCl, pyridine, r.t., 82%, d) but-3-enylamine, K_2CO_3, MeCN, 70 °C, 86%; e) i. PhSH, K_2CO_3, DMF, 70°C; ii. benzyl chloroformate, 0 °C, 86%; f) [$Cl_2(Cy_3P)_2Ru$= CHPh], CH_2Cl_2, reflux, 87%; g) H_2, Pd/C (10%), MeOH, r.t., 87%; h) HCl, EtOH, r.t., 90%; i) $(Boc)_2O$, TEA, MeOH, 50 °C, 98%; j) PCC, CH_2Cl_2, r.t., quant.; k) 3 N HCl, MeOH, r.t., quant.

The synthesis recently proposed by del Pozo *et al*. is based on a different strategy, involving the double use of *N*-sulfinyl amines as both chiral auxiliaries and as nucleophiles in an intramolecular aza-Michael reaction.[161] The general retrosynthetic approach is depicted in Scheme 36.

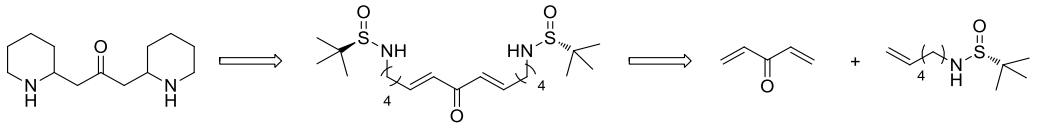

Scheme 36. Retrosynthetic pathway for the synthesis of anaferine, proposed by del Pozo and co-workers, taking advantage of an intramolecular aza-Michael reaction and of a bidirectional cross-metathesis.

Compared with the previously reported synthesis, this one presents the advantage of being a really concise one, consisting of only three steps.

The first step was a bidirectional cross metathesis (CM), between the proper sulfinyl amine and divinyl ketone. Considering the volatility and the tendency toward polymerisation of divinyl ketone, it was synthesised *in situ* oxidizing divinyl alcohol with DDQ (2,3-Dichloro-5,6-dicyano-1,4-benzoquinone) and used for the cross metathesis without being isolated. 2nd generation Hoveyda–Grubbs catalyst and Ti(i-PrO)$_4$ co-catalyst were used to promote the CM reaction. A *N*—sulfinyl amine/: divinyl ketone ratio of 1 : 2 was required to obtain the desired product with satisfactory yield. Then, a double intramolecular aza-Michael reaction allowed the formation of the bis-piperidine core, generating at the same time the two stereocenters.

The stereochemical outcome of this reaction is usually strongly dependent on the type of substrate and base, and on the size of the ring that could be formed. Several reaction conditions were tested. The best result was obtained exploiting potassium hydride as base and THF as solvent, at room temperature. In this case a 10 : 1 mixture of A : B diastereomers (see Scheme 37) was obtained, with 97 % yield (on the mixture). It is noteworthy that also in all the other tested conditions, the formation of A diastereomer (precursor of (+)-anaferine) proved to be favoured over B diastereomer. The stereoselectivity arises from a double chair-like transition state (Scheme 37), in which nitrogen attacks the Si face of both sides of the bis-enone, affording (*S,S*)-bispiperidine as major product.

Diastereomer A was isolated and converted in (+)-anaferine dihydrochloride, cleaving the sulfinyl moiety upon acid treatment. The desired product was accessed in only three steps (or four, if the *in situ* generation of divinyl ketone is considered) and with 70% overall yield.

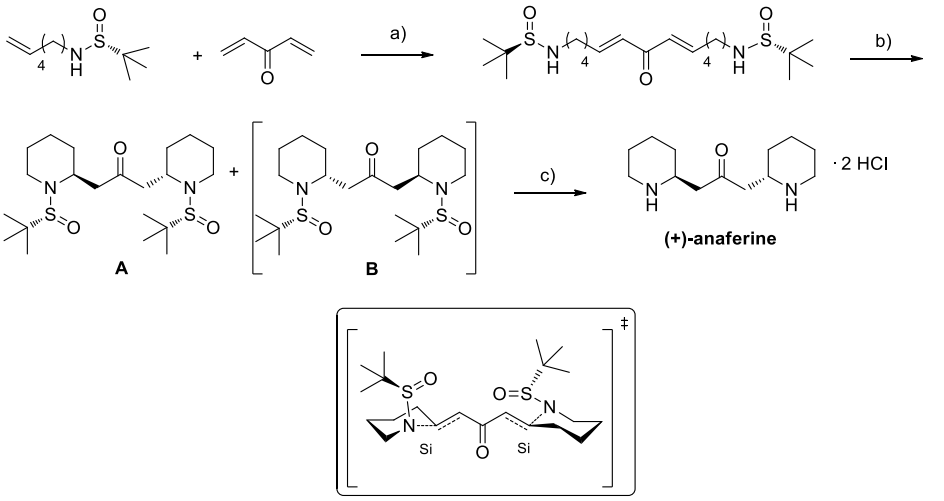

Scheme 37. *Reaction and conditions.* a) HG-II (10 mol %), Ti(i-PrO)$_4$ (10 mol %), CH_2Cl_2, r.t., 16h, 78%; b) KH, THF, r.t., 2h, 97%, A:B = 10:1; c) HCl/dioxane, MeOH, 0°C, 2h, 99%.
In box the transition state for the intramolecular aza-Michael reaction is represented.

4.3 (-)-anaferine: our DOS approach

The presence of (-)-anaferine (**49**) in our library of piperidine-based derivatives was quite serendipitous, resulting a sort of unexpected encounter. In fact, we realised that its obtainment could constitute another branch of our diversifying approach, exploiting intermediate **10**, already exploited in the synthesis of the potential Hh inhibitor **19**. In fact, **10** already bears a piperidine ring and a 2-hydroxypropane bridge, that could be easily oxidize to the ketone present in (-)-anaferine. On the other hand, the homoallylic alcohol could be converted into a lactam, analogously to the previously reported synthesis of compound **14** (Chapter 2), that could be properly reduced, giving the second piperidine ring present in **49**. A simplified representation of this approach is reported in Scheme 38, in which the useful elements of compounds **10** and **14** are highlighted in different colours.

In detail, enantiopure **(*R,R,S*)-10**, would be used as starting material, and its homoallylic alcohol would be converted into the corresponding amine, exploiting the Mitsunobu-Staudinger reduction approach already depicted in Chapter 2. After acylation and RCM, the second nitrogen-containing hexacycle would be formed and converted into a piperidine through a sequence of reductions. Finally, oxidation of the hydroxyl group to ketone and the cleavage of the protecting groups would give (-)-anaferine.

For what concern the control over the stereochemical outcome, Brown's allylation would be exploited once again, considering that it proved to be a good approach, compared with the method based on Leighton's strained silacyles.

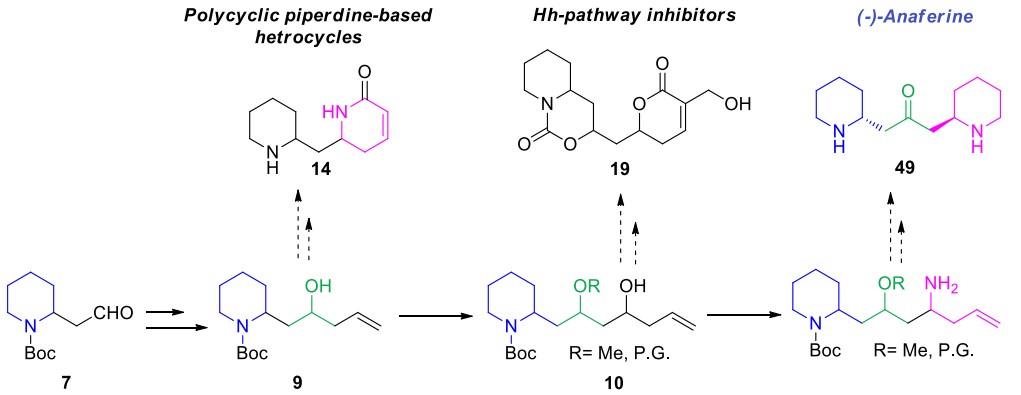

Scheme 38. Our diversity-oriented approach, starting from 2-piperidine ethanol. The fragments of the intermediates that would be exploited for the synthesis of (-)-anaferine are highlighted in different colours.

As already mentioned, this approach shares the first synthetic steps with the previously reported synthesis of the potential Hedgehog inhibitor **19**, leading to enantiopure compound **10**. To secure the correct stereocenters configuration, both the two stereoselective Brown's allylations were performed in the presence of (–)- B-allyl diisopinocampheylborane (e.e.= 84% for compound **9**, *d.r.*=85:15 for compound **10**). Accordingly to the previously discussed chair-like transition state model, the desired (*R,R,S*)- product was obtained (Scheme 39).

The second allylation step proved to be quite challenging for what concern the purification. In fact, when we tried to isolate the desired homoallylic alcohol through column chromatography (Hex : EtOAc = 4 :1), we realised that it tended to be eluted together with the di-isopinocampheole, obtained as by-product of this reaction. Crystallisation attempts failed, as well as the idea of washing away the di-isopinocampheole with pentane.

Finally, we managed to obtain clean alcohol **10**, removing as much as possible the by-product through sublimation and then performing a column chromatography in dichloromethane.

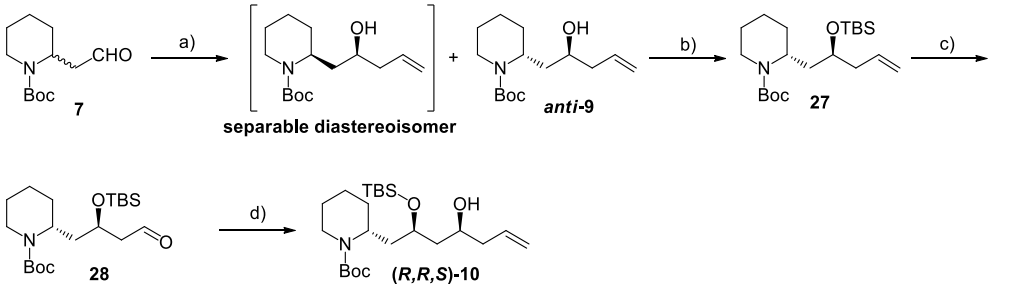

Scheme 39. *Reaction and conditions*. a) (–)-allyl-BIpc$_2$, THF, –78 °C to r.t., 4 h, 90 % overall yield, 84% ee on the *anti*-alcohol; b) TBSCl, imidazole, CH_2Cl_2, 0°C to r.t., 5h, 90%; c) i. O_3, CH_2Cl_2, -78°C, 1 h; ii. PPh_3, -78°C to r.t., 3h, 60%; d) (–)-allyl-BIpc$_2$, THF, –78 °C to r.t., 16 h, 92%

Once obtained alcohol **10**, a Mitsunobu reaction in the presence of diphenylphosphoryl azide assured the conversion of the alcohol into the corresponding azide, with inversion of configuration. In this way, the required *R*-configuration of the second piperidine ring stereocenter was secured. Azide **50** was reduced under Staudinger conditions to the corresponding amine **51**, that was acylated in turn with the commercially available acryloyl chloride. For the subsequent key ring closing metathesis, fundamental to build the second piperidine core, the M73-SIMes catalyst was used. The presence of two monosubstituted olefins didn't required a catalyst such as the Stewart-Grubbs one, exploited in the synthesis of the potential Hh inhibitors, and so we took advantage of the higher activity of M73-SIMes catalyst. In this way, the desired lactam **53** was obtained with high yield and no trace of cross metathesis product was appreciable.

This reaction afforded the fundamental skeleton of (-)-anaferine, composed by two nitrogen containing hexacycles, bearing (*R*)-configuration at the stereocenters, connected by a 2-hydroxy propanone chain.

Therefore, the last part of the synthetic route was focused on the conversion of the α,β-unsaturated lactam to the corresponding piperidine and on the oxidation of the silylether to ketone.

First of all, the double bond was reduced selectively through a catalytic hydrogenation, in the presence of Pd/C. The obtained amide **54** was protected at the nitrogen as Boc, and then reduced to the corresponding piperidine **56** exploiting $BH_3{\cdot}SMe_2$ complex as reducing agent.

The silylether protecting group was selectively cleaved using TBAF, affording one of the intermediates reported in Blechert and Stapper's synthesis of (-)-anaferine (**57**).[162] The use of TBAF instead of acid conditions left unchanged the two Boc protecting groups: this was a fundamental requirement, because two basic nitrogens would have

interfered with the following oxidation of the hydroxyl group to ketone. Dess-martin periodinane (DMP) was used instead of PCC, that was the oxidizing agent of choice in the previously reported synthesis.[162] DMP is a less toxic reagent and easier to handle. Moreover, the reaction was really clean and the iodinane by-product was removed simply through a basic work-up, affording the desired product **58** in quantitative yield, without need of further purification. Finally, cleavage of the two Boc protecting groups, gave the desired (-)-anaferine dihyrochloride **49**, whose identity was confirmed comparing analytical and spectroscopic properties with data reported in literature.

The synthetic route, that allowed the synthesis of the desired product from the key intermediate **10** (18% overall yield, over 10 steps) is summarised in Scheme 40.

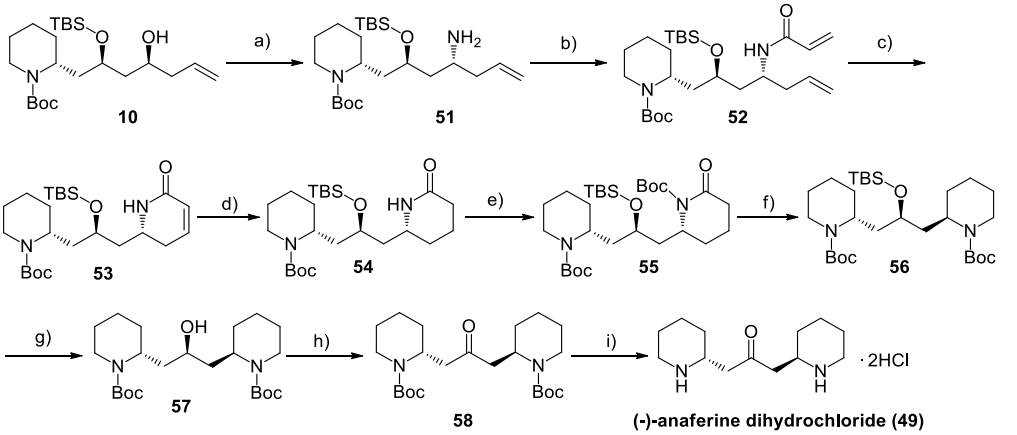

Scheme 40. *Reaction and conditions*. a) i. PPh_3, DIAD, DPPA, THF, r.t., 16h, 85%; ii. PPh_3, THF/H_2O, 40°C, 8h, 80%; b) acryloyl chloride, TEA, CH_2Cl_2, 0°C to r.t., 5h, 88%; c) M73 SIMes cat. (1 mol %) CH_2Cl_2, 50°C, 5h, 71%; d) H_2, Pd/C (10 % wt), MeOH, r.t., 16h, quant.; e) Boc_2O, TEA, DMAP, CH_2Cl_2, r.t., 48h, 82%; f) $BH_3{\cdot}SMe_2$, THF, 0°C, 5h, 76%; g) TBAF, THF, -15°C to 0°C, 16h, 71%; h) DMP, CH_2Cl_2, r.t., 16h, quant.; i) HCl 4M in dioxane, CH_2Cl_2, 0°C to r.t., 16h, quant.

Of course, the tuning of the chiral ligand used in the two allylation steps would open the possibility of synthesizing also the enantiomer and the meso-form of (-)-anaferine, exploiting a (+)-allylBIpc$_2$ / (+)-allylBIpc$_2$ combination for (+)-anaferine and (-)-allylBIpc$_2$ / (+)-allylBIpc$_2$ or (+)-allylBIpc$_2$ / (-)-allylBIpc$_2$ combinations for the meso-anaferine.

4.4 (-)-anaferine and meso-anaferine: future perspectives

The future development of this work will be focused on the improvement of the developed synthetic route (Scheme 40).
The first possibility that will be innnvestigated will concern the obtainement of amine **51** in a more direct fashion, starting from the key intermediate **27** and avoiding the "ozonolysis-allylation-Mitsunobu-Staudinger reduction" sequence.
To this extent, the formation of an activated aziridine on **27** double bond, followed by aziridine opening with a vinylcuprate appeared to be the best choice, as represented in Scheme 41.

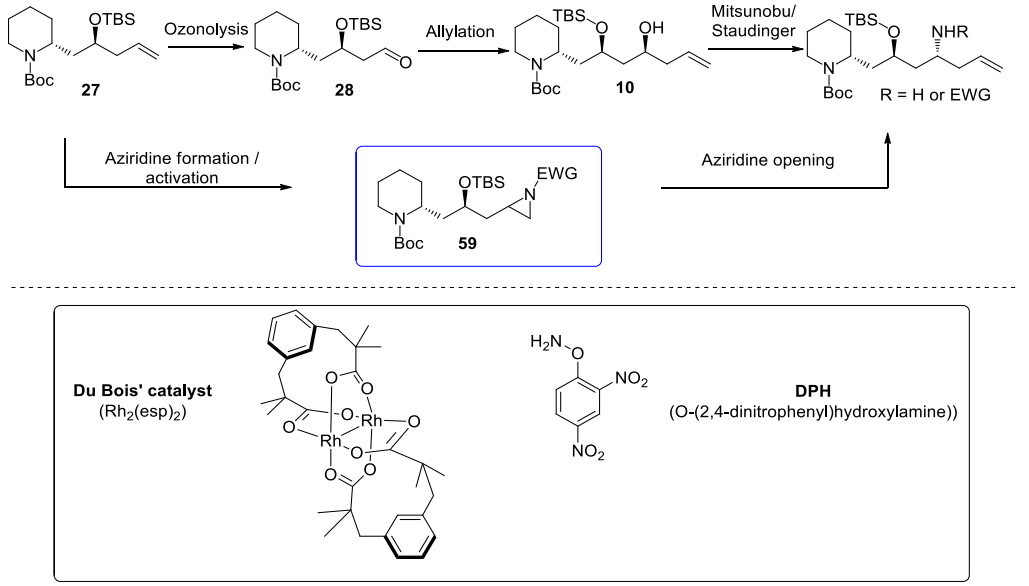

Scheme 41. Aziridine-based approach, for the conversion of intermediate **27** into the key homoallylic amine. In the box, strctures of Du Bois' catalyst and DPH are reported.

Despite being only one step shorter than the previous synthesis, this approach would avoid the ozonolysis step, characterised by the lowest yield of the whole synthetic route. For the aziridination step, Kurti's method appears as an intriguing one.[163]
In fact, it allows the direct aziridination of not activated mono-, di-, tri- and tetrasubstituted olefins. The reaction is homogeneously catalysed by Rh (II) and O-(2,4-dinitrophenyl)hydroxylamine (DPH) acts as aziridinating agent. This one-pot

[163] a) J. L. Jat, M. P. Paudyal, H. Gao, Q.-L. Xu, M. Yousufuddin, D. Devarajan, D. H. Ess, L. Kürti, J. R. Falck, *Science* **2014**, *343*, 61–65. b) Z. Ma, Z. Zhou, L. Kürti, *Angew. Chem. Int. Ed.,* **2017**, *56*, 9886–9890.

methodology is operationally simple, exploits mild conditions, tolerates several functional groups and doesn't required external oxidizing agents. The best catalyst for this reaction is $Rh_2(esp)_2$, also known as Du Bois' catalyst. Evidently, the limit of this procedure would be the lack of stereoselectivity, depending on the use of an achiral catalysts. Therefore, the aziridination of intermediate **27**, would generate a diastereomeric mixture of aziridines, because the reaction should occur on both the faces of the double bond. However, we realised that after aziridine activation with an electron withdrawing group, followed by alkylation, the two separated diastereomers could be used for the parallel synthesis of (-)-anaferine and its meso-form.

4.5 Experimental part

General

Unless otherwise stated, reagents and solvents were purchased from Sigma Aldrich, Fluorochem or TCI and used without further purification. Unless otherwise stated, all reactions were carried out in oven-dried glassware and dry solvents, under nitrogen atmosphere and were monitored by thin layer chromatography (TLC) on silica gel (Merck precoated 60F254 plates), with detection by UV light (254 nm) or by solutions of potassium permanganate stain, or ninhydrin, or p-anisaldehyde stain.
Flash chromatography was performed using silica gel (240-400 mesh, Merck) as stationary phase.
^{1}H-NMR spectra were recorded on a Bruker Avance Spectrometer (400 MHz) and are reported relative to residual $CDCl_3$ or CD_3OD. ^{13}C-NMR spectra were recorded on the same instruments (100 MHz) and are reported relative to residual $CDCl_3$ or CD_3OD. All 1D and 2D NMR spectra were collected using the standard pulse sequences available with Bruker Topspin 1.3. Chemical shifts (δ) for proton and carbon resonances are quoted in parts per million (ppm) relative to tetramethylsilane (TMS), used as an internal standard. Data for ^{1}H-NMR are reported as follows: chemical shift (δ/ppm) (multiplicity, coupling constant (Hz), integration). Multiplicities are reported as follows: s = singlet, d = doublet, t = triplet, m = multiplet, bs = broad singlet. Data for ^{13}C-NMR are reported in terms of chemical shift (δ/ppm).
Mass spectra were registered exploiting the electrospray ionisation (ESI) technique, on a Q-Tof micro mass spectrometer.
Specific rotation values were measured on a P-1030 Jasco polarimeter, using 1 mL cells, with path length of 10 cm. Measures were collected at 20-25°C, using sodium D line wavelength λ=589 nm.

Synthesis of tert-butyl (R)-2-((2R,4R)-4-azido-2-((tert-butyldimethylsilyl)oxy)hept-6-en-1-yl)piperidine-1-carboxylate (50).

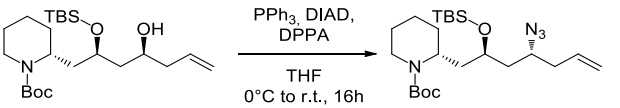

85%

10 (0.932 g, 2.18 mmol) and PPh_3 (0.687 g, 2.62 mmol) were dissolved in anhydrous THF (18 mL) and cooled at 0°C. DIAD (0.52 mL, 2.62 mmol) was added dropwise. The reaction mixture was stirred for 10' at 0°C and then DPPA (0.57 mL, 2.62 mmol) was added dropwise. The reaction was warmed to r.t.and stirred overnight. The mixture was concentrated, and the crude product was purified by column chromatography on silica gel (Hex: EtOAc = 97:3), to give **50** (0.839 g, 85%) as light yellow oil.

^{1}H NMR (400 MHz, $CDCl_3$) δ 5.82 (ddt, *J* = 17.1, 10.1, 7.0 Hz, 1H), 5.21 – 5.08 (m, 2H), 4.36 – 4.22 (m, 1H), 4.09 – 3.94 (m, 1H), 3.80 (m, 1H), 3.66 – 3.54 (m, 1H), 2.77 (t, *J* = 13.1 Hz, 1H), 2.35 (m, 2H), 2.10 – 1.98 (m, 1H), 1.80 – 1.66 (m, 1H), 1.64 – 1.53 (m, 5H), 1.51 (m, 1H), 1.47 (s, 9H), 1.44 – 1.36 (m, 2H), 0.89 (s, 9H), 0.09 (s, 3H), 0.08 (s, 3H).
^{13}C NMR (100 MHz, $CDCl_3$) δ 154.06, 134.06, 118.36, 79.38, 67.16, 58.62, 47.30, 41.09, 39.61, 38.64 (2 CH_2), 29.84, 28.62 (3 CH_3), 26.07 (3 CH_3), 25.84, 19.43, 18.17, -3.82, -4.69.
$[\alpha]_D^{20}$: -29.7 (*c*= 0.54, $CHCl_3$).
MS (ESI) m/z $[M + Na]^+$ calcd. for $C_{23}H_{44}N_4O_3SiNa$: 475.30, found: 475.44.

Synthesis of (R)-tert-butyl 2-((2S,4R)-4-amino-2-((tert-butyldimethylsilyl)oxy)hept-6-en-1-yl)piperidine-1-carboxylate (51).

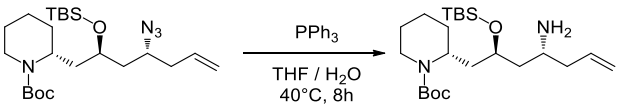

80%

50 (0.821 g, 1.81 mmol) and PPh_3 (0.951 g, 3.63 mmol) were dissolved in a mixture of THF and H_2O (10:1, 25 mL) and heat at 40°C for 8 hours. At that point water was added (10.4 mL). The layers were separated and the aqueous one was extracted with Et_2O. The combined organic layers were washed with brine, dried over Na_2SO_4, filtered and concentrated under vacuum. The crude product was purified by column chromatography on silica gel (CH_2Cl_2:MeOH = 95:5), to give **51** (0.601 g, 78%) as light yellow oil.

^{1}H NMR (400 MHz, $CDCl_3$) δ 5.79 (ddt, *J* = 17.2, 10.2, 7.1 Hz, 1H), 5.31 – 4.94 (m, 2H), 4.28-4.12 (m, 1H), 4.08-3.90 (m, 1H), 3.87-3.80 (m, 1H), 3.10- 3.05 (m, 1H), 2.90 – 2.59 (m, 1H), 2.40-2.20 (m, 2H), 2.09 – 2.01 (m, 1H), 1.76 – 1.48 (m, 7H), 1.45 (s, 9H), 1.40 – 1.30 (m, 2H), 0.96 – 0.75 (m, 9H), 0.10 – -0.15 (m, 6H).

^{13}C NMR (100 MHz, $CDCl_3$) δ 155.31, 135.29, 117.87, 79.57, 68.41 (2 CH), 47.77, 42.47 (2 CH_2), 38.99, 37.77, 29.83, 28.68 (3 CH_3), 25.98 (3 CH_3), 25.83, 19.40, 18.12, -4.17, -4.47.

$[\alpha]_D^{20}$: +6.8 (*c*= 0.46, $CHCl_3$).

MS (ESI) m/z $[M + H]^+$ calcd. for $C_{23}H_{47}N_2O_3Si$: 427.33, found: 427.63.

Synthesis of (R)-tert-butyl 2-((2S,4R)-4-acrylamido-2-((tert-butyldimethylsilyl)oxy) hept-6-en-1-yl)piperidine-1-carboxylate (52)

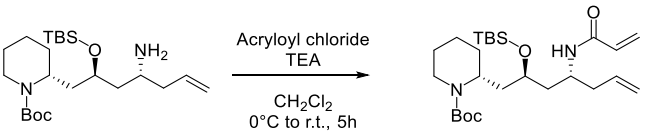

51 (0.558 g, 1.31 mmol) was dissolved in anhydrous CH_2Cl_2 (5.5 mL) and cooled at 0°C. anhydrous TEA (547 µL, 3.92 mmol) was added and the reaction was stirred for 10 minutes. Acryloyl chloride (160 µL, 1.96 mmol) was added dropwise; the mixture was warmed to r.t. and stirred for 5 hours. At that point, cold water (0°C) was added. The layers were separated and the aqueous one was extracted with CH_2Cl_2. The combined organic layers were washed twice with a saturated solution of NH_4Cl, dried over Na_2SO_4, filtered and concentrated under vacuum. The crude product was purified by column chromatography on silica gel (CH_2Cl_2:MeOH = 95:5), to give **52** (0.548 g, 88%) as a brown oil.

^{1}H NMR (400 MHz, $CDCl_3$) δ 6.42 (bs, 1H), 6.29 – 6.03 (m, 2H), 5.81 (ddt, J = 19.2, 9.6, 7.2 Hz, 1H), 5.65 – 5.51 (m, 1H), 5.16 – 4.94 (m, 2H), 4.22 – 4.09 (m, 1H), 4.05 – 3.91 (m, 2H), 3.77 – 3.60 (m, 1H), 2.86 (m, 1H), 2.53 – 2.30 (m, 1H), 2.14 – 2.02 (m, 1H), 1.80 (t, J = 12.8 Hz, 1H), 1.66 – 1.53 (m, 6H), 1.45 (m, 11H), 1.31 (m, 1H), 0.91 (s, 9H), 0.02 (s, 6H).
^{13}C NMR (100 MHz, $CDCl_3$) δ 165.29, 134.61, 131.72, 125.38, 117.43, 79.56, 66.82, 46.61, 39.28 ($3CH_2$), 31.44, 30.50 ($2CH_2$), 28.58 ($3CH_3$), 25.89 ($3CH_3$), 25.56, 19.30 (2 CH_2), 17.91, -4.46 ($2CH_3$).
$[\alpha]_D^{20}$: -8.1 (*c*= 0.42, $CHCl_3$).
MS (ESI) m/z $[M + Na]^+$ calcd. for $C_{26}H_{48}N_2O_4SiNa$: 503.33, found: 503.71.

Synthesis of (R)-tert-butyl 2-((S)-2-((tert-butyldimethylsilyl)oxy)-3-((R)-6-oxo-1,2,3,6-tetrahydropyridin-2-yl)propyl)piperidine-1-carboxylate (53).

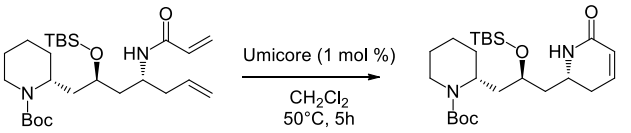

52 (0.540 g, 1.12 mmol) was dissolved in anhydrous degassed CH_2Cl_2 (47 mL). A solution of Umicore catalyst 14% wt (59.0 mg, 0.01 mmol) in degassed CH_2Cl_2 (16.2 mL) was added dropwise and the reaction was stirred for 5 hours at 50°C. The reaction mixture was concentrated under vacuum. The crude product was purified by column chromatography on silica gel (CH_2Cl_2:MeOH = 98:2), to give **53** (0.364 g, 71%) as a light yellow oil.

^{1}H NMR (400 MHz, $CDCl_3$) δ 6.67 (bs, 1H), 6.60 – 6.51 (m, 1H), 5.91 – 5.83 (m, 1H), 4.19 (m, 1H), 3.99 – 3.94 (m, 1H), 3.80 – 3.76 (m, 2H), 2.81 – 2.73 (m, 1H), 2.17 – 2.16 (m, 2H), 1.84-1.75 (m, 2H), 1.54 – 1.46 (m, 6H), 1.45 (s, 9H), 1.36 – 1.28 (m, 2H), 0.89 (s, 9H), 0.06 (s, 6H).
^{13}C NMR (100 MHz, $CDCl_3$) δ 165.99, 155.53, 140.37, 125.21, 79.91, 68.24, 48.00 (2 CH), 31.51 (2 CH_2), 30.04, 29.79, 28.63 (3 CH_3), 25. 97 (3 CH_3), 25.92, 25.72, 19.35, 18.07, -4.35, -4.76.
$[\alpha]_D^{20}$: +46.2 (*c*= 0.66, $CHCl_3$).
MS (ESI) m/z $[M + Na]^+$ calcd. for $C_{24}H_{44}N_2O_4SiNa$: 475.30, found: 475.52.

Synthesis of (R)-tert-butyl 2-((S)-2-((tert-butyldimethylsilyl)oxy)-3-((R)-6-oxopiperidin-2-yl)propyl)piperidine-1-carboxylate (54).

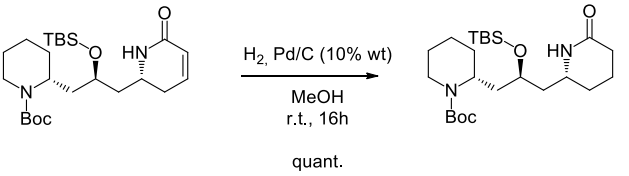

53 (0.205 g, 0.45 mmol) and Pd/C 10% wt (0.205 g) were dissolved in MeOH (10 mL). The reaction mixture was put under H_2 atmosphere and stirred overnight. The mixture was filtered over celite, washed with MeOH and CH_2Cl_2 and concentrated to give **54** (0.206 g, quant.) as a dark yellow oil.

^{1}H NMR (400 MHz, $CDCl_3$) δ 6.73 (s, 1H), 4.23 – 4.19 (m, 1H), 4.00 – 3.96 (m, 1H), 3.82 – 3.77 (m, 1H), 3.59 – 3.54 (m, 1H), 2.78 (t, J = 13.2 Hz, 1H), 2.44 – 2.32 (m, 1H), 2.25 (ddd, *J* = 17.7, 11.1, 6.5 Hz, 1H), 2.07 (ddd, *J* = 14.6, 11.4, 3.7 Hz, 1H), 1.88 (m, 1H), 1.84 – 1.66 (m, 4H), 1.66 – 1.48 (m, 6H), 1.45 (s, 9H), 1.37 (m, 2H), 0.91 (s, 9H), 0.08 (s, 6H).
^{13}C NMR (100 MHz, $CDCl_3$) δ 171.60 , 155.21 , 79.84 , 68.59 , 49.92 , 47.67, 41.54 , 39.20 , 31.28 , 30.31 , 29.98 , 29.89 , 28.69 (3 CH_3) , 26.06 (3 CH_3), 25.81 , 20.55 , 19.44, 18.17, -4.59, -4.91.
$[\alpha]_D^{20}$: +1.4 (*c*= 0.70, $CHCl_3$).
MS (ESI) m/z $[M + Na]^+$ calcd. for $C_{24}H_{46}N_2O_4SiNa$: 477.31, found: 477.91.

General procedure for the synthesis of (R)-tert-butyl 2-((R)-3-((R)-1-(tert-butoxy carbonyl)piperidin-2-yl)-2- ((tert-butyldimethylsilyl)oxy)propyl)-6-oxopiperidine-1-carboxylate (55).

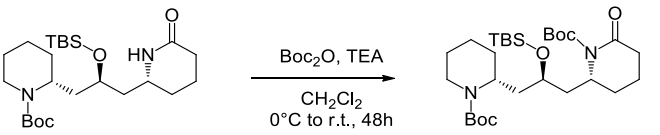

54 (0.206 g, 0.45 mmol) was dissolved in anhydrous CH_2Cl_2 (1.5 mL) and cooled to 0°C. TEA (190 µL, 1.36 mmol), DMAP (0.012 g, 0.09 mmol) and Boc_2O (0.298 g, 1.36 mmol) were added. The mixture was stirred at r.t. for 48h and concentrated under vacuum. The crude product was purified by column chromatography on silica gel (Hex:EtOAc = 7:3), to give **55** (0.204 g, 82%) as a dark yellow oil.

^{1}H NMR (400 MHz, $CDCl_3$) δ 4.48 – 4.33 (m, 1H), 4.23 (m, 1H), 4.08 – 3.92 (m, 1H), 3.78 (quint., *J* = 6.2 Hz, 1H), 2.77 (t, *J* = 12.7 Hz, 1H), 2.55 – 2.38 (m, 2H), 1.96 – 1.70 (m, 7H), 1.88- 1.56 (m, 5H), 1.52 (s, 9H), 1.44 (s, 9H), 1.31 – 1.19 (m, 2H), 0.88 (s, 9H), 0.07 (s, 6H).
^{13}C NMR (100 MHz, $CDCl_3$) δ 171.30 , 154.82 , 152.82 , 82.93 , 79.23 , 68.48 , 53.74 , 47.30 , 41.58 , 39.23 , 36.75 , 34.12 , 29.69 , 28.56 (3 CH_3), 28.04 (3 CH_3), 26.69 , 25.89 (3 CH_3), 25.59 , 19.16 , 17.95 , 17.06 , -4.27 (2 CH_3).
$[\alpha]_D^{20}$: +23.2 (*c*= 0.82, $CHCl_3$).
MS (ESI) m/z $[M + Na]^+$ calcd. for $C_{29}H_{54}N_2O_6SiNa$: 577.36, found 577.48.

Synthesis of (2R,2'R)-di-tert-butyl 2,2'-(2-((tert-butyldimethylsilyl)oxy)propane- 1,3-diyl)bis(piperidine-1-carboxylate) (56).

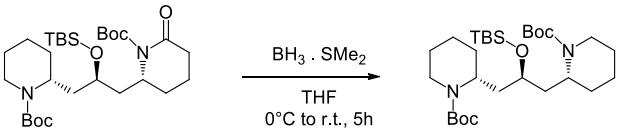

55 (0.170 g, 0.31 mmol) was dissolved in anhydrous THF (7.5 mL) and cooled to 0°C. BH_3·SMe_2 (68 µL, 0.67 mmol), was added dropwise. The mixture was stirred at r.t. for 5h and quenched with a saturated solution of NH_4Cl. The layers were separated, and the organic one was extracted with Et_2O. The combined organic layers were dried over Na_2SO_4, filtered and concentrated under vacuum. The crude product was purified by column chromatography on silica gel (Hex:EtOAc = 8:2), to give **56** (0.126 g, 76%) as a yellow oil.

^{1}H NMR (400 MHz, $CDCl_3$) δ 4.40 – 4.24 (m, 2H), 4.00 – 3.87 (m, 2H), 3.72 – 3.61 (m, 1H), 2.84 – 2.71 (m, 2H), 1.94 – 1.63 (m, 6H), 1.60-1.51 (m, 6H), 1.45 (s, 18H), 1.39 – 1.34 (m, 4H), 0.89 (s, 9H), 0.06 (s, 6H).
^{13}C NMR (100 MHz, $CDCl_3$) δ 154.9 (2 Cq), 79.1 (2 Cq), 68.7, 47.4 (2 CH), 39.5 (2 CH_2), 37.6 (2 CH_2), 29.68 (2 CH_2), 28.5 (6 CH_3), 25.7 (3 CH_3), 25.6 (2 CH_2), 19.1 (2 CH_2), 18.01, -4.2, - 4.4.
$[\alpha]_D^{20}$: +28.0 (*c*= 0.48, $CHCl_3$).
MS (ESI) m/z $[M + Na]^+$ calcd. for $C_{29}H_{56}N_2O_5SiNa$: 563.38, found: 563.99.

Synthesis of (2R,2'R)-di-tert-butyl 2,2'-(2-hydroxypropane-1,3- diyl)bis(piperidine-1-carboxylate) (57)

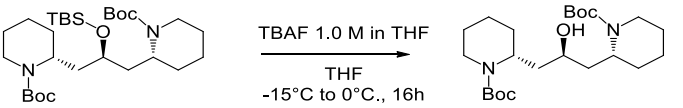

71%

56 (0.112g, 0.21 mmol) was dissolved in anhydrous THF (1.5 mL) and cooled to -15°C. TBAF 1.0 M in THF (620 µL, 0.62 mmol), was added dropwise. The mixture was stirred for 16h slowly warming to 0°C. The mixture was quenched with a saturated solution of NH_4Cl. The layers were separated, and the organic one was extracted with Et_2O. The combined organic layers were dried over Na_2SO_4, filtered and concentrated under vacuum. The crude product was purified by column chromatography on silica gel (Hex:EtOAc = 85:15), to give **57** (0.090 g, 71%) as a white solid.

^{1}H NMR (400 MHz, $CDCl_3$) δ = 4.28−4.52 (m, 2 H), 3.70−3.98 (m, 2 H), 3.08−3.34 (m, 1 H), 2.60−2.92 (m, 2 H), 1.80−2.38 (m, 2 H), 1.00−1.74 (m, 14 H), 1.42 (s, 18 H).
^{13}C NMR (100 MHz, $CDCl_3$) δ = 156.5, 155.0, 79.9, 79.0, 64.7, 47.4, 46.3, 39.3, 39.0, 37.0, 36.7, 29.7, 29.4, 28.5 (3 CH_3), 28.3 (3 CH_3), 25.6, 25.5, 19.1 (detected signals).
$[\alpha]_D^{20}$: +43.3 (*c*= 0.53, $CHCl_3$). Ref: **$[\alpha]_D^{20}$** : +41.4 (*c*= 0.72, $CHCl_3$)
MS (ESI) m/z $[M + Na]^+$ calcd. for $C_{23}H_{42}N_2O_5Na$: 449.30, found: 449.71.

Synthesis of (2R,2'R)-di-tert-butyl 2,2'-(2-oxopropane-1,3-diyl)bis(piperidine-1-carboxylate) (58).

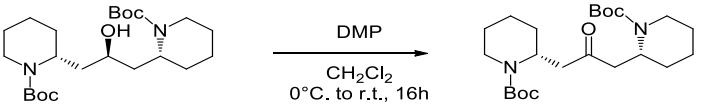

quant.

57 (0.043 g, 0.10 mmol) was dissolved in anhydrous CH_2Cl_2 (1 mL) at 0°C, and DMP (50.7 mg, 0.12 mmol) was added. The mixture was stirred for 16h at r.t.. The mixture was concentrated; a 10% solution of NaOH was added and the mixture was extracted with Et_2O. The combined organic layers were washed with NaOH (10%) and H_2O. The aqueous layers were extracted with Et_2O, and the combined organic layers were dried over Na_2SO_4, filtered and concentrated under vacuum to give **58** (0.042 g, quant.) as a colourless solid.

^{1}H NMR (400 MHz, $CDCl_3$) δ = 4.60−4.76 (m, 2 H), 3.82−4.02 (m, 2H), 2.50−2.86 (m, 6 H), 1.20−1.71 (m, 12 H), 1.41 (s, 18 H).
^{13}C NMR (100 MHz, $CDCl_3$) δ = 207.2, 154.8 (2 Cq), 79.6 (2 Cq), 47.3 (2 CH), 43.4 (2 CH_2), 39.6 (2 CH_2), 28.5 (6 CH_3), 28.4 (2 CH_2), 25.4 (2 CH_2), 19.1 (2 CH_2).
$[\alpha]_D^{20}$: +19.9 (*c*= 0.77, $CHCl_3$).
MS (ESI) m/z $[M + Na]^+$ calcd. for $C_{23}H_{40}N_2O_5Na$: 447.28, found: 447.81.

Synthesis of 1,3-di((R)-piperidin-2-yl)propan-2-one (49).

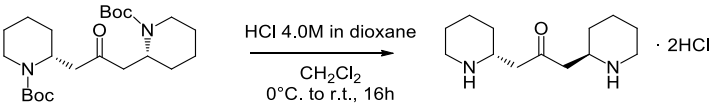

quant.

58 (0.030 g, 0.07 mmol) was dissolved in CH_2Cl_2 (2 mL) and cooled to 0°C. A 4M solution of HCl (75 µL, 0.21 mmol) in dioxane was added dropwise. The mixture was stirred for 16h at r.t. The mixture was concentrated to give (-)-anaferine dihydrochloride (0.021 g, quant.) as a colourless solid, without need of further purification.

^{1}H NMR (400 MHz, CD_3OD) δ = 3.50−3.61 (m, 2 H), 3.32−3.40 (m, 2 H), 2.88−3.05 (m, 6 H), 1.82−1.95 (m, 6 H), 1.00−1.74 (m, 6 H).
^{13}C NMR (100 MHz, CD_3OD) δ = 205.0, 52.3 (2 CH), 44.8 ($2CH_2$), 44.7 ($2CH_2$), 28.3 ($2CH_2$), 22.0 ($2CH_2$), 21.6 ($2CH_2$).
$[\alpha]_D^{20}$: -47.9 (*c*= 0.65, MeOH/H_2O = 1:1).
MS (ESI) m/z calcd. for $[C_{13}H_{24}N_2O]^+$: 224.19; found 224.31.

5. Thiocolchicine-based bivalent compounds

5.1 Microtubules targeting bivalent compounds from 2-piperidine ethanol

The last part of this project, was inspired by the structure of the fundamental dumetorine-pironetin hybrid **60,** previously synthesised in our laboratory, starting once again from 2-piperidine ethanol, as reported in Chapter 1.[42] The hybrid was identified as a key building block for the synthesis of bivalent compounds able to target tubulin and microtubules (MTs). In fact, compound 63 contains a key portion on (-)-pironetin, one of the few α-tubulin binders to be known.[164] On the other hand, the piperidine ring, deriving from (+)-dumetorine, could be exploited as an anchor point, to connect a linker and then an other active compounds, as reported in Figure 26.

These considerations inspired the synthesis of bivalent compounds bearing an α- and a β-tubulin biners, able to target tubulin and microtubules, to achieve a multiple and synergic effect on tubulin polymerisation.

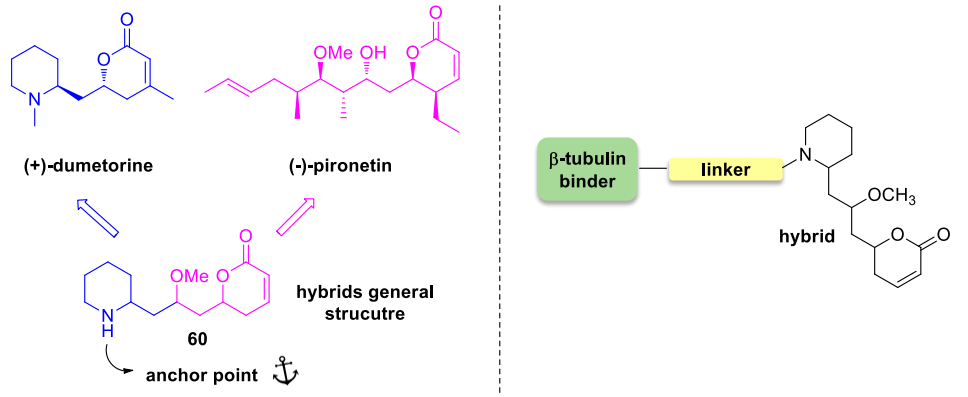

Figure 26. General structure of the pironetin-dumetorine hybrids previously synthesised in our laboratory (left); general structure of the bivalent compounds (right).

But before dealing with the synthesis of these conjugates, a brief introduction about microtubules as target in medicinal chemistry and about the use of microtubules-targeting bivalent compounds will follow.

[164] a) A. E. Prota, J. Setter, A. B. Waight, K. Bargsten, J. Murga, J. F. Díaz, M. O. Steinmetz, *J. Mol. Biol.* **2016**, *428*, 2981-2988. b) J. Yang, Y. Wang, T. Wang, J. Jiang, C. H. Botting, H. Liu, Q. Chen, J. Yang, J. H. Naismith, X. Zhu, L. Chen, *Nat. Commun.* **2016**, *7*, 1–9.

5.2 Tubulin and microtubules.

Tubulins are a superfamily of globular proteins, diffused in eukaryotic cells, as well as in some bacteria.[165]

This superfamily contains five different families: α, β, γ, δ, ε- tubulins and among them, α and β subtypes are the most widely diffused in eukaryotic cells. α - and β-tubulins tend to form heterodimers, that through a polymerisation process, originate the so called microtubules (MTs). MTs are fundamental structural components of cells cytoskeleton and are involved in diverse cellular processes, including cell division, locomotion, intracellular transport and cell shape definition.

The first event in the polymerisation process is the binding between the β-subunit of a heterodimer and a unit of guanosine triphosphate (GTP), that starts the polymerisation of α/β-tubulin heterodimers in a head-to-tail arrangement. In this way, a protofilament is formed and then thirteen protofilaments are assembled in a cylindrical structure. The polymerisation endures until the GTP molecule is hydrolysed to GDP. Considering the head-to-tail arrangement of tubulin heterodimers, the microtubule possesses a termination constituted by β -tubulin, called (+)-end, and a termination composed by α-tubulin, called (-)-end.[166] The structural features of a microtubule are summarised in Figure 27.

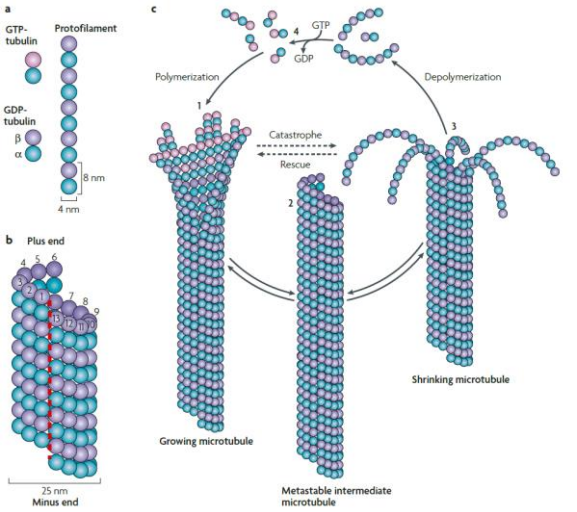

Figure 27. Structural features of a MT (left) and MTs dynamic polymerisation-shrinkage cycle (right). Adapted from "Tracking the ends: a dynamic protein network controls the fate of microtubule tips", A. Akhmanova, M. O. Steinmetz, nature reviews, molecular cell biology, 9, 2008, 309-322, with permission from Nature-Springer, copyright 2008.

[165] M. Pilhofer, M. S. Ladinsky, A. W. McDowall, G. Petroni, G. J. Jensen, *PLoS Biol.* **2011**, *9*, e1001213.
[166] Bollang, D.; McQueney, P.A.; Zhu, J.; Hensens, O.; Koupal, L.; Liesch, J.; Goetz, M.; Lazarides, E.; Woods, C.M.; *Cancer Research* **1995**, *55*, 2325-2333.

Once that have been built in the aforementioned process, MTs don't remain static structures. In physiological conditions, MTs are in fact characterised by the so called "dynamic" instability", that consist in alternating phases of growth and shrinkage or in the phenomenon of "treadmilling", which is the net growth at one end of the microtubule, accompanied by a shortening at the opposite side.[167,168]

Also in this case, the process is regulated by GTP. In fact, during the growth phase, tubulin binds GTP in solution and the tubulin-GTP unit is added to the end of a growing microtubule. After that, GTP is gradually hydrolysed to GDP. The exchange between the polymerisation phase to the shrinkage one appears to be regulated by the presence of GTP or GDP at the microtubule end. If the end is characterised by the stabilizing GTP cap, the microtubule grows, while the loss of the GTP cap, after hydrolysis to GDP, results in the depolymerisation process. It is noteworthy that the two extremities of a microtubule are not equivalent. It has been demonstrated that the plus end is more dynamic than the minus end, from a kinetically point of view. The global result is that although each one of the extremity of a microtubule can polymerize and shrink, the modifications in length at the plus end are more prominent that at the minus end.

The dynamic instability and treadmilling typical of microtubules are crucial for their correct functionality, in particular for the formation of the mitotic spindle during the mitosis process.[169]

In this context, the highly dynamic microtubules allow the correct attachment of the chromosomes to the spindle and control their alignment and separation at metaphase and anaphase, respectively. Thus, the perturbation of microtubules dynamics has deleterious effects on the cell, interfering with the cell replication mechanism and often resulting in cell apoptosis.

For this reason, tubulin and microtubules are well known targets in medicinal chemistry and in the last decades several antimitotic drugs have been developed and approved by FDA as anticancer agents. More recently, the use of antimitotic compounds found applications in the treatment of neurodegenerative diseases, considering that several neuronal activities are regulated by tubulin post translational modifications.[170,171]

---

[167] M. Jordan, *Curr. Med. Chem. Agents* **2002**, *2*, 1–17.

[168] T. J. Mitchison, M. Kirschner, *Nature* **1984**, *312*, 237-242.

[169] J. Zhou, P. Giannakakou, *Curr. Med. Chem. Anticancer. Agents* **2005**, *5*, 65–71.

[170] D. Cartelli, F. Casagrande, C. L. Busceti, D. Bucci, G. Molinaro, A. Traficante, D. Passarella, E. Giavini; G. Pezzoli, G. Battaglia, G. Cappelletti, *Sci. Rep.* **2013**, *3*, 1837-1847.

[171] K. R. Brunden, J. Q. Trojanowski, A. B. Smith, V. M. Lee, C. Ballatore, *Bioorg. Med. Chem.* **2014**, *22*, 5040-5049.

It is noteworthy that the perturbation of the dynamic instability can occur either by stabilisation and destabilisation of microtubules, leading to the same result of blocking the cell replication cycle and eventually resulting in cellular apoptosis. Thus, two classes of antimitotic drugs exist: MTs destabilizing agents and MTs stabilizing agents.[172] These drugs bind to diverse sites on the tubulin dimers and at different regions of the microtubule.
Thus, despite the opposite mechanism of action on microtubules, the perturbation of the dynamic instability leads to the same effects: in fact, both MTs stabilizing and destabilizing agents interferes with mitosis at the metaphase/anaphase transition, and induce cell death. The effects of the administration of antimitotic drugs on the cell replication cycle can be appreciated in Figure 28, in which the physiological mitotic spindle is compared with the situation in the presence of Taxol.

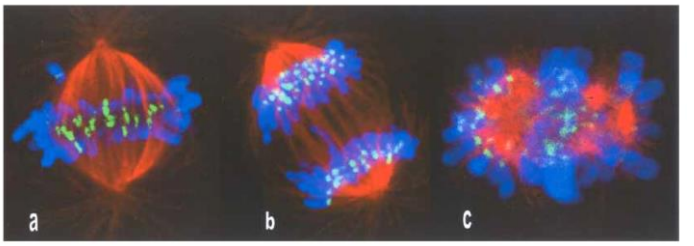

Figure 28. Human osteosarcoma cells (U2Os) in a) early metaphase and b) anaphase of the cell cycle and c) after incubation with 1 µM taxol. Microtubules are reported in red, chromosomes in blue and kinetochores in green. In the presence of taxol, the mitotic spindle is disrupted, and the chromosomes remain at the poles. Adapted from ref 167, with permission from EUREKA SCIENCE, copyright 2002.

5.1.1 MTs destabilizing agents

MTs destabilizing agents inhibit microtubules polymerisation, interacting essentially on two possibile sites located on β-tubulin: the vinca-site and the colchicine site.[172]
Vinca-site binders include of course the vinca alkaloids. Two well-known members of this class are vinblastine and vincristine, that have been used for the treatment of several tumour types, such as Hodgkin and non-Hodgkin lymphomas (vinblastine) and hematological tumours (vincristine). The employment of vinca alkaloid in anticancer therapy is limited by the side effects, that include the suppression of the bone marrow and marked neurotoxicity. However, vinflunine, a synthetic fluorinated vinca alkaloid characterised by an excellent safety profile has been recently approved in Europe for the second-line treatment of metastatic urothelial carcinoma.

[172] C. Dumontet, M. A. Jordan, *Nat. Rev. Drug Discovery* **2010**, *9*, 790-803.

Other classes of vinca-binders are the cryptophycins (such as Cryptophycin-52, a potent antimitotic agent, active also on multi-drug resistant cells) and the dolastatins (eribulin, spongistatin, rhizoxin, maytansinoids and tasidotin).
On the other hand, colchicine-site binders include colchicine, a compound characterised by anti-inflammatory properties and use for gout treatment, and combretastatins (such as combretastatin A), a class of molecules structurally related with colchicine, that displays an additional vascular-disrupting action (VDAs), useful in anticancer treatment.
Other know colchicine-binders are podophyllotoxin, combretastatins, 2-methoxyoestradiol, phenylahistins, and steganacins.
The structures of some of the aforementioned mictrotubules-destabilizing agents are reported in Figure 29.

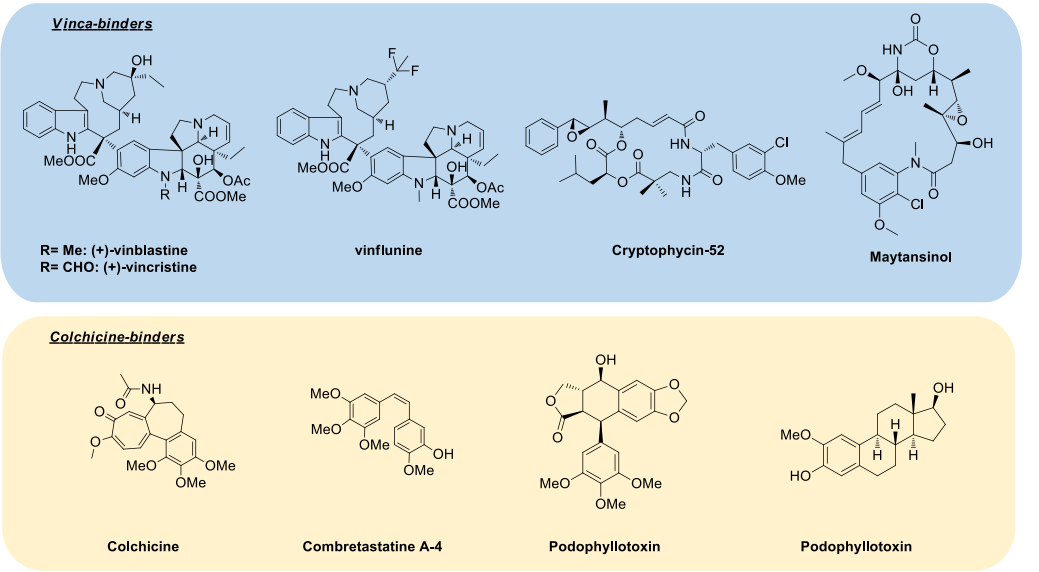

Figure 29. Structures of some of the principal microtubules destabilizing agents.

5.1.2 MTs-stabilizing agents

Microtubules-stabilizing agents favour microtubules polymerisation. Among this class of antimitotic agents, taxanes are probably the most famous family and paclitaxel, or taxol, was the first MTs-stabilizing agent used in anticancer therapy for the treatment of multiple solid tumours such as ovarian, breast and prostate cancer.[173]

[173] M. C. Wani, H. L. Taylor, M. E. Wall, P. Coggon, A. T. McPhail, *Journal of the American Chemical Society* **1971**, *93*, 2325–2327

Unfortunately, the occurrence of multi-drug resistance limited taxanes applications in chemotherapy.

Other well-known MTs stabilizing agents are epothilones, discodermolide, dictyostatin, sarcodictyins, and laulimalide and peloruside A, which are characterised by different chemical structures, but similar mechanism of action.

Epothilones, discodermolide, dictyostatin and sarcodictyins seem to bind to the same site of taxoles, located on β-tubulin, on the inner surface of the microtubule, or at least to an overlapping site, as it is demonstrated by the fact that these compounds act as competitive inhibitors of paclitaxel.

Epothilones are naturally occurring polyketide macrolides, well-known for antifungal and anticancer activity. Ixabepilone is a synthetic aza-derivative of epothilone B, and is the only approved member of this family as anticancer agent. Moreover, Epothilone D could find applications in the treatment of different tauopathies, such as Alzheimer's disease.[174]

Discodermolide and dictyostatin are two structurally related macrocycles, which induce tubulin polymerisation more rapidly than paclitaxel and displaying a marked activity also against paclitaxel-resistant cancer cells, as a result of β-tubulin mutations.[175]

Sarcodictyins are a class of compounds structurally and functionally correlated to eleutherobin, a natural glycosylate diterpene. Sarcodictyins display a better safety-profile compared with eleutherobin, that is active against paclitaxel-resistant cells, but resulting too toxic also for healthy cells.[176]

Also laulimalide and peloruside A display a MTs polymerizing activity similar to the one of the aforementioned compounds. However, they don't act as competitive binders of paclitaxel, and for this reason they are supposed to interact with a novel site on tubulin.[177,178,] Moreover, laulimalide proved to be active against P-glycoprotein-resistant cells, preventing blood vessel formation.

The structures of some of the aforementioned molecules are reported in Figure 30.

---

[174] K. R. Brunden, C. Ballatore, V. M.-Y. Lee, A. B. Smith, J. Q. Trojanowski, *Biochem. Soc. Trans.* **2012**, *40*, 661–666.

[175] C. Madiraju, M. C. Edler, E. Hamel, B. S. Raccor, R. Balachandran, G. Zhu, K. A. Giuliano, A. Vogt, Y. Shin, J. H. Fournier, Y. Fukui, A. M. Bru¨ckner, D. P. Curran, B. W. Day, *Biochemistry* **2005**, *44*, 15053–15063.

[176] B. H. Long, J. M. Carboni, A. J. Wasserman, L. A. Cornell, A. M. Casazza, P. R. Jensen, T. Lindel, W. Fenical, C. R. Fairchild, *Cancer Res.* **1998**, *58*, 1111–1115.

[177] D. E. Pryor, A. O'Brate, G. Bilcer, J. F. Díaz, Y.Wang, Y. Wang, M. Kabaki, M. K. Jung, J. M. Andreu, A. K. Ghosh, et al., *Biochemistry* **2002**, *41*, 9109–9115.

[178] J. T. Huzil, J. K. Chik, G. W. Slysz, H. Freedman, J. Tuszynski, R. E. Taylor, D. L. Sackett, D. C. Schriemer, *J. Mol. Biol.* **2008**, *378*, 1016–1030.

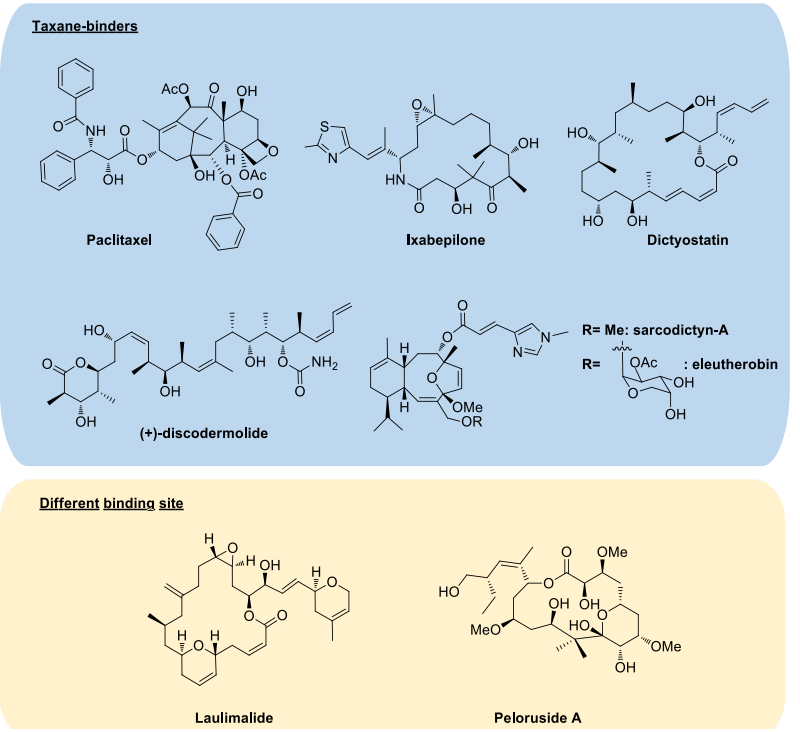

Figure 30. Structures of some of the principal microtubules stabilizing agents.

5.1.3 Bivalent compounds targeting tubulin and microtubules

In the last decades, the importance of MTs in both anticancer therapy and neurodegenerative diseases treatment became increasingly evident, and this encouraged the development of potential MT-targeting drugs.

However, nowadays it's clear that single drugs cannot completely cure very complex diseases. Thus, multi-target therapies emerged as one of the best strategies to contrast these complex diseases. The combination of drugs allows a multiple action at different targets at the same time. Therefore, multi-target therapies display enhanced efficacy and reduced adaptive resistance compared to mono- therapies. Moreover, the simultaneous action on different targets often leads to a synergic effect. In fact, a cocktail of multiple drugs often shows an increased efficacy, compare with the sum of the effects of the single components.[179]

In this context, bifunctional drugs are a class of multi-target therapies, with the advantage of presenting the two active units bound in the same chemical entity, eliciting a multiple effect and increasing the global pharmacological activity.

[179] G. R. Zimmermann, J. Lehár, C. T. Keith, *Drug Discov. Today* **2007**, *12*, 34–42.

The idea of exploiting diverse microtubules binders, connecting them with a linker is not new, and several examples of microtubules-targeting bivalent compounds are reported in literature. A brief overview of some interesting examples will follow below, starting with the efforts already performed in our laboratory. The structures of the mentioned hybrids are reported in Figure 31.

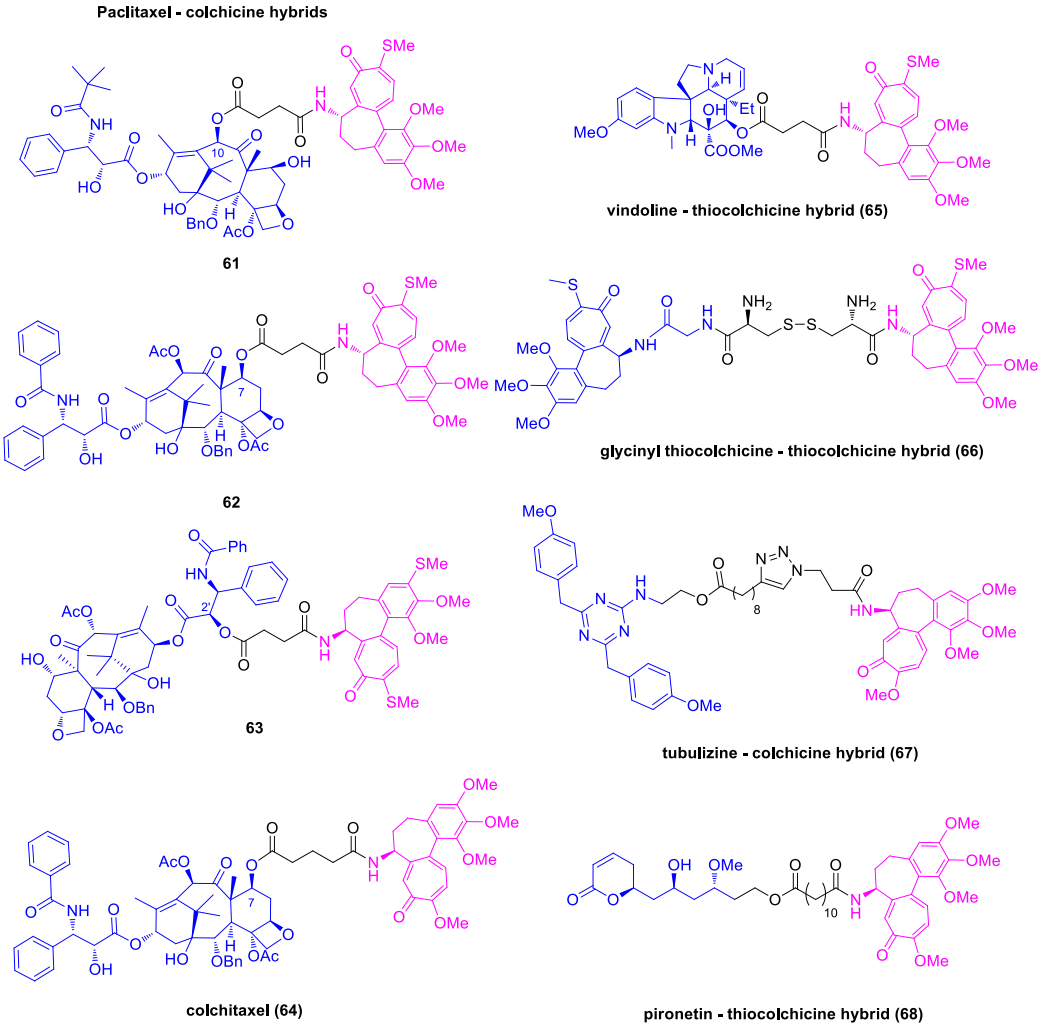

Figure 31. Structures of the cited hybrid compounds.

An interesting example involved the synthesis of a small library of taxoid-colchicinoid conjugates.[180] In detail, a succinate spacer was used to connect thiocolchicine (a more stable version of colchicine, in which the enolic oxygen group was replaced by a sulfur) and tow toxoids: paclitaxel and deacetylbaccatin III. The latter is a taxane devoid of the aminoacidic lateral chain, used with the intent to work with a simpler structure, adding the lateral chain in an advance stage of the synthesis. Despite the simplified structure of deacetylbaccatin III, the obtainment of the corresponding bivalent compounds proved to be quite difficult from a synthetic point of view and in the most of the cases paclitaxel proved to be the best taxoid candidate. To construct out conjugates, the thiocolchicine was converted into the corresponding *N*-deactyl thiocolchicine, in order to obtain an amine group exploitable for the attachment of the linker, through the formation of an amide bond. To connect the taxoid moiety, the hydroxyl groups in position 7, 2' and 10 (originated after the removal of the acetyl group) were exploited. In this way, three candidates **61-63** were synthetised. Two of them (**61** and **62**) showed a taxoid-like activity, but less marked than paclitaxel alone. A comparison with a control experiment in which an equimolar mixture of paclitaxel and thiocolchicine was tested, suggested that in our conjugate the taxoid −phenotype prevails over the colchicine one in tubulin assembly/disassembly experiments. On the other hand, compound **63** displayed an excellent cytotoxicity, but resulting inactive in assays of colchicine- and taxoid-type activity, suggesting a binding with a different site on tubulin.

A similar example, reported by Bombuwala and coworkers, dealt with the synthesis of the so-called "colchitaxel" (**64**), a dimeric compound composed by colchicine and paclitaxel, bound by a longer glutarate linker.[181] Also in this case, colchicine was converted into the corresponding *N*-deactyl colchicine, to obtain an anchor point. For what concern the paclitaxel, the more accessible hydroxyl group was protected with a bulky silane, that was cleaved after the coupling reaction between the other alcohol and the complex colchicine – glutarate. The obtained bivalent compound underwent biological test, that revealed a shortening and fragmentation of the plus end cap on microtubules. Microtubules conformations was similar to the one of microtubules treated with a combination of the two drugs, but the mechanism of action of the bivalent compounds remained quite unclear. Different bivalent compounds, originated by the merging of *Vinca* alkaloids (anhydrovinblastine, vinorelbine, and

[180] B. Danieli, A. Giardini, G. Lesma, D. Passarella, A. Silvani, G. Appendino, A. Noncovich, G. Fontana, E. Bombardelli, O. Sterner, *Chem. Biodivers.* **2004**, *1*, 327–345.

[181] K. Bombuwala, T. Kinstle, V. Popik, S. O. Uppal, J. B. Olesen, J. Viña, C. A. Heckman, *Beilstein J. Org. Chem.* **2006**, *2*, 1–9.

vindoline) to taxoid- binders such as thiocolchicine, podophyllotoxin, and baccatin III.[182] Twelve hybrids conjugates were accessed combining a vinca-binder and a taxoid-binder, through diacyl spacers of different chain length. The most active compound of this series (**65**), composed by vindoline and thiocolchicine, connected through a C-4 linker, inhibited tubulin polymerisation, and was even more effective as antiproliferative agent than thiocolchicine alone.

An evolution of this approach concerned the development of an innovative dynamic combinatorial library (DCL). This kind of strategy is based on the use of known high-affinity scaffolds that could reversibly self-assemble with several complementary building blocks. The reversibility ensures that all of the members of the library are in thermodynamic equilibrium. Thus, when the members of the library are in the presence of a molecular target, a selection process can alter the composition of the mixture.

This results in a stabilisation of the compounds that bind to the target, triggering the equilibrium of the mixture towards the formation of the strongest binders. On the contrary, the poor binders are suppressed. This rational was employed for the synthesis of homodimeric compounds bearing thiocolchine and podophyllotoxin as active components and connecting them through linkers of different length, but presenting a fundamental disulfide bond.[183,184] The general idea is that disulfide bond exchange could occur even under mild conditions, leading to the formation of heterodimeric bivalent compounds in the presence of microtubules, as reported in Figure 32.

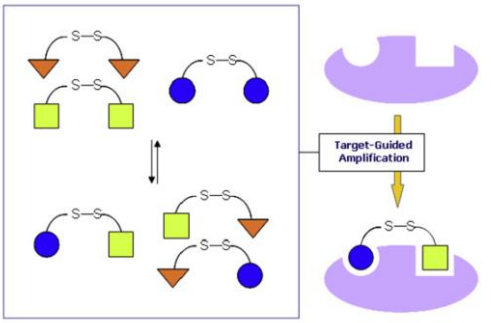

Figure 32. General concept for the target-guided DCL based on the disulfide-exchange reaction.

[182] D. Passarella, A. Giardini, B. Peretto, G. Fontana, A. Sacchetti, A. Silvani, C. Ronchi, G. Cappelletti, D. Cartelli, J. Borlak, B. Danieli, *Bioorganic Med. Chem.* **2008**, *16*, 6269–6285.

[183] B. Danieli, A. Giardini, G. Lesma, D. Passarella, B. Peretto, A. Sacchetti, A. Silvani, G. Pratesi, F. Zunino, *J. Org. Chem.* **2006**, *71*, 2848–2853.

[184] G. Cappelletti, D. Cartelli, B. Peretto, M. Ventura, M. Riccioli, F. Colombo, J. S. Snaith, S. Borrelli, D. Passarella, *Tetrahedron* **2011**,

A proof of concept was performed, synthesizing few homodimeric hybrids, with the two active parts connected by two dithiodicarboxylic acids differing into the chain length and demonstrating that they could generate heterodimers in solution. However, the first generation homodimers weren't soluble enough in water, forbidding the possibility of test them in the presence of tubulin. Then a modification in the spacer was considered, coupling podophyllotoxin, *N*-deacetyl thiocolchicine and *N*-deacetylglycinyl thiocolchicine with *N*-Boc-cystine. After the cleavage of the Boc protecting group, water soluble homodimers were finally obtained.

After a proof of concept in aqueous solution, aimed at confirming the formation of the heterodimers, the same experiment was performed in the presence of tubulin. In this case, an amplification of the production of heterodimer **66**, composed by a unit of *N*-deacetyl thiocolchicine and a unit of *N*-deacetylglycinyl thiocolchicine reported in Figure 28.

Then, the analog of **66** bearing an ethylene spacer instead of the labile disulfide bond was synthesised, to guarantee the maintenance of the dimeric structure in cellular environment. In this way a compound that inhibits the polymerisation of tubulin in a dose-dependent manner was obtained.

Other examples of antimitotic hybrids include colchicine-tubulizine bivalent compounds, in which the two tubulin binders were linked exploiting a huisgen 1, 3-dipolar cycloaddition between an azido-derivative of colchicine and acetylene-substituted tubulizine-type derivatives.[185] Different chain lengths were tested, in order to find the optimal distance to ensure the simultaneous binding of both the active units on tubulin. The obtained compounds displayed a good cytotoxicity against HBL100 epithelial cells and the ones bearing a linker of 14-20 carbon atoms proved to act as sub-stoichiometric inhibitors of microtubule assembly. The structure of the best candidate **67** is reported in Figure 31.

Finally, a library of synthetic hybrids composed by colchicine and a fragment structurally related to pironetin, was developed. In this case a β- and an α-tubulin binders were respectively used, and connected through a spacer of variable length, containing an ester and an amide. Although none of the spacers was long enough to allow the simultaneous interaction of colchicine and pironetin moieties with the respective binding sites. For this reason, competitive binding was expected to take place. Biological test revealed that the hybrids compounds was less cytotoxic than the two parental compounds.

[185] Y. B. Malysheva, S. Combes, D. Allegro, V. Peyrot, P. Knochel, A. E. Gavryushin, A. Y. Fedorov, *Bioorganic Med. Chem.* **2012**, *20*, 4271–4278.

However, the linker length played a crucial role, in particular for the interaction at the pironetin binding site. In fact, when short spacers were employed, the sterically bulky colchicine moiety hinders the hybrid molecules from arriving at the pironetin binding site and only a reversible activity at colchicine binding site was observed. The structure of the best hybrid **68** is reported in Figure 31.

5.2 Thiocolchicine-based bivalent compounds: synthetic efforts

Al the previously reported examples of MTBCs indicates that linker chemical and physical features play a crucial role in the activity of MTBCs. In fact, despite their great pharmacological potential, bivalent compounds often display in vitro and in cell performances similar or poorer than their individual components. One of the possible cause is the linker nature. It's quite clear that the use of too short or rigid linkers could prevents the interaction with the desired binding site and leads to steric clashes, while too long and flexible linkers may lead to solubility and cell internalisation problems.[186] Thus, to better understand the role of the chemical spacer in the synthesis of bifunctional tubulin binders, we planned the synthesis of conjugates, constituted by the aforementioned dumetorine-pironetin hybrids, previously developed in our laboratory (**60a-c**, Figure 33), and a known β-tubulin binder, connected by linkers differing in chemical nature and chain length, to investigate how their properties affect the binding capability.

For the first explorative studies, a ten-atom all-carbon chain and a 24-atom pseudo-peptidic chain were taken into account. As active units, we choose thiocolchicine, as a well-known model of β-tubulin binder, and three isomers of dumetorine-pironetin hybrid (**60a-c**), that were already available in our laboratory. The general scheme for the assembling of our MTBCs is reported in Figure 33.

[186] J. Marangon, M. S. Christodoulou, F. V. M. Casagrande, G. Tiana, L. Dalla Via, A. Aliverti, D. Passarella, G. Cappelletti, S. Ricagno, *Biochem. Biophys. Res. Commun.* **2016**, *479*, 48–53.

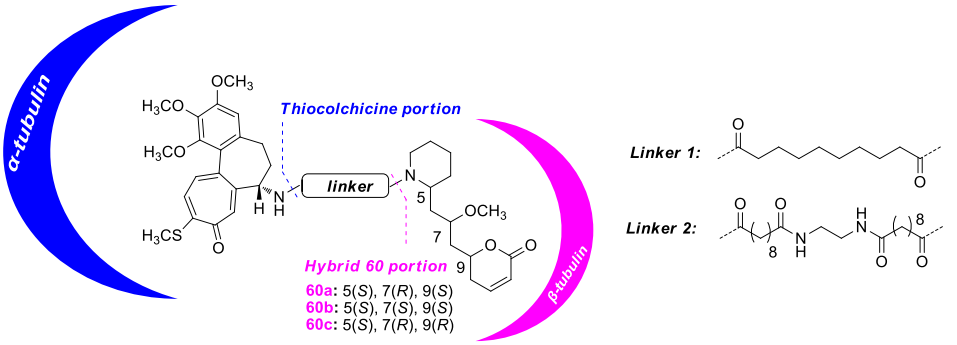

Figure 33. General scheme for the assembly of the conjugate compounds and representation of the employed specific components.

The hybrid should bind preferentially to α-tubulin, thanks to the presence of the pironetin-like α, β-unsaturated lactone.[187] It has been demonstrated that in pironetin, this moiety serves as Michael acceptor for the Cys316 residue inside α-tubulin binding site.[164]

This type of covalent interaction could be fundamental to escape P- glycoprotein-induced drug resistance. P-glycoprotein is a common ATP-dependent efflux pumps, member of the ATP-binding cassette (ABC) transporter family. This protein is present on cellular membrane and is overexpressed in a wide range of human cancers. The drug resistance arises from the ability of P-glycoprotein of pump drugs outside the cells. Thus, drugs interacting with a receptor through a covalent bond are less sensible to this drug resistance mechanism.

Thus, to prepare the first class of bivalent compounds, characterised by the ten-carbons chain, *N*-deacetyl-10-thiocolchicine **69**, was obtained through acidic hydrolysis of thiocolchicine.[188] The free amine was condensed with sebacic acid, giving compound **70**. A strict control over the amount of sebacic acid avoided the undesired reaction on both the carboxylic moieties. Finally, reaction of **70** with compound **60a** in the presence of HATU and DIPEA, afforded the first MTCBs, (**71**), characterised by a linker of 10 carbon atoms (Scheme 42). Unfortunately, the condensation of compound **70** with **60b** and **60c** gave unexpectedly complex mixture of compounds, impossible to purify.

[187] E. Bonandi, F. Foschi, C. Marucci, F. Dapiaggi, M. Sironi, S. Pieraccini, M. S. Christodoulou, F. de Asís Balaguer, J. F. Díaz, N. Zidar, D. Passarella, *ChemPlusChem* **2019**, *84*, 98–102.
[188] Q. Shi, P. Verdier-Pinard, A. Brossi, E. Hamel, K. Lee, *Bioorg. Med. Chem.* **1997**, 5, 2277-2282.

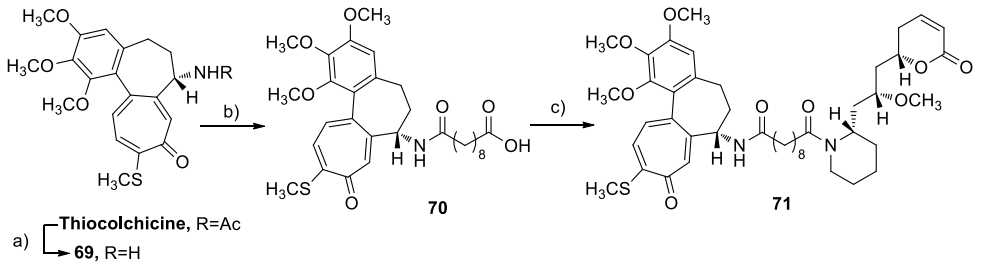

Scheme 42. *Reagents and conditions:* a) HCl 2M, MeOH, 85°C, 3 days; b) sebacic acid, HATU, DIPEA, CH_2Cl_2, rt, 3h; c) **60a**, HATU, DIPEA, CH_2Cl_2, rt, 4 h.

Then, the synthesis of the conjugates characterised by a longer spacer was faced. In particular, we decided to elongate compound **70** chain, adding a short di-amidic linker and another unit of sebacic acid. In this way, a 24-atoms pseudo-peptidic linker should be obtained. The first step of this synthetic sequence, reported in Scheme 43, was the HATU-mediated coupling between **70** and the tert-butyl 2-aminoethylcarbamate fragment **72**, obtained according to reported procedure.[189] The Boc protecting group was removed upon acidic treatment, and the resulting free amine was exploited for a further with sebacic acid. In this way, the thiocolchicine derivative **75** was obtained as main product.

Final MTBCs **76a–c** were accessed condensing **78** with the proper **63** stereoisomer, under the same conditions exploited for the previous couplings.

In this case all the three expected conjugates were obtained, without particular purification issues.

[189] J. P. Holland, V. Fisher, J. A. Hickin, J. M. Peach, *Eur. J. Inorg. Chem.* **2010**, 48–58.

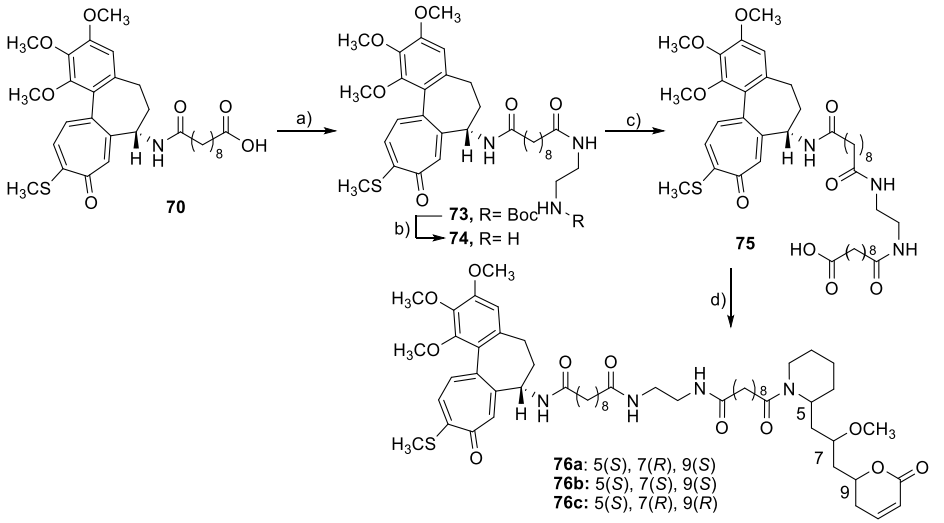

Scheme 43 *Reagents and conditions:* a) **72**, HATU, DIPEA, CH_2Cl_2, rt, 3h; b) TFA, CH_2Cl_2, 0°C to rt, 1h; c) sebacic acid, HATU, DIPEA, CH_2Cl_2, rt, 3h; d) **60a-c**, HATU, DIPEA, CH_2Cl_2, rt, 3h.

5.2.1 Biological Data

At the end of the synthetic process, four potential microtubules targeting bivalent compounds were obtained: compounds **71**, characterised by a ten all-carbon chain and **76a–c**, bearing the longer pseudo-peptidic spacer. Preliminary biological tests were performed on all of them. Firstly, they were tested on wild-type and resistant ovarian cancer cells lines (A2780 and A2780AD respectively). The results are summarised in Table 4. Unfortunately, cytotoxicity data seem to suggest that our compounds do not interact through the pironetin-like unit.

In fact, if this was the case, they would have accumulated inside the cells like other MTs covalent binders, avoiding the P-glycoprotein resistance, but in this situation it's evident that the activity drops on A2780AD cells.[190]

For what concern the differences in linker length, **71** is almost as toxic as *N*-deacetyl-10-thiocolchicine **69** in non-resistant cells, but 100 times less toxic in resistant cells, while compounds **76a–c** displayed even less toxicity. Also in this case the trend is more marked on resistant cells. These results suggest that our bivalent compounds interact with tubulin only through the thiocolchicine moiety, justifying in this way the partially

[190] a) R. M. Buey, E. Calvo, I. Barasoain, O. Pineda, M. C. Edler, R. Matesanz, G. Cerezo, C. D. Vanderwal, B. W. Day, E. J Sorensen, J. A. Lopez, J. M. Andreu, E. Hamel, F. J. Díaz, *Nat. Chem. Biol.* **2007**, *3*, 117-125; b) A. J. Marco, J. Garcia-Pla, M. Carda, J. Murga, E. Falomir, C. Trigili, S. Notararigo, F. J. Díaz, I. Barasoain, *Eur. J. Med. Chem.* **2011**, *46*, 1630-1637; c) J. J. Field, B. Pera, E. Calvo, A. Canales, D. Zurwerra, C. Trigili, J. Rodriguez-Salarichs, R. Matesanz, A. Kanakkanthara, S. Wakefield, J. A. Singh, J. Jimenez- Barbero, P. Northcote, J. H. Miller, J. A. Lopez, E. Hamel, I. Barasoain, K. Altmann, F. J. Díaz, *Chem. Biol.* **2012**, *19*, 686-698.

retained bioactivity. The fact that compound **71**, characterised by the shortest spacer is the most active conjugate indicates that the longer linker of **76a-c** hinders the interaction of the pironetin moiety with the target. Moreover, the activity drop in the case of resistant cancer cells suggests that the hydrophobic linker render these hybrids better substrates for P- glycoprotein. This assumption is somehow confirmed considering that A2780AD cells overexpress this protein and that the activity decreases with the length- and the hydrophobicity- of the chemical spacer.

Table 4. Cytotoxicity data.

Compound	IC_{50} [nM][a]		R/S[b]
	A2780	***A2780AD***	
71	11.8±1	4300±600	364
76a	252±7	20500±500	81
76b	205±15	19000±6000	93
76c	196±0.2	46000±1500	235
Colchicine	13.6±2	663±23	49
N-deacetyl-10-thiocolchicine	7.8±1	30.9±0.6	4
Paclitaxel	0.4±0.08	1400±200	3500
Podophyllotoxin	8±1	10.1±0.7	1.2

[*a] IC_{50} values determined in the parental ovarian carcinoma A2780 line and the MDR P-glicoprotein-overexpressing ovarian carcinoma A2780/AD10. IC_{50} values in nm were determined after two days' exposure to drugs using the MTT cell proliferation assay. Data are the mean ± SE of at least four independent experiments. [b] Ratio of IC_{50}(resistant cell line)/IC_{50}(parental cell line). Values are the calculated relative resistance of each mutant cell line obtained by dividing the IC_{50} value of the resistant line by the IC_{50} value of the parental line, A2780.*

To confirm that the partially retained antiproliferative activity of **71** and **76a-c** was actually related to their capacity to destabilize tubulin in a typical "thiocolchicine-fashion", a tubulin polymerisation assay was performed, testing also podophyllotoxin and *N*-deacetyl-10-thiocolchicine as models of MTs destabilizing agents and DMSO as negative control. The results are reported in Figure 34.

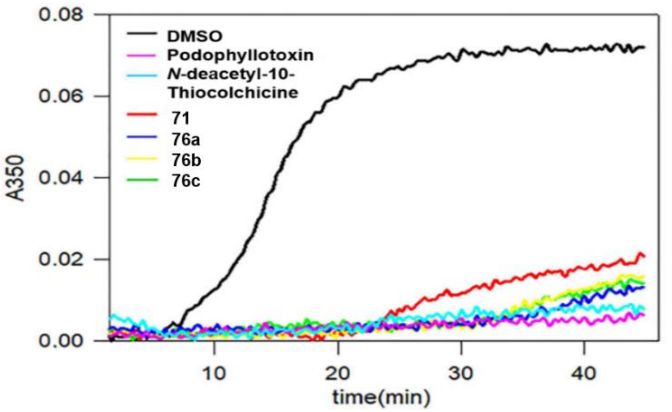

Figure 34. Time course of 25 µM tubulin polymerisation at 37°C measured by 350 nm turbidimetry in the presence of DMSO vehicle (control) or 27.5 µM of ligand. The assay was performed in triplicate and the graph represents the mean of the three experiments.

Observing the graphic, it's evident that all the tested compounds display a strong destabilizing effect on tubulin, indicating that the observed toxicity is exerted through inhibition of tubulin assembly. This is coherent with the assumption that the partial activity of these bivalent compounds depends from the interaction of the thiocolchicine moiety with tubulin. These results highlight only a slight activity difference between compound **71** and compounds **76a–c**.

In summary, biological data highlighted the plain inability of the obtained bivalent compounds to exploit the dual interaction with tubulin/microtubules, with the retained activity due to the thiocolchicine moiety.

These observations prompted us to investigate the binding mode of these compounds through *a posteriori* molecular modelling studies.

5.2.2 Molecular Dynamics Simulations

Molecular dynamics (MD) simulations are a useful tool to assess the conformational stability of a ligand within the binding site. MD simulations were performed on compounds **71**, **76a** (as example of the long-chain MTBc class), colchicine and *N*-deacetyl-10-thiocolchicine in complex with a tubulin α-β dimer. PDB 4O2B[191] (tubulin-colchicine complex) was chosen as the starting structure for MD simulations. This choice was justified by a higher resolution compared to any tubulin-thiocolchicine solved structure.

[191] A. E. Prota, F. Danel, F. Bachmann, K. Bargsten, R. M. Buey, J. Pohlmann, S. Reinelt, H. Lane, M. O. Steinmetz, *J. Mol. Biol.* **2014**, *426*, 1848-1860.

Moreover, colchicine and thiocolchicine are very similar molecules and the conformation of the residues forming the binding site is largely super- imposable. The biological evaluation suggested that ligands interact with tubulin through the *N*-deacetyl-10-thiocolchicine moiety. Accordingly, in the MD starting structures the *N*-deacetyl-10-thiocolchicine nucleus of each ligand was placed into the colchicine binding site, while the pironetin-like part was placed between α-β subunits. A 50 ns MD simulation for each complex was performed and subsequently the root mean square deviation (RMSD) were computed with respect to the staring structure for each ligand after least square fit to protein Cα (Figure 35, left). From these data it resulted that the longer is the linker, the greater is the displacement of the ligands within the binding site. On the other hand, colchicine and *N*-deacetyl-10-thiocolchicine show a low and stationary RMSD trend.

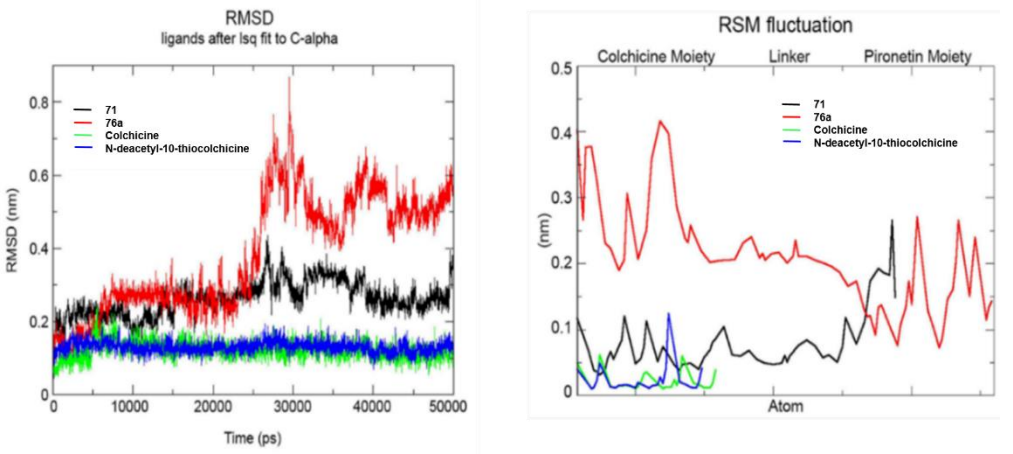

Figure 35. RMSD plot for the ligands. Colchicine and *N*-deacetyl-10-thiocolchicine show a low and stationary RMSD value, while the linker of compounds **71** and **76a** has a negative effect on the conformational stability of the molecules within the binding site (left). RMSF plot for the ligands. The fluctuations are higher for compound **76a**, which has the longest linker (right).

This result was confirmed through a second experiment, in which the root mean square fluctuations (RMSF) for ligands with heavy atoms were considered (Figure 35, right). Also in this case, it's quite clear that the presence of a long spacer (compound **76a**, red line) increases the mobility of the thiocolchicine moiety, while this effect is less marked for **71** (black line), bearing the shorter linker. On the other hand, colchicine and *N*-deacetyl-10- thiocolchicine present the lowest RMSF values, indicating that both of the linker types display a negative impact on the ligands binding mode.

In conclusion, four different bivalent compounds have been efficiently synthesised by linking thiocolchicine nucleus with pironetin-inspired derivatives. One of them presents 10 atoms linker and three of them present 24-atom (C10-N-C2-N-C10) linker. Biological test suggested that the drug conjugates weren't able to exploit the dual interaction and the partially retained activity seemed to depend by the thiocolchicine moiety. Moreover, the chemical nature of the spacers and in particular their intrinsic hydrophobicity, appears to make these conjugates better substrates for P-glycoprotein. These results were confirmed by *a posteriori* MD studies, suggesting that a longer linker has a displacing effect on the thiocolchicine nucleus, resulting in the loss of activity.

Thus, this study demonstrates that the idea to improve tubulin/microtubules targeting by an α,β-bivalent binder seems to be unlikely, due to the required dimension and the tricky relevance of the linker. However, the use of less hydrophobic linkers and of stronger α-tubulin binders could be the first elements that required to be investigated to try to improve the performance of this kind of conjugates.

5.3 Experimental part

General

Unless otherwise stated, reagents and solvents were purchased from Sigma Aldrich, Fluorochem or TCI and used without further purification. All reactions were carried out in oven-dried glassware and dry solvents, under nitrogen atmosphere and were monitored by thin layer chromatography (TLC) on silica gel (Merck precoated 60F254 plates), with detection by UV light (254 nm) or by solutions of potassium permanganate stain or pancaldi solution (molybdatophosphorus acid and Ce(IV)sulphate in 4% sulphuric acid), upon heating.

Flash chromatography was performed using silica gel (240-400 mesh, Merck) as stationary phase.

^{1}H-NMR spectra were recorded on a Bruker Avance Spectrometer (400 MHz) and are reported relative to residual $CDCl_3$ or CD_3OD. ^{13}C-NMR spectra were recorded on the same instruments (100 MHz) and are reported relative to residual $CDCl_3$ or CD_3OD. All 1D and 2D NMR spectra were collected using the standard pulse sequences available with Bruker Topspin 1.3. Chemical shifts (δ) for proton and carbon resonances are quoted in parts per million (ppm) relative to tetramethylsilane (TMS), used as an internal standard. Data for ^{1}H-NMR are reported as follows: chemical shift (δ/ppm) (multiplicity, coupling constant (Hz), integration). Multiplicities are reported as follows: s = singlet, d = doublet, t = triplet, m = multiplet, bs = broad singlet. Data for ^{13}C-NMR are reported in terms of chemical shift (δ/ppm).

Mass spectra were registered exploiting the electrospray ionisation (ESI) technique, on a Q-Tof micro mass spectrometer.

Specific rotation values were measured on a P-1030 Jasco polarimeter, using 1 mL cells, with path length of 10 cm. Measures were collected at 20-25°C, using sodium D line wavelength λ=589 nm.

Melting points were measured on a StuartTM melting point apparatus SMP3.

Synthesis (S)-7-amino-1,2,3-trimethoxy-10-(methylthio)-6,7-dihydrobenzo [a]heptalen-9(5H)-one (69)

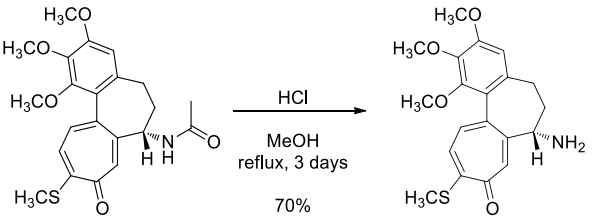

A solution of thiocolchicine (0.500 g, 1.20 mmol) in MeOH (20 mL) and 2 N HC1 (9.5 mL) was heated at 85-90 °C for 3 days. The reaction mixture was neutralised with saturated $NaHCO_3$ solution, extracted with CH_2Cl_2, and washed with brine. The organic layer was dried over Na_2SO_4, filtered and concentrated under reduced pressure. The crude product was purified by flash chromatography (CH_2Cl_2 /MeOH, 9:1) followed by crystallisation from CH_2Cl_2/MeOH, affording **69** (0.320 g, 70%), as yellow solid.

^{1}H NMR (400 MHz, $CDCl_3$) detected signals: δ= 7.56 (s, 1H), 7.17 (d, *J* = 10.4 Hz, 1H), 7.01 (d, *J* = 10.4 Hz, 1H), 6.52 (s, 1H), 3.89 (s, 6H), 3.74 – 3.66 (m, 1H), 3.64 (s, 3H), 2.52 – 2.44 (m, 1H), 2.42 (s, 3H), 2.41– 2.33 (m, 1H), 2.29 (m, 1H), 1.66 – 1.54 (m, 1H).
^{13}C NMR (100 MHz, $CDCl_3$): δ= 182.67, 157.98, 153.91, 153.58, 150.85, 141.30, 138.27, 136.01, 134.25, 129.49, 126.04, 125.64, 107.15, 61.23 (2 CH_3), 56.18, 53.76, 40.45, 30.71, 15.23.
MS (ESI): *m/z* $[M+Na]^+$ calcd for $C_{20}H_{23}NO_4SNa$: 396.1245, found 396.1250.
Melting point: 198°C.
$[\alpha]_D^{25}$: -160.6 (*c*= 0.31, MeOH).

Synthesis of (S)-10-oxo-10-((1,2,3-trimethoxy-10-(methylthio)-9-oxo-5,6,7,9-tetrahydrobenzo[a]heptalen-7-yl)amino)decanoic acid (70)

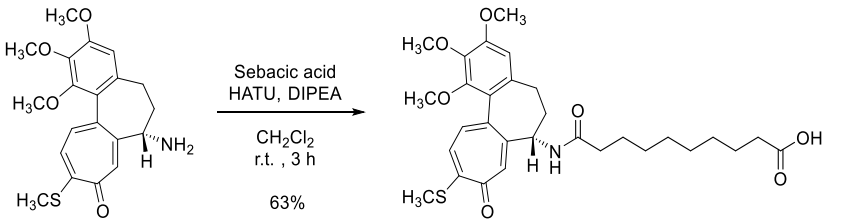

A solution of sebacic acid (0.175 g, 0.87 mmol), HATU (0.165 g, 0.43 mmol) and DIPEA (202 µL, 1.16 mmol) in anhydrous CH_2Cl_2 (3 mL) was stirred at room temperature for 0.5 h, then a solution of **69** (0.108 g, 0.29 mmol) in anhydrous CH_2Cl_2 (1 mL) was added. The reaction mixture was stirred at room temperature for 3 h, then diluted with CH_2Cl_2 (15 mL), washed with water (10 mL), saturated aqueous $NaHCO_3$ solution (10 mL), 1 M HCl (2 × 10 mL) and brine (10 mL). The organic layer was dried over Na_2SO_4, filtered and concentrated under reduced pressure. The crude product was purified by flash chromatography (CH_2Cl_2 /MeOH: 20/1), to afford **70** (0.085 g, 63%) as a yellow amorphous solid.

^{1}H NMR (400 MHz, $CDCl_3$) detected signals: δ=7.61 (s, 1H), 7.37 (d, *J* = 10.5 Hz, 1H), 7.14 (d, *J* = 10.5 Hz, 1H), 7.02 (bs, 1H), 6.54 (s, 1H), 4.76 – 4.65 (m, 1H), 3.94 (s, 3H), 3.91 (s, 3H), 3.65 (s, 3H), 2.52 (dd, *J* = 13.3, 6.0 Hz, 1H), 2.44 (s, 3H), 2.42 – 2.29 (m, 3H), 2.28 – 2.19 (m, 3H), 1.90 (m, 1H), 1.59 (m, 4H), 1.26 (m, 8H).
^{13}C NMR (100 MHz, $CDCl_3$): δ= 182.21, 177.55, 173.42, 158.48, 153.96, 152.97, 151.30, 141.82, 139.64, 135.61, 134.66, 128.67, 127.83, 125.64, 107.67, 61.87, 61.51, 56.26, 52.13, 37.07, 36.43, 34.16, 30.12, 29.03, 28.83, 28.61 (2 CH_2), 25.35, 24.70, 15.31.
MS (ESI): *m/z* $[M+Na]^+$ calcd for $C_{30}H_{39}NO_7SNa$: 580.2339, found 580.2346.
$[\alpha]_D^{25}$: -148.28 (*c*= 0.51, $CHCl_3$).

Synthesis of 10-((S)-2-((R)-2-methoxy-3-((S)-6-oxo-3,6-dihydro-2H-pyran-2-yl) propyl)piperidin-1-yl)-10-oxo-N-((S)-1,2,3-trimethoxy-10-(methylthio)-9-oxo-5,6,7,9 -tetrahydrobenzo[a]heptalen-7-yl)decanamide (71)

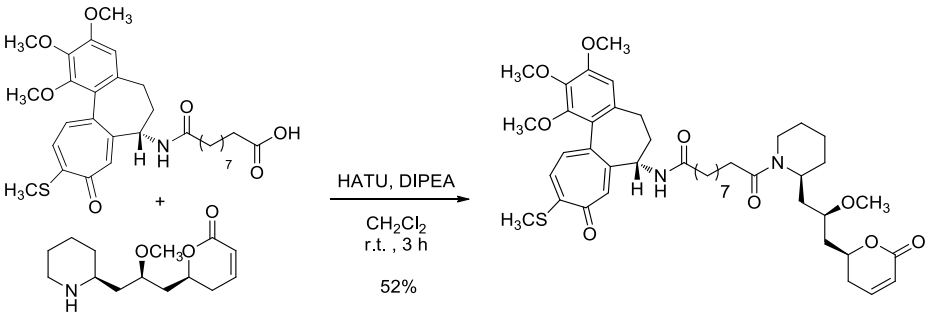

A solution of **70** (0.030 g, 0.06 mmol), HATU (0.037 g, 0.10 mmol) and DIPEA (23 µL, 0.13 mmol) in anhydrous CH_2Cl_2 (1mL) was stirred at room temperature for 0.5 h, then a solution of hybrid compound **60a** (0.020 g, 0.08 mmol), in anhydrous CH_2Cl_2 (1 mL) was added. The solution was stirred for with 5 h, then diluted with CH_2Cl_2 (5 mL), washed water (4 mL), saturated aqueous $NaHCO_3$ solution (4 mL), 1 M HCl (2 × 4 mL) and brine (4 mL). The organic layer was dried over Na_2SO_4, filtered and concentrated under reduced pressure. The crude product was purified by flash chromatography (CH_2Cl_2 /MeOH: 98/2) to afford **71** (0.027 g, 52%) as dark yellow oil.

^{1}H NMR (400 MHz, $CDCl_3$) detected signals: *δ*= 7.46 (s, 1H), H3), 7.40 (d, *J* = 8.7 Hz, 1H), 7.16 (d, *J* = 8.7 Hz, 1H), 6.93-6.90 (m, 1H), 6.56 (s, 1H), 6.06-6.02 (m, 1H'), 4.78-4.51 (m, 2H), 4.18-4.02 (m, 1H'), 3.98 (s, 3H), 3.92 (s, 3H), 3.73-3.68 (m, 1H), 3.67 (s, 3H), 3.39-3.23 (m, 4H), 3.21-3.05 (m, 1H), 2.61-2.52 (m, 1H), 2.47 (s, 3H), 2.42-2.18 (m, 8H), 1.97-1.83 (m, 1H), 1.72-1.51 (m, 8H), 1.48-1.18 (m, 14H).
^{13}C NMR (100 MHz, $CDCl_3$): *δ*= 181.61, 173.05, 172.50, 164.29, 158.51, 153.93, 152.52, 151.35, 145.49, 141.85, 139.33, 135.51, 134.57, 128.43, 127.43, 125.70, 121.50, 107.62, 75.28, 74.86, 61.87, 61.52, 56.79, 56.26, 52.19, 49.70, 41.48, 37.09, 36.71 - 19.37 (15 CH_2), 15.33.
MS (ESI): *m/z* $[M+Na]^+$ calcd. for $C_{44}H_{60}N_2O_9SNa$: 815.3917; found 815.3925.
$[\alpha]_D^{25}$: -115.9 (*c*= 0.46, $CHCl_3$).

Synthesis of (S)-tert-butyl (2-(10-oxo-10-((1,2,3-trimethoxy-10-(methylthio)-9-oxo-5,6,7,9-tetrahydrobenzo[a]heptalen-7-yl)amino)decanamido)ethyl)carbamate (73).

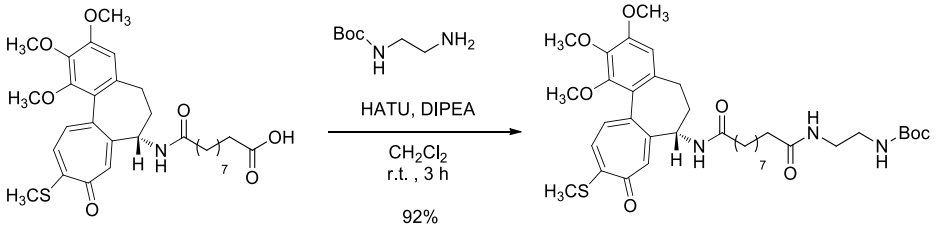

A solution of **70** (0.680 g, 1.22 mmol), HATU (0.695 g, 1.83 mmol) and DIPEA (425 µL, 2.44 mmol) in anhydrous CH_2Cl_2 (20 mL) was stirred at room temperature for 0.5 h, then a solution of *tert*-butyl (2-aminoethyl)carbamate **72** (0.254 g, 1.58 mmol) in anhydrous CH_2Cl_2 (10 mL) was added. The mixture was stirred at room temperature for 3 h, then diluted with CH_2Cl_2 (50 mL) and washed with water (2 × 20 mL), saturated aqueous $NaHCO_3$ solution (3 × 20 mL), 1N HCl (3 × 20 mL) and brine (2 × 20 mL). The organic layer was dried over Na_2SO_4, filtered and concentrated under reduced pressure. The crude product was purified by gradient flash chromatography (CH_2Cl_2 /MeOH : 50/1 to 20/1) to afford **73** (0.789 g, 92%) as a yellow solid.

^{1}H NMR (400 MHz, $CDCl_3$): δ= 7.71 (bs, 1H), 7.66 (bs, 1H), 7.32 (d, *J* = 10.5 Hz, 1H), 7.27 (s, 1H), 7.07 (d, *J* = 10.5 Hz, 1H), 6.93 (bs, 1H), 6.53 (s, 1H), 4.70 – 4.58 (m, 1H), 3.93 (s, 3H), 3.90 (s, 3H), 3.67 (s, 3H), 3.46 (m, 2H), 3.27 (m, 2H), 2.53 (dd, *J* = 13.3, 6.1 Hz, 1H), 2.43 (s, 3H), 2.38 (dd, *J* = 13.3, 6.1 Hz, 1H), 2.34 – 2.14 (m, 5H), 1.88 (m ,1H), 1.65 – 1.46 (m, 4H), 1.43 (s, 9H), 1.36 – 1.11 (m, 8H).
^{13}C NMR (100 MHz, $CDCl_3$) detected signals: δ=182.49, 174.51, 173.07, 158.30, 153.82, 151.61, 151.41, 141.90, 138.57, 134.91, 134.50, 128.57, 126.75, 125.89, 107.60, 61.88, 61.52, 56.27, 52.21, 40.95 (2 CH_2), 37.36, 36.84, 36.38, 36.26, 30.13, 29.13 (superimposition of CH_2), 28.53, 25.69 (superimposition of CH_2), 15.25.
MS (ESI) *m/z* $[M+Na]^+$ calcd. For $C_{37}H_{53}N_3O_8SNa^+$: 722.3451; found 722.3459
$[\alpha]_D^{25}$: -156.36 (*c*= 0.55, $CHCl_3$).
Melting point: 66-70 °C.

Synthesis of (S)-N^1-(2-aminoethyl)-N^{10}-(1,2,3-trimethoxy-10-(methylthio)-9-oxo-5,6,7,9-tetrahydrobenzo[a]heptalen-7-yl)decanediamide (74).

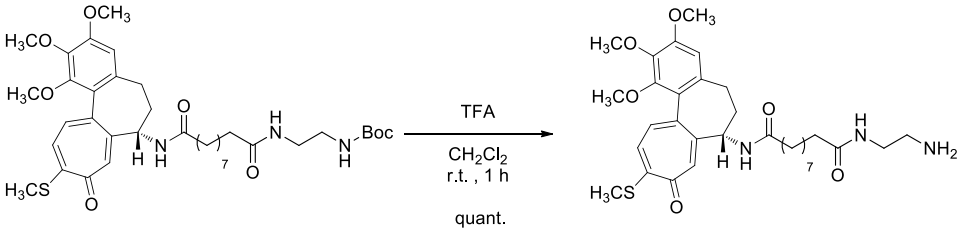

Trifluoroacetic acid (0.37 mL, 4.84 mmol) was added to a solution of **73** (0.678 g, 0.97 mmol) in CH_2Cl_2 (7 mL), cooled at 0°C. The reaction mixture was allowed to warm to room temperature and then stirred for 1 h. The solvent was removed under reduced pressure, then the residue was dissolved in CH_2Cl_2 (50 mL) and washed with saturated aqueous solution of $NaHCO_3$ (2 × 30 mL) and brine (2 × 30 mL). The organic layer was dried over Na_2SO_4, filtered and concentrated under reduced pressure. The obtained yellow solid **74** (0.570 g, quant.) didn't required further purification.

^{1}H NMR (400 MHz, $CDCl_3$) detected signals: δ=7.31-7.28 (m, 2H), 7.06 (d, *J*= 10.7 Hz, 1H), 6.70 (bs, 1H), 6.53 (s, 1H), 4.67 (m, 1H), 3.93 (s, 3H), 3.89 (s, 3H), 3.66 (s, 3H), 3.33 (m, 2H), 2.84 (m, 2H), 2.62 – 2.47 (m, 1H), 2.43 (s, 3H), 2.39-2.10 (m, 6H), 1.85 (m, 1H), 1.70-1.49 (m, 4H), 1.33-1.15 (s, 8H).
^{13}C NMR (100 MHz, $CDCl_3$): δ=182.49, 174.13, 173.04, 158.23, 153.78, 151.61, 151.36, 141.84, 138.58, 134.86, 134.47, 128.61, 126.76, 125.84, 107.55, 61.82, 61.51, 56.25, 52.08, 41.97, 41.53, 36.57, 36.47 (2 CH_2), 30.10, 29.16, 29.03, 28.90, 28.80, 25.66 (2 CH2), 15.26.
MS (ESI) *m/z* $[M+Na]^+$ calcd for $C_{32}H_{45}N_3O_6SNa$: 622.2927; found 622.2932.
$[\alpha]_D^{25}$: -164.73 (*c*= 0.61, $CHCl_3$).
Melting point: 108-112 °C.

Synthesis of (S)-10-oxo-10-((2-(10-oxo-10-((1,2,3-trimethoxy-10-(methylthio)-9-oxo-5,6,7,9-tetrahydrobenzo[a]heptalen-7-yl)amino)decanamido)ethyl)amino)decanoic acid (75).

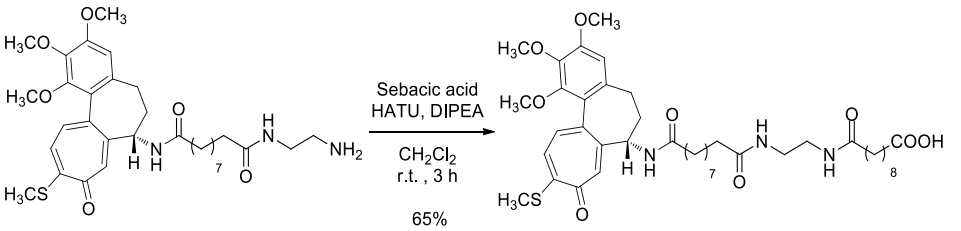

A solution of sebacic acid (0.433 g, 2.14 mmol), HATU (0.407 g, 1.07 mmol) and DIPEA (497 µL, 2.85 mmol) in anhydrous CH_2Cl_2 (20 mL) was stirred at room temperature for 0.5 h, then a solution of **74** (0.428 g, 0.71 mmol) in anhydrous CH_2Cl_2 (10 mL) was added. The reaction mixture was stirred at room temperature for 3 h, then diluted with CH_2Cl_2 (30 mL), washed with water (2 × 20 mL) and brine (20 mL). The organic layer was dried over Na_2SO_4, filtered and concentrated under reduced pressure. The crude product was purified by gradient flash chromatography (CH_2Cl_2 / MeOH : 50/1 to 5/1), to afford **75** (0.420 g, 65%) as yellow solid.

^{1}H NMR (400 MHz, $CDCl_3$): δ= 10.97 (bs, 1H), 7.80 (bs, 1H), 7.70 (bs, 1H), 7.44 (s, 1H), 7.31 (d, *J* = 10.6 Hz, 1H), 7.13 (bs, 1H), 7.08 (d, *J* = 10.6 Hz, 1H), 6.52 (s, 1H), 4.70 – 4.55 (m, 1H), 3.91 (s, 3H), 3.88 (s, 3H), 3.65 (s, 3H), 3.57-3.37 (m, 2H), 3.35 – 3.13 (m, 2H), 2.52 (m, 1H), 2.41 (s, 3H), 2.37 (m, 1H), 2.34 – 2.15 (m, 9H) 2.04-1.88 (m,1H), 1.73 – 1.37 (m, 8H), 1.32-1.20 (m, 16H,).
^{13}C NMR (100 MHz, $CDCl_3$): δ=182.60, 176.65, 175.42, 174.83, 173.56, 158.15, 15.75, 152.48, 151.22, 141.67, 139.01, 135.01, 134.61, 128.68, 127.13, 125.72, 107.52, 61.82, 61.48, 56.20, 52.17, 40.22, 39.33, 36.66, 36.16 -24.84 (17 CH_2), 15.23.
MS (ESI) *m/z* $[M+Na]^+$ calcd. for $C_{42}H_{61}N_3O_9SNa$: 806.4026; found 806.4033
$[\alpha]_D^{25}$: -142.16 (*c*= 0.70, $CHCl_3$).
Melting point: 65-69 °C.

General Procedure for the synthesis of 76a-c

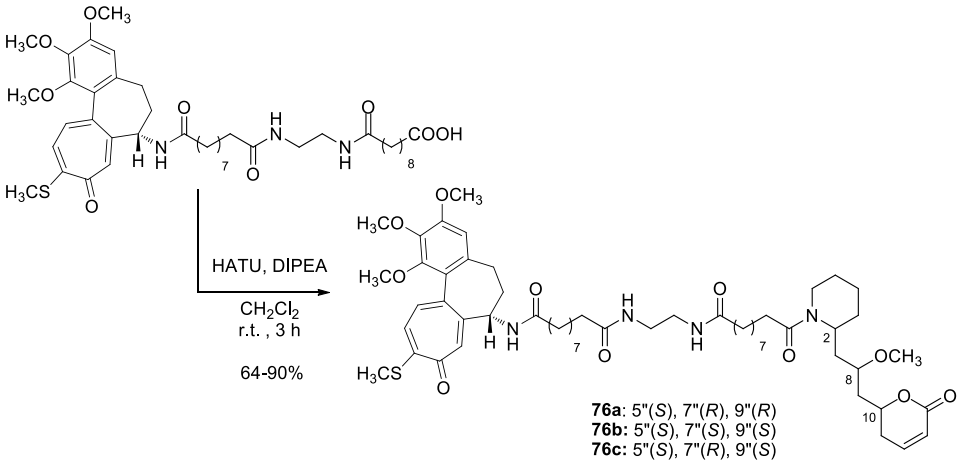

A solution of **75** (0.043 g, 0.06 mmol), HATU (0.031 g, 0.08 mmol) and DIPEA (190 µL, 0.11 mmol) in anhydrous CH_2Cl_2 (2 mL) was stirred at room temperature for 0.5 h, then a solution of hybrid **60** (0.017 g, 0.07 mmol) in anhydrous CH_2Cl_2 (2 mL) was added. The mixture was stirred at room temperature for 3 h, then diluted with CH_2Cl_2 (30 mL), washed with water (20 mL), saturated aqueous solution of $NaHCO_3$ (3 × 20 mL), 0.5 N HCl (3 × 20 mL) and brine (20 mL). The organic layer was dried over Na_2SO_4, filtered and concentrated under reduced pressure. The crude product was purified by gradient flash chromatography (CH_2Cl_2 / MeOH : 50/1 to 20/1 for all the compounds **76a-c**), to afford product **76**.

N^1-(2-(10-((S)-2-((R)-2-methoxy-3-((R)-6-oxo-3,6-dihydro-2H-pyran-2-yl)propyl) piperidin-1-yl)-10-oxodecanamido)ethyl)-N^{10}-((S)-1,2,3-trimethoxy-10-(methylthio) -9-oxo-5,6,7,9-tetrahydrobenzo[a]heptalen-7-yl)decanediamide 76a

Yield: 90%.

^{1}H NMR (400 MHz, $CDCl_3$) δ 7.54 (m, 1H), 7.48 (m, 1H), 7.31 (d, *J* = 10.4 Hz, 1H), 7.27 (s, 1H), 7.07 (d, *J* = 10.4 Hz, 1H), 6.88 (m, 1H), 6.74 (s, 1H), 6.54 (s, 1H), 6.02 (m, 1H), 5.07 –4.88 (m, 1H), 4.71 – 4.60 (m, 1H), 4.60 – 4.51 (m, 1H), 3.93 (s, 3H), 3.90 (s, 3H), 3.67 (s, 3H), 3.65 – 3.60 (m, 2H), 3.60 – 3.48 (m, 1H), 3.35-3-25 (m, 5H), 3.20 – 3.08 (m, 2H), 2.53 (m, 1H), 2.43 (s, 3H), 2.42 – 2.14 (m, 12H), 2.02 (m, 1H), 1.91-1.17 (34H).
^{13}C NMR (100 MHz, $CDCl_3$) δ 182.54, 175.41, 174.51, 173.27, 172.02, 158.20, 153.79, 152.01, 151.39, 145.44, 141 .88, 138.70, 134.90, 134.53, 128.54, 127.03, 125.91, 121.61, 107.57, 74.83, 73.85, 61.89, 61.53, 56.28 (2 CH_3), 52.35, 45.55, 41.30 - 19.43 (27 CH_2), 15.26.

MS (ESI) *m/z* $[M+Na]^+$ calcd. for $C_{56}H_{82}N_4O_{11}SNa$: 1041.5598; found 1041.5606.
$[\alpha]_D^{25}$: -108.95 (*c*= 0.61, $CHCl_3$).
Melting point: 40-44 °C.

N^1-(2-(10-((S)-2-((S)-2-methoxy-3-((S)-6-oxo-3,6-dihydro-2H-pyran-2-yl)propyl) piperidin-1-yl)-10-oxodecanamido)ethyl)-N^{10}-((S)-1,2,3-trimethoxy-10-(methylthio) -9-oxo-5,6,7,9-tetrahydrobenzo[a]heptalen-7-yl)decanediamide (76b).

Yield: 77%.
^{1}H NMR (400 MHz, $CDCl_3$): δ= 7.64 (bs, 1H), 7.50 (bs, 1H), 7.27 – 7.25 (m, 2H), 7.03 (d, *J* = 10.5 Hz, 1H), 6.88 (s, 1H), 6.82 (bs, 1H), 6.50 (s, 1H), 5.95 (m, 1H), 4.89 (m, 1H), 4.68 – 4.54 (m, 2H), 3.89 (s, 3H), 3.86 (s, 3H), 3.62 (s, 3H), 3.60 – 3.54 (m, 2H), 3.50 – 3.45 (m, 1H), 3.42 -3.25 (m, 5H), 3.34 – 3.20 (m, 1H), 3.20 – 3.11 (m, 1H), 2.62 – 2.45 (m, 1H), 2.39 (s, 3H), 2.34 -2.15 (m, 12H), 2.22 – 2.10 (m, 1H), 1.79 -1.13 (m, 34H).
^{13}C NMR (100 MHz, $CDCl_3$): δ=182.50, 175.21, 174.52, 173.27, 171.85, 158.16, 153.75, 152.07, 151.33, 145.31, 141.81, 138.73, 134.84, 134.54, 128.60, 126.77, 125.88, 121.50, 107.55, 74.91, 74.35, 61.83, 61.47, 56.91, 56.24, 52.25, 44.45, 41.34 -19.24 (27 CH_2), 15.22. **MS (ESI)** *m/z* $[M+Na]^+$ calcd for $C_{56}H_{82}N_4O_{11}SNa$: 1041.5598; found 1041.5601.
$[\alpha]_D^{25}$: -112.29 (*c*= 0.58, $CHCl_3$).
Melting point: 57-61 °C.

N^1-(2-(10-((S)-2-((R)-2-methoxy-3-((S)-6-oxo-3,6-dihydro-2H-pyran-2-yl)propyl) piperidin-1-yl)-10-oxodecanamido)ethyl)-N^{10}-((S)-1,2,3-trimethoxy-10-(methylthio) -9-oxo-5,6,7,9-tetrahydrobenzo[a]heptalen-7-yl)decanediamide (76c)

Yield: 64%
^{1}H NMR (400 MHz, $CDCl_3$): δ= 7.55 (bs, 1H), 7.48 (bs, 1H), 7.33 (d, *J* = 10.6 Hz, 1H), 7.30 (s, 1H), 7.08 (d, *J* = 10.6 Hz, 1H), 6.94 – 6.84 (m, 1H), 6.76 (bs, 1H), 6.54 (s, 1H), 6.01 (m, 1H), 4.86 (m, 1H), 4.63 – 4.56 (m, 2H), 3.93 (s, 3H), 3.90 (s, 3H), 3.67 (s, 3H), 3.66 – 3.64 (m, 2H), 3.51 (m, 1H), 3.46 – 3.26 (m, 5H), 3.16 (m, 1H), 3.07 (m, 1H), 2.59 – 2.47 (m, 1H), 2.43 (s, 3H), 2.39– 2.18 (m, 12H), 1.99 (m, 1H), 1.97 – 1.16 (m, 34H).
^{13}C NMR (100 MHz, $CDCl_3$): δ= 182.43, 175.42, 174.53, 173.28, 158.22, 153.81, 152.18, 151.37, 145.47, 141.86, 138.83, 134.99, 134.55, 128.51, 126.89, 125.88, 121.64, 107.57, 75.02, 74.68, 61.89, 61.52, 57.82, 56.27, 52.36, 45.10, 41.44 – 19.21 (27 CH_2), 15.27.
MS (ESI) *m/z* $[M+Na]^+$ calcd. for $C_{56}H_{82}N_4O_{11}SNa$: 1041.5598; found 1041.5604.

$[\alpha]_D^{25}$: -90.51 (*c*= 0.64, $CHCl_3$).
Melting point: 63-67 °C.

6. Novel Approaches for the Chemoenzymatic Generation and Isolation of ‘Unnatural’ Polyethers

6.1 Introduction

The work reported in this chapter was performed during a period of six months spent at the University of Warwick (UK), in the laboratory of Professor Manuela Tosin.
The project was aimed at the chemoenzymatic generation of "unnatural" and "diversified" versions of polyketides such as lasalocid A and salinomycin; these are polyether ionophores that recently emerged as potential anticancer agents, targeting different signalling pathways such as K-ras and Hedgehog.[192,193]
The fundamental difference with the general approach presented in this thesis is the way through which the diversity is achieved. In this case, natural products derivatives are not synthesised by a chemist, but by a microorganism, forcing it to produce modified versions of the natural products that it physiologically biosynthesises, exploiting methodologies that will be explained in the following paragraphs. For this reason, the microorganism could be considered as a sort of "cell factory".
This approach presents an evident advantage: it exploits the ability of the microorganism to synthesise compounds characterised by highly complex structures and by a defined stereochemistry, in a way that could be almost impossible for a chemist. As a sort of demonstration, it's enough to observe the structures of lasalocid A and salinomycin, that were the focus of this project (Figure 36).

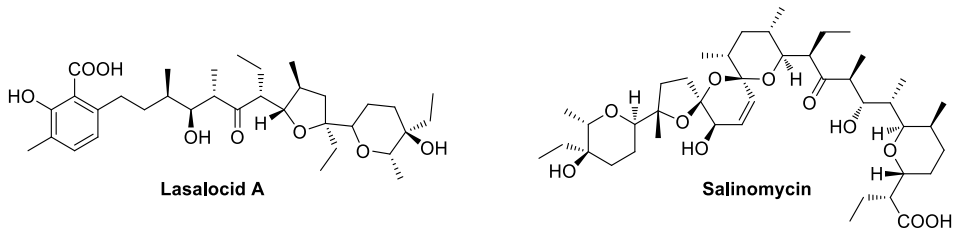

Figure 36. Structures of the principal polyether ionophores that were investigated in this chapter.

However, before getting into the details of this work, a brief overview about the crucial aspects of polyketides biosynthesis and about the methods to force microorganisms to produce unnatural products, will be given.

[192] A. K. Najumudeen, A. Jaiswal, B. Lectez, C. Oetken-Lindholm, C. Guzmán, E. Siljamäki, I. M. D. Posada, E. Lacey, T. Aittokallio, D. Abankwa, *Oncogene* **2016**, *35*, 5248–5262.
[193] J. Dewangan, S. Srivastava, S. K. Rath, *Tumor Biol.* **2017**, *39*, 1-12.

6.1.1 Polyketides Biosynthesis

Polyketides are a large family of natural products comprising macrolides, polyphenols, polyenes and polyethers. They are widespread in nature, being found as secondary metabolites in plants, fungi, bacteria and some marine organisms. Although their specific functions in the natural source have not been completely elucidated, in general they seem to play different roles, participating to defense mechanisms or acting as virulence factors or constituting pigments.
More importantly, polyketides are well-known for their great pharmacological potential. In fact, this class of natural products contains antibiotics, immunosuppressants, anticancer and cholesterol-lowering compounds.[194] Some examples are reported in Figure 37.

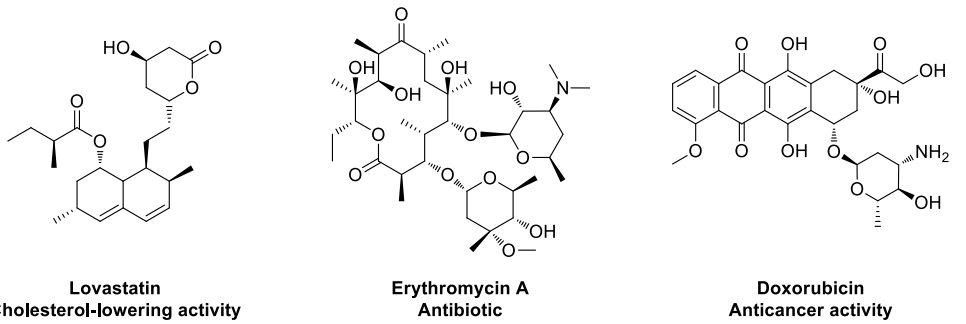

Figure 37. structure differences between three key members of polyketide family.

Despite their apparent structural diversity, polyketides are biosynthesised through a common mechanism involving a sequence of decarboxylative Claisen condensation steps that take place between acyl carrier protein (ACP) bound-malonyl units and ketosynthase (KS)-bound acyl intermediates; this chemistry is carried out by complex multifunctional enzymes called polyketide synthases (PKSs). The mechanism of carbon chain formation in polyketide (PK) formation is very similar to that of fatty acid (FA) biosynthesis, as shown in Figure 38. For this reason, PKSs are classified with a similar nomenclature to that of fatty acid synthases.

[194] C. Hertweck, *Angew. Chemie - Int. Ed.* **2009**, *48*, 4688–4716.

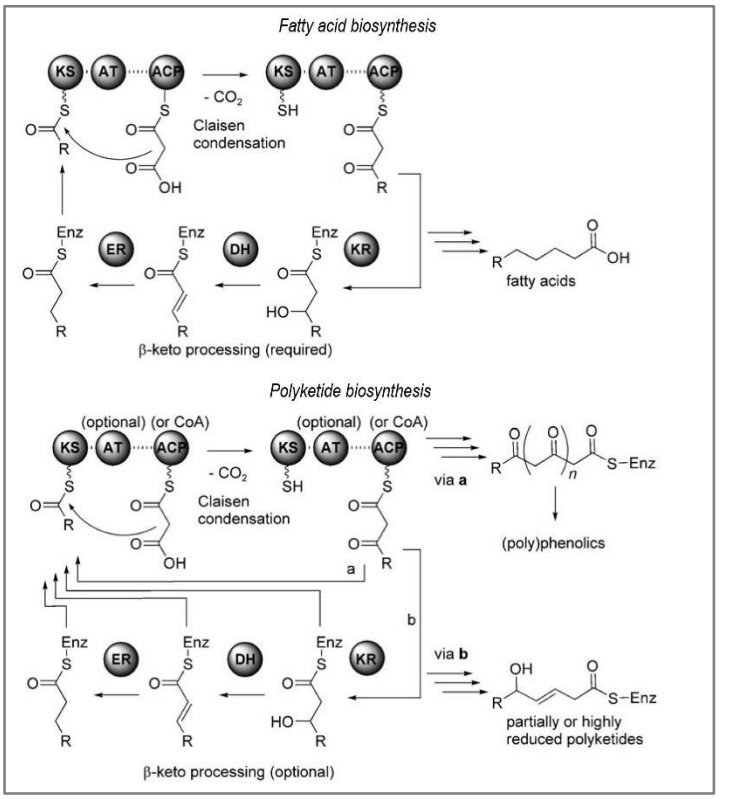

Figure 38. Comparison between fatty acids and polyketides biosynthesis. Adapted from ref 194, with the permission from Wiley -VCH Verlag GmbH & Co. Copyright 2009.

Both PK and FA biosynthetic pathways present also similar enzymatic domains and share the same building blocks, such as acetyl- coenzyme A (CoA) and malonyl-CoA (MCoA).

As well as a β-ketoacylsynthase (KS) domains, other key domains include: an acyl transferase domain (AT), which transfer the acetyl-CoA starter unit to a cysteine thiol of KS, and a phosphopantetheinylated acyl carrier protein (ACP) that acts as the mediator of carbon chain extension and modification by shuttling malonyl units and intermediates to and from different catalytic domains in the form of thioesters. The KS, AT and ACP domains are the minimal requirements to constitute a so-called "module" (Fig. 4), which is responsible for at least one round of Claisen condensation. However, additional domains are present, and are responsible of the carbon chain tailoring through a process known as "β-keto processing". In fact, after Claisen condensation, the carbon chain can undergo a sequence of:

- ✓ ketoreduction (KR), in which the carbonyl group of the elongating chain is reduced to the corresponding hydroxyl group;
- ✓ dehydration (DH), leading to the formation of an α,β-unsaturated thioester;
- ✓ enoyl reduction (ER), reducing selectively the double bond.

PKSs mediated biosynthesis involved several modules, each of them constituted by the aforementioned domains.
The global result of this process is the elongation of the carbon chain of two carbon atoms, for every Claisen condensation cycle.[194,195]
The described process is mandatory in fatty acid biosynthesis and leads to the formation of a fully saturated acyl backbone, while it's somehow optional in the case of PKSs. In fact, the major difference between the two biosynthetic pathways is that in PKSs some steps can be omitted before the subsequent Claisen condensation. For example, the omission of a dehydration step, will result in the propagation of a hydroxyl moiety in the growing carbon chain. It's evident that these deviations from the "classical" fatty acids biosynthetic mechanism are responsible of the great structural diversity found in polyketides family. When the carbon chain reaches the proper length, it is released from the PKS enzyme (generally through a thioester hydrolysis) and then is further modified by post-PKS enzymes.[196]
On the basis of the mechanisms and enzyme architectures involved in the biosynthesis, PKSs can be classified in different ways.
A first distinction is between 'iterative' and 'modular' PKSs.
Iterative PKSs are typical of fungi and are usually single-module proteins, constituted by the proper set of domains. For them, the single module is able to catalyze multiple rounds of Claisen condensation - β-keto processing sequences, originating the entire polyketide backbone.[197]
On the other hand, modular or non-iterative PKSs are composed by several modules and the KS domain of each module is responsible of only one elongation cycle. Thus, to build a certain polyketide chain, it's required that the number of modules correspond to the number of required elongation steps.
A second classification is based on the different architecture in which the catalytic domains are arranged. On this basis, three different families are identified and named

[195] Y. A. Chan, A. M. Podevels, B. M. Kevany, M. G. Thomas, *Nat. Prod. Rep.* **2009**, *26*, 90–114.
[196] C. Olano, C. Méndez, J. A. Salas, *Nat. Prod. Rep.* **2010**, *27*, 571–616.
[197] H. Chen, L. Du, *Appl Microbiol Biotechnol*. **2016**, *100*, 541–557.

in analogy with fatty acids synthases classification: PKSs I, PKSs II and PKSs III. A brief description of each family will follow.[198]

Type I PKSs.

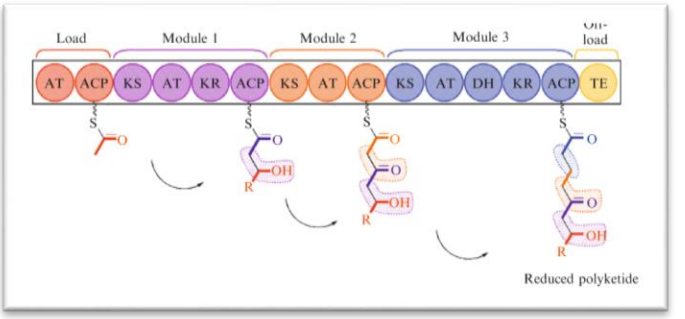

Figure 39. Schematic representation of a type I modular PKS. Adapted from ref 198, Copyright 2009, with permission from Elsevier.

Type I PKSs are the most complex of the three classes. They are multi-functional polypeptides, composed by several modules that incorporate a set of catalytic domains, as presented in Figure 39. PKSs I can be either modular or iterative.

The first modular PKS to be discovered was the 6-deoxyerythronolide B synthase DEBS in the soil bacterium *Saccharopolyspora erythraea*, responsible of erythromycin A biosynthesis. Nowadays DEBS is one of the most studied and has become a model to illustrate how type I PKS enzymes work.[199,200] As in several other modular PKSs, the biosynthesis of erythromycin A displays a perfect co-linearity between the number of active modules and the required elongating steps, as reported in Figure 40.

DEBS is constituted by three main subunits, called DEBS 1, DEBS 2 and DEBS 3, each one including multiple modules. The first module is responsible of the beginning of the bioassembly, through the loading of a propionyl-CoA starter unit. The other modules (1 – 6) participate to the polyketide chain elongation, employing six (2*S*)-methylmalonyl Coenzyme A extender units, while the last thioesterase domain (TE) is responsible for the cyclisation and release of the 6-deoxyerythronolide B scaffold from the PKS. The action of post-PKS enzymes ultimately converts -deoxyerythronolide B into erythromycin A.

[198] K. J. Weissman, *Methods Enzymol.* **2009**, *459*, 3–16.
[199] H. Zhang, J. Wu, K. Skalina, B. A. Pfeifer, *Chem. Biol.* **2010,** *17,* 1232–1240.
[200] K. J. Weissman, *Nat. Prod. Rep.* **2016**, *33*, 203–230.

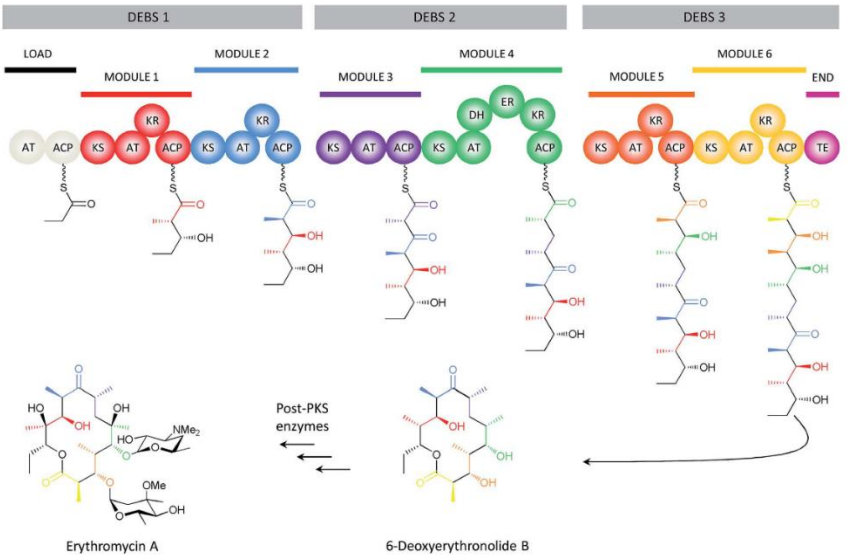

Figure 40. Bioassembly of erythromycin A by the DEBS polyketide synthase (type I modular). Adapted from ref 200, with the permission of Royal Society of Chemistry, copyright 2016.

The same core domains of modular type I PKSs are exploited by iterative PKSs I, but in this case only a single module is present and it is used by the PKS for several elongating cycles, originating the entire polyketide backbone.

Cholesterol-lowering agent lovastatin is an example of polyketide molecule biosynthesised by this type of PKS. In this case, a starter unit of acetyl-CoA reacts with eight extender units of malonyl CoA and *S*-adenosylmethionine (SAM), giving the key intermediate dihydromonacolin L, which is converted in lovastatin through post-PKS modifications (Figure 41).

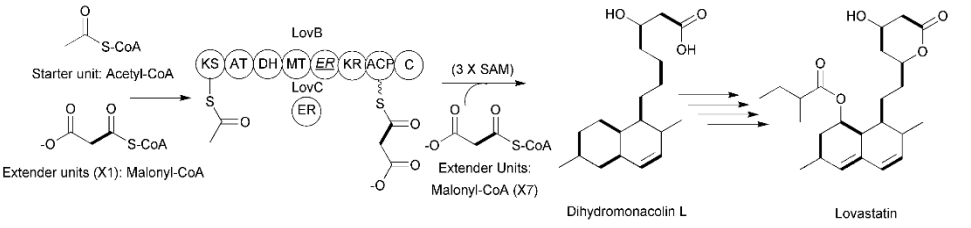

Figure 41. Biosynthesis of lovastatin by a type I iterative PKS. Adapted from ref 195, with the permission of Royal Society of Chemistry, copyright 2009.

Although iterative PKSs I are typical of fungi, they have been recently found in several bacteria.[195] In addition, these type of enzymes are responsible of the biosynthesis of long-chain polyunsaturated fatty acids, found in some marine microbes. This is really interesting, considering that iterative PKSs I were believed to be present only in terrestrial eukaryotes.[198] Nevertheless, it is necessary to stress out that the assembly mechanism of these particular marine PKSs is quite different compared with fungal iterative PKS I.

Type II PKSs.

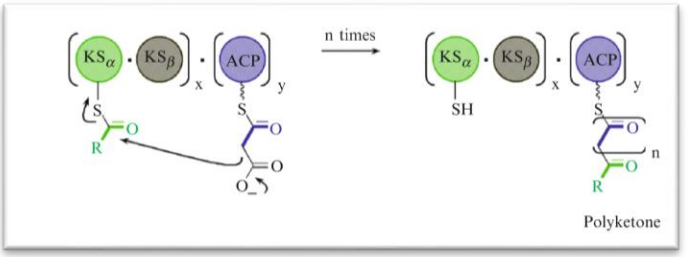

Figure 42. Schematic representation of a type II PKS. Adapted from ref 198, Copyright 2009, with permission from Elsevier.

Type II PKSs are iterative discrete enzymes, composed essentially by three types of domains, associated to form an active complex. The involved domains are a KSα, a KSβ and an ACP, as reported in Figure 42, which constitute a 'minimal' PKS This complex catalyses several extension cycles, to reach the proper chain length.
The KS condensing enzymes are responsible of the chain initiation process, mostly involving an acetate moiety; then, chain elongation with malonyl extender units takes place with the intermediates all covalently attached to the ACP as thioesters. The activity of the minimal PKS is sided by the action of additional domains, such as cyclases, ketoreductases, oxygenases and aromatases, that are responsible of the tailoring of the nascent polyketide into the final natural product structure. Polyketides that are originated from type II PKSs usually present aromatic and polyphenolic structures. Despite huge efforts, the exact mode of action of several PKSs II still remains not elucidated, considering that the interdependence between the different domains makes the attempts of study really challenging.[198]

Type III PKSs.

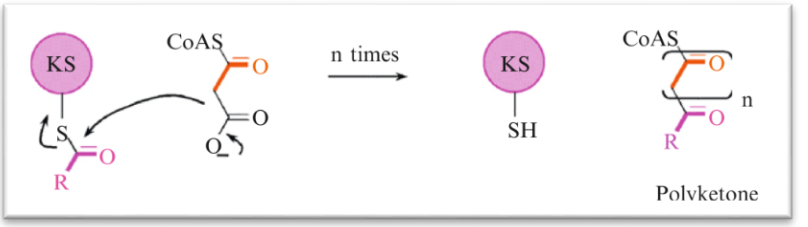

Figure 43. Schematic representation of a type III PKS. Adapted from ref 198, Copyright 2009, with permission from Elsevier.

Type III PKSs are quite diffused in nature, being found in bacteria, plants and fungi. They are known also as chalcone synthases, being involved in the biosynthesis of natural products bearing this type of scaffold; they are iterative enzymes and are typically responsible of the bioassembly of small cyclic aromatic compounds.
In comparison with type I and type II, type III PKSs appear to be quite simple, being composed by a single KS domain that is responsible of the repeated condensation of acetate units on an acyl- CoA starting moiety (Figure 43). In addition to the common chain elongation process, other reactions occur in the same PKS active site, including aromatisation and cyclisation of the growing linear chain. The possibility of using different acyl-CoA starting units, the modulation of the number of elongation steps, as well as modifications induced by downstream enzymes, generate an impressive structural diversity of the natural products synthesised by type III PKSs. Moreover, the structural simplicity of these enzymes has provided good insights into their mode of action, as evidence by X-ray protein crystallographic data.

6.1.2 Polyether ionophores: lasalocid A and salinomycin

Polyether ionophores are an important class of natural products that display potent antibiotic activity.[201,202] The first two members of this family to be discovered were nigericin and lasalocid A, isolated in the 50s, from two different *Streptomyces* strains. Nowadays, this family includes more than 120 members, biosynthesised by almost 50 microorganisms, belonging majorly to three different genera: *Streptomyces, Dactylosporangium* and *Actinomadura*. Notably, *Streptomyces* are the main carboxyl ionophores producers, and almost a half of the known members of this family are biosynthesised by two strains: *Streptomyces albus* and *Streptomyces hygroscopicus*.
The term "ionophore" indicates the ability of a molecule to bind a metal ion, forming lipo-soluble complexes able to cross cellular membranes, transporting the metal ions inside or outside the cell.
Naturally occurring polyether ionophores possess a marked affinity for Na^+ and K^+ cations, with the exception of lasalocid, that prefers to interact with Mg^{2+} and Ca^{2+}, forming dimers and divalent complexes. The ability to interact with these cations arises from the intrinsic structure of polyether ionophores that includes several coordinating sites, such as carboxylic, carbonyl and hydroxyl groups. In addition to the aforementioned lasalocid A and salinomycin, other well-known members of this family are narasin, monesin A, maduramycin and lysocellin. Their structures are reported in Figure 44.

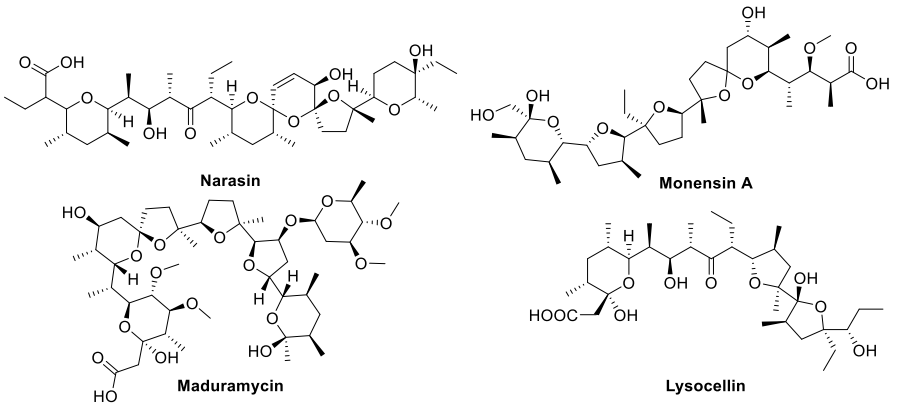

Figure 44. Structures of some important polyethers, in addition to lasalocid A and salinomycin, whose structures are reported in Figure 36.

[201] C. J. Dutton, B. J. Banks, C. B. Cooper, *Nat. Prod. Rep.* **1995**, *12*, 165-181.
[202] J. Rutkowski, B. Brzezinski, *Biomed Res. Int.* **2013**, *2013*, 1–31.

From a biological point of view, polyether ionophores display a wide range of pharmacological activities. They are well-known antibiotics, active in particular against Gram-positive bacteria, including *S. aureus* and *S. epidermidis* strains that have developed drug resistance against other antibiotics. They possess also antifungal, antimalarial, antiparasitic, anti-inflammatory, antiviral and anticancer properties.[203,204]

This impressive set of pharmacological activities arises from the ability of these compounds to travel across cellular membranes, in complex with metal cations. This leads to an alteration of the cellular membranes permeability towards cationic species, that results in the perturbation of the intracellular cation balance. [205,206]

Ion concentration gradients are essential for the maintenance of cellular functions. For example, in several healthy cells, the intracellular concentration of K^+ should be higher than that of Na^+, and the situation should be reverse in the extracellular environment, originating the gradient. Modifications of these gradients could have deleterious effects on the cell, inducing even apoptosis, and this is the paradigm on which the biological properties of polyether ionophores are based.

On the basis of the mechanism of action, polyether antibiotics can be classified into three groups.[205]

- ✓ Group 1. Includes polyethers that bind the cation in an internal cavity, masking its charge. Then, thanks to their lipophilic nature, polyethers cross the cellular membrane, carrying the cation with themselves. In general, they are carboxylic compounds. Some examples include salinomycin, lasalocid A and nigericin.
- ✓ Group 2. Constituted by neutral ionophores, such as valinomycin and nonactin, able to promote the diffusion of cations through the membranes according to the membrane potential, acting as cations carriers.
- ✓ Group 3. This group is composed by the so called "quasi-ionophores". These compounds form transmembrane hydrophilic channels, through which metal cations can easily cross the cellular membranes. Examples are alamethicin C and Gramicidin S.

[203] A. Huczyński, *Bioorganic Med. Chem. Lett.* **2012**, *22*, 7002–7010.
[204] D. A. Kevin, D. A. Meujo, T. H. Mark, *Expert Opin. Drug Discov.* **2016**, *4*, 109–146.
[205] B. C. Pressman, M. Fahim, *Annu Rev Pharmacol Toxicol.* **1982**, *22*, 465–90.
[206] J. W. Westley, Polyether Antibiotics: Naturally Occurring Acid Ionophores, Edition. Marcel Dekker Inc; New York: **1982**, 1.

Nowadays, some polyether ionophores are marketed as coccidiostats for animal farming, taking advantage of the possibility of producing them at industrial level through predictable fermentation processes, exploiting cheap microorganisms. Examples of polyethers that reached the market as coccidiostats are monensin, lasalocid, salinomycin, narasin, maduramycin and semduramycin.
As already mentioned, lasalocid A and salinomycin appear to possess interesting anticancer properties, that attracted our attention. Thus, accordingly to the importance that they had in the project described in this chapter, their biosynthesis will be discussed more in detail in the next paragraphs.

Lasalocid A

Lasalocid A (structure reported in Figure 36) is a polyether ionophore characterised by a potent antibiotic activity. On this basis, it is used coccidiostat under the trade names of Avatec and Bovatec. These drugs are used as additives in chickens, turkeys and cattle feed. More recently, additional pharmacological properties, such as antischistosomiasis and antimalarial have emerged. [207]
In contrast with other ionophores, lasalocid A displays a preferential interaction with divalent cations, such as Mg^{2+} and Ca^{2+}, and its structure presents an aromatic ring. This feature is quite atypical: in fact, lasalocid A is produced by *Streptomyces lasaliensis*, and its biosynthesis is mediated by a type I modular PKS, that usually doesn't generate aromatic products.
The biosynthesis of this polyether has been subject of debate in the scientific community, in particular for what concern the formation of the cyclic ethers.
Scientists agree that the PKS that produces lasalocid A is composed by a loading module and eleven extension modules, for a total of twelve modules that originate a linear dodecaketide chain. The elongating process involves the addition of five malonyl-CoA, four methylmalonyl-CoA and three ethylmalonyl-CoA units, as appreciable in the biosynthetic scheme reported in Figure 45. [208,209]

[207] M.-H. Abdulla, D. S. Ruelas, B. Wolff, J. Snedecor, K.-C. Lim, F. Xu, A. R. Renslo, J. Williams, J. H. McKerrow, C. R. Caffrey, PLoS Neglected Trop. Dis. 2009, 3, e478, 1 – 14.
[208] A. Migita, M. Watanabe, Y. Hirose, K. Watanabe, T. Tokiwano, H. Kinashi, H. Oikawa, *Biosci. Biotechnol. Biochem.*, **2009**, *73*, 169–176.
[209] D. E. Cane, W. D. Celmer, J. W. Westley, *J. Am. Chem. Soc.* **1983**, *105*, 3594 – 3600.

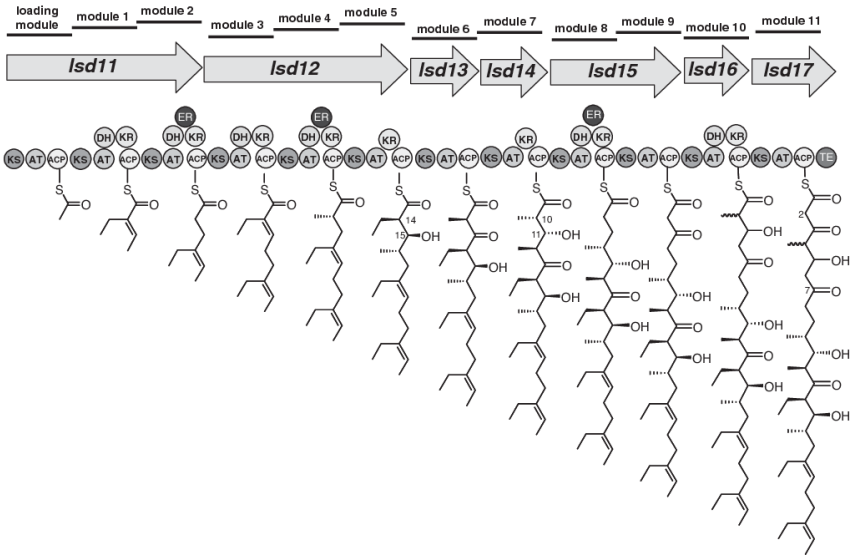

Figure 45. Architecture of the PKS responsible of lasalocid A biosynthesis. Adapted from ref 208, with the permission of Taylor & Francis, free of charge.

Examining in detail every module, it emerges that a complete Claisen condensation / β-keto processing sequence occurs in modules 2, 4 and 8 (following the module numeration in Figure 45), while the other modules present partial reductive loops. Thus, the module organisation seems to reflect well the structure of lasalocid A chain. However, major issues arose regarding the following biosynthetic steps, in particular for what concern the formation of the cyclic ethers and of the aromatic ring.

The determination of the temporal sequence in which these rings are built and whether these events occur on PKS or are mediated by tailoring enzymes, were objects of debate.

Some research groups agreed that the formation of the aromatic ring anticipates the synthesis of the cyclic ethers.[210,211]

A possible mechanism for aromatic ring biosynthesis was reported by Oikawa and co-workers and is represented in Figure 46A.[210]

This mechanism suggests that a deactivation of the DH domain in module 10 should lead to a non-dehydrated product, reported in Figure 46A. Then, a condensation between C2 and C7 carbon occurs, followed by dehydration and aromatisation.

[210] Y. Shichijo, A. Migita, H. Oguri, M. Watanabe, T. Tokiwano, K. Watanabe, H. Oikawa, *J. Am. Chem. Soc.* **2008**, *130,* 12230 – 12231.

[211] J. W. Westley, J. F. Blount, R. H. Jr Evans, A. Stempel, J. Berger*, J. Antibiot.* **1974**, *27*, 597 – 604.

Finally, the polyketide chain, now bearing its aromatic ring and named prelasalocid, should be released from the enzyme by a thioesterase in the TE domain; however, prelasalocid as such has never been detected nor isolated from wild-type nor mutant strains.

For what concerns the formation of the cyclic ethers, Westley *et al.* proposed that a stereoselective double epoxidation occurred on prelasalocid, followed by hydrolysis of the epoxides and by a cascade-like cyclisation, affording lasalocid A and its isomer isolasalocid. This process appears to be catalysed by epoxide hydrolase Las B, that would favour firstly the formation of the tetrahydrofuran (THF) ring and then of the tetrahydropyran (THP) of lasalocid A. This hypothesis is schematised in Figure 46B and represents an elegant example of how nature can escape the basic rule of chemistry, favouring the formation of an "anti-Baldwin" six-membered polyether.[212,213]

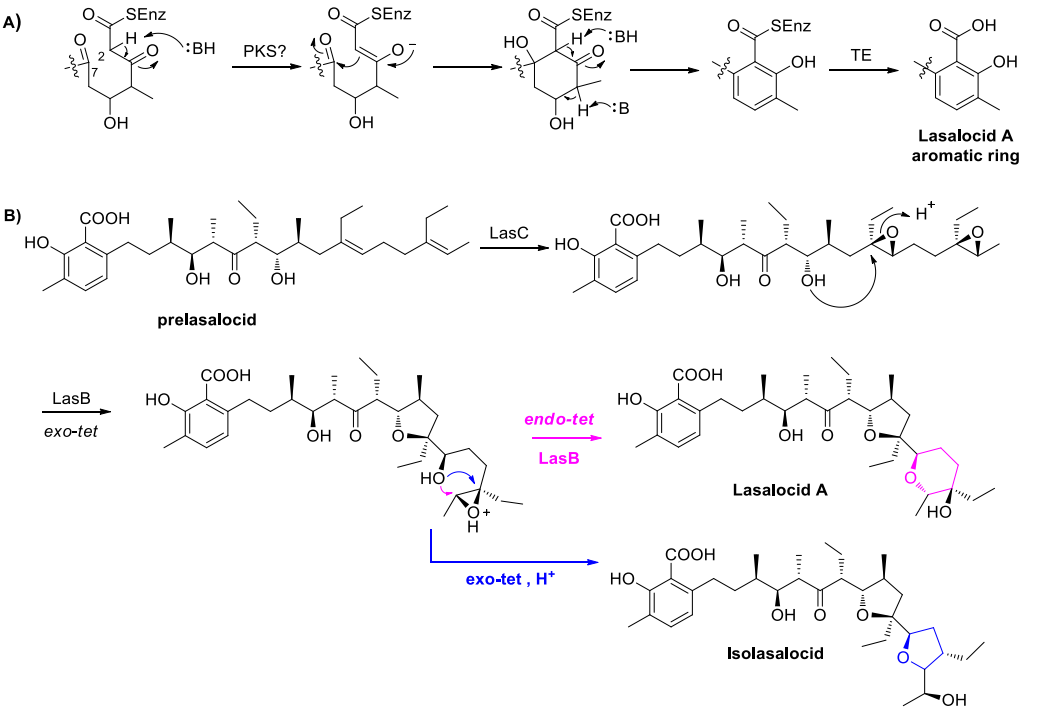

Figure 46. Proposed mechanisms for the formation of the aromatic ring (A) and of polyether cycles in lasalocid A and isolasalocid (B).[213]

[212] D. E. Cane, *Nature* **2012**, *483*, 285-286.

[213] K. Hotta, X. Chen, R. S. Paton, A. Minami, H. Li, K. Swaminathan, I. I. Mathews, K. Watanabe, H. Oikawa, K. N. Houk and C.-Y. Kim, *Nature* **2012**, *483*, 355–358.

However, a more recent study by Tosin *et al.* contradicts this hypothesis.[214] In fact, exploiting an approach based on the administration of particular chemical probes to *S. lasaliensis* fermentation broth, Tosin was able to determine that the formation of the cyclic ethers anticipates the introduction of the aromatic ring and, more importantly, that this process happens on PKS, more specifically in module 11 (or module 10 exploiting the numeration of modules of Figure 45), as reported in Figure 47.

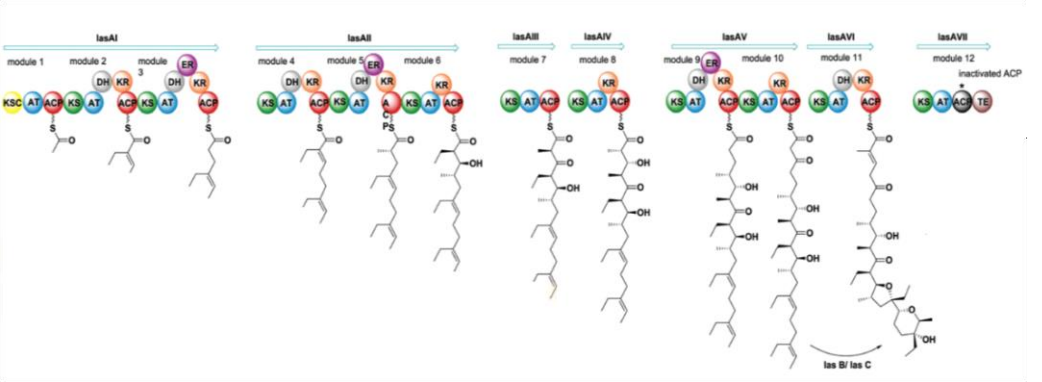

Figure 47. Proposed biosynthetic pathway for lasalocid A by the lasA PKS enzymes, showing the presence of the cyclic ethers, but not of the aromatic ring on module 11.[214]

This approach will be explained in detail in paragraph 6.1.3. For what concerns the formation of the aromatic ring, early results suggest that can occur on the PKS as well, as soon as the dodecaketide chain is formed.

Salinomycin

Salinomycin (structure reported in Figure 36), is a polyether ionophore produced by different strains of *Streptomyces albus*. As lasalocid A, it is a potent antibiotic that elicits its biological activity binding majorly K^+ ions and transporting them across cellular membranes.[215] Although its toxicity limits its therapeutic use for humans, salinomycin is marketed with the trade names of Bio-Cox and Sacox as coccidiostat in animal farming.

In the last years, the interest of the scientific community for this compound was rekindled by the discovery that salinomycin possesses interesting anticancer properties and is particularly active against cancer stems cells (CSCs). The activity

[214] M. Tosin, L. Smith, P. F. Leadlay, *Angew. Chemie - Int. Ed.* **2011**, *50*, 11930–11933.
[215] J. W. Westley, *Antibiotics* **1981**, *4*, 41–73.

appears to derive from the multiple targeting of different signalling pathways, including Akt, Wnt/β-catenin, Hedgehog, and Notch. Moreover, salinomycin contrasts the overexpression of ABC transporters, usually related to the development of multidrug resistance in cancer cells.[193,216]

The importance of Hh signalling targeting in anticancer therapy and for the treatment of CSCs has been already discussed in Chapter 3.

In this field, salinomycin proved to contrast the proliferation of human breast carcinoma MCF-7 cancer stem cells, targeting both Smo protein and Gli1.[217] The activity toward Gli1 could be really promising, considering the possibility of Smo downstream regulation that renders ineffective several Smo inhibitors, as reported in Chapter 3.

The mechanism through which salinomycin elicits its activity towards CSCs, targeting such an impressive number of different signalling pathways has not been completely elucidated yet. However, a study performed on metastatic breast cancer stem cells, demonstrated that salinomycin and one of its synthetic derivatives, induced cellular apoptosis sequestering iron ions from lysosomes. To contrast the depletion in iron concentration, the cell promotes the degradation of ferritin in lysosomes, but the consequent production of iron ions triggers the formation of reactive oxygen species (ROSs). ROSs increase the cellular membrane permeabilisation, inducing the cell death process.[218]

The interest toward the peculiar anticancer properties of salinomycin, encouraged the synthesis of several derivatives, also in the attempt to understand the so called "SARs" (structure-activity relationships). The principal adopted strategies involved the functionalisation of the carboxyl and hydoxyl groups, protecting them or converting them in other entities, such as amides, esters, hydroxamic acids, amines, azides, triazoles and so on. A complete list of the possible functionalisation was reviewed by Versini *et al.*[216]

From a structural point of view, salinomycin presents a more complex scaffold than lasalocid A. It doesn't bear any "exotic" aromatic ring but an atypical *cis*- double bond is present at C18-C19 junction. Salinomycin contains five cyclic ethers (four with a

[216] A. Versini, L. Saier, F. Sindikubwabo, S. Müller, T. Cañeque, R. Rodriguez, *Tetrahedron* **2018**, *74*, 5585–5614.

[217] Y. Lu, W. Ma, J. Mao, X. Yu, Z. Hou, S. Fan, B. Song, H. Wang, J. Li, L. Kang, P. Liu, Q. Liu, L. Li, *Chem. Biol. Interact.* **2015**, *228*, 100–107.

[218] T. T. Mai, A. Hamaï, A. Hienzsch, T. Cañeque, S. Müller, J. Wicinski, O. Cabaud, C. Leroy, A. David, V. Acevedo, A. Ryo, C. Ginestier, D. Birnbaum, E. Charafe-Jauffret, P. Codogno, M. Mehrpour, R. Rodriguez, *Nat. Chem.* **2017**, *9*, 1025–1033.

THP-like ring, one with a THF-like ring), and three of them constitute a complex spiro-system, conferring some structural rigidity.

The biosynthesis of the polyketide chain occurs on an assembly line of nine modular PKS, for a total of fourteen fatty acids synthase-like modules, reported in Figure 48.[219] As in the case of lasalocid A, a correspondence between the order of the modules and the structure of the natural product can be inferred.

This biosynthetic pathway starts with the loading of the malonyl-CoA on SalA1, followed by several condensation steps, involving as extender units five malonyl- CoA, six methylmalonyl-CoA and three ethylmalonyl-CoA.

Dehydration to form the double bonds between C18–C19 appears to occur at a late stage of the biosynthesis, after the transfer of the growing polyketide chain from the module 14 of the PKS to a discrete SalX protein. The cyclisation mechanism seems to be initiated by a SlnM enzyme, homologous to O-methyltransferases.[220] The formation of the cyclic ethers involves a stereoselective epoxidation, followed by epoxide opening and cyclisation, catalysed by the epoxide hydrolases/cyclases (SalBI, SalBII and Sal- BIII), similarly to the case of lasalocid A. Carbon C20 is hydroxylated by a cytochrome P450- SalD. However, the exact timing of the dehydrations and epoxidation/cyclisations reactions is still quite controversial.[219,221]

A representation of salinomycin biosynthesis is reported in Figure 48. In Figure 48, the post PKS SalAIX process is represented, assuming that the formation of *cis* C18-C19 double bond happened after the formation of the spiro-system.

[219] M. E. Yurkovich, P. A. Tyrakis, H. Hong, Y. Sun, M. Samborskyy, K. Kamiya, P. F. Leadlay, *ChemBioChem* **2012**, *13*, 66–71.

[220] C. Jiang, Z. Qi, Q. Kang, J. Liu, M. Jiang, L. Bai, *Angew. Chem. Int. Ed.* **2015**, *54*, 9097–9100.

[221] C. Jiang, H. Wang, Q. Kang, J. Liu, L. Bai, *Appl. Environ. Microbiol.* **2012**, *78*, 994–1003.

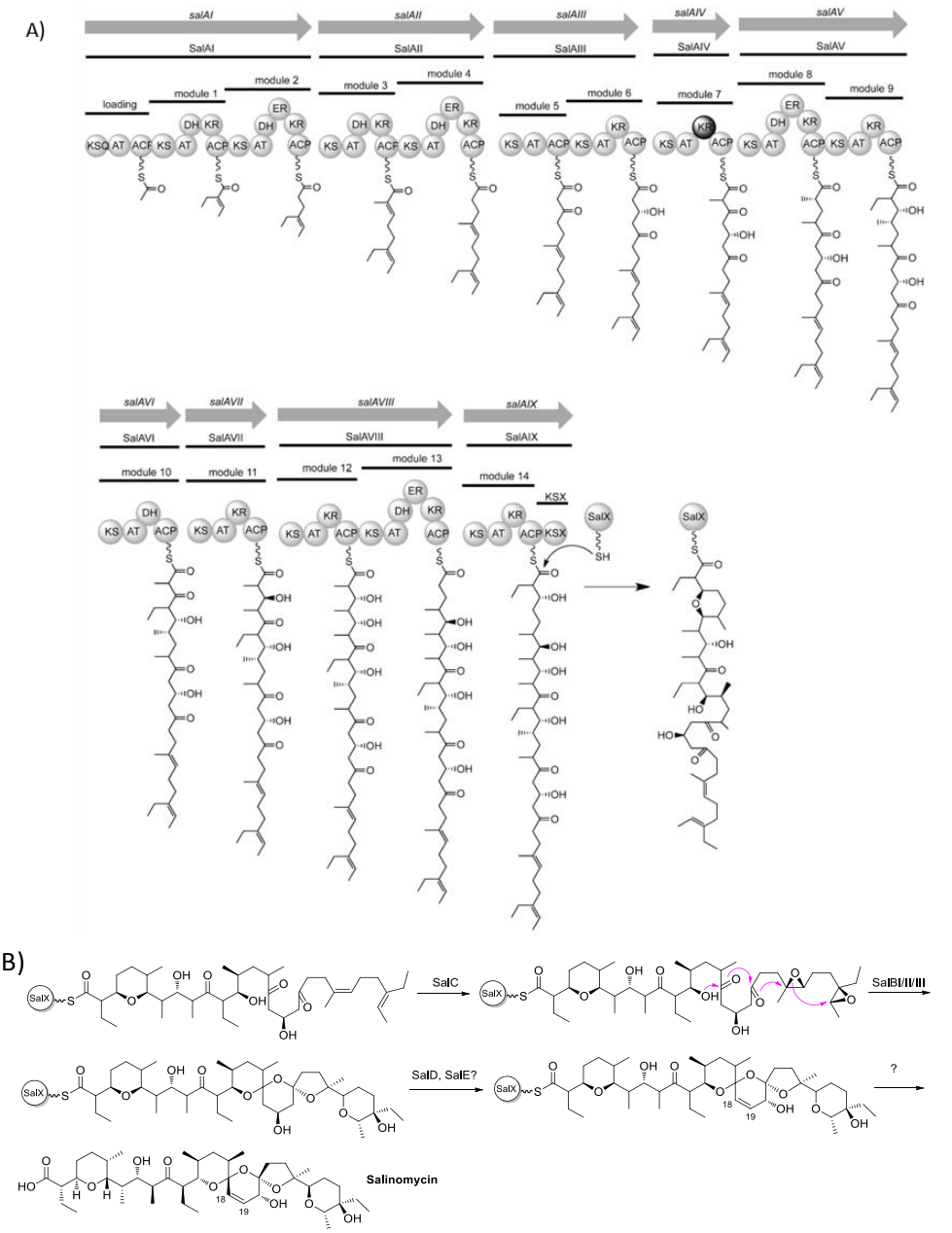

Figure 48. A) Proposed biosynthetic pathway for salinomycin by PKS enzymes. Adapted from ref 219, with the permission of WILEY-VCH Verlag GmbH & Co. Copyright 2012. B) Proposed mechanism for the post-tailoring modifications, leading to salinomycin (Note that in this case the dehydration is supposed to occur after cyclic polyethers formation).

6.1.3 Biosynthesis of diversified "unnatural" products

The elucidation of natural products bioassembly pathways appears to be fundamental, when the microorganism producers are intended to be used as "cell factories", to obtain these compounds. In this field, a good knowledge of the biosynthetic mechanism could be exploited essentially in two ways: to enhance the fermentation yield of the natural product that it is meant to biosynthesised, or to force the microorganism to produce "unnatural" and "diversified" versions of the natural product, as in the case of the project reported in this chapter.

In the first case, a rational genetic manipulation of the microorganism gene cluster is generally performed to improve the production of the expected natural products. To this extent, two strategies could be considered:

- ✓ the overexpression of the biosynthetic genes for the involved extender units;
- ✓ the deletion of other gene clusters that should compete for the same extender units.

For example, both these approaches were simultaneously applied to *Streptomyces Albus* DSM 41398, to enhance salinomycin yielding, disrupting the competing PKS gene clusters and overexpressing a crotonyl-CoA reductase, that enhance the supply of extender units for the bioassembly.[222] In another case, performed on *Streptomyces platensis* MA7327, the deletion of a *ptmR1* gene, sequentially similar to a family of transcriptional repressors, generated a microorganism that overproduced platensimycin and platencin, two natural antibiotic leads. [223]

For what concern the approaches aimed at the biosynthesis of "unnatural" versions of natural products, different strategies have been established in the last decades and will be described hereafter.

- ✓ ***Precursor-directed biosynthesis***

Precursor-directed biosynthesis is probably the most intuitive method to induce a microorganism to biosynthesize a novel "unnatural" product. The general idea at consists into the feeding of an analog of the natural precursor of the producing organism, to induce it to incorporate the new precursor into a modified version of the final natural product.[224] This approach proved to be quite efficient for the synthesis of

[222] C. Lu, X. Zhang, M. Jiang, L. Bai, *Metab. Eng.* **2016**, *35*, 129–137.
[223] M. J. Smanski, R. M. Peterson, S. R. Rajski, B. Shen, *Antimicrob. Agents Chemother.* **2009**, *53*, 1299–1304.
[224] J. Kennedy, *Nat. Prod. Rep.* **2008**, *25*, 25–34.

penicillin V, a phenoxymethylated-version of penicillin. In that case, phenoxyacetic acid was simply added to the fermentation broth of *Penicillium chrysogenum*.[225]
The major drawback of this strategy is that usually a mixture of the natural and unnatural products is produced by the microorganism, which are difficult to separate. Moreover, a huge amount of unnatural precursor is usually required to compete with the natural biosynthesis. For this reason, this approach found and evolution into the bioassembly line reprogramming and mutasynthesis strategies that involve the genetic manipulation of the microorganism, to block the production of the natural product and favouring the synthesis of the unnatural one. These methods are discussed in the next paragraph.

Bioassembly line reprogramming and mutasynthesis.
Considering the strict relationship between gene cluster and protein function, and with the elucidated biosynthetic pathway in hands, every bioassembly line could be potentially reprogrammed, manipulating genes to favour the synthesis of new metabolites, enhancing the chemical diversity.[226] A typical example of this strategy regarded the synthesis of doramectin, an antiparasitic drug obtained reprogramming the PKS-like bioassembly of avermectin in *Streptomyces avermitilis*.[227] The fundamental requirement was the modification of the PKS starter unit, from the isobutyryl-coenzyme A (CoA) used by the wild type microorganism, to an atypical cyclohexanecarboxylic (CHC) unit in doramectin case.
A CHC loading module had been found in *Streptomyces platensis* phoslactomycin PKS; therefore, a *Streptomyces avermitilis* mutant was produced, replacing its loading module with the one of *Streptomyces platensis*, as reported in Figure 49. In addition, to secure a supply of CHC starter unit for the biosynthesis, five putative genes responsible of CHC-CoA formation in *Streptomyces platensis*, were cloned and placed into the mutant.

[225] A. L. Demain, E. P. Elander, *Antonie van Leeuwenhoek* **1999**, *75*, 5-19.
[226] J. M. Winter, Y. Tang, *Curr. Opin. Biotechnol.* **2012**, *23*, 736–743.
[227] J. B. Wang, H. X. Pan, G. L. Tang, *Bioorg. Med. Chem. Lett.* **2011**, *21*, 3320-3323.

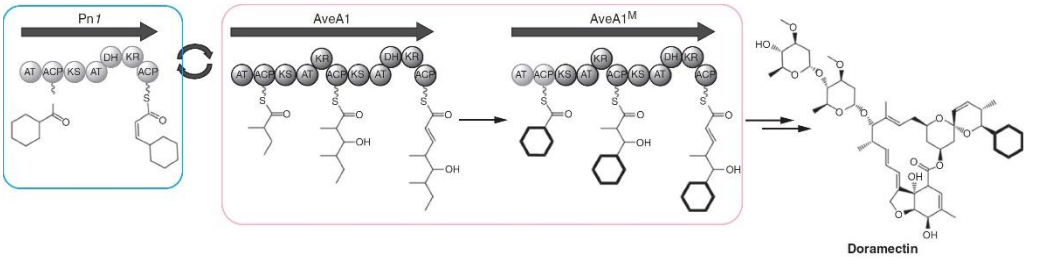

Figure 49. Representation of the bioassembly of doramectin in *Streptomyces avermitilis* mutant, showing the merging of *Streptomyces platensis* starting module (cyan) with the modules of wild type of *Streptomyces avermitilis* (light orange). Adapted from ref 226, with the permission of Elsevier, copyright 2011.

An analogous strategy was exploited for the synthesis of fluorinated unnatural derivatives of salinosporamide A, an anticancer agent produced by *Salinispora tropica* and naturally bearing a chlorine atom. To generate fluorinated version of this compound, the chlorinase gene salL was replaced with a fluorinase gene of *Streptomyces cattleya*. The obtained *Salinispora tropica* mutant was able to produce the fluorosalinosporamide (Figure 50), but only if the fermentation media was enriched with inorganic fluorine.[228]

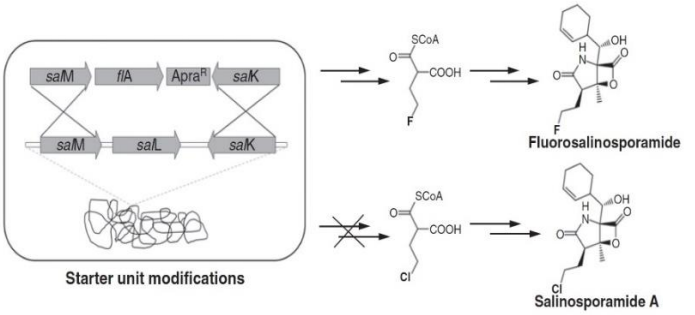

Figure 50. Reprogramming of Salinosporamide A biosynthesis, replacing the gene salL in *Salinospora tropica* with a *S. cattleya* fluorinase flA. The obtained mutant generates florosalinosporamide. Adapted from ref 226, with the permission of Elsevier, copyright 2011.

Mutasynthesis can be consider as a sub-group of the bioassembly line reprogramming strategy, and it is an evolution of the precursor-directed biosynthesis approach. In this case, mutant microorganism, lacking a key factor of the biosynthetic pathways are used, to block the production of the natural product. Therefore, the supplement of a

[228] A. S. Eustaquio, D. O'Hagan, B. S. Moore, *J. Nat. Prod.* **2010**, *73*, 378-382.

different starting material, affords a modified version of the natural products, in which the new precursor has been incorporated. In this way, the drawback of the simultaneous synthesis of natural and unnatural products is avoided, and an increasing in the chemical diversity of natural products can be efficiently achieved.

In the past, this technique was applied majorly to obtain modified versions of antibiotics. At the beginning the process was quite random: in fact, casual mutations were induced in the microorganisms that were then isolated, characterised and tested with different modified precursors, to evaluate which type of compounds could have been biosynthesised.

One of the first reported applications of this strategy was the synthesis of analogs of the antibiotic neomycin B. In that case, the natural producer, *Streptomyces fradiae*, was randomly mutated. Interestingly, one of the mutants was still able to produce neomycin B, when supplemented with deoxystreptamine, but when the precursor was replaced with streptamine and epistreptamine, two new antibiotics, hybrimycin A1 and hybrimycin B2 respectively, were obtained.[229]

With the passing of time, the new insight into the bioassembly mechanisms of different natural products biosynthesis, made mutasynthesis more rational, and applicable to different families of natural products.

Of course, PKSs emerged as optimal candidates to undergo mutasynthesis, considering that their bioassembly lines have been elucidated in several cases and that in type I PKSs a strict correlation between the different modules and the structure of the final compound is inferable.

This approach is so common, that application of mutasynthesis to PKSs is often referred as chemobiosynthesis.

A typical example of chemobiosynthesis is the pioneering work of Jacobsen *et al.*, aimed at the synthesis of erythromycin derivatives.[230] To this extent, the 6-deoxyerythronolide B synthase (DEBS) was inactivated, replacing a key cysteine in the active site of the module 1 KS with an alanine. The feeding of the natural substrate of module 2, as diketide *N*-acetylcysteamine thioester resulted again in the obtainment of the natural 6-deoxyerythronolide B, that was then converted into erythromycin by tailoring enzymes. More interestingly, feeding of diketide analogues (as thioesters), to the mutated PKS, afforded new analogs of 6-deoxyerythronolide B, including

[229] W. T. Shier, K. L. Rinehart Jr, D. Gottlieb, *Proc. Natl. Acad. Sci. U. S. A.* **1969**, *63*, 198-204.

[230] J. R. Jacobsen, C. R. Hutchinson, D. E. Cane, C. Khosla, *Science* **1997**, *277*, 367–369.

aromatic and ring-expanded derivatives, impossible to obtain through chemical synthesis (Figure 51).

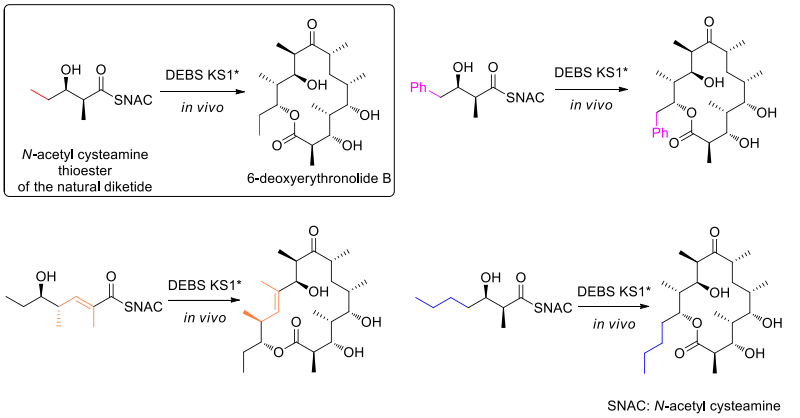

Figure 51. Summary of the main 6-deoxyerythronolide B analogs obtained through a chem-biosynthetic approach.[230]

- ✓ ***Heterologous expression in surrogate hosts***

The technique of heterologous expression found applications in the implementation of natural products or their derivatives production, when the wild type producer is difficult to be manipulate or to be genetically modified, or doesn't growth in a satisfactory way. In all of these situations, the biosynthetic pathway needs to be reconstructed in a heterologous host, chosen on the basis of the metabolite that is required.

This technique is generally exploited to facilitate the manipulation of natural products biosynthesis, as in the case of salinomycin which can be produced by a *Streptomyces coelicolor* M1154 heterologous host,[231] but it is also useful for the synthesis of modified version of natural products. An interesting example, in the field of polyketides, concerns the synthesis of doxorubicin glycosylated derivatives.[232]

Doxorubicin potent anticancer activity is related to the presence of a deoxysugar L-daunosamine. However, the acute toxicity and severe side effects prompted the synthesis of modified derivatives of doxorubicin that must contain a deoxysugar moiety to preserve the biological properties. To this extent, *Streptomyces venezuelae*, a strain not able to biosynthesize aminoglycoside units as wild type, was used as

[231]H. Luhavaya, S. R. Williams, H. Hong, L. Gonzaga de Oliveira, P. F. Leadlay, *ChemBioChem* **2014**, *15*, 2081-2085.

[232] A. R. Han, J. W. Park, M. K. Lee, Y. H. Ban, Y. J. Yoo, E. J. Kim, E. Kim, B. G. Kim, J. K. Sohng, Y. J. Yoon, *Appl. Environ. Microbiol.* **2011**, *77*, 4912-4923.

heterologous host of different plasmids coding for several nucleotide deoxysugars. The host was also equipped with the enzymes (namely glycotranferases) necessary to transfer the sugar on the aglycon, to force the production of doxorubicin analogs characterised by unnatural sugar moieties.

- ✓ **Tosin's bio-chem approach**

The methods for the generation of diversified "unnatural" products, reported in the previous sections, required a deep understanding of the bioassembly mechanism adopted by the producer microorganism. In the case of polyketides, a great advantage is constituted by the aforementioned correspondence between the structure of the polyketide chain and the functions of the PKS modules. However, some essential features often remained poorly understood, such as the exact timing of the individual steps on the PKS assembly line or the general biosynthetic mechanism for unconventional PKSs that don't follow exactly the collinearity rule. In these cases, the strategies based on the modification of the bioassembly line cannot necessarily provide an answer, and general approaches for PKS mechanism elucidation, ideally isolating directly the biosynthetic intermediates, could be extremely valuable.

In this context, the strategy developed in the Tosin's research group emerged as an interesting solution. It is based on intercepting the biosynthetic intermediates of the elongating polyketide chain, inducing their release from the PKS into the fermentation media, where they can be extracted and analysed by LC-MS techniques. The release of these intermediates is achieved feeding the fermentation broth with chemical nonhydrolysable probes that mimic the malonyl-CoA extender units and compete with them in the chain elongation steps, as illustrated in Figure 52.[233]

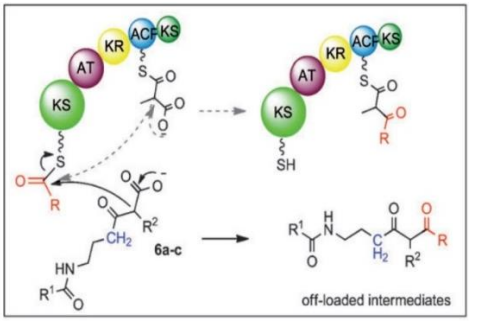

Figure 52. Mechanism of chain termination on a type I PKS, leading to the release of off-loaded intermediates in the fermentation media.[214]

[233] M. Tosin, L. Betancor, E. Stephens, W. M. A. Li, J. B. Spencer, P. F. Leadlay, *ChemBioChem* **2010**, *11*, 539–546.

The nonhydrolysable chemical probes that act as chain terminators are designed to mimic the malonyl-CoA extender unit. For this reason, they contain a β-ketomethyl ester group and a side chain in place of the pantetheine moiety of the ACP. The methyl ester is hydrolised *in vivo* by esterases, affording a malonyl carba(dethia) substrate that, after decarboxylation, compete for the fundamental Claisen condensation between the polyketide elongating unit (on KS domain in Figure 52) and the malonyl-CoA extender unit. If the condensation with the chemical probe was successful, the elongating intermediate would be intercepted and off loaded from the PKS enzyme. At this point, the intercepted intermediated could be simply extracted from the fermentation media and analysed.[233]

One of the most interesting aspect of this strategy is that it can be applied in two different field: to get insights into the details of PKSs bioassembly, or to generate unnatural polyketides.

A good example of the first application is the aforementioned determination of the timing of aromatisation and cyclisation steps in lasalocid A biosynthesis.[214]

In that study, the administration of a small library of chemical probes designed to mimic malonyl-mimic unit, afforded the off-loaded intermediates reported in Figure 53.

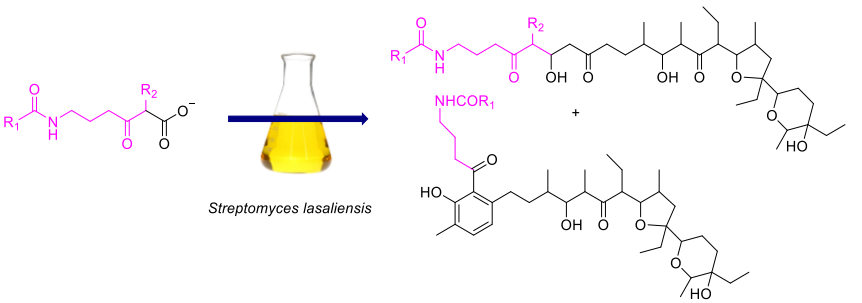

Figure 53. Feeding experiment on *S. lasaliensis*, leading to the detection of the two key intermediates. The presence of the first one, bearing the cyclic ethers, but not the aromatic ring, suggested that the formation the aromatic ring occurs in a later stage.

The detection of a fragment containing only the two cyclic ethers and a fragment presenting in addition the aromatic ring, demonstrated that the epoxidation opening-cyclisation sequence anticipates the aromatisation. A similar approach was employed

also to study the biosynthesis of 6-methylsalicylic acid, performed by an iterative type I PKSs.[234]

For what concern the generation of novel polyketides, the use of chemical probes could be seen as a particular case of chemobiosynthesis, because the fermentation would generate unnatural version of the target polyketide in which the probe has been incorporated.

To demonstrate the effectiveness of this idea, derivatised probes were synthesised and tested on a proper engineered bacterial strain by Tosin and co-workers.[235]

The probes were modified at the *N*-acyl side chain to introduce diversity, testing carbon skeletons differing in length and presenting eventually handles such as azides and alkynes, or CF_3 substituents. On the other hand, the β-ketoester moiety, fundamental for the interaction with the elongating polyketide chain, remained essentially unchanged, with the only variability of a fluorine or methyl atom as substituent of the methylene bridge between the carbonyl groups. The obtained probes were tested on engineered modified *Streptomyces lasaliensis* strains, to generate modified versions of lasalocid A, taking advantage of the knowledge of the biosynthetic pathway acquired during the previous studies. The strains were generated form *S. lasaliensis* NRRL 3382, mutating the active serine of ACP12 or ACP5 domains of the PKS into an alanine.

These mutants cannot produce lasalocid A, but can proceed with the biosynthesis until the mutation point. Obviously, this should lead to an accumulation of the intermediates on the PKS, favouring the interference of the chemical probe with the biosynthetic pathway.

The results of the feeding experiments on *S. lasaliensis* ACP12 are summarised in Figure 54, reporting the structures of the unnatural lasalocid A off-loaded intermediates, inferred by micro-LC-HR-MS analyses of the fermentation broth extract. It is interesting that the most abundant products in ACP12 strain were the late stages derivatised intermediated, bearing both the cyclic ethers and the aromatic ring (light blue in Figure 54).

[234] J. S. Parascandolo, J. Havemann, H. K. Potter, F. Huang, E. Riva, J. Connolly, I. Wilkening, L. Song, P. F. Leadlay, M. Tosin, *Angew. Chemie Int. Ed.* **2016**, *55*, 3463–3467.

[235] E. Riva, I. Wilkening, S. Gazzola, W. M. A. Li, L. Smith, P. F. Leadlay, M. Tosin, *Angew. Chemie Int. Ed.* **2014**, *53*, 11944–11949.

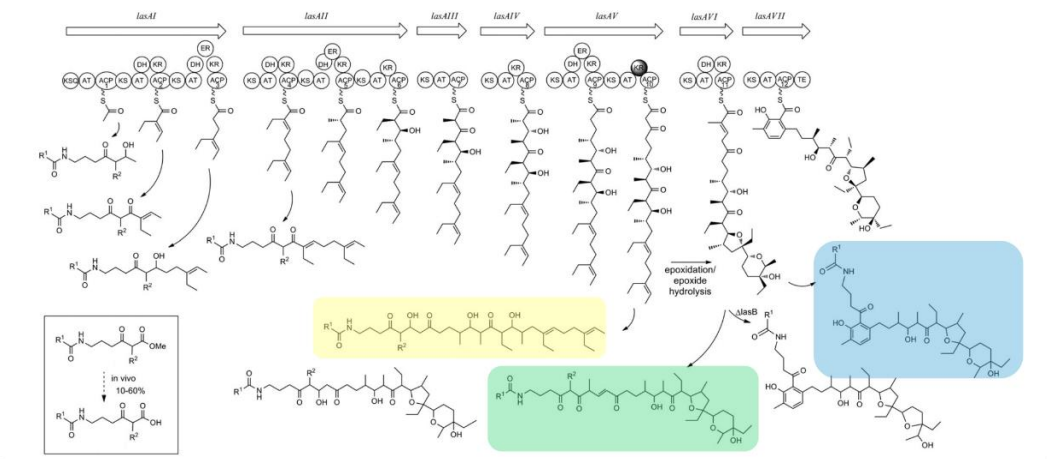

Figure 54 Generation of putative unnatural polyketide intermediates by fermentation of *S. lasaliensis* in the presence of chemical probes. In the light blue box, the main obtained scaffold is reported. In yellow and green boxes, the main structures obtained fermenting fluoro and methylmalonate probes, respectively, are appreciable.[235]

Fluoromalonated probes were processed as well, demonstrating that is possible to incorporate fluorine *in vivo*, leading to the formation of products bearing a fluorine atom in a specific α-carbonyl position. However, fluorinated undecaketides were preferentially obtained instead of the dodekatides presenting the cyclic ethers (yellow in Figure 54).

Moreover, the feeding with methyl malonated probes, generated a novel linear polyether, on which the aromatisation step didn't occur (green in Figure 54).

The presence of an alkyne or azide handle in the obtained unnatural lasalocid A derivatives was exploited to further enhance the diversity, performing a Huisgen 1,3-dipolar cycloaddition or Staudinger-phosphite reaction.

This chemoenzymatic approach constitutes a promising platform, to generate diversified polyether analogs, but obviously requires further optimisation, to improve the yields of the obtained off-loaded intermediates and to facilitate their detection and isolation. However, in comparison to other existing chemoenzymatic methodologies, Tosin's approach should allow a higher degree of polyketide diversification, taking advantage of the versatility of the genetic manipulation of the microorganism and of the diversity easily introduced by the chemical synthesis of the probes.

6.2 Aim of the project

On the basis of the background studies reported in the previous paragraph, the aim of this project was to develop of a robust chemoenzymatic protocol, not only to generate unnatural polyketides with possible biological application, but also for an easier detection and recovery of these compounds from the complex mixture of fermentation broth.

My investigation focused in particular on the preparation of diversified derivatives of lasalocid A and salinomycin, because of the bioactivities of these two polyethers ionophores that include anticancer properties against CSCs for the latter compound.

The main idea was to synthesise new chemical probes, perform feeding experiments on *Streptomyces lasaliensis* and *Streptomyces albus* strains, isolate the modified polyethers and, hopefully, perform a preliminary biological evaluation of the obtained compounds.

The chemical probes should be properly design, in order to contain the malonate unit fundamental for the targeting of the biosynthetic pathway, and a handle useful for the detection and isolation of the unnatural off-loaded intermediates, like a sort of "bait" for a selective "fishing".

In particular, three different baits were considered for different recovery approaches (Figure 55):

- ✓ azido probes, for their isolation through a Staudinger reaction with a supported phosphine;
- ✓ desthiobiotin-based probes, to exploit the strong interaction with avidin-labelled resins;
- ✓ ionic liquid (IL) probes, taking advantage of the peculiar properties of ILs, that can be efficiently separated from mixtures and, being charged molecules, are easily detectable at mass spectroscopy.

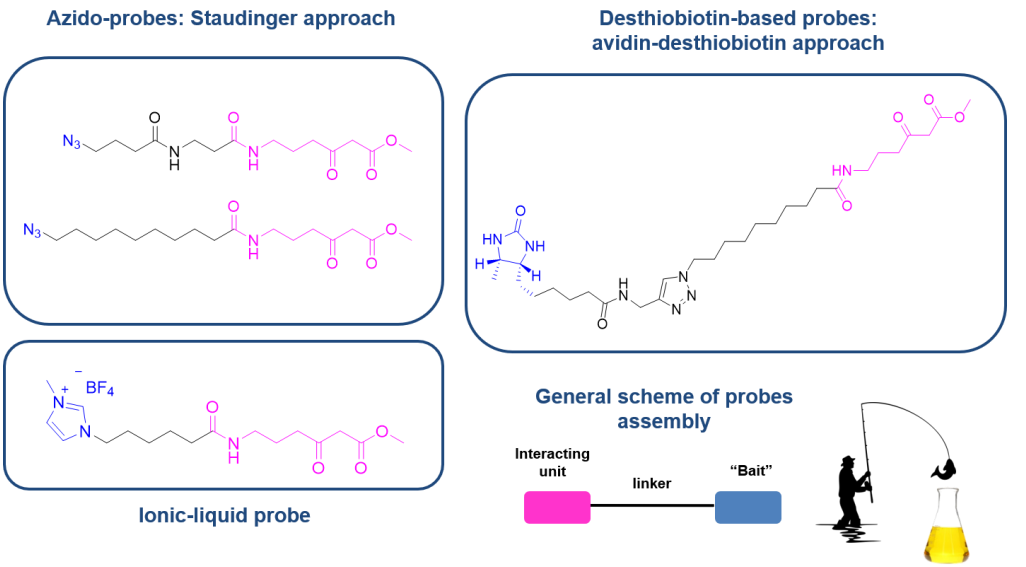

Figure 55. General assembly of the new probes, showing the "bait" in blue and the malonate interacting unit in pink.

In addition, preliminary semisynthetic studies were planned on commercially available lasalocid A and salinomycin to obtain possible active simple derivatives for biological studies and structure-activity relationships (SARs) elucidation.

6.3 Main results

6.3.1 Synthesis of azido probes for Staudinger approach

The idea of synthesizing azido probes wasn't new in Tosin's research group, as has been reported in paragraph 6.1.3. The demonstration that off-loaded intermediates bearing an azido moiety were detected in *Streptomyces lasaliensis* fermentation broths, prompted us to consider a recovery approach based on the Staudinger reduction of azides.

This reaction is a mild method to convert an azide to amine, upon treatment with a phosphine, typically PPh_3.[50] The mechanism, depicted in Figure 56a, involves the formation of an iminophosphorane, favoured by the elimination of nitrogen.

Hydrolysis of the iminophosphorane affords the amine; the generation of phosphine oxide is the driving force of this reaction.

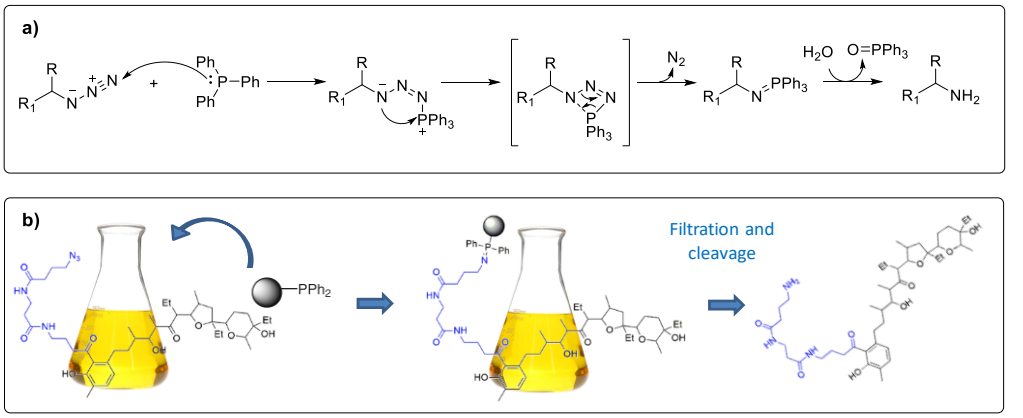

Figure 56. a) Mechanism of Staudinger reduction of azides to amines. b) Schematic representation of the recovery approach based on Staudinger reaction directly in the fermentation media, exploiting a polymer-bound phosphine.

Considering that polymer-bound PPh_3 is commercially available from different suppliers, the protocol schematised in Figure 56b was envisaged.

Addition of the resin to the extracts of fermentation media, should catch selectively the off loaded-intermediates that bear an azido moiety, through the formation of the iminophosphorane. The washing of the resin should remove all the undesired fermentation products, while the unnatural polyketides derivatives should remain

bound to the resin. Finally, in hydrolytic conditions, the desired fragments should be cleaved from the resin, and easily recovered and isolated.
With this idea in mind, our efforts were oriented at the design and synthesis of a novel azido-probe and at demonstrating the proof of concept of the applicability of this methodology.

Synthesis of a novel azido probe.

For the design of probe **77**, the retrosynthetic pathway depicted in Scheme 44 was envisaged. It was built upon a series of condensation reactions between simple and inexpensive building blocks, such as β-alanine and γ-aminobutyric acid (GABA), with the introduction of the malonate-interacting unit as the last step of the synthesis. This was not the first azido-probe synthesised in Tosin's laboratory, but compared with the others, **77** possess two amides in the "linker" portion of the probe. The increased polarity could be beneficial for the affinity of **77** toward the PKS enzyme, hopefully leading to and easier interaction with the chain-elongating fragments.

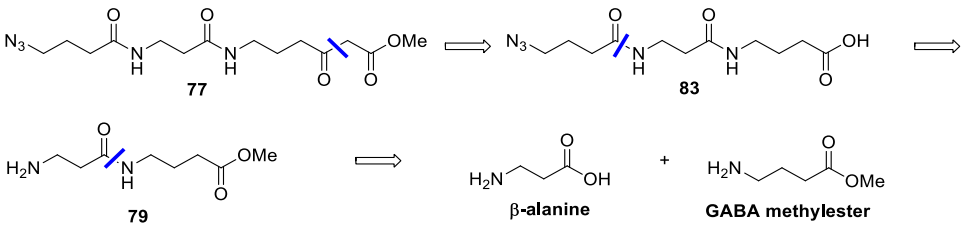

Scheme 44. Retrosynthetic approach for the synthesis of the novel azido-probe **77**.

The first step to be performed was the protection of β-alanine as benzyloxy carbamate (Cbz), as reported in literature.[236] The obtained compound was coupled with the methylester of γ-aminobutyric acid, using EDC hydrochloride as condensing agent. The Cbz protecting group was cleaved through hydrogenation in the presence of pallidum on carbon. The free amine **79** was coupled with the Cbz-protected GABA, obtained accordingly to the procedure used for β-alanine.[236,237]
In this case EDC gave unsatisfactory yield of 30%. The employment of a stronger condensing agent, such as HATU (1-[Bis(dimethylamino)methylene]-1H-1,2,3-triazolo[4,5-b]pyridinium 3-oxid hexafluorophosphate), gave an improvement of the

[236] M. Y.H.Lai, M. A. Brimble, D. J.Callis, P. W.R. Harris, M. S.Levi, F. Sieg, *Bioorg. Med. Chem.* **2005**, *13*, 533–548.
[237] Đ. Š kalamera, V. Blazek Bregovič, I. Antol, C. Bohne, N. Basaric, *J. Org. Chem*. **2017**, *82*, 12554−12568.

yield to 68%. However, from this point onwards, the poor solubility of the obtained products in organic solvents became a problem that accompanied us for the rest of the synthesis. The Cbz-protecting group of product **80** was cleaved once again through catalytic hydrogenation, and the resulting amine **81** was converted into the corresponding azide **82** through a diazotransfer reaction in the presence of triflic azide. [238] This reagent is explosive when dried, but a protocol in which it remained always in solution was applied. The methylester of compound **82** was hydrolysed in basic conditions, giving the corresponding carboxylic acid **83**. The acidic work-up proved to be quite challenging, because the product tended to remain in aqueous solution. However, multiple extraction of the aqueous phase allowed the recovery of **83** in satisfactory yield. Disappointingly, the last step was the most challenging of the whole synthesis. In the Tosin's research group, the conversion of the carboxylic acid into the fundamental malonate methylester moiety usually involved the coupling of the acid with Meldrum's acid, leading to the formation of a cyclic adduct, that is converted into the desired β-ketoester upon alcoholysis (Scheme 45, in dashed arrows).[235]

However, considering the polarity of our compound, that rendered the last purification steps really difficult, we preferred to exploit a different approach, based on the activation of the carboxylic acid with carbonyldiimidazole (CDI), followed by coupling with methyl potassium malonate. This strategy was previously applied for similar reactions and usually gave the desired product with moderate yield and without need of purification.

Unfortunately, in this case, probe **77** was obtained in very low yield, and as a mixture of byproducts. The crude proved to be impossible to purified by column chromatography on silica gel. Purification attempts by semi-preparative HPLC are currently in progress, but new reaction conditions for the last step of this synthetic route will be investigated, maybe considering the alternative procedure with Meldrum's acid.

The global synthetic pathway is reported in Scheme 45.

[238] T. L. Mindt, C. Muller, M. Melis, M. de Jong, R. Schibli, *Bioconjugate Chem*. **2008**, *19*, 1689-1695.

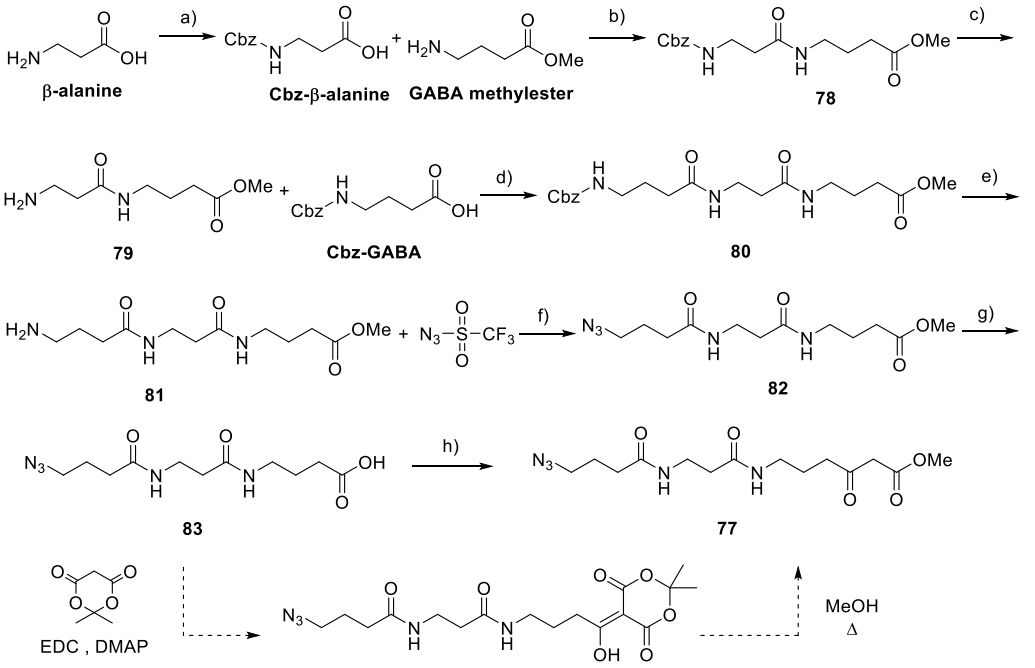

Scheme 45. Synthetic pathway leading to probe **77** formation, displaying also the alternative procedure for the final step. *Reagents and conditions*. a) Cbz-Cl, Na_2CO_3, H_2O/dioxane, r.t., 16 h, 85%; b) EDC HCl, TEA, DMAP, THF, 0°C to r.t., 16 h, 74%; c) H_2, Pd/C, MeOH, r.t., 6 h, quant.; d) HATU, DIPEA, THF, 0°C to r.t, 24 h, 68%; e) H_2, Pd/C, MeOH, r.t., 6 h, quant.; f) $CuSO_4$ $5H_2O$, K_2CO_3, MeOH / H2O; r.t., 20 h, 82%; g) LiOH, THF / H_2O, r.t., 16 h, 70%; h) CDI, $MgCl_2$, methyl potassium malonate, CH_3CN, 0°C to 30°C,16 h.

Staudinger-based approach: a proof of concept.

Considering the problematic synthesis of probe **77,** the proof of concept experiments on Staudinger reduction were performed on a different azido-probe **84**, that was synthesised in high scale and in few steps starting from 10-bromodecanoic acid, according to a reported procedure[235] (Scheme 46).

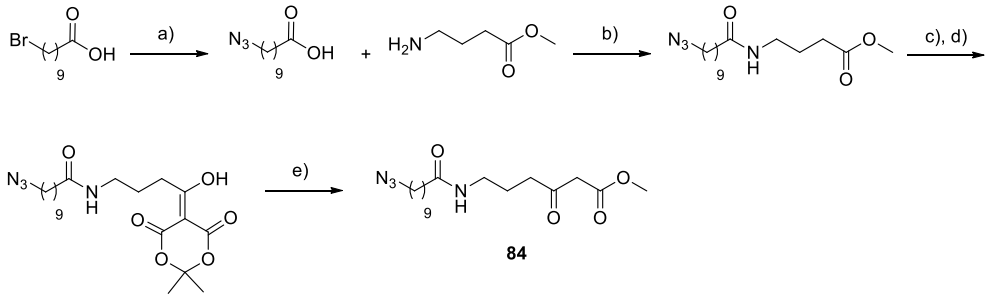

Scheme 46. Synthetic pathway giving azido-probe **84**. *Reagents and conditions.* a) NaN_3, DMSO, r.t., 16h, quant.; b) EDC HCl, TEA, CH_2Cl_2, r.t., 18h, 66%; c) NaOH, MeOH, r.t., 2h; d) EDC HCl, Meldrum's acid, DMAP, CH_2Cl_2, r.t., 18h, 74% over two steps; e) MeOH, reflux, 18h, 41%

As phosphine, we chose triphenylphosphine supported on polystyrene (200-400 mesh, loading: 1.4-2.0 mmol/g). The first explorative studies weren't performed directly on complex fermentation mixtures or extracts, but only on the azido-probe itself, to demonstrate the possibility of reducing it to amine upon treatment with a polymer-bound phosphine. However, we tried to mimic extract-like conditions, working on a very small scale (5 mg of probe **84**, in 1 mL of THF, 0.015 mM). The results of the screening of conditions are reported in Table 5. Reactions were monitored only by mass spectroscopy, to gain a qualitative information about the consumption of the azide and the eventual formation of the amine. Quantitative analysis to determine a yield of conversion, or the monitoring through TLC or NMR weren't considered, because they wouldn't be feasible when applied on the concentrations typical of extracts.

Table 5. Screening of extract-like conditions for Staudinger-based approach.[a]

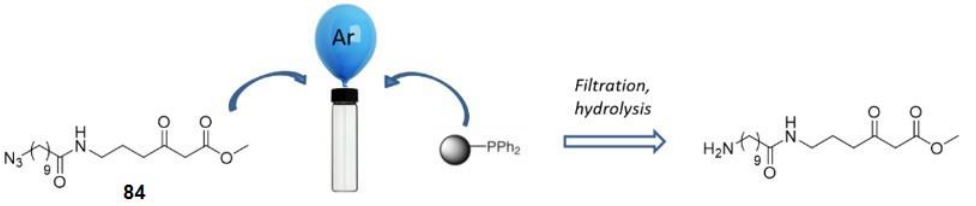

	Iminophosphorane formation				Hydrolysis			
Entry	**Solvent[b]**	**T (°C)**	**Time**	**Result**	**Solvent[c]**	**T (°C)**	**Time**	**Result**
1	THF	40°C	18 h	No azide Present	MeOH	40°C	16 h	Amine formation
2	MeOH	40°C	18 h	No azide Present	MeOH	40°C	16 h	Amine formation
3	THF	r.t.	3 days	No azide Present	MeOH	r.t.	2 days	Amine formation
4	MeOH	r.t.	3 days	Azide still Present	MeOH	r.t.	2 days	Amine formation
5	THF	r.t.	3 days	No azide Present	MeOH+ CH_3CN	r.t.	2 days	Resin degradation
6	THF	r.t.	3 days	Amine formation before azide consumption	-	-	-	Day 5: resin degradation
7	THF	r.t.	4 days	No azide Present	MeOH	r.t.	1 day	Day 5: resin degradation
8	THF	r.t.	4 days	Amine formation before azide consumption	-	-	-	Day 5: resin degradation

[a]: probe / resin ratio = 1 : 6 (5 mg : 55 mg), both the steps performed in 1 mL of solvent.

[b]: for the iminophosphorane formation, anhydrous solvents were used.

[c]: for the cleavage step, anhydrous solvents weren't required.

In the first experiment (entry 1), the reaction was performed in anhydrous THF, as reported in literature[239], with a ration azide: resin of 1 : 6. The reaction mixture was stirred at 40 °C, and after 18 h at that temperature, no unreacted azide was detected in the supernatant solution, indicating that the imino phosphorane had been formed. The resin was filtered and washed with THF, then it was dissolved in methanol and stirred at 40°C for the cleavage step. A mixture of MeOH and KOH was reported to hydrolyze iminophosphorane intermediates,[239] but in our case we preferred to avoid, if possible, the use of strong bases, that would not be compatible with experiments

[239] S. Ayesa, B. Samuelsson, B. Classon, *Synlett* **2008**, *1*, 97-99.

performed on extracts. To our delight, after 16 h, MS analysis revealed the formation of the desired amine.

This experiment constitutes a proof of concept for the applicability of this approach to the recovery of unnatural off-loaded intermediates from extraction mixtures.

A second experiment was performed in the same reaction conditions but using anhydrous methanol as solvent for the iminophosphorane formation step (entry 2). In fact, fermentation broth extracts are usually preserved in MeOH, and the possibility to avoid a change of solvent should facilitate the process. Also in this case the azide was completely consumed and the mass peak of the amine was detected, although the resin appeared to be less swelled when suspended in methanol.

At this point, we investigate if the reaction could work also at room temperature, considering that if this method was applied to extracts, the heating probably would be a problem for the stability of the off-loaded intermediates.

The best result was obtained in entry 3, a reproduction of entry 1 conditions, but at r.t. instead of at 40°C. In that case, longer reaction times for the iminophosphorane formation led to the complete binding of the azide to the resin. Also the cleavage phase required longer reaction times, but the amine peak was easily detected at MS analysis. When MeOH was used instead of THF (entry 4), maintaining unchanged the other reaction conditions, free azide was still detectable at mass analysis. For this reason, THF became the solvent of choice for the iminophosphorane formation step.

The other tested conditions involved changing the cleavage solvent (CH_3CN, also used sometimes for extract storage), leading to resin degradation (entry 5), and several unsuccessful attempts to replicate the results obtained in entry 3. In fact, in some cases (entry 6 and 8) the amine began to be released from the polymer before the complete formation of the iminophosphorane. Moreover, in the last attempts we started to observed resin degradation during the last days of experiments. In particular, in entry 7, the azide was promisingly bound on the polymer before amine release, although the completion of the reaction required one day more than the usual. Unfortunately, when the cleavage was performed in the usual conditions, after one day the resin completely degraded.

These results globally highlighted a lack of reproducibility of reactions initially promising. The fact that after some uses the resin seemed to be less reactive could be explained by a progressive oxidation of the phosphines that labelled the surface of the polymer to phosphineoxide. In fact, despite the resin was carefully preserved under argon atmosphere, a little bit of moisture probably entered the packaging every time that the resin was weighted. This could explain the progressive reactivity decreasing

and, if the resin incorporated moisture, also the unexpected anticipated hydrolysis of the iminophosphorane to amine, as well as the degradation of the resin.
The other drawback is given by the prolonged reaction times. This reaction isn't fast even under heating (18h for the iminophosphorane formation, 16 h for the hydrolysis), but when performed at room temperature it becomes really slow, leading to resin degradation due to the prolonged time in solution.
For this reason, this approach has been temporarily set aside. The proof of concept remained valid and in future new attempts will be performed, but using phosphines supported on more stable polymers developed *ad hoc* by collaborators at the University of Warwick.

6.3.2 Synthesis of desthiobiotin probes: avidin-desthiobiotin approach

The second approach to be tested exploited the strongest non-covalent interaction between a ligand and a protein, in particular the one involving D-biotin and avidin (*K*d in the order of 4 x 10^{-14} M).

Avidin is a protein commonly found in chicken egg white, and it can accommodate four biotin molecules in its binding sites (Figure 57). The binding is not only really strong, but it is also formed quickly and remains stable over a wide range of pH and temperatures, being almost irreversible in physiological conditions.

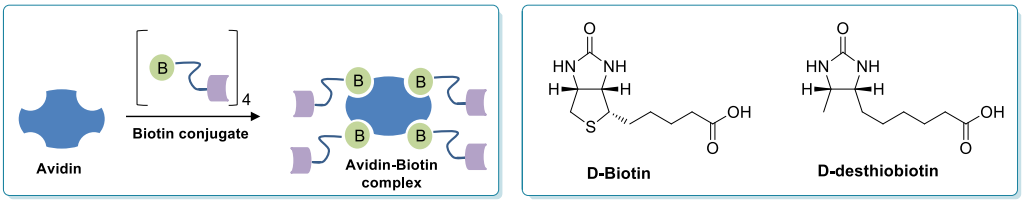

Figure 57. Schematic representation of the interaction between four biotin conjugates and avidin (left box); structures of D-Biotin and D-desthiobiotin (right box).

A bacterial homologus of this protein exists: it is called streptavidin and it has been isolated from the actinobacterium *Streptomyces avidinii*. Also streptavidin displays similar characteristics in binding biotin and for this reason both these proteins found wide applications in biotechnology, for example in proteins and nucleic acids detection or in protein isolation and enrichment.[240,241,242] Commonly, to facilitate these applications, avidin and streptavidin (*K*d in the order of 10^{-15} M) are commercially available as engineered forms, usually bound upon a support, such as a resin or magnetic beads. In this way the protein can catch rapidly and selectively the biotinylated entities from even complex mixtures and the undesired components could be eliminated simply filtering and washing the support. The main drawback of this methodology is the recovery of the biotinylated molecules. In fact, the interaction between biotin and avidin or streptavidin is so strong that can be broken only in harsh

[240] D. Savage, G. Mattson, S. Desai, G. Nielander, S. Morgensen, E. Conklin, Avidin-Biotin Chemistry: A Handbook, Pierce Chemical Company, Rockford, 1992, 1-23.
[241] X. Tong, L. M. Smith, *Anal. Chem.* **1992**, *64*, 2672–2677.
[242] A. Holmberg, A. Blomstergren, O. Nord, M. Lukacs, J. Lundeberg, M. Uhlén, *Electrophoresis* **2005**, *26,* 501–510.

conditions (high temperatures, acid pH, formamide treatment), that usually denature the protein and can damage the molecules of interest. [241,242]

However, it has been demonstrated that D-desthiobiotin (Figure 57), a modified version of biotin lacking the sulfur atom, still gave quite a strong interaction with avidin-like proteins, but weaker than that of biotin. For this reason, desthiobiotin can be displaced by biotin from avidin (K_d= 10^{-11} M).[243]

This prompted us to think about a desthiobiotin-based probe, with the aim of exploiting a monomeric avidin resin for the recovery of off-loaded fragments from extracts. When we reasoned about how to connect desthiobiotin with a malonate-mimicking probe, we immediately thought of click chemistry. In fact, the functionalisation of biotin with propargylamine, to introduce an alkyne handle exploitable in different ways (including click chemistry with azides), is a common strategy in biochemistry.[244]

Thus, we planned to label desthiobiotin in the same way and to connect it to azido-probe **84**, through a Huisgen 1,3-dipolar cycloaddition, exploiting click chemistry.

The synthetic route that afforded probe **86** is depicted in Scheme 47.

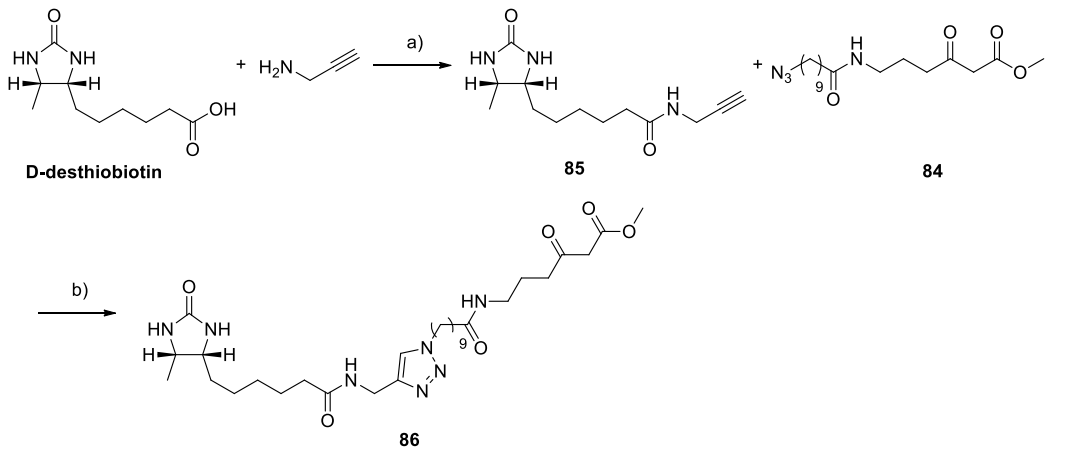

Scheme 47. Synthetic route leading to probe **86** formation. *Reagents and conditions.* a) EDC HCl, CH_3CN/MeOH, 0°C to r.t., 16 h, 90%; b) CuI, MeOH, r.t., 6h, 70%.

[243] J. D. Hirsch, L. Eslamizar, B. J. Filanoski, N. Malekzadeh, R. P. Haugland, J. M. Beechem, R. P. Haugland, *Analytical Biochemistry* **2002**, *308*, 343–357.

[244] S. Nainar, M. Kubota, C. McNitt, C. Tran, V. V. Popik, R. C. Spitale, *J. Am. Chem. Soc.* **2017**, *139*, 8090-8093.

D-desthiobiotin was coupled with propargyl amine, exploiting the same protocol applied to D-biotin.[244] Then the propargyl-desthiobiotin (**85**) was mixed with an equimolar amount of probe **84** and a catalytic amount of copper (I) iodide. The Huisgen 1,3-dipolar cycloaddition afforded the desthiobiotin-based probe **86.**

86 was employed as substrate in small-scale fermentations on WT and ACP12 *Streptomyces lasaliensis* strains*.* We chose to begin our feeding experiments on this microorganism, considering the expertise derived from the previous studies performed on lasalocid A biosynthesis; experiments on salinomycin producers would have followed, once that the protocol had been established.

Cultures were performed in both liquid (10 mL) and solid (5 mL), and were fed with the probe, to reach a final to reach a final 2.0 mM concentration. After 5 days at 30°C, all the cultures were extracted with ethylacetate. The positive thing was that both the microorganisms grow well also in the presence of the probe, that didn't result toxic for them.

The extracts were analysed by UPLC-HR-ESI-MS analyses: these revealed that our probe had been hydrolysed and decarboxylated *in vivo* (as demonstrated by the presence of the corresponding mass peak with *m/z* 548.3919, $[M+H]^+$, see Figure 58), but that it was not processed by the PKS enzymes.

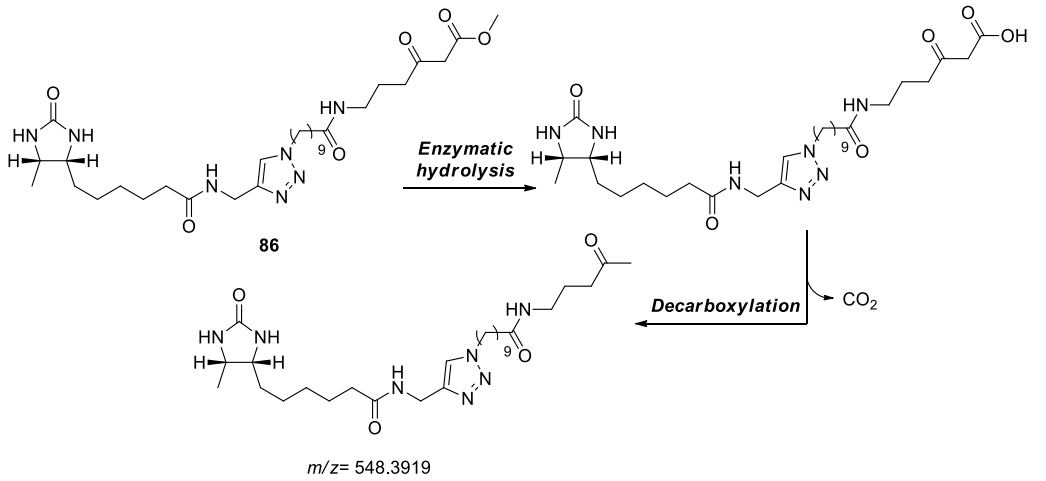

Scheme 58. In vivo hydrolysis/decarboxylation process, leading to the detected fragment characterised by *m/z* 548.3919.

In fact, we observed only peaks corresponding to **86** fragmentation, and the usual peaks relative to lasalocid A, but none of the expected unnatural lasalocid A off-loaded intermediates was detected.

In conclusion, the lack of incorporation of our probe in unnatural derivatives of lasalocid A could be explained by the metabolism of the microorganism, that may be prefers to employ desthiobiotin-conjugates for other functions. We mustn't forget that desthiobiotin is a modified version of a vitamin widely diffused in cells. Also, it is possible that the addition of the triazole and the desthiobiotin moiety to the probe may interfere with the ability of the probe to diffuse into PKS active sites. For these reasons, future efforts will involve:

1) The testing of the newly generated probe for applications *in vitro*, instead that *in vivo* (*e.g*. on recombinant functional enzymes);
2) the feeding of microorganisms with azido-probe **84**, performing the click reaction on the extracts and then purifying the reaction mixture on the avidin resin.

Once optimised, this protocol will be applied also on the salinomycin producer *Streptomyces albus*.

6.3.3 Synthesis of ionic liquid-based probes

Ionic liquids (ILs) are described as salts that result in a liquid phase at room temperature or, at least, below 100°C. The reason for this is that the characteristic ions forming the salt are poorly coordinated and prevent the formation of a defined and stable crystal lattice. The poor coordination is the result of the interaction between an organic, bulky and asymmetric cation and weekly coordinating anion.
Compared with conventional liquids, ILs display unique properties, behaving as nanoheterogeneous media. In fact, the ions in liquid state tend to form quite stable amphiphilic nanostructures, through a self-assembly process. Thus, in contrast to conventional liquids, ILs display a certain structural organisation, even in liquid phase, that is probably related with their peculiar properties.
A list of the most common cations and anions that compose ILs is reported in Figure 59, but the number of possible combinations is incredibly high, approaching 10^{18}. Clearly, this means that almost every desirable property, could be potentially satisfied by the proper combination of the ions that compose the IL. [245]

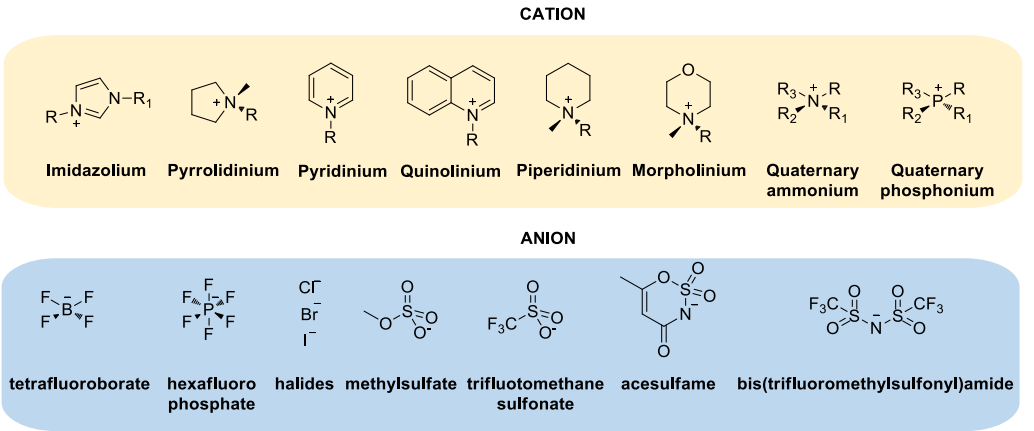

Figure 59. List of the most common cations and anions in ILs.[245]

Since the discovery of the first ionic liquids back in 1992, based on 1-ethyl-3-methylimidazolium salts, the interest of the scientific community for this topic steadily growth.[246] In a first moment, the focus of these research were applications in chemical synthesis, catalysis, electrochemistry, fuel production and processing. In particular, ILs became quite famous as green solvents, able to dissolve also high molecular weight

[245] K. S. Egorova, E. G. Gordeev, V. P. Ananikov, *Chem. Rev.* **2017**, *117*, 7132−7189.
[246] J. S. Wilkes, M. J. Zaworotko, *J. Chem. Soc., Chem. Commun.* **1992**, 965−967.

molecules, such as cellulose. In fact, they are widely exploited in carbohydrate synthesis.[247,248]

However, in the last years ILs found applications in life science and medicine areas, thanks to their bioactivities (cytotoxic, antimicrobial) and the possibility of employment in drug delivery, drug synthesis and biomedical analytics.[245]

In this field, we were attracted by the works of Galan and co-workers, in which ionic liquids were used inexpensive and versatile probes for an easier monitoring of enzymatic reactions on carbohydrates, allowing also a quantitative kinetic analysis.[249,250] These ILs-based probes were attached to the substrate of the enzymatic reaction and were exploited with a dual purpose. On one hand, the presence of an IL handle facilitates the purification process during the synthesis of the probe. In fact, ionic liquids can be easily separated from the other components of even complex mixtures, because non-ILs compounds can be simply washed away in solvents like hexane or diethyl ether, in which ILs are insoluble.

On the other hand, ILs are perfect probes for MS analysis, because, being charge molecules, they possess great spectral peak intensities and lower limits of detection, compared with the other components that can be present in the enzymatic reaction mixture.

These features facilitate the reaction monitoring by LC-MS, avoiding the use of expensive radioactive of fluorescent labelled carbohydrates.

Thus, the peculiar characteristics of ILs could find a perfect application in the analysis of fermentation extracts. An ionic liquid probe would solve the problem of the separation of the unnatural off-loaded intermediates from the extract mixture, exploiting the aforementioned easy washing procedure. Moreover, the ILs tag would increase the peak intensities of the off-loaded intermediates at mass spectroscopy analysis, making them more easily detectable than the not-ILs components eventually present in the sample.

With this goal in mind, ionic liquid-based probe **87** was designed (Scheme 48). To the best of our knowledge, it should be the first time that an IL is used to probe a biosynthetic pathway.

[247] M. C. Galan, R. A. Jones, A. Tran, *Carbohydrate Research* **2013***, 375*, 35–46.
[248] I. Sittel, A. Tran, D. Benito-Alifonso, M. C. Galan, *Chem. Commun.* **2013***, 49,* 4217-4219.
[249] M. C. Galan, A. Tran, C. Bernard, *Chem. Commun.* **2010,** *46*, 8968–8970.
[250] M. C. Galan, A. Tran, K. Bromfield, S. Rabbani, B. Ernst, Org. Biomol. Chem. **2012**, *10*, 7091–7097.

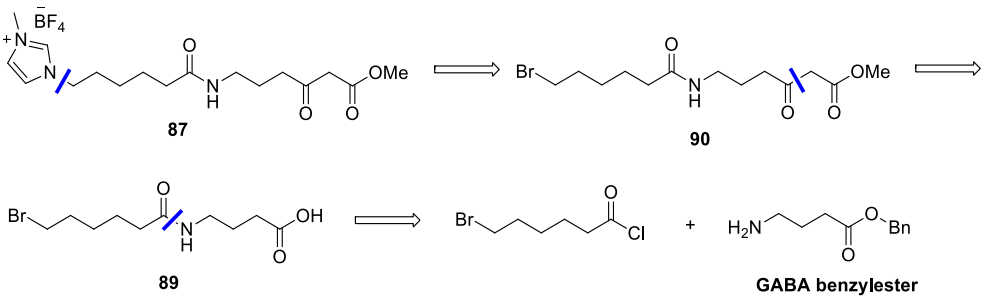

Scheme 48. Retrosynthetic pathway for the synthesis of probe **87**.

As appreciable from the retrosynthetic approach, we reasoned to introduce the IL liquid moiety as last step of the synthesis, anticipating possible solubility problems in reactions performed on the ionic liquid.

As IL we choose the couple methylimidazolium / tetrafluoroborate, which is one of the most commonly used and better characterised in literature. In this case, the "bait" was connected to the interacting malonate unit simply through a pseudo-peptidic carbon chain.

The synthesis started from the benzyl ester of GABA, synthesised according literature.[251] The amine was acylated with the commercially available 6-bromo hexanoylchloride. A strict control over reaction stoichiometry was required, to avoid the nucleophilic substitution of the bromine by the amine. The obtained compound **88** underwent hydrogenation in the presence of palladium (0) supported on carbon. In this case, the reaction was performed in ethylacetate. In fact, when methanol was employed as usual, a complete conversion of the benzylester into the corresponding methylester was observed after 3 hours.

The carboxylic acid **89** was converted into the malonate methylester **90** using the mild CDI -mediated procedure, exploited for the synthesis of azido-probe **77**. Also in this case the yield wasn't really high (37%), but acceptable, considering that the substrate was quite delicate due to the presence of the labile bromine.

Finally, we tried to displace the bromine, adding 1-methyl imidazole and KBF_4. The reaction was performed in acetonitrile, one of the few organic solvents in which ionic liquids are soluble. In literature, this reaction is usually performed at 70°C, but when we tried on our substrate, a complex mixture of products was obtained. The reaction was replicated at room temperature and, after 48h we obtained the desired product.

[251] H. Kimura, S. Sampei, D. Matsuoka, N. Harada, H. Watanabe, K. Arimitsu, M. Ono, H. Saji, *Bioorganic Med. Chem.* **2016**, *24*, 2251–2256.

After filtration and concentration under vacuum, thee crude residue was purified with the peculiar method employed for ILs. Diethyl ether was added, and the mixture was sonicated for 5 minutes. After decantation, the supernatant was carefully removed. The ionic liquid that appeared as a dense yellow oil remained stacked at the bottom of the flask. The procedure was repeated three times. The obtained product clearly still contained a white solid, probably KBF_4. To remove it, the probe was dissolved in cooled EtOH and filtered. After evaporation of the solvent, our clean ionic liquid probe **87** was obtained with 25% yield. Increasing the amount of 1-methyl imidazole (form 1.2 eq to 2 eq) and KBF_4 (from 1.4 eq to 2.5 eq) the yield was increased to 55%. This is a quite good result, considering that also the malonate portion of our probe could be sensible to the nucleophilic substitution by 1-methylimidazole. The synthetic pathway is summarised in Scheme 49.

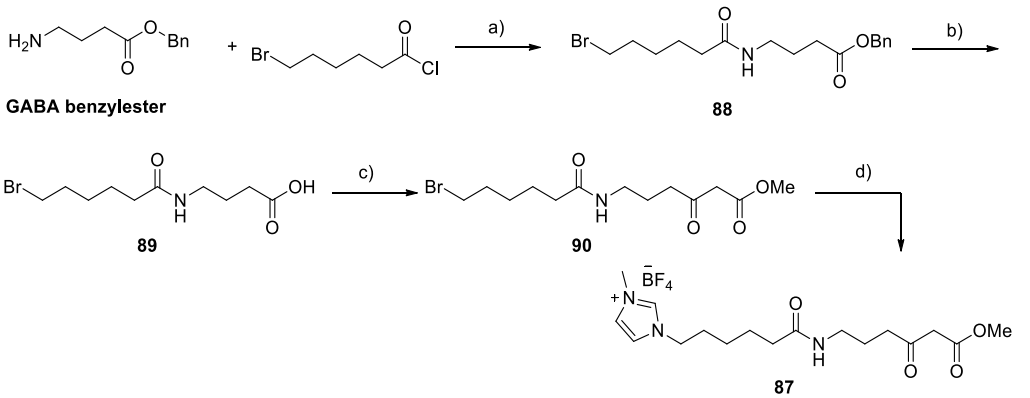

Scheme 49. Synthetic pathway leading to the formation of probe **87**. *Reagents and conditions*. a) TEA, CH_2Cl_2, 0°C to r.t., 4h, 90%; b) H_2, Pd/C, EtOAc, r.t., 3h, quant.; c) CDI, methylpotassium malonate, $MgCl_2$, CH_3CN, 0°C to r.t., 18 h, 37%; d) 1-methyl imidazole, KBF_4, CH_3CN, r.t., 48 h, 55%.

With probe **87** in my hands, preliminary feeding experiments on *Streptomyces lasaliensis* (WT and ACP12) were performed, in both liquid and solid phase, reaching a final concentration of 2.0 mM. Analogous experiments on *Streptomyces albus* DSM 41398 and *S. coelicolo*r harbouring the sal PKS enzymes were later completed in in the Tosin research group.

Feeding experiments revealed that all the microorganisms grew well in the presence of probe **87**, producing a considerable amount of the expected natural products and demonstrating that the probe was not toxic for the two microorganisms.

Unfortunately, as occurred in the case of the desthiobiotin probe, **87** wasn't incorporated in unnatural polyketides, probably because of the ionic nature of the probe affecting its distribution in cells and preventing its specific migration within the PKS active sites.

To bypass these issues and still gather information on whether the probe may be capable of off-loading biosynthetic intermediates, preliminary *in vitro* experiments were recently performed in the Tosin research group (by PhD student Panward Prasongpholchai) with a recombinant iterative type I PKS. The exact origins and details of this enzyme cannot be herein provided for confidentiality reasons. A KS-AT construct derived from the type I iterative PKS was first primed with hexanoyl-CoA and then incubated with probe **91** generated by prior treatment of **87** with pig liver esterase (PLE). The idea behind these experiments was to verify whether **91** would be capable of offloading KS-bound hexanoyl by decarboxylative Claisen condensation catalysed by the KS domain itself.

Orbitrap analysis of assay extracts led to the identification of *m/z* 378.5375, attributable to species **92**, and diagnostic fragments for it including *m/z* 296.2214 and m/z 182.1537. Considering the typical mass fragmentation of our ionic liquid probe, in which the methylimidazole moiety is usually lost, we hypothesised that *m/z* 296.2214 peak, could derived from the fragmentation of compound **92**, leading to **93**, as reported in Figure 60. Moreover, m/z 182.1537 appears to derive from further **93** fragmentation, followed by the loss of water, as reported again in Figure 60.

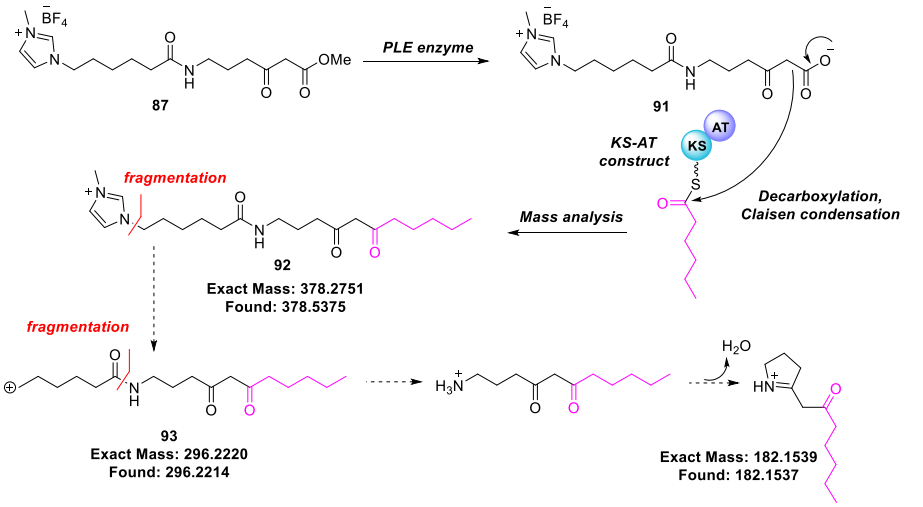

Figure 60. Preliminary results of the *in vitro* experiments on a type I iterative PKS construct KS-AT, showing the incorporation of the hexanoyl chain (pink) on probe **87**, leading to fragments **92** and **93**.

The mass spectrum obtained from the orbitrap analysis, showing the peaks corresponding to fragments **92** and **93** is appreciable in Figure 61.

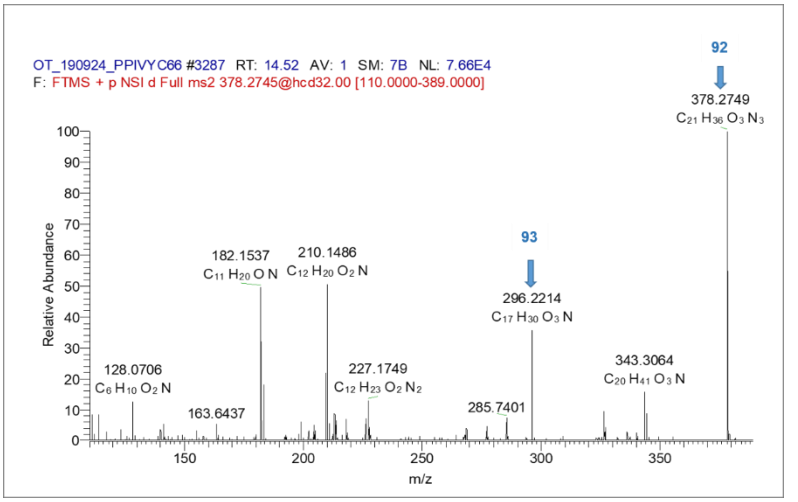

Figure 61. Orbitrap mass spectrum, showing the presence of the peaks corresponding to fragments **92** and **93**.

These preliminary results seemed to support that the ionic-liquid probe **91** effectively underwent decarboxylative Claisen condensation with the hexanoyl chain, resulting in its off-loading from the enzyme. However, in this instance the malonyl extending unit bound to ACP was not present to compete in this process. Further studies in the presence of malonyl-bound ACP will be soon performed to verify whether probe **91** can effectively interfere in the biosynthesis to generate a series of IL-tagged unnatural structures. If successful, this kind of approach would open up new avenue of investigations for the generation of functionalised polyketides and their isolation/ quantification.

6.3.4 Semisynthesis of Lasalocid A and Salinomycin derivatives

In the last part of the period at the University of Warwick, preliminary studies aimed at the semisynthesis of analogs of lasalocid A and salinomycin were performed.
Several studies dealing with the semisynthesis of salinomycin bioactive derivatives are reported in literature.[216] These analogs could be useful not only to obtain new active compounds, but also to increase their structural diversity and better understand the SARs of this interesting polyether ionophore.
In this field, our efforts were oriented in two different directions: the first involved the synthesis of amides of the carboxylic acid present in both lasalocid A and salinomycin. The latter exploited a retroaldol reaction, already reported on lasalocid A. This reaction breaks the polyether in two fragments, one containing the cyclic ethers and the other the aromatic ring. We reasoned that it would have been interesting to test this reaction on both the polyether ionophores, and to test the simplified fragments independently, in order to understand which portion of every molecule is responsible of the bioactivity.

Synthesis of amide derivatives of lasalocid A and salinomycin

Considering that both our polyketides of interest bear a carboxylic acid moiety, a functionalisation through the formation of an amide appeared to be the most intuitive choice. The alternative would have involved the exploitation of the hydroxyl groups, with all the consequent problems relative to the selectivity.
For a preliminary study, we simply decided to synthesise amides characterised by a different chain length.
To this extent, two different amines, previously synthesised in Tosin's research group (*N*-(2-aminoethyl) butyramide, **94** and *N*-(2-aminoethyl) decanamide, **95**)[252] were coupled with lasalocid A and salinomycin.
These reactions, performed in the presence of HATU and DIPEA, proceeded well for lasalocid A, leading to the obtainment of amides **96** and **97**. Salinomycin proved to be considerably less reactive, but after subsequent additions of condensing agent and prolonged reaction times, the corresponding amides **98** and **99** were obtained as well.
The reactions were performed on small scale and the purification of the crude products by semipreparative HPLC is still in progress. However, LC-HRMS analysis of

[252] Y. T. C. Ho, D. J. Leng, F. Ghiringhelli, I. Wilkening, D. P. Bushell, O. Köstner, E. Riva, J. Havemann, D. Passarella, M. Tosin, *Chem. Commun.* **2017**, *53*, 7088–7091.

the crudes, confirmed the obtainment of all the desired amides, whose structures are reported in Figure 62.

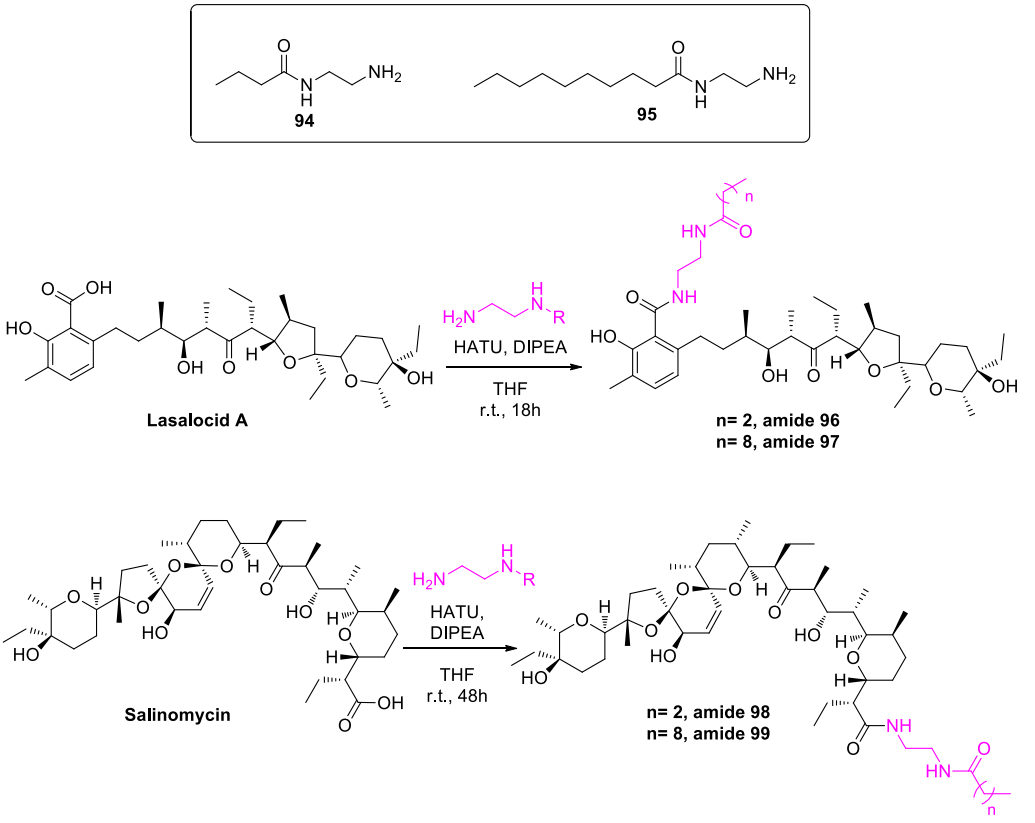

Figure 62. Structures of the amines **94** and **95**, used for the synthesis of amide derivatives of lasalocid A (**96** and **97**) and salinomycin (**98** and **99**).

Once purified, these amides will be tested, to check their antibacterial activity and, for what concern salinomycin derivatives, antiproliferative test against CSCs will be performed as well.

Interestingly, LC-HRMS analysis of amides **98** and **99** revealed the presence of two peaks characterised by the same m/z, and their intensity varied with the concentration (Figure 63, left box). A similar phenomenon was previously observed in Tosin's group, analysing different off-loaded intermediates obtained probing lasalocid A biosynthesis (an example is reported in Figure 63, right box).

At that time, it was hypothesised that the two peaks could correspond to isomerisation or the adoption of different monomeric/dimeric structures of the polyethers in complex with sodium, but the very low amount of product prevented

the structural analysis aimed at confirming those assumptions. However, in salinomycin amides cases, it should be possible to purify and isolated the pure compounds by semipreparative HPLC. The elucidation of the structure of the two compounds by NMR should help us to better understand this behaviour, supporting eventually also the hypothesis previously formulated.

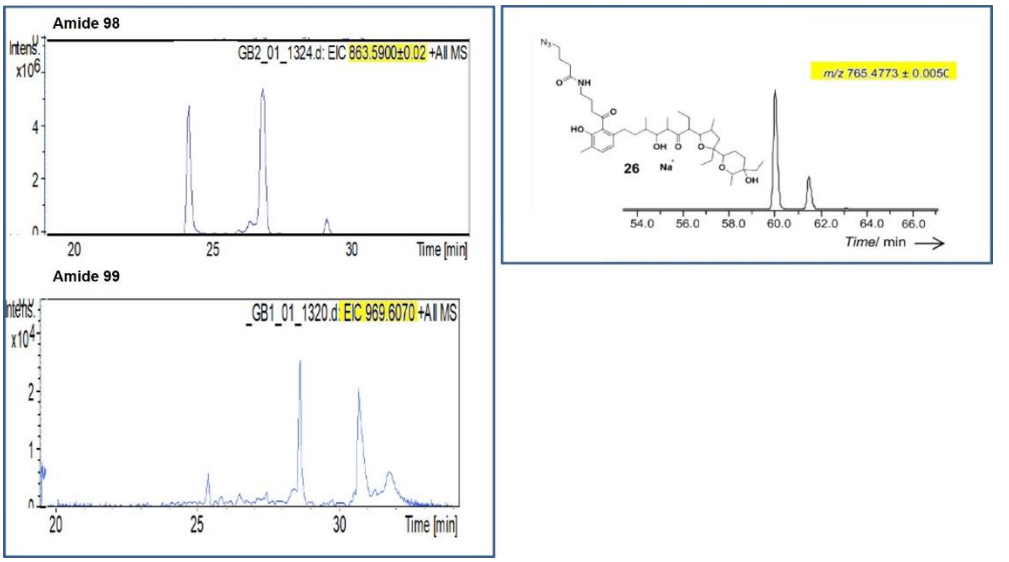

Figure 63. LC-HRMS analysis of amides **98** and **99** (left box) and of an unnatural off-loaded intermediate previously identify in the Tosin's group. In all of these cases it's possible to observe the presence of two peaks characterised by the same mass.

Retroaldol reaction on lasalocid A and salinomycin

Finally, attempts of breaking the scaffolds of both the polyethers ionophores through retroaldol reaction were made.

Back in the seventies, several groups reported that upon heating or in basic conditions, lasalocid A underwent retroaldol reaction, as reported in Scheme 50, affording an ethylketon, bearing the two cyclic ethers, and an aromatic aldehyde, that spontaneously cyclize to form a bicyclic compound. Moreover, a mixture of the *cis*- and *trans*- dehydration products was obtained as byproducts. [211,253,254]

[253] J. W. Westley, E. P. Oliveto, J. Berger, R. H. Evans, R. Glass, A. Stempel, V. Toome, T. Williams, *J. Med. Chem.* **1973**, *16*, 397–403.

[254] D. L. Coffen, D. A. Katonak, *Helv. Chim. Acta* **1981**, *64*, 1645–1652.

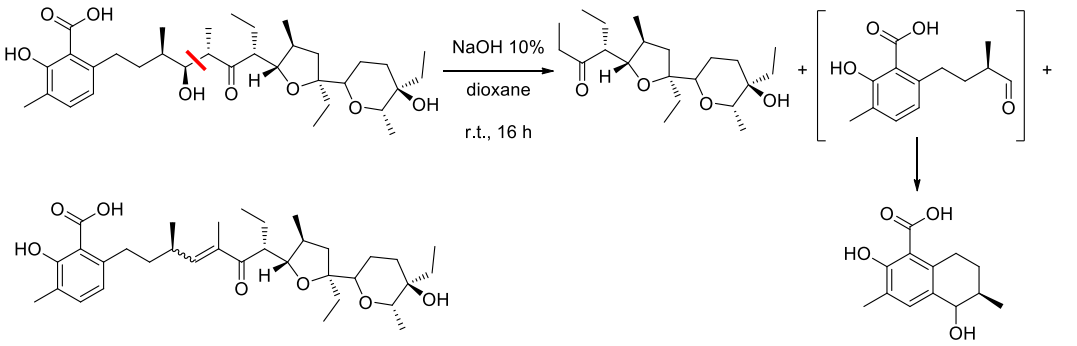

Scheme 50. Outcome of retroaldol reaction on lasalocid A.

We tried to replicate this reaction on small scale (10 or 15 mg), and we confirmed by mass analysis the formation of the ethyl ketone and the dehydration products. HPLC purification of these products is currently in progress.

However, also in this case, salinomycin prove to be definitely less reactive than lasalocid A. in fact, in the same reaction conditions, even after 5 days in basic environment, almost only the starting material was detected by MS analysis, accompanied by traces of the ketone and dehydration products.

Thus, this approach did not seem to be feasible on salinomycin, while once isolated, the fragments obtained through the retroaldol reaction on lasalocid A will be tested to evaluate their antibacterial activity.

6.4 Experimental part

General

Unless specified otherwise, chemicals were purchased from Sigma Aldrich, Fisher Scientific, Carbosynth and Alfa Aesar and Fluorochem and were used without further purification.

Analytical thin-layer chromatography (TLC) was performed on aluminium sheets precoated with silica gel 60 (F254, Merck) and visualised under ultra-violet light (short and long-wave) and using potassium permanganate ($KMnO_4$) or vanillin or ninhydrin stains. Silica gel was purchased from Sigma Aldrich (Tech Grade, pore size 60Å, 230-400 mesh).

^1H and ^{13}C NMR spectra were recorded in CD_3OD, $CDCl_3$ or CD_3CN on the following Bruker Avance instruments: DPX-300 300 MHz, DPX-400 400 MHz, DRX-500 500 MHz. High-resolution mass spectra (HRMS) were obtained using electrospray ionisation (ESI) on a MaXis UHR-TOF (Bruker Daltonics) or on Bruker MaXis (ESI-HR-MS).

Compounds were purified by preparative or semipreparative HPLC (Agilent 1260) on Phenomenex synergi™ Polar RP 80Å (250 x 10.0 mm, 4µm) column. The mobile phase consisted of a gradient of water and acetonitrile (HPLC grade, containing 0.1 % trifluoroacetic acid or 0.1% formic acid) at a flow rate of 0.5 mL/min, with UV detection at 210 nm.

Chemistry

Synthesis of methyl 4-(3-(((benzyloxy)carbonyl)amino)propanamido)butanoate (78)

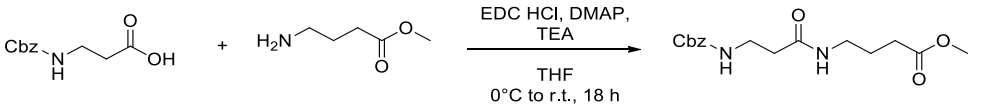

EDC HCl (0.670 g, 3.49 mmol) was added to a solution of Cbz-protected β-alanine (0.600 g, 2.69 mmol) and DMAP (0.476 g, 3.90 mmol) in anhydrous THF (40 mL), cooled at 0°C. The reaction mixture was stirred at 0°C for 30 min, then methyl 4-(4-chlorobutanamido) butanoate (0.454 g, 2.96 mmol) was added. The reaction was stirred for 1 hour at 0°C and then at r.t. for 18 h.

The solvent was removed under vacuum and the residue was dissolved in CH_2Cl_2. The organic layer was washed with 1M HCl and brine, then dried over $MgSO_4$, filtered and concentrated.

The crude product was purified by column chromatography (gradient elution, from EtOAc: petrol 4:1 to ethyl acetate), affording **78** (0.636 g, 74%) as a white solid.

^{1}H-NMR (400 MHz, $CDCl_3$) δ 7.33 (bs, 5H), 5.95 (bs, 1H), 5.49 (bs, 1H), 5.08 (s, 2H), 3.66 (s, 3H), 3.56 – 3.37 (m, 2H), 3.26 (q, *J* = 6.1 Hz, 2H), 2.36 (m, 4H), 1.81 (quint., *J* = 6.2, 5.6 Hz, 2H).

^{13}C-NMR (100 MHz, $CDCl_3$) δ 173.94, 171.42, 156.67, 136.67, 128.62- 128.20- 128.11 (5 CH of Cbz), 66.75, 51.87, 39.07, 37.23, 36.12, 31.57, 24.66.

MS (ESI) *m/z* $[M+Na]^+$ calcd. for $C_{16}H_{22}N_2O_5Na$: 345.1421, found: 345.1416.

Synthesis of methyl 4-(3-aminopropanamido)butanoate (79)

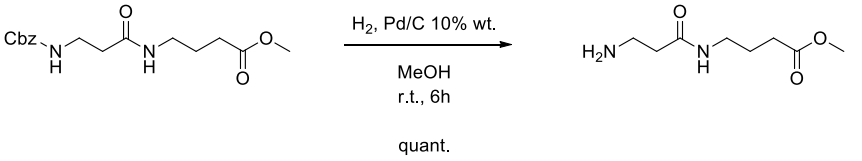

Pd/C (0.350 g, 10% wt) was added to a solution of **78** (0.350 g, 1.08 mmol) in anhydrous MeOH (25 mL). The reaction mixture was stirred under hydrogen atmosphere for 6 h, then the palladium was filtered through a small plug of Celite and washed with MeOH. The filtrate was concentrated under vacuum, affording **79** (0.196 g, quant.) as an amorphous solid, which didn't require further purification.

^{1}H-NMR (400 MHz, CD_3OD) δ 3.69 (s, 3H), 3.24 (t, *J* = 6.8 Hz, 2H), 2.92 (t, *J* = 6.3 Hz, 2H), 2.50 – 2.31 (m, 4H), 1.82 (quint., *J* = 7.1 Hz, 2H).
^{13}C-NMR (100 MHz, CD_3OD) δ 175.31, 174.41, 52.08, 39.54, 39.17, 38.98, 32.05, 25.71.
MS (ESI) m/z $[M+H]^+$ calcd. for $C_8H_{17}N_2O_3$: 189.1234, found: 189.1231.

***Synthesis of methyl 3,8,12-trioxo-1-phenyl-2-oxa-4,9,13-triazaheptadecan-17-oate (*80)**

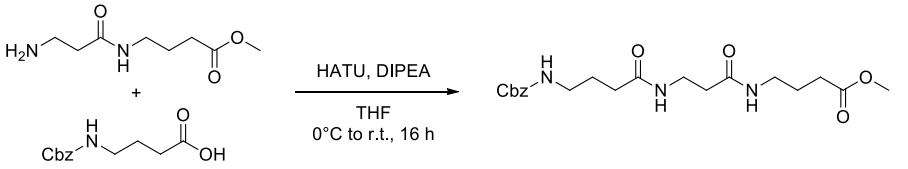

DIPEA (278 µL, 1.59 mmol) was added to a solution of **79** (0.150 g, 0.78 mmol) and *N*-Cbz-protected GABA (0.190 g, 0.78 mmol) in anhydrous THF (12 mL), cooled at 0°C. After 15 min at 0°C, HATU (0.394 g, 1.04 mmol) was added as well. The reaction mixture was stirred for 30 min at 0°C, then at r.t. for 24 h.

The solvent was removed under vacuum and the residue was dissolved in CH_2Cl_2 and washed with 1M HCl, $NaHCO_3$ and brine. The combined aqueous layers were extracted with CH_2Cl_2. The combined organic layers were dried over $MgSO_4$, filtered and concentrated.

The crude product was purified by column chromatography (ethyl acetate to ethyl acetate : methanol 85:15), affording **80** (0.215 g, 68%) as a white solid.

^{1}H-NMR (400 MHz, CD_3OD) δ 7.36 (bs, 5H), 5.08 (s, 2H), 3.67 (s, 3H), 3.42 (t, *J* = 6.5 Hz, 2H), 3.21 (t, *J* = 6.8 Hz, 2H), 3.14 (t, *J* = 6.7 Hz, 2H), 2.37 (dd, *J* = 15.7, 7.5 Hz, 4H), 2.21 (t, *J* = 7.3 Hz, 2H), 1.87 – 1.73 (m, 4H).

^{13}C-NMR (100 MHz, CD_3OD) δ 175.60, 175.32, 173.76, 129.46 - 128.97 - 128.80 (5 CH of Cbz), 67.38, 52.09, 41.21, 39.62, 37.05, 36.69, 34.22, 32.06, 27.23, 25.70. (detected signals).

MS (ESI) m/z $[M+Na]^+$ calcd. for $C_{20}H_{29}N_3O_6Na$: 430.1949, found: 430.1950.

Synthesis of methyl 4-(3-(4-aminobutanamido)propanamido)butanoate (81)

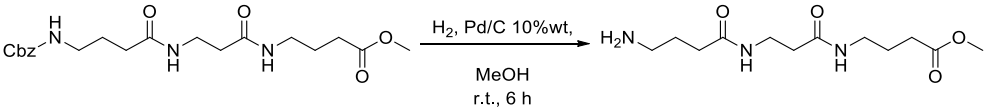

Pd/C (0.125 g, 10% wt) was added to a solution of **80** (0.125 g, 0.31 mmol) in anhydrous MeOH (8 mL). The reaction mixture was stirred under hydrogen atmosphere for 6 h, then the palladium was filtered through a small plug of Celite and washed with MeOH. The filtrate was concentrated under vacuum, affording **81** (0.085 g, quant.) as an amorphous solid which didn't require further purification.

^{1}H-NMR(400 MHz, CD_3OD) δ 3.68 (s, 3H), 3.44 (t, *J* = 6.7 Hz, 2H), 3.22 (t, *J* = 6.8 Hz, 2H), 2.70 (t, *J* = 7.1 Hz, 2H), 2.39 (dd, *J* = 14.5, 7.2 Hz, 4H), 2.25 (t, *J* = 7.4 Hz, 2H), 1.88 – 1.73 (m, 4H).
^{13}C-NMR: (100 MHz, CD_3OD) δ 203.79, 203.48, 201.86, 80.24, 69.92, 67.77, 65.19, 64.81, 62.49, 60.22, 57.34, 53.88.
MS (ESI) m/z $[M+Na]^+$ calcd. for $C_{12}H_{23}N_3O_4Na$: 3296.1581, found: 296.1582

Synthesis of methyl 4-(3-(4-azidobutanamido)propanamido)butanoate (82)

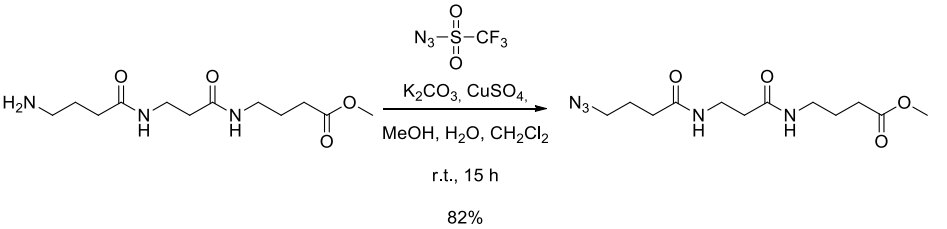

NaN_3 (0.200 g, 3.10 mmol) was dissolved in water (1.2 mL) and CH_2Cl_2 (1.9 mL). The mixture was cooled at 0°C and trifluoromethanesulfonic anhydride (130 µL, 0.61 mmol) was added dropwise. After 2 hours at r.t., the layers were separated, and the water was extracted with CH_2Cl_2 (2 x 0.5 mL). The combined organic phases were washed with brine and then added to a solution of **81** (0.084 g, 0.31 mmol), K_2CO_3 (0.098 g, 0.71 mmol), $CuSO_4$ pentahydrate (1 mg) in MeOH (2.5 mL) and water (1.5 mL). The reaction mixture was stirred at r.t. for 15 h, then the layers were separated and the organic one was washed with water. The aqueous layer was back extracted with CH_2Cl_2, then the collected organic phases were dried over $MgSO_4$, filtered and concentrated, affording **82** (0.076 g, 82%) as a white solid that didn't required further purification.

^{1}H-NMR (400 MHz, $CDCl_3$) δ 6.50 (bs, 1H), 6.11 (bs, 1H), 3.67 (s, 3H), 3.51 (dd, *J* = 11.6, 5.8 Hz, 2H), 3.30 (dt, *J* = 20.7, 6.6 Hz, 4H), 2.37 (dd, *J* = 15.6, 6.7 Hz, 4H), 2.25 (t, *J* = 7.2 Hz, 2H), 1.98 – 1.76 (m, 4H).
^{13}C-NMR (100 MHz, $CDCl_3$) δ 173.94, 172.08, 171.81, 51.92, 50.93, 39.11, 35.58 (2 CH_2), 33.34, 31.61, 24.91, 24.66.
MS (ESI) m/z $[M+Na]^+$ calcd. for $C_{12}H_{21}N_5O_4Na$: 322.1487, found: 322.1486.

Synthesis of 4-(3-(4-azidobutanamido)propanamido)butanoic acid (83)

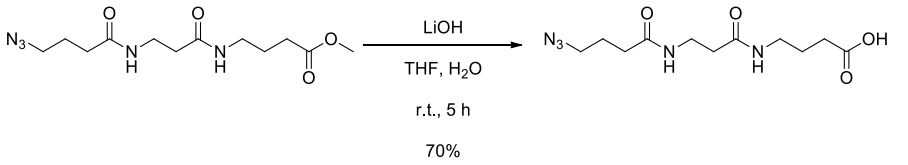

LiOH (0.006 g, 0.23 mmol) as added to a solution of **82** (0.058 mg, 0.19 mmol) in THF: water 1:1 (2 mL). The reaction mixture was stirred vigorously for 5 h, then the aqueous layer was acidified to pH= 2 with 1M HCl and extracted with ethyl acetate (12 X 4 mL). The collected organic phases were dried over $MgSO_4$, filtered and concentrated under vacuum, affording **83** (0.038 g, 70%) as a white solid which didn't required further purification.

^{1}H-NMR (400 MHz, CD_3OD) δ 3.44 (t, *J* = 6.8 Hz, 2H), 3.38 – 3.31 (m, 2H), 3.23 (t, *J* = 6.9 Hz, 2H), 2.40 (t, *J* = 6.8 Hz, 2H), 2.35 (t, *J* = 7.4 Hz, 2H), 2.28 (t, *J* = 7.4 Hz, 2H), 1.87 (quint., *J* = 7.0 Hz, 2H), 1.81 (quint., *J* = 7.2 Hz, 2H).
^{13}C-NMR (100 MHz, CD_3OD) δ 176.91, 175.13, 173.72, 51.86, 39.75, 37.05, 36.65, 33.88, 32.24, 26.15, 25.80.
MS (ESI) m/z $[M+Na]^+$ calcd. for $C_{11}H_{19}N_5O_4Na$: 308.1329, found: 308.1330.

Synthesis of methyl 6-(3-(4-azidobutanamido)propanamido)-3-oxohexanoate (77)

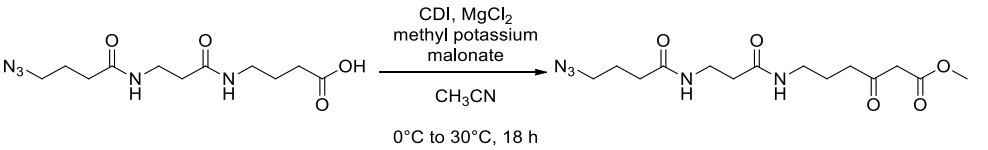

CDI (0.050 g, 0.30 mmol) was added to a solution of **83** (0.084 g, 0.29 mmol) in anhydrous THF (10 mL), previously cooled at 0°C. The reaction mixture was stirred at r.t. fo 3 h, then methyl potassium malonate (0.073 g, 0.47 mmol) and anhydrous magnesium chloride (0.067 g, 0.71 mmol) were added as well. The reaction mixture was stirred at 30°C for 18 h, then the solvent was removed under vacuum. The residue was dissolved in ethyl acetate and washed with an acid aqueous solution (pH=3-4). The aqueous phase was extracted 12 times with ethyl acetate. The collected organic phases were washed with a saturated aqueous solution of $NaHCO_3$ and brine, then dried over $MgSO_4$, filtered and concentrated under vacuum. Crude purification through column chromatography failed. The conditions for semi-preparative HPLC were established as follows:

Column: Phenomex Synergi 4u Polar-RP 80 Å 250 x 10 mm, flux: 2.5 ml/min, solvents: water (solvent A) and MeOH (solvent B). Gradient: 0 min- 15 min -> 70 : 30 A/B; 15 min - 30 min -> 5 : 95 A/B; 30 min – 50 min -> 5 : 95 A/B; 50 min- 51 min -> 70:30 A/B. In this way 3 mg of **77** (white solid) were obtained and characterized through ^{1}H-NMR and HR-MS. The purification of the crude through preparative HPLC will be performed in future, when the synthesis will be replicated on a higher scale.

^{1}H-NMR (400 MHz, $CDCl_3$) δ 6.45 (bs, 1H), 5.89 (bs, 1H), 3.75 (s, 3H), 3.53 (bd, *J* = 5.1 Hz, 2H), 3.47 (s, 2H), 3.34 (t, *J* = 6.4 Hz, 2H), 3.27 (dd, *J* = 12.1, 5.9 Hz, 2H), 2.63 (t, *J* = 6.5 Hz, 2H), 2.43 – 2.35 (m, 2H), 2.27 (t, *J* = 7.2 Hz, 2H), 1.98 – 1.87 (m, 2H), 1.87 – 1.77 (m, 2H).

MS (ESI) m/z $[M+Na]^+$ calcd. for $C_{14}H_{23}N_5O_5Na$: 364.1591, found: 364.1591.

General procedure for the Staudinger reduction of azides with polymer-bound triphenylphosphine.

55 mg of polymer-bound PPh_3 (loading 1.6 mol/g) were allowed to swell in 1 mL of anhydrous solvent (THF or MeOH), then the azido-probe **84** (5 mg, 0.014 mmol) was added in the minimum amount of solvent. The mixture was stirred at r.t. until the disappearing of free azide from the supernatant solution. The solvent was carefully removed, and the resin was washed three times with the reaction solvent. Then the resin was resuspended in 1 mL of MeOH and stirred at r.t. for two days, affording the desired amine, which was detected by MS analysis.

Synthesis of 6-((4R,5S)-5-methyl-2-oxoimidazolidin-4-yl)-N-(prop-2-yn-1-yl) hexanamide (85)

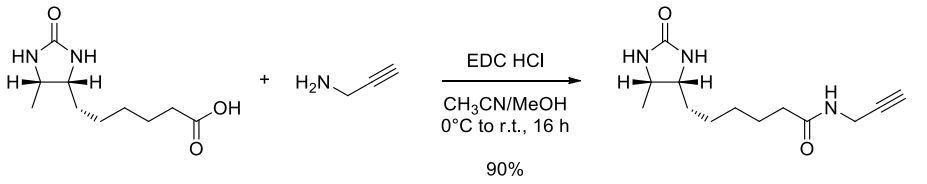

Desthiobiotin (0.900 g, 4.20 mmol) and propargyl amine (425 µL, 6.64 mmol) were dissolved in CH_3CN (30 mL) and MeOH (9 mL). The solution was cooled at 0°C, then EDC HCl (1.25 g, 6.55 mmol) was added. The reaction mixture was stirred at 0°C for 15 minutes and then allowed to warm to r.t. for 16 h. The solvent was removed under vacuum and the residue was purified by column chromatography (CH_2Cl_2 to CH_2Cl_2: MeOH = 9:1), affording **85** (0.952 g, 90%) as a yellow solid.

^{1}H-NMR (400 MHz, $CDCl_3$) δ 6.72 (bs, 1H), 6.12 (s, 1H), 5.05 (s, 1H), 4.02 (m, 2H), 3.94 – 3.76 (m, 1H), 3.69 (t, *J* = 7.7 Hz, 1H), 2.29 – 2.12 (m, 3H), 1.75 – 1.59 (m, 2H), 1.58 – 1.21 (m, 6H), 1.10 (d, *J* = 6.3 Hz, 3H).
^{13}C-NMR (100 MHz, $CDCl_3$) δ 172.98, 164.21, 80.32, 71.33, 56.12, 51.54, 35.54, 29.54, 29.02, 28.39, 25.72, 25.10, 15.89.
MS (ESI) m/z $[M+Na]^+$ calcd. for $C_{13}H_{21}N_3O_2Na$: 274.1526, found: 274.1529.

Synthesis of methyl 6-(2-(4-((6-((4R,5S)-5-methyl-2-oxoimidazolidin-4-yl)hexanamido)methyl)-1H-1,2,3-triazol-1-yl)acetamido)-3-oxohexanoate (86)

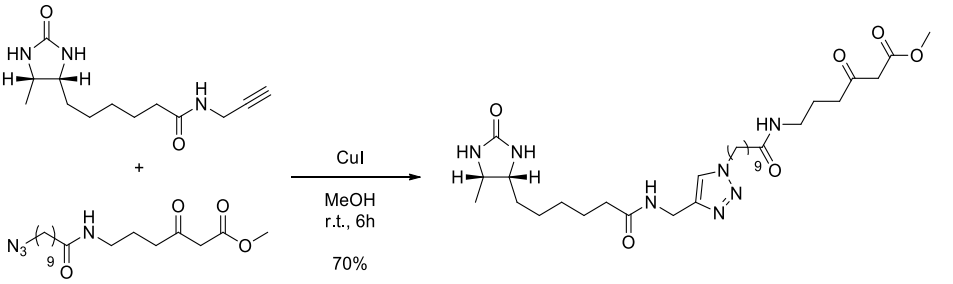

CuI (0.040 g, 0.20 mmol) was added to a solution of **85** (0.170 g, 0.68 mmol) and **84** (0.240 g, 0.68 mmol) in anhydrous methanol (20 mL). The reaction mixture was stirred 6 h at r.t., then the solvent was removed under vacuum. The residue was purified by flash chromatography (from pure EtOAc to ethyl EtOAc : MeOH = 4 : 1), affording **86** (290 mg, 70%) as a white solid.

^{1}H-NMR (400 MHz, $CDCl_3$) δ 7.54 (s, 1H), 6.24 (s, 1H), 5.95 (bs, 1H), 5.52 (s, 1H), 4.46 (dd, J = 13.3, 5.4 Hz, 2H), 4.29 (t, J = 7.0 Hz, 2H), 3.85 (d, J = 6.6 Hz, 2H), 3.72 (s, 3H), 3.46 (s, 2H), 3.25 (dd, J = 12.5, 6.1 Hz, 2H), 2.61 (t, J = 6.8 Hz, 2H), 2.34 – 2.09 (m, 4H), 1.97 – 1.74 (m, 6H), 1.74 – 1.63 (m, 2H), 1.59 (m, 2H), 1.52 - 1.35 (m, 4H), 1.30 (m, 10H), 1.13 (d, J = 6.2 Hz, 3H).
^{13}C-NMR (100 MHz, $CDCl_3$) δ 202.69, 173.43, 173.29, 164.17, 122.21, 56.20, 52.41, 51.53, 50.34, 48.98, 40.37, 38.60, 36.67, 35.20, 34.36, 30.10, 29.27, 29.11, 29.02, 29.00, 28.72, 27.78, 26.28, 25.62, 25.43, 24.68, 23.31, 15.76. (detected signals)
MS (ESI) m/z $[M+Na]^+$ calcd. for $C_{30}H_{51}N_7O_6Na$: 628.3793, found: 628.3794.

Synthesis of benzyl 4-(6-bromohexanamido)butanoate (88)

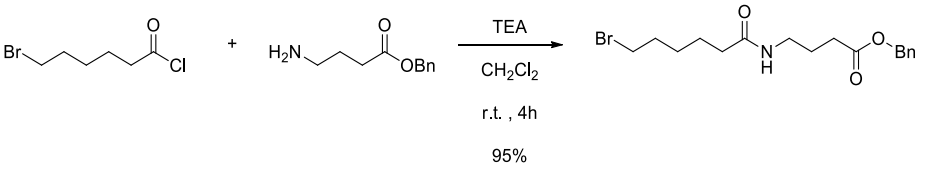

6-bromo hexanoylchloride (0.33 mL, 2.39 mmol) was added dropwise to a solution of benzyl 4-aminobutanoate hydrochloride (0.500 g, 2.18 mmol) and TEA (0.90 mL, 6.53 mmol) in CH_2Cl_2 (14 mL), previously cooled at 0°C. The reaction mixture was stirred at r.t. for 4 h, then washed with a saturated aqueous solution of NH_4Cl, water and brine. The organic layer was dried over $MgSO_4$, filtered and concentrated, affording **88** (0.843 g, 95%) as a white solid which didn't require further purification.

^{1}H-NMR (400 MHz, $CDCl_3$) δ 7.26 (m, 5H), 5.91 (bs, 1H), 5.03 (s, 2H), 3.30 (t, *J* = 6.6 Hz, 2H), 3.19 (dd, *J* = 12.6, 6.3 Hz, 2H), 2.32 (t, *J* = 7.1 Hz, 2H), 2.05 (t, *J* = 7.4 Hz, 2H), 1.75 (dd, *J* = 12.8, 6.2 Hz, 4H), 1.55 (quint., *J* = 7.5 Hz, 2H), 1.35 (quint., *J* = 8.0 Hz, 2H).
^{13}C-NMR (100 MHz, $CDCl_3$) δ173.28, 172.91, 135.81, 128.62, 128.34, 128.22, 66.42, 38.91, 36.36, 33.70, 32.44, 31.78, 27.76, 24.85, 24.65.
MS (ESI) m/z $[M+Na]^+$ calcd. $C_{17}H_{24}BrNO_3Na$: 392.0832, found: 392.0835.

Synthesis of 4-(6-bromohexanamido)butanoic acid (89)

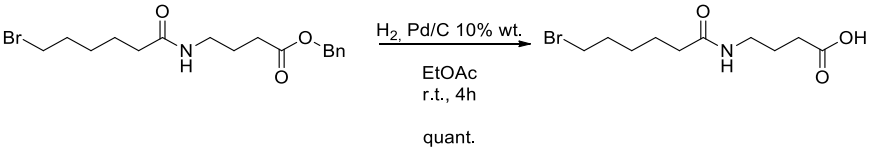

Pd/C (0.200 g, 10% wt.) was added to a solution of **88** (0.200 g, 0.54 mmol) in ethyl acetate (11 mL). The reaction mixture was stirred under hydrogen atmosphere for 4 h. The palladium was filtered through a plug of Celite and the filtrate was concentrated, affording **89** (0.153 g, quant.) as a white wax which didn't require further purification.

R_f: 0.09 (EtOAc 100%).

^{1}H-NMR (400 MHz, $CDCl_3$) δ 6.13 (bs, 1H), 3.34 (t, *J* = 6.1 Hz, 2H), 3.25 (bd, *J* = 5.6 Hz, 2H), 2.33 (m, 2H), 2.15 (t, *J* = 7.0 Hz, 2H), 1.79 (m, 4H), 1.56 (m, 2H), 1.39 (dd, *J* = 15.0, 7.6 Hz, 2H).

^{13}C-NMR (100 MHz, $CDCl_3$) δ 177.41, 173.94, 39.05, 36.45, 33.78, 32.48, 31.66, 27.81, 24.89, 24.72.

MS (ESI) m/z $[M+Na]^+$ calcd. for $C_{10}H_{18}BrNO_3Na$: 302.0362, found: 302.0360.

Synthesis of methyl 6-(6-bromohexanamido)-3-oxohexanoate (90)

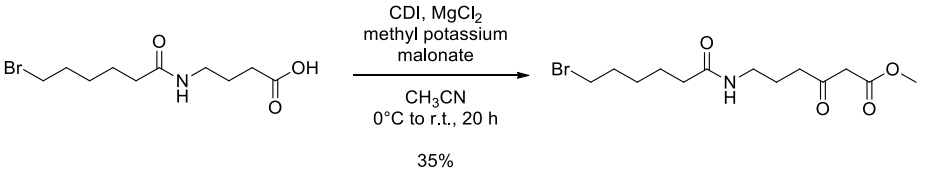

CDI (0.240 g, 1.48 mmol), was added to a solution of **89** (0.400 g, 1.43 mmol) in anhydrous CH_3CN (30 mL), cooled at 0°C. The reaction mixture was stirred at r.t. for 3h, then a solution of methyl potassium malonate (0.246 g, 1.58 mmol) and anhydrous magnesium chloride (0.218 g, 2.29 mmol) in anhydrous CH_3CN (10 mL) was added (the solution of methyl potassium malonate and $MgCl_2$ in CH_3CN was stirred 30 min before the addition).

The reaction mixture was stirred 16 h at r.t., then the solvent was removed under vacuum. The residue was dissolved in ethyl acetate and washed with acid water (pH= 5). The aqueous layer was extracted with ethyl acetate. The collected organic phases were washed with a saturated aqueous solution of $NaHCO_3$ and brine, dried over $MgSO_4$, filtered and concentrated under vacuum. The crude was purified by flash chromatography (EtOAc: petrol from 1:1 to 7:3), affording **90** (0.161 g, 34%) as a white wax.

^{1}H-NMR (400 MHz, $CDCl_3$) δ 5.77 (bs, 1H), 3.74 (s, 3H), 3.47 (s, 2H), 3.42 (t, *J* = 6.6 Hz, 2H), 3.27 (q, *J* = 6.3 Hz, 2H), 2.62 (t, *J* = 6.6 Hz, 2H), 2.18 (t, *J* = 7.4 Hz, 2H), 1.92 – 1.78 (m, 4H), 1.66 (quint., *J* = 7.4 Hz, 2H), 1.47 (quint., *J* = 8.4 Hz, 2H).

^{13}C-NMR (100 MHz, $CDCl_3$) δ 202.64, 172.91, 167.73, 52.44, 48.95, 40.37, 38.73, 36.44, 33.67, 32.35, 27.77, 24.81, 23.21.

MS (ESI) m/z $[M+Na]^+$ calcd. for $C_{13}H_{22}BrNO_4Na$: 358.0624, found: 358.0624.

Synthesis of compound 3-{5-[(6-methoxy-4,6-dioxohexyl)carbamoyl]pentyl}-1-methyl-1H-imidazol-3-ium trifluoroborane fluoride (87)

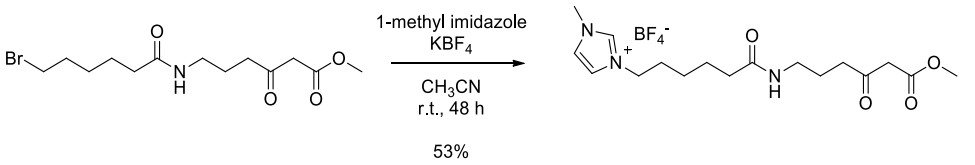

1-methyl imidazole (20 µL, 0.24 mmol) and KBF_4 (0.038 g, 0.30 mmol) were added to a solution of **90** (0.040 g, 0.12 mmol), in anhydrous CH_3CN (2.5 mL). The reaction mixture was stirred at r.t. for 2 days, then filtered and concentrated under vacuum. Et_2O was added and the mixture was sonicated for 5 minutes. After decantation, the surnatant was removed. The procedure was repeated 3 times, then the ionic liquid, which remained stacked on the bottom of the flask, was dissolved in cooled EtOH and filtered to remove the residual KBF_4. **87** (0.028 g, 53%) was obtained as a yellow oil.

^{1}H-NMR (400 MHz, CD_3CN) δ 8.92 (s, 1H), 7.47 (s, 1H), 7.36 (s, 1H), 7.05 (bs, 1H), 4.17 (t, *J* = 7.1 Hz, 2H), 3.85 (s, 3H), 3.65 (s, 3H), 3.50 (s, 2H), 3.07 (dd, *J* = 12.1, 5.9 Hz, 2H), 2.55 (t, *J* = 6.8 Hz, 2H), 2.14 (t, *J* = 7.1 Hz, 2H), 1.91 – 1.80 (m, 2H), 1.61 (dh, *J* = 27.0, 6.6 Hz, 4H), 1.29 (quint., *J* = 7.1 Hz, 2H).
^{13}C-NMR (100 MHz, CD_3CN) δ 204.20, 173.53, 168.87, 136.82, 124.43, 123.22, 52.58, 50.04, 49.71, 40.63, 38.73, 36.76, 36.16, 30.04, 25.85, 25.36, 24.16.
MS (ESI) m/z calcd. for $[C_{17}H_{28}N_3O_4]^+$: 338.2074, found: 338.2075

General procedure for the synthesis of amides derivatives of lasalocid A and salinomycin.

DIPEA (2 eq) was added dropwise to a solution of polyether ionophore (lasalocid A or salinomycin, 1 eq) and amine (1.1 eq) in anhydrous THF (0.05 M), previously cooled at 0°C. After 15 minutes, HATU (1.3 eq) was added as well. The solution was stirred at 0°C for 30 minutes and then at r.t. for 18 h. If necessary (as in the case of salinomycin, which is less reactive than lasalocid A), HATU, DIPEA and amine were added to reach reaction completion. The solvent was removed under vacuum. The products will be purified by semipreparative HPLC, but LC-MS analysis confirmed the obtainment of the desired amides.

6-((3R,4S,5S,7R)-7-((2S,3S,5S)-5-ethyl-5-((5R,6S)-5-ethyl-5-hydroxy-6-methyl tetrahydro-2H-pyran-2-yl)-3-methyltetrahydrofuran-2-yl)-4-hydroxy-3,5-dimethyl-6-oxononyl)-2-hydroxy-3-methyl-N-(2-pentanamidoethyl)benzamide (96).

MS (ESI) m/z $[M+H]^+$ calcd. for $C_{40}H_{67}N_2O_8$: 703.4897, found: 703.4800.

N-(2-decanamidoethyl)-6-((3R,4S,5S,7R)-7-((2S,3S,5S)-5-ethyl-5-((5R,6S)-5-ethyl-5-hydroxy-6-methyltetrahydro-2H-pyran-2-yl)-3-methyltetrahydrofuran-2-yl)-4-hydroxy-3,5-dimethyl-6-oxononyl)-2-hydroxy-3-methylbenzamide (97).

MS (ESI) m/z $[M+H]^+$ calcd. for $C_{46}H_{79}N_2O_8$: 787.5836, found 787.5800.

(2R)-N-(2-butanamidoethyl)-2-[(2R,5S,6R)-6-[(2S,3S,4S,6R)-6-[(2S,5S,7R,9S,10S,12R, 15R)-2-[(2R,5R,6S)-5-ethyl-5-hydroxy-6-methyloxan-2-yl]-15-hydroxy-2,10,12-trimethyl-1,6,8-trioxadispiro[4.1.5^7.3^5]pentadec-13-en-9-yl]-3-hydroxy-4-methyl-5-oxooctan-2-yl]-5-methyloxan-2-yl]butanamide (98).

MS (ESI) m/z $[M+H]^+$ calcd. for $C_{48}H_{83}N_2O_{11}$: 863.5997, found 863.5900.

N-{2-[(2R)-2-[(2R,5S,6R)-6-[(2S,3S,4S,6R)-6-[(2S,5S,7R,9S,10S,12R,15R)-2-[(2R,5R, 6S)-5-ethyl-5-hydroxy-6-methyloxan-2-yl]-15-hydroxy-2,10,12- trimethyl-1,6,8-trioxadispiro[4.1.5^7.3^5]pentadec-13-en-9-yl]-3-hydroxy-4-methyl-5-oxooctan-2-yl]-5-methyloxan-2-yl]butanamido]ethyl}decanamide (99).

MS (ESI) m/z $[M+Na]^+$ calcd. for $C_{54}H_{94}N_2O_{11}Na$: 969.6755, found 969.6070.

Feeding experiments

Microbiology methods.

All media and glassware were sterilized prior to use by autoclave (Astell). Liquid cultures were grown with shaking in Innova 44 incubator/shaker (New Brunswick scientific).

M79 medium: 2.5 g glucose, 2.5 g peptone, 0.5 g yeast extract, 1.5 g NaCl, 2.5 g casein hydrolysate in 250 ml of distilled water adjusted to pH 7.1.

MYM medium: 1.0 g maltose, 1.0 g yeast extract, 2.5 g malt extract in 250 ml of distilled water adjusted to pH 7.1.

TSBY medium: tryptone soy broth 3%, sucrose 10.3%, yeast extract 0.5%. in distilled water.

R2YE agar: sucrose 103 g, K_2SO_4 0.25 g, $MgCl_2 \cdot 6H_2O$ 10.12 g, glucose 10 g, Difco casaminoacids 0.1 g, distilled water 80 mL, Bacto agar 2.2 g for 80 mL of solution. Just before use, the following components were added to 80 mL of solution: KH_2PO_4, 0.5%, 1mL; $CaCl_2 \cdot 2H_2O$, 3.68% - 8 mL; L-proline, 20% -1.5 mL; TES buffer, 5.73% pH7.2 - 10 mL; trace element solution - 0.2 mL; NaOH 1N - 0.5 mL; Difco yeast extract 10% - 5 mL; trace element solution (per 1L): $ZnCl_2$ - 40 mg, $FeCl_3 \cdot 6H_2O$ -200 mg, $CuCl_2 \cdot 2H_2O$ - 10 mg, $MnCl_2 \cdot 4H_2O$ - 10 mg, $Na_2B_4O_7 \cdot 10H_2O$ - 10 mg, $(NH_4)_6Mo_7O_{24} \cdot 4H_2O$ - 10 mg).

General procedure for feeding experiments on Streptomyces lasaliensis cultures in liquid phase.

The *Streptomyces lasaliensis* strains, wild type and ACP12 (S970A) were grown in 10 mL of M79 medium for 3 days at 30°C. Then, 100 µL of seed culture were used to inoculate 10 mL of MYM medium. The cultures were incubated at 30°C for 5 days. After one day of incubation, the feeding began. The probe was dissolved in a known amount of HPLC-grade methanol (e.g. 200 µL) and four additions of this solution (e.g. 50 µL) were performed over four days, to reach a final concentration of 2.0 mM.

These experiments were performed in duplicate in sterile 50 mL Erlenmeyer flasks with springs. Control liquid cultures were prepared as well, in the absence of probe.

At the end of the fermentation process, the cultures were extracted with ethyl acetate. After evaporation of the solvent, the residues were redissolved in 1 mL of HPLC-grade methanol for MS analysis.

General procedure for feeding experiments on Streptomyces lasaliensis cultures in solid phase.

50 µL of seed culture of *Streptomyces lasaliensis* strains (WT or S970A, prepared as above) were used to inoculate 5 mL of MYM-agar and transferred in sterile Petri dishes. The plates were allowed to solidify in sterile conditions. The amount of probe necessary to reach a final 2.0 mM concentration was dissolved in100 µL of HPLC-grade methanol. The solution was dispersed over the plate. The solid cultures were incubated at 30 °C for 5 days, then the agar was cut in small pieces and extracted with ethyl acetate. After concentration under vacuum, the extracts were redissolved in 1 mL of HPLC-grade methanol for MS analysis.

The experiments were performed in duplicate and control cultures with no probe were prepared.

Growth of S. albus DSM 41398

Preculture: the microorganism was rehydrated in TSBY medium and used to inoculate 10 mL of the seed medium (sucrose 4%, yeast 0.5%, soybean flour 1%, $CaCO_3$ 0.2%, pH: 7.5). The preculture was gently shaken at 30°C for 7 days.

Culture: 100 µL of preculture were added to 10 mL of fermentation medium (soybean flour 1%, starch 0.5%, $CaCO_3$ 0.5%, $(NH_4)_2SO_4$ 0.3%, NaCl 0.2%, $MgSO_4$ 0.01%, KH_2PO_4 0.02%, pH= 7.5. After sterilization in autoclave, 6% of sunflower oil was added). The culture was gently shaken for 7 days at 30°C.

Growth of S. coelicolor M1154, harbouring the sal PKS

Preculture: A spore taken from the petri dish was used to inoculate 10 mL of TSBY medium. The preculture was gently shaken at 30°C for 7 days.

Culture: 100 µL of preculture were used to inoculate R2YE agar. The Petri dish was maintained at 30°C for 5 days.

Modification to the protocol for feeding experiments with ionic-liquid probes.

Feeding experiments performed with the ionic-liquid probe required a modification in the extraction protocol. The fermentation broth was freeze-dried to remove water. The residue was dissolved in diethylether and sonicated. After decantation, the supernatant solution was removed. The process was repeated twice and the collected diethylether fractions were concentrated under vacuum. The residue was dissolved in 1 mL of HPLC methanol for MS analysis.

The residue left after decantation was concentrated under vacuum to remove residual diethylether, then it was dissolved in 1mL of HPLC methanol for MS analysis.

7. Remarks and future perspectives

Diversity-oriented approach

During these three-years project, the library of piperidine-based derivatives previously obtained in the Passarella's research group through a diversity-oriented approach starting from 2-piperidine ethanol, was enriched with different scaffolds.
DOS is still an important strategy in drug discovery and development, in particular for the obtainment of diversified libraries of compounds, exploring in this way new portions of the chemical space, that could result more prolific for the individuation of interesting bioactive species.
The individuation of a good starting point to achieve diversification is always mandatory in DOS strategy, and 2-piperidine ethanol prove to be an optimal choice.
In fact, this compound is commercially available, cheap and characterized by structural features that make it easily functionalisable, including a piperidinic nitrogen and a hydroxyl group. The latter could be oxidized, leading to the key highly reactive aldehyde **7**, widely exploited in the Passarella's research group. Moreover, the presence of a stereocenter allows the synthesis of the different stereoisomers of the scaffolds obtained after the diversification process. Different strategies, such as the enzymatic kinetic resolution of the racemic 2-piperidine ethanol, or the use of asymmetric reactions on aldehyde **7**, could be exploited to this extent.
Finally, the presence of a piperidine ring, a widespread motif in several bioactive natural products suggests the possibility of obtaining interesting derivatives.
The versatility of 2-piperidine ethanol, proved in the previous works performed by Passarella *et al*, was demonstrated once again in this thesis.
The main results and the future perspectives will be summarised hereinafter.

- **Synthesis of novel piperidine-based heterocycles.**
  In this project three diversified compounds, resembling the structures of alkaloids natural products, were efficiently synthesised in a stereoselective fashion, starting from the common precursor **13**, and exploiting the diverse reactivity under acidic or Eschweiler-Clarke conditions, resulting from its *syn*- or *anti*- stereocenters configuration. Preliminary citotoxicity tests performed on three cancer cells lines did not show any particular activity. Nevertheless, the members of this small library of piperidine-based derivatives will remain available for both *in silico* and biological tests on different biological targets.

- **Hedgehog signalling p athway as target.**
  In this project, we decided to exploited the key homoallylic alcohol **10** to build the fundamental α,β-unsaturated lactone motif present in some withanolides and withanolides-inspired inhibitors of Hh signalling pathway. After that, docking simulations help us to identify a promising scaffold **19**. Its synthesis proved to be highly challenging, but we finally managed to obtain two out of the four possible racemic stereoisomers (**19a-b**). Preliminary biological evaluation through an Hh-dependent luciferase reporter assay revealed that the final compounds did not display the expected activity, while two intermediates, **33b** and **34b**, proved to significantly inhibit the Hh signalling, with IC_{50} of 7.44 and 12.95μM, respectively. These data suggest that **19a-b** could possess a poor pharmacokinetic profile, being too polar to cross the cellular membranes, while **33b** and **34b**, characterised by a similar structure but including a TBDPS protecting group on the primary alcohol could eventually reach Hh target proteins.
  The enantiomers of each active compound were synthesized, adapting the synthetic protocol in a stereoselective fashion, exploiting two asymmetric Brown's allylations. Biological tests are currently ongoing, to determine whether both the enantiomers of **33b** and **34b** are active. Moreover, further tests will be performed on the obtained compounds, to exactly determine at which stage of the Hh signalling the inhibition occurs.
  The identification of two active compounds will be exploited in future for the development of new Hh-inibitors characterized by increased activity.

  In parallel, the synthesis of 2nd generation inhibitors **35** and **36** was considered.
  Recently the first stereoisomer of the urea-based scaffold **35** was accessed in our laboratory. The developed synthetic strategy would open the possibility of easily obtaining the other stereoisomers.
  On the other hand, the separation of the diastereomeric mixture of the arylated precursor **48** of scaffold **36** is currently in progress. After that, **48** will be exploited in the same synthetic pathway developed for compounds **19**, in order to obtain arylated analogs that should be characterized by an improved activity.

- **(-)-anferine**

  The peculiar structures of scaffolds **10** and **14** guided our DOS approach towards a natural product, (-)-anaferine. In fact, the proper combination of the structural features of these two compounds was envisaged to access (-)-anaferine scaffold, constituted by two piperidine rings connected by a 2-propanone bridge. The synthesis of this natural compound was easily accomplished. The future efforts in this field will be focused on the optimization of the synthetic strategy, taking advantage of a Kurti's aziridination, followed by nucleophilic opening, leading to two diastereoisomeric homoallylic amines that could be exploited for the parallel synthesis of (-)- and meso-anaferine.

- **Thiocolchicine-based bivalent compounds.**

  In this project, a hybrid compound, previously synthesised in our laboratory starting from 2-piperidine ethanol, was exploited as building block for the synthesis of bivalent conjugates, considering that its structure contained an analog of pironetine (a known α-tubulin binder), and a piperidine ring, exploitable as anchor point for the attachment of a linker and a second active unit (in our case, thiocolchicine, a model of β-tubulin binder). In this way, four bivalent compounds, characterized by two different linkers, were easily synthesised. Biological evaluation of our conjugates revealed that both the linkers disrupted the interaction of the two active units in their binding sites. More importantly, the hydrophobic nature of the linkers, made the bivalent compounds better substrates for P-glycoprotein, an efflux pump responsible of the drug resistance in several cancer types. However, these results will help us to develop new conjugates characterized by improved features, in particular for what concern the physical and chemical nature of the linker.

Chemoenzymatic approach

Mutasynthesis- based strategies could be a good alternative to obtain diversified analogs of natural products characterised by highly complex structures, for whom a classical synthesis would be unfeasible and time consuming. The chemoenzymatic approach recently developed in the Tosin's research group, exploiting the administration of malonate-mimicking chemical probes to different bacterial strains, allowed the generation of unnatural, diversified analogs of different polyketides. In this context, my aim was the obtainment of unnatural derivatives of two polyether ionophore antibiotics (lasalocid A and salinomycin) and, more importantly, the development of a system for an easier recovery of these compounds from extract mixtures.

Thus, during my period abroad, four different probes were efficiently synthesised (two azido probes **77** and **84**, a desthiobiotin-based probe **86** and an ionic-liquid probe, **87**), to be exploited in three different approaches aimed at allowing an easier detection and recovery of diversified off-loaded intermediates generated from feeding experiments in different bacterial strains.

- The feasibility of the Staudinger-based approach was confirmed by a proof of concept experiment, leading to the reduction of the azido-probe **84** to the corresponding amine. However, the lack of reproducibility limited the application of this strategy on extracts. Therefore, different polymers will be tested in the near future, and efforts will be focused on the optimization of reaction conditions. This approach would be ultimately tested on extracts deriving from feeding experiments in the presence of azido probes.

- Feeding experiments on *S. lasaliensis* performed with the desthiobiotin probe **86** confirmed the hydrolysis and decarboxylation of **86**, as well as its lack of toxicity inferred by the inaffected growth of the microorganism and production of lasalocid A. However, probe **86** wasn't incorporated in unnatural polyketides *in vivo*. This is likely due to a change in distribution of the probe within cells due to the presence of the desthiobiotin tag. Therefore, we envisage two possible near-future solutions: *in vitro* experiments with recombinant PKSs, and performing of the click reaction with propargyl desthiobiotin on extracts originated by feeding experiments with azido-probe **84**). Extract purification exploiting avidin resin would be implemented for the best approach.

- Feeding experiments on *S. lasaliensis*, *S. albus* DSM 41398 and *S. coelicolo*r harbouring the sal PKS enzymes were performed in the presence of the ionic-liquid probe **87**. As occurred in the case of probe **86**, **87** was not incorporated in unnatural polyketide species. However, preliminary *in vitro* experiments performed on a KS-AT construct from a type I iterative PKS by a co-worker gave encouraging results, and an unnatural polyketide derivative **92** was allegedly generated. Future efforts will be aimed at verifying if **87** could compete with malonyl-CoA in the generation of unnatural fragments.

For what concerns the semisynthesis of lasalocid A and salinomycin derivatives, two amides characterised by different chain length were synthesised for each natural product. A retroaldol-based approach led to lasalocid A fragmentation in three different compounds, while it was ineffective on salinomycin. The obtained derivatives will be tested to evaluate their antibacterial properties. The results will help us to better understand the SARs (structure-activity relationships) at the basis of the antibiotic activity of the two natural polyether ionophore antibiotics.

Acknowledgements

At the end of this three-years journey, I would like to express my gratitude to my supervisor, Professor Daniele Passarella, that gave me the opportunity of working in its research group, always encouraging me to face new and challenging projects. Thanks also to all the research group members, in particular to the bachelor and master students that contributed to the work reported in this thesis.
I would also like to warmly thank Prof. Manuela Tosin of the University of Warwick (UK) and her research group, that kindly hosted me for almost 6 months, giving me the opportunity to discover different branches of chemistry and microbiology.

A special acknowledgement goes to our network of collaborators, for their precious expertise in different research field:

- Computational studies were performed by Prof. Maurizio Sironi and Dr. Stefano Pieraccini (Università degli Studi di Milano), and by Dr. Mattia Mori (Università degli Studi di Siena).
- Biological evaluations of my products were made in collaboration with Professor Bruno Botta and Dr. Lucia Di Marcotullio (La Sapienza, Università di Roma), Dr. Paola Infante (Center for Life Nano Science@Sapienza Istituto Italiano di Tecnologia), Prof. Fernando Diaz (Centro de Investigaciones Biológicas Consejo Superior de Investigaciones Cientificas CIB–CSIC, Madrid), Prof. Lisa Dalla Via (Università degli studi Padova) and Dr. Arvind Singh Negi and co-workers, (CSIR-Central Institute of Medicinal and Aromatic Plants, Lucknow, India).
- X- rays analysis were performed by Prof. Leonardo Lo Presti (Università degli Studi di Milano).

Finally, my gratitude goes to COST action CM1407 “Challenging organic syntheses inspired by nature - from natural products chemistry to drug discovery”, to MIUR (PRIN 2017) 2019-2022 “Targeting Hedgehog pathway: Virtual screening identification and sustainable synthesis of novel Smo and Gli inhibitors and their pharmacological drug delivery strategies for improved therapeutic effects in tumors” and to the MAECI Italia-India Strategic Projects 2017-2019 MAE0105301 “Development of nature inspired bivalent antitubulins as anticancer agents” for the financial support of my research work.